AD-763 811

GEOPHYSICS APPLIED TO GEOTECHNICAL PROBLEMS IN A MARINE ENVIRONMENT: A CASE STUDY - MONTEREY BAY, CALIFORNIA

B. B. Barnes, et al

National Oceanic and Atmospheric Administration

Prepared for:

Advanced Research Projects Agency
Bureau of Mines

June 1973

U.S. DEPARTMENT OF COMMERCE
NATIONAL OCEANIC AND ATMOSPHERIC ADMINISTRATION
Environmental Research Laboratories

Geophysics Applied to Geotechnical Problems in A Marine Environment A Case Study: Monterey Bay, California

B. B. Barnes, R. F. Corwin, T. G. Hildenbrand, L. Jackson
R. Kessler, W. Takeyama, M. Hornick and R. Jenkins

Annual Report— January 20, 1972 through March 20, 1973
Amount of Contract: $32,544.00
Principal Investigator and Project Scientist: B. B. Barnes (415) 383-6016
Short title— Marine Geophysics

Sponsored by:
Advanced Research Projects Agency
ARPA Order No. 1579, Amend. 3
Program Code 2F10

This research was supported by the Advanced Research Projects Agency of the Department of Defense and was monitored by the Bureau of Mines under Purchase Order No. H0220019.

June 1973

AB DOCUMENT CONTROL DATA FORM

UNCLASSIFIED

Security Classification

3200.8 (Att 1 to Encl 1)
Mar 7, 66

DOCUMENT CONTROL DATA - R & D

(Security classification of title, body of abstract and indexing annotation must be entered when the overall report is classified)

1. ORIGINATING ACTIVITY (Corporate author)
Marine Minerals Technology Center
(U.S. Dept. of Commerce)
3150 Paradise Drive, Tiburon, Ca. 94920

2a. REPORT SECURITY CLASSIFICATION
Unclassified

2b. GROUP
N/A

3. REPORT TITLE
Geophysics Applied to Geotechnical Problems in a Marine Environment
A Case Study: Monterey Bay, California

4. DESCRIPTIVE NOTES (Type of report and inclusive dates)
Annual Report, January 19, 1972 through January 19, 1973

5. AUTHOR(S) (First name, ...)
B. B. Barnes, L. Jackson, M. Hornick, R. F. Corwin, R. Kessler, R. Jenkins, T. G. Hildenbrand, W. Takeyama

6. REPORT DATE
May, 1973

7a. TOTAL NO. OF PAGES
vi, 282

7b. NO. OF REFS
127

8a. CONTRACT OR GRANT NO.
H0220019

b. PROJECT NO.

c.

d.

9a. ORIGINATOR'S REPORT NUMBER(S)
N/A

9b. OTHER REPORT NO(S) (Any other numbers that may be assigned this report)

10. DISTRIBUTION STATEMENT

11. SUPPLEMENTARY NOTES
This contract was monitored by the U. S. Bureau of Mines

12. SPONSORING MILITARY ACTIVITY
Advanced Research Project Agency
Dept. of Defense
Washington, D. C. 20301

13. ABSTRACT

Geophysical systems consisting of electrical and acoustical tools were developed and special mapping techniques applied to obtain geotechnical data in Monterey Bay, California. The objective of the field exercise was to try and relate geophysical measurements to the mass physical properties and engineering properties of seafloor sediments. Measurements consisted of; (1) mapping the Rayleigh Reflection Coefficient continuously by a ship underway, (2) measuring *in situ*, the propagation velocities of compressional and transverse (shear) waves, and (3) taking both underway and *in situ* measurements of sediment conductivity.

P and S wave velocities were measured using a prototype seismic shear wave generator. Measurements of sediment conductivity were taken with a direct current resistivity system deployed in a surface-towed configuration and as a diver-operated expandable array implanted in the seafloor. These data, along with the computed reflection coefficients (bottom loss) data, were correlated to analysis of samples taken using a unique diver-operated core sampler and vibracorer sampler that were specially designed for the field experiment.

The surveys and sampling programs were carried out in Santa Cruz Harbor, Monterey Bay, California. Surveys were conducted on a fine-grained scale. Grid patterns for profiling and sampling covered an area of 30 square miles. A high-accuracy precision radiolocation navigation and positioning system was employed throughout the field exercise.

The experiments, equipment employed, and corroboration of data to previous studies of a similar nature are described. It was concluded that each of the systems employed have potential application for measuring remotely and directly (*in situ*) parameters of mass physical properties of seafloor sediments, and that only the shear wave system showed potential for measurement of the engineering properties of seafloor sediments.

DD FORM 1 NOV 65 1473

UNCLASSIFIED

Security Classification

Ia

14 KEY WORDS	LINK A		LINK B		LINK C	
	ROLE	WT	ROLE	WT	ROLE	WT
Reflectivity measurement						
Acoustic velocity measurement						
Shear wave velocity						
Electromagnetic sounding						
Direct current resistivity						
Resistivity measurement						
Geologic prediction						
Marine sediment properties						
Seismic velocity						
Sediment properties						
Electrical properties of marine sediments						
Seismic properties of marine sediment						

DISTRIBUTION OF THIS DOCUMENT IS UNLIMITED

*U. S. Government Printing Office: 1972-781-435/8 Region 8

*GPO 781-435

II

NOTICE

The NOAA Environmental Research Laboratories do not approve, recommend or endorse any proprietary product or proprietary material mentioned in this publication. No reference shall be made to the NOAA Environmental Research Laboratories, or to this publication furnished by the NOAA Environmental Research Laboratories, in any advertising or sales promotion which would indicate or imply that the NOAA Environmental Research Laboratories approve, recommend or endorse any proprietary product or proprietary material mentioned herein, or which has as its purpose an intent to cause directly or indirectly the advertised product to be used or purchased because of this NOAA Environmental Research Laboratories publication.

The views and conclusions contained in this document are those of the authors and should not be interpreted as necessarily representing the official policies, either expressed or implied, of the Advanced Research Projects Agency or the U. S. Government.

I

TABLE OF CONTENTS

TECHNICAL REPORT SUMMARY

Geophysical systems consisting of electrical and acoustical tools were developed and special mapping techniques applied to obtain geotechnical data in Monterey Bay, California. The objective of the field exercise was to try and relate geophysical measurements to the mass physical properties and engineering properties of seafloor sediments. Measurements consisted of; (1) mapping the Rayleigh Reflection Coefficient continuously by a ship underway, (2) measuring *in situ*, the propagation velocities of compressional and transverse (shear) waves, and (3) taking both underway and *in situ* measurements of sediment conductivity.

P and S wave velocities were measured using a prototype seismic shear wave generator. Measurements of sediment conductivity were taken with a direct current resistivity system deployed in a surface-towed configuration and as a diver-operated expandable array implanted in the seafloor. These data, along with the computed reflection coefficients (bottom loss) data, were correlated to analysis of samples taken using a unique diver-operated core sampler and vibracorer sampler that were specially designed for the field experiment.

The surveys and sampling programs were carried out in Santa Cruz Harbor, Monterey Bay, California. Surveys were conducted on a fine-grained scale. Grid patterns for profiling and sampling covered an area of 30 square miles. A high-accuracy precision radiolocation navigation and positioning system was employed throughout the field exercise.

The experiments, equipment employed, and corroboration of data to previous studies of a similar nature are described. It was concluded that each of the systems employed have potential application for measuring remotely and directly (*in situ*) parameters of mass physical properties of seafloor sediments, and that only the shear wave system showed potential for measurement of the engineering properties of seafloor sediments.

GEOPHYSICS APPLIED TO GEOTECHNICAL PROBLEMS IN A MARINE ENVIRONMENT
A CASE STUDY: MONTEREY BAY, CALIFORNIA

B. B. Barnes, R. F. Corwin, T. G. Hildenbrand, L. Jackson
R. Kessler, W. Takeyama, M. Hornick and R. Jenkins

1. INTRODUCTION

The purpose of this work is to demonstrate the value of applying geophysical remote sensing techniques to the classification of engineering and mass physical properties of seafloor sediments commonly referred to as "geotechnical properties" and to suggest specific studies in which the methods could be further utilized to obtain geotechnical information necessary for seafloor excavation, such as in mining marine mineral deposits of shallow and deep sea origin.

Tools and techniques recently developed in this laboratory for obtaining acoustical and electrical resistivity measurements on target areas in San Francisco Bay (Barnes et al., 1972), Baja California, Mexico (Corwin and Conti, 1973) and more recently in Monterey Bay, California, have greatly enhanced the usefulness of geophysical methods in determining subtle variations observed in a wide variety of sediment types from both estuarine and continental shelf environments. Acoustical and electrical resistivity variations within individual sediment types, detectable by applying fine-grained surveying practices and employing advanced instrumentation, can reflect information useful in depicting geotechnical variations occurring in these two environments. Thus, the methods described herein are powerful tools for use in site selection for undersea foundation emplacement and in predicting a geologic situation before seafloor excavation and mining. To demonstrate this, the present report will give as an example geotechnical variations obtained using geophysical methods which are verified by sediment analyses of core samples in selected test sites. The analyses depict several different mass physical properties and engineering properties, each systematically obtained from diverse kinds of sediments located within a geographical province in the primary

test area located in Monterey Bay, California. An additional advantage of applying advanced sampling equipment to enable more accurate and reliable correlations of acoustical and electrical resistivity measurements to sediment analyses is also described in the report.

The distribution of changes in mass physical properties, consisting of porosity, density, mean grain size, and sorting coefficients, and of engineering properties, such as measured by penetrometer and vane shear apparatus, is made complex by a host of oceanographic operators — pressure, currents, mineralogy, biology, geochemistry, and structural deformation, to mention a few. The complexity is further enhanced by the interrelation and interdependence of parameters related to the sediment properties. In this study we are mainly concerned with the static situation — the seafloor as it is in one place in space and time.

During the last decade, interest in geotechnical measurements has been steadily growing because of the utilization of our coastal zone and adjacent shelf for engineering purposes, such as, for example, emplacement of oil pipelines, drilling platforms, bridge and dam foundations, and submerged nuclear power plants. More recently the United States mining industry has indicated an interest in developing more rapid and accurate methods to obtain geotechnical data in deep sea areas where ferromanganese deposits are located. Although the feasibility of applying remote sensing instrumentation to geotechnical problems is still widely debated, considerable progress has been made in the development of methods and instrumentation for this purpose. We still have insufficient knowledge of the full potential to reliabily predict sediment property variations and to understand the mechanisms that cause such changes to occur. Knowledge can only be derived from making many empirical measurements in the actual environment, utilizing computed analyses and the best in sediment sampling equipment in conjunction with advanced geophysical tools and methods.

Elements in this study consist of: (1) two separate acoustic experiments based on continuously mapping reflection coefficients by a ship underway and using *in situ* apparatus implanted in the seafloor capable of generating and detecting P and S waves in a saturated medium, (2) an electrical resistivity experiment utilizing especially configured arrays for

obtaining *in situ* and surface towed direct current resistivity measurements that indicate sediment conductivity taken in place and by a ship underway and, (3) the use of unique sampling equipment for obtaining cores of the near surface seafloor sediments. The report defines in detail the interrelationship and correlation of data obtained from each of these three sources and relating these data to the overall objective and purpose of the project.

1.1 Discussion of Problems

Application of geophysics to the solution of marine civil engineering problems, or "geotechnics", constitute the subject of this report. The point of view is that of the engineer, and the earth sciences, particularly geophysics, have been brought into the engineering pattern only when they have direct bearing upon a problem. Our goal is to present only those basic geotechnical problems connected with depicting the natural environment of an engineering structure and/or trafficability of seafloor systems, such as mining implements, that may be used for excavation. The case history of Monterey Bay has been used to elucidate the value of applying geophysics to standard practices for determining seafloor properties.

Several cases of differential settlement of oil drilling platforms in the Gulf of Mexico and huge pipelines shifting from their anchorages in the North Sea and Mediterranean Sea have resulted in the loss of production and a considerable amount of revenue. Before these events, not all marine engineers could see clearly that the design of a structure should be preceded by a careful study of its environment, particularly the foundation material on which the structure was to be placed. The problems are more complicated than those encountered on land because of the overlying water column and unusual behavior of marine sediments. The past 15 years have seen great emphasis placed towards diagnosing in advance the state of sediment properties. With the advent of offshore mining on our continental shelves and in the deep sea, undoubtedly more requirements for rapid, but accurate determinations will be necessary; thus,

a new type of technology is needed to assist standard methods of geotechnical measurements.

1.2 Operational Constraints

Certain constraints to applying geophysical methods must be identified before proceeding further. Acoustical measurements taken by a ship underway are particularly affected by topography, acoustic beam width, power, system stability in a hostile environment, and water depth. *In situ* measurements are likewise affected, but to a lesser degree, their greatest limitation being time and cost factors.

A level seafloor terrain is most desirable for acoustic measurements. Micro topographic changes have greater influence on acoustic sources that possess characteristics of narrow beam width and high frequency. Ideally, a flat bottom with little variation of sediment type produces the most reliable data. Water depth becomes an important factor if source and receiver transducers are on the surface. Attenuation of energy by spreading and absorption are neglible in shallower water but can become an appreciable factor with depth. The stability of the systems, in particular the source and receiver orientation to the reflecting surface, are obviously a consideration in obtaining accurate signal ratios between the transmitted and received (reflected) energy. In the case of the towed electrical array, similar constraints apply. In this instance, the sensitivity of the measurement is affected causing the information to be less accurate than *in situ* measurement. These tolerances and the errors induced will be described in this report.

2. PREVIOUS INVESTIGATIONS

2.1 Application of Acoustics

The earliest work in applying reflection acoustical methods began during World War II when the Division of War Research and several Navy research agencies looked into submarine warfare applications. Slant angle measurements at various frequencies and distances provided the first data on the seafloor geological environment. Attention was focused

on two aspects relating wave propagation phenomena and sediments. In the period following the war several investigators (Liebermann, 1948; Urick, 1954; Urick and Saling, 1962; Mackenzie, 1960; McKinney and Anderson, 1964; and Jones et al., 1964) directed their efforts toward identifying the characteristics of sound transmission and reflection. Attention was not given to sediment properties until the mid-1950's, when investigations by Hamilton (1956), Shumway (1960); Sarmiento and Kirby (1962), Richards (1962), and Nafe and Drake (1963) produced much of the deductive theory relating sediment properties to acoustics. Direct measurements made by a ship underway did not begin until the mid-1960's (Breslau, 1964, 1967; Taylor-Smith and Li, 1966; Taylor-Smith, 1968).

Recent work by Pawlowicz (1971) indicates that it is possible, with caution, to describe the porosity of seafloor sediments in terms of reflectivity, Furthermore, the strong correlation which exists between reflectivity and porosity can be used to infer qualitatively, the potential load-bearing properties of the substrate. If a more quantitative description is desired, computer data processing, either in the laboratory or aboard ship, could be used. Pawlowicz suggests that it should be feasible to relate porosity to sediment type in general terms, i.e., high porosity relates to silts and clays, and low porosity to sands and gravels; however, for porosities greater than 55 percent, there is a great overlap in sediment type and precise designations may be inconclusive (Taylor-Smith and Li, 1966; Faas, 1969).

The Mine Defense Laboratory has developed a Sea Bottom Classifier (SBC) which determines the softness of a sea bottom by measuring the elongation of reflected acoustic pulses using a standard depth sounder (Stanley and Harris, 1968). If a short narrow-beam acoustic pulse is transmitted into a hard bottom, the received echo is about the same length as the transmitted pulse. On the other hand, in a soft bottom, the acoustic pulse penetrates the bottoms, and volume reverberation within the bottom causes elongation of the echo pulse proportional to pulse penetration.

Li and Taylor-Smith (1969) believed that by profiling with a repeating broad-band acoustic pulse source over areas where a wedge of sediment was underlain by a strong reflector it should be possible, by

comparing a sub-bottom reflection (and in some cases its associated multiples) to the pulse reflected from the sea-floor and/or to its adjacent reflections, that one could give a reasonable analysis of the bulk properties of the sea-floor medium in terms of variations in the frequency spectrum. The values so obtained from laboratory and *in situ* probe measurements, would thus provide data about the mechanical properties of the sediment.

Sub-bottom profiling devices as conventionally used, no matter how complex, can only provide an assessment of the geology of the sediments, not the sediment types or their properties. While it should be possible to obtain a feeling for the hardness of the sea-floor from observed multiples on a sub-bottom record and, to a certain extent, the material sizes making up the surface shown by scattering or lack of penetration observed on a record. In analysing multiples, few attempts have related the energy decay rate of multiples to varying sediment properties.

Other studies by Li and Taylor-Smith (1966) and Breslau (1965), and Shumway (1960), have also pointed out that frequency analysis of seismic energy reflected from the bottom may provide the information needed to absolutely fix acoustic reflection values to sediment types. Experimental studies by Taylor-Smith and Li (1966 and 1969), and Breslau (1965) have used spectrum analysis measurements utilizing the attenuation factors of various sediment types versus grain sizes with the comparison of the various frequency components of an acoustical source.

Results of work done by McCann (1966) and Buchan et al. (1967) show that attenuation plotted against grain size varies for various frequencies within the low-frequency sound source range (fig. 1). According to McCann (1966), two mechanisms are responsible for the acoustic energy loss in saturated sediments: (1) A solid friction loss for sediments with grain-to-grain contact, this being characterized by a linear variation of the attenuation coefficient with frequency, and (2) a viscous loss caused by interaction between solids and liquids, this being characterized by an attenuation coefficient which is proportional to the square root of the frequency.

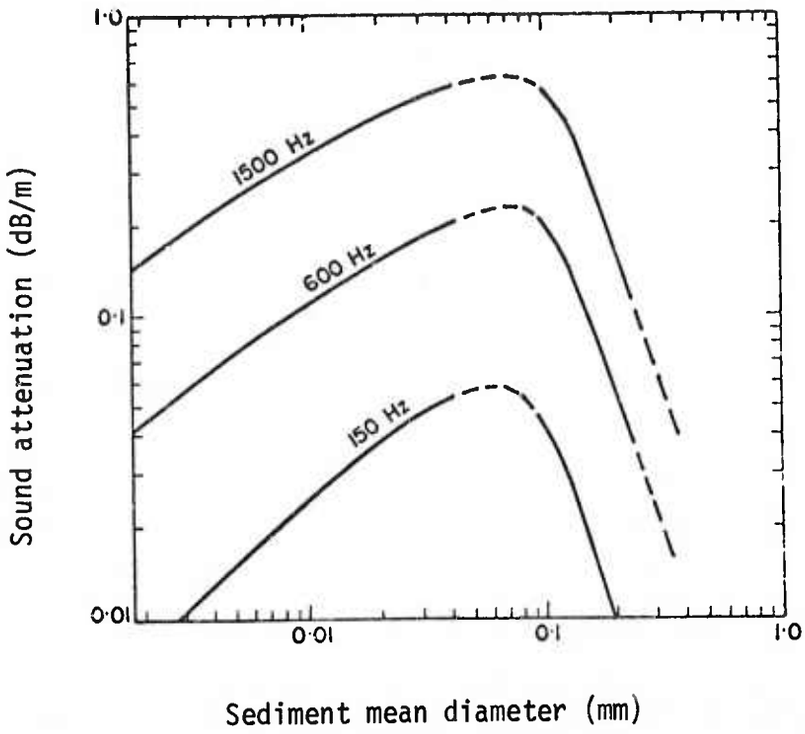

Figure 1. Sound attenuation plotted against mean grain diameter. (McCann, 1966).

Reflection coefficients measured continuously by a ship underway have been made Breslau (1965), Li and Taylor-Smith (1965), and Barnes et al. (1972). These consisted of measuring the amplitudes and/or energy in the transmitted and reflected pulses and correlating attenuation to various bottom sediment properties.

Another way of ascertaining sediment properties is by *in situ* measurement, from which one can obtain direct information on the compressional wave velocity, shear wave velocity, attenuation, and Poisson's ratio. Direct measurement of the shear wave velocity in ocean sediments has been restricted to the seismology of high energy sources that produce returns from the deeply buried material and no returns from the soft superficial sediment. This is because shear waves do not propagate at all in a fluid and, consequently, are transmitted poorly in a saturated porous medium. The shear wave velocity for the saturated sediments of the

sea floor has been determined indirectly through measuring *in situ* the Stoneley wave velocity (Hamilton et al., 1970; Davies, 1965; Jones, 1958; Cohen, 1968; and Bieda, 1970). It has been demonstrated in laboratory experiments that the generation of torsional waves by a viscoelastometer provides information on the shear wave velocity in saturated sediments.

The compressional wave, unlike the transverse (shear) wave, is transmitted readily in water and in saturated sediments. Its velocity in marine sediments has been documented in several reports (Nafe and Drake, 1963; Hamilton, 1970a; Lewis, 1971; Horn et al., 1968). If, in addition to the compressional wave velocity and the shear wave velocity, density is known, one can calculate the dynamic values of rigidity, bulk modulus, Young's modulus, and other elastic constants (Hamilton, 1970a; Nafe and Drake, 1963). Due to the difficulty in measuring the shear wave velocity, the elastic constants have been derived by assuming a value of the sediment bulk modulus from an aggregate theory (Hamilton, 1971; Laughton, 1957; Lewis, 1971).

Other marine sediment properties of interest are porosity, grain size, shear strength, and percent of clay, sand, or silt. Acoustical properties are determined by these physical properties and, thus, have been empirically related to them. The reader is referred to excellent discussions on this subject in Hamilton (1970b, 1971), Horn et al. (1968), Schreiber (1968), and Lewis (1971).

2.2 Application of Electrical Resistivity

Apart from acoustics there has been an appreciable amount of effort devoted to resistivity techniques applied to prediction of porosity in marine sediments.

The earliest marine methods evolved from the application of theory and technology used in land borehole logging to marine investigations, (Bouma et al., 1971; Erchul and Nacci, 1971; Kermabon et al., 1969; Wyllie, 1963). A horizontal array for measuring seafloor resistivity has resulted from this evolution (Corwin and Conti, 1973). For marine use, a horizontal array may be towed over the sea surface or deployed on the seafloor. The

first application provides a fast and convenient method of mapping horizontal changes of average bottom resistivity over large areas. An array deployed in the second manner, however, provides a more detailed picture of the bottom resistivity distribution at a given location.

There has been little previous use of horizontal resistivity arrays on the seafloor. An array of fixed spacing dragged over the seafloor off the coast of Cornwall, England, was used to map lateral changes in seafloor resistivity (Marke, 1965). The fixed electrode spacing used by Marke, however, precluded the acquisition of information about the vertical distribution of bottom resistivity. Schlumberger and Leonardon (1934) used a bottom-deployed array to measure depth to bedrock below seafloor sediments. Dunlap and Johnson (1958) mapped offshore faults and salt domes, also using a fixed array dragged over the seafloor.

The deployment of a surface towed resistivity array in work done by this laboratory is believed to be the first such application using this mode. Several other electrical studies, including self potential, direct current resistivity and electromagnetic sounding have been carried out in this laboratory and are reported in Barnes et al. (1972), Beyer (1972), and Crowin and Conti (1973).

3. THEORY AND TECHNIQUE

3.1 Reflection Coefficient Mapping

A simplified approach to a very complex physical process involving wave propagation, attenuation, and absorption has been used in developing the model of the sea floor-water interface. The sea floor is considered a plane interface between two fluids. Energy is focused on a zone of about one square meter surface area. The backscattering strength associated with this surface area depends greatly on the roughness of the sea bottom. A smooth bottom acts as a mirror such that the reflected energy is concentrated in a specular direction. A rough bottom will reflect the energy more evenly in all directions. It is important to note that the terms "smooth" and "rough" must be considered in relation to the acoustical wave length. Where the wave length is only a few centimeters, it is seen that a 100 percent smooth bottom is rare. Even small

stones, holes or ripples will make the bottom rough in the sense considered here. When a sound wave strikes the sea bottom, part of the incident energy will be reflected. The reflected energy is spread in all directions with a typical distribution, as shown in figure 2. The distribution is totally dependent on the roughness of the sea bottom. Figure 3 illustrates how the roughness of the topography can influence the bottom backscattering strength as a function of the grazing angle. The

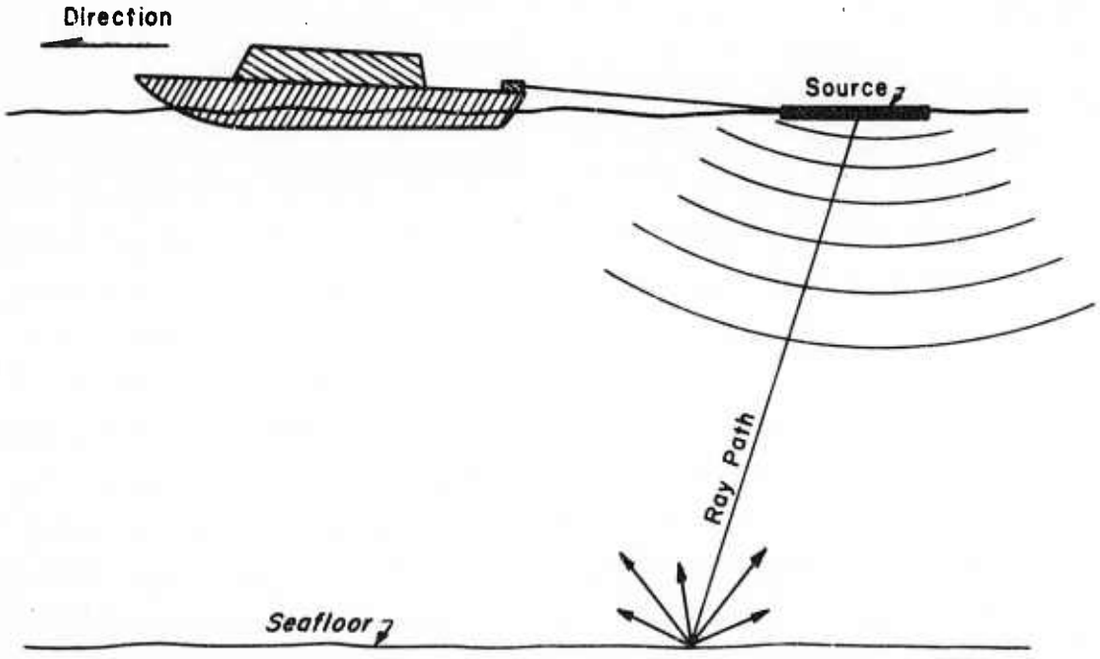

Figure 2. Seafloor scattering – specular energy.

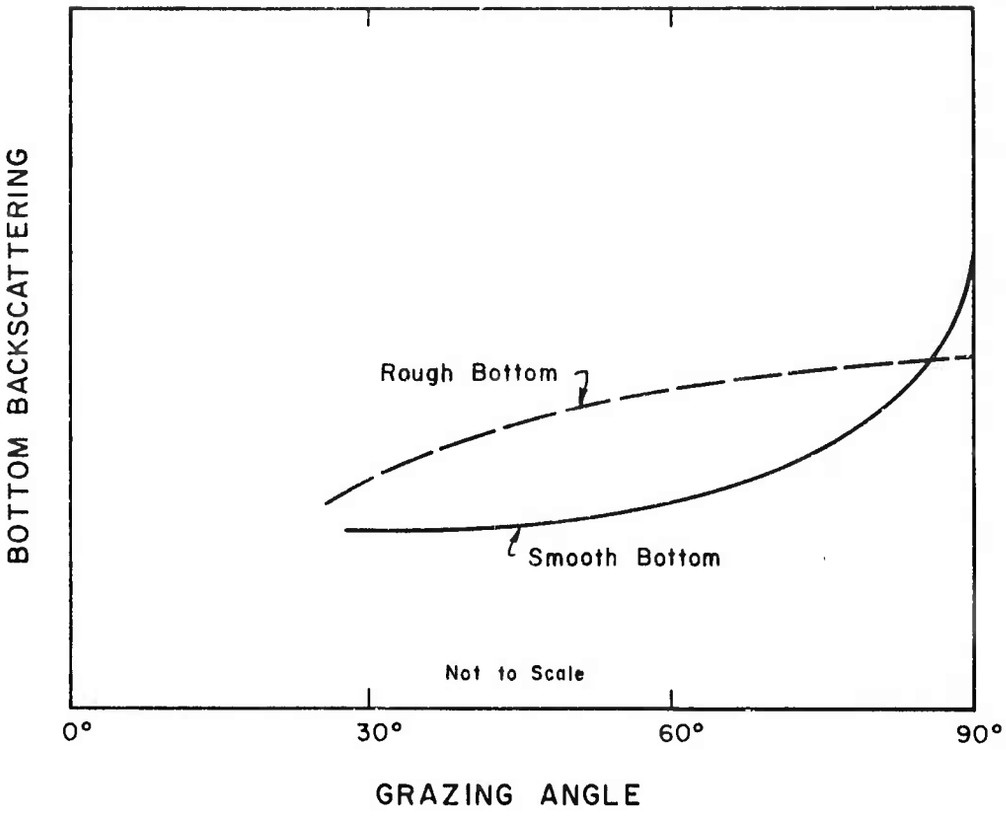

Figure 3. Typical curves for bottom backscattering strength. (After Bodholt, 1969).

angle of incidence is seen to also play an important role in determining the strength of the echo signal. The experiments described in this report were all conducted with the source and receiver set up to record normal incidence. It can be shown that theoretically the most accurate measurements of bottom backscattering strength should be obtained with a narrow beam transducer. If the beam width is 5-10°, the bottom backscattering strength will vary only a few dB or less within the beam, of course

depending on the type of bottom. The magnitude of the bottom sampling area will depend on the pulse length of the transmitted sound. The shorter the pulse the smaller the sampling area. Figure 4 illustrates the beam width, pulse length, and area concept.

In the exercise conducted for this investigation, two sources are employed. One is an uncontrolled beam width emitting a .5 millisecond pulse length and the other is a wide beam (35°) echo sounder having a pulse length of .25 millisecond.

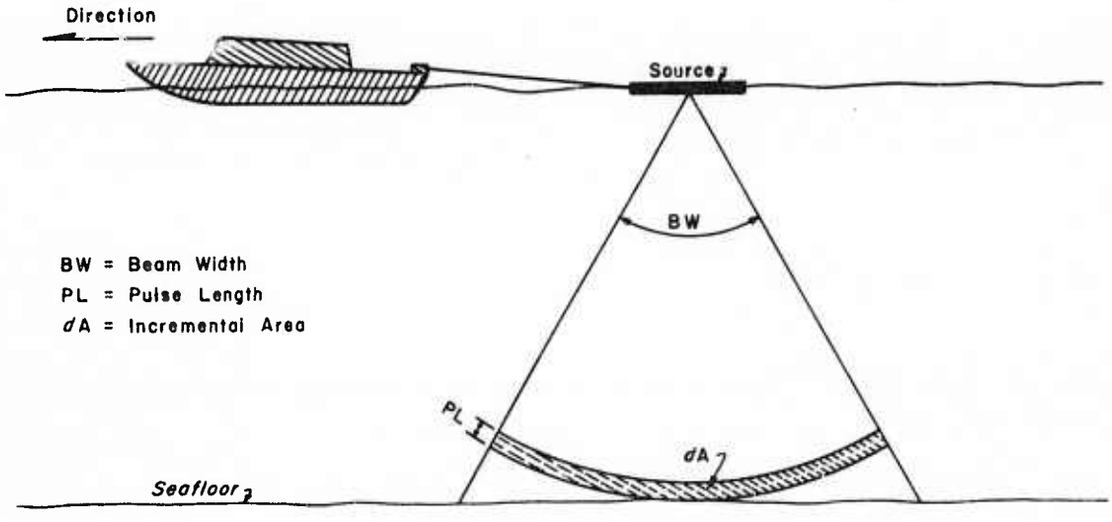

Figure 4. Transmitted sound pulse.

Details of the mathematical description for acoustic wave propagation, reflection and absorption (bottom loss) is contained in a previous report by Barnes et al. (1972). Several references were consulted and the best mathematical expressions relating to the experiments conducted in this investigation were taken from derivations by Breslau (1967).

From the derivations the most useful equations applicable to data reduction and processing are represented by defining the relationship between the fractional loss of intensity at the sea floor, K, and the Rayleigh Reflection Coefficient, R, i.e.,

$$K = R^2 \tag{1}$$

where K is defined on a peak pressure basis,

$$K = \frac{P_{R^2}}{P_{S^2}} (2D)^2 \frac{1}{e^{-\alpha 2D}} \tag{2}$$

where

P_R = pressure of the echo pulse,

P_S = pressure of the source pulse,

D = transmission loss due to spherical spreading, and

$e^{-\alpha 2D}$ = transmission loss due to dissipative attenuation of sound in seawater.

An expression of the fundamental equation for bottom loss, BL, is defined by Breslau (1967) as

$$BL = S_{PL} - E_{PL} - TL_S - TL_A \ , \tag{3}$$

where

BL = bottom loss (in dB) and is equal to -10 log K,

S_{PL} = pressure level of the source pulse (in dB//1 dyne/cm^2) and is equal to 20 log P_S,

E_{PL} = pressure level of the echo pulse (in dB//1 dyne/cm^2) and is equal to 20 log P_R,

TL_S = spreading loss (in dB) and is equal to 20 log 2D,

TL_A = attenuation loss (in dB) and is equal to 10 2D log e.

A final expression relates bottom loss, BL, to reflectivity, R, expressed in decibels;

$$BL = 20 \log R. \qquad (4)$$

Other manifestations of these basic expressions that include measurements dealing with the energy versus time waveform of the echo are described in Breslau (1967). Since this investigation was concerned only with peak pressure measurements, the derivations relating to energy in the echo strength are not included in this discussion.

The computational basis for correcting data related to the field configurations (geometry) of acoustic sources and their respective receivers, as used in the Monterey Bay experiment, are contained in Appendix A-1. The mathematical expressions and constants derived were used in computer analyses and processing of the data (see section 7.1.1).

3.1.1 Relation of Bottom Loss to Mass Physical Properties

The mass characteristics of the bottom sediment are related to bottom loss through the Rayleigh Reflection coefficient and the acoustic impedance contrast at the interface, and it has been shown that the Rayleigh Reflection Coefficient is related to bottom loss through equation (4) (Breslau, 1967). It is possible to establish a relationship between porosity and bottom loss using the impedance which is dependent upon density and compressional velocity, both factors that relate to the porosity of natural sediments (Barnes et al., 1972; Breslau, 1964, 1967).

In summary, several investigations have ascertained that a linear relationship exists between porosity and density, in particular that bottom loss, as deduced from many measurements made on sediments, bears a definite relationship to the porosity of the sediment. And furthermore, since the porosities of natural sediments are somewhat related to sediment grain size, it is also possible to establish a general relationship between bottom loss and the geological properties of sediments.

For further discussion of the sediment bulk properties and variations within the physical makeup of the grains, interstitial properties, etc., and more specifics on how these factors influence porosity, the

reader is directed to the papers by Nafe and Drake (1963), Birch et al. (1942), Hamilton et al. (1956), Shumway (1960), Sutton et al. (1967), Breslau (1964), and Barnes et al. (1972). The information available on this subject is too voluminous to be discussed here.

3.2 In Situ Shear Wave Generation

In an earlier report (Barnes et al., 1972), it was concluded that the best method to generate and directly detect shear waves in saturated marine sediments is by implanting both receivers and a S_H-source into the sediments and by timing the direct S_H-wave. Assuring a large response to the direct S_H-wave, a linear array of horizontal geophones was implanted with the sensitive axis of each geophone parallel to the ground motion of direct S_H-wave. The S_H-source was placed at one end of the geophone array. Theoretically, in a homogeneous half space the first arrival detected by each horizontal geophone will be the direct S_H-wave. The shear wave velocity is, thus, obtained from a time distance graph constructed from the first arrival at each horizontal geophone.

The shear wave source was also employed to generate compressional waves. Little concern was given to the detection of the compressional wave since it is transmitted and detected with little difficulty in saturated sediments. However, it was thought best to implant source and receivers into the sediment. This would avoid the confusion that might exist in differentiations between the direct compressional wave propagating through the sediment and the direct compressional wave propagating through the water.

A linear array of vertical geophones was used to record the arrival time of the direct compressional wave. Theoretically, a vertical geophone will not respond to the direct compressional wave if source and receiver are at the same depth; however, because of the predictable increase in density of natural sediments with depth, the direct P-wave will propagate in an arcuate path and, thus, be detected by a vertically sensitive geophone. The advantage of using a geophone sensitive to vertical displacement instead of a standard omnidirectional geophone or a horizontal geophone is that information on the direct S_V-wave might be obtained

from the vertical geophone. Barnes et al. (1972) describes in detail successful applications of this technique in moist sand and saturated beach sands.

3.2.1 Viscoelastic Model

There remains the question of what model to employ for the sea floor. Recent reports by Hamilton (1970a, 1972) have clarified this problem. From his data and from an extensive literature search, Hamilton (1972) arrived at the following conclusions for a water saturated porous media: (1) for the small stresses produced by sound waves, marine sediments act essentially as a closed system (interstitial water and solids move together); (2) viscosity of the interstitial water is neglible; (3) dispersion of velocity with frequency is insignificant in the frequency range of interest for geophysical studies; (4) Hookean model and the equations of elasticity that follow may be used in most cases to compute the compressional and shear wave velocity; and (5) a linear viscoelastic model with attenuation proportional to frequency and energy damping independent of frequency can be used if wave energy losses are to be considered. These conclusions will not be discussed in great detail except the usefulness of the Hookean model to determine wave velocities.

In geophysical and soil mechanic studies of rocks and minerals, the equations of Hookean elasticity have been shown to adequately define the compressional and shear velocity (Anderson and Liebermann, 1968) (Hardin and Richards, 1963). The widespread use of the elastic model is primarily due to the fact that this model does not provide for wave energy losses and that these losses are small in most materials. To investigate whether saturated marine sediments can be considered as a low-loss material, an appropriate model providing for energy absorption was studied and then compared to the elastic model.

An appropriate anelastic model is to consider the seafloor as a homogeneous, isotropic linear viscoelastic medium. Linear viscoelasticity has been discussed in various forms by Borcherdt (1972), Ferry (1961), White (1965), and others. The basic equations of linear viscoelasticity were derived (Appendix A-2) following the approach by Borcherdt (1972).

A linear viscoelastic model accounts for wave energy losses by replacing the Lamé constants of the Hookean equations with complex Lamé constants. In the expressions for rigidity, $\mu_R + i\mu$, and bulk modulus, $K_R + iK_I$, μ_R and K_R denote the elastic response; and μ_I and K_I denote the damping of wave energy. μ_I, μ_R, K_I and K_R are all real and positive.

Anelasticity can be measured in terms of the dimensionless quantity Q^{-1} (specific attenuation factor). It is defined as the $(2\pi)^{-1}$ times the ratio of the energy dissipated per cycle of forced oscillation to the peak energy stored during the cycle (Borcherdt, 1972, p. 12). The specific attenuation factor in terms of velocity (V), attenuation (a), and circular frequency (ω) is found to be

$$Q^{-1} = \frac{2Va/\omega}{1 - (aV/\omega)^2} \quad . \tag{5}$$

The specific attenuation factor for dilatation, Q_p^{-1}, and shear Q_s^{-1}, are found by substituting the appropriate subscript p or s in equation (5). Note that because velocity is independent of frequency and attenuation is proportional to frequency, Q^{-1} is independent of frequency.

For a low-loss material ($0 < Q^{-1} <, 1$), $aV/\omega << 1$; and therefore, (5) may be approximated by

$$Q^{-1} \quad \frac{2Va}{\omega} \quad . \tag{6}$$

The expressions for the phase velocity of a homogeneous plane compressional wave (V_p) and shear wave (V_s) in a linear viscoelastic medium is given by:

$$V_p = q_p \quad \frac{K_R + \frac{4}{3}\mu_R}{\phi} \tag{7}$$

$$V_s = q_s \quad \frac{\mu_R}{\phi} \tag{8}$$

where ϕ = sediment density

$$q_p = \frac{2(1 + Q_p^{-2})}{1 + Q_p^{-2} + 1} \tag{9}$$

$$q_s = \frac{2(1 + Q_s^{-2})}{1 + Q_s^{-2} + 1} \; . \tag{10}$$

As energy losses become small, Q_p^{-1} (or Q_s^{-1}) $\rightarrow 0$ and q_p (or q_s) approach unity. Thus, (7) and (8) can be simplified to the familiar expressions for velocities in an elastic medium:

$$V_p = \frac{K_R + \frac{4}{3}\mu_R}{\phi} \tag{11}$$

$$V_s = \frac{\mu_R}{\phi} \; . \tag{12}$$

The question remains whether ocean bottom sediment can be classified as a low-loss medium. If so, the low-loss approximations, equations (6), (11), and (12) can be employed to describe wave propagation. Figure 5 illustrates the low-loss error percentages as a function of Q_s^{-1}. Values of Q_s^{-1} ranging from approximately .5 to 2.0 have been reported by Hamilton (1970a, p. 4048) for ocean bottom sediments off San Diego, California [assumption of no absorption in bulk ($K_I = 0$) was used]. Referring to figure 5 and to the viscoelastic equations discussed above, error percentages ranging from 8 to 43 percent can be introduced in determining the velocity of a homogeneous shear wave, and the error percentage for the corresponding absorption coefficient is between 15 and 184 percent. Because these large errors are not permissible, the linear viscoelastic equations are needed in determining the shear wave velocity or Lamé constants.

Hamilton (1972, p. 635) also reports Q_p^{-1} values ranging from 0.002-0.044 for sediments off San Diego. The low-loss approximations, equations (6) and (11) can be used without any significant error.

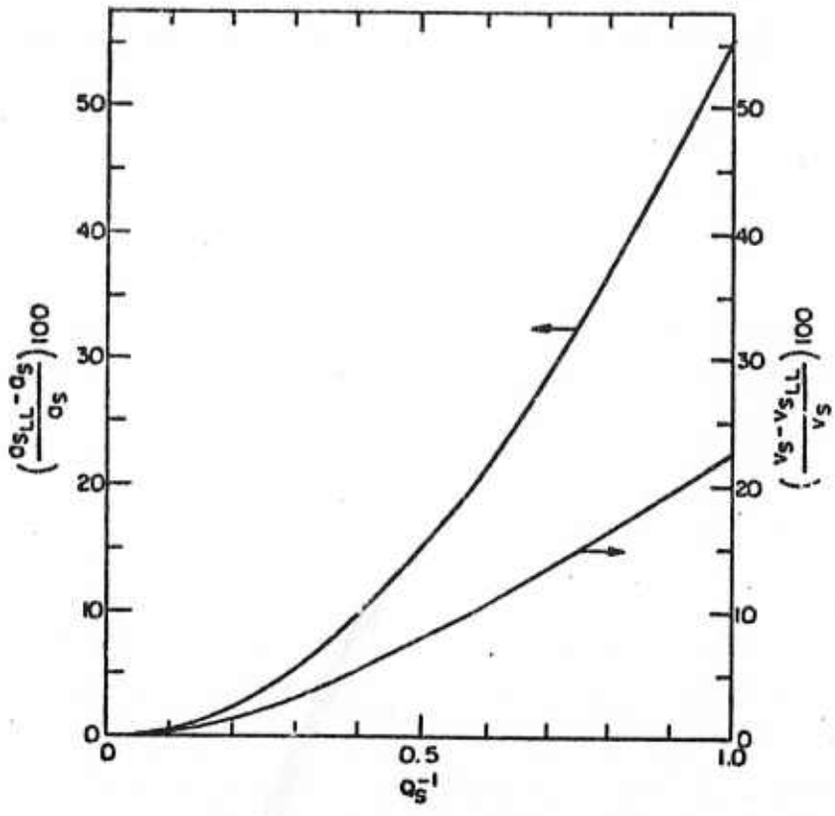

Figure 5. Low-loss error percentages for the velocity and absorption coefficient of a homogeneous shear wave with $0.05 \leq \cdot Q^{-1} \leq 1.0$.

Density, V_p, V_s, a_p, and a_s were measured to calculate Q_s^{-1}, μ_R, μ_I, K_I, K_R, Poisson's Ratio, and Young's modulus. Appendix A-3 lists equations that can be employed to determine various sediment properties from the measured properties.

3.3 Direct Current Resistivity

The electrical resistivity of a geologic material is related to the porosity of the material (Archie, 1942) with low resistivity implying high porosity. Resistivity (ρ) is numerically equal to the electrical resistance between opposite faces of a cube of the material of unit dimensions, and usually is measured in ohm-centimeters (ohm-cm) or ohm-meters (ohm-m) (Grant and West, 1965). As porosity is related to sediment composition

and engineering properties, *in situ* measurement of the vertical variation of the electrical resistivity of marine sediments can provide information about sea-floor structure.

Resistivity techniques are well established on land, and increasing use is being made of them in the offshore environment. Measurements of resistivity and porosity of sea-floor sediments indicate that, except for some highly conductive clays, the formation factor of a marine sediment predicts the porosity of the sediment to within 5 or 10 percent. Formation factor F is defined by the equation:

$$F = \frac{\rho_s}{\rho_\omega} \quad , \tag{13}$$

where ρ_s is the resistivity of the sediment and ρ_ω is the resistivity of the overlying water. Figure 6 summarizes some of these measurements. Measurement of the vertical resistivity distribution of the sea floor, therefore, provides a method of determining sub-bottom porosity, and thus geologic and engineering properties.

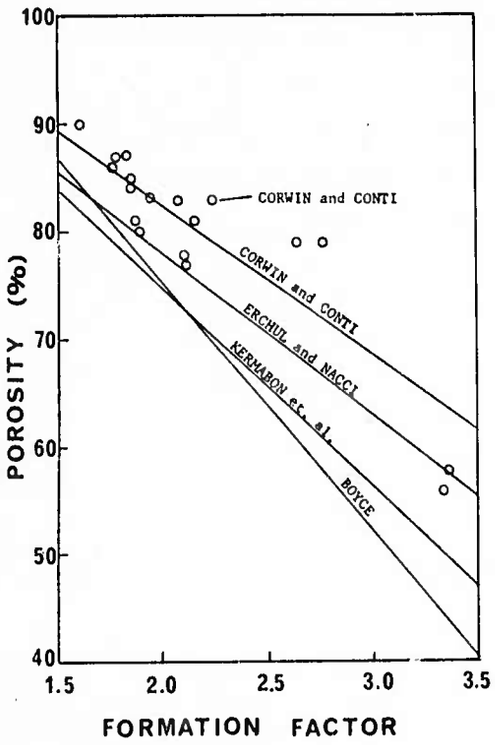

Figure 6. Porosity vs formation factor for marine sediments.

Resistivity is measured on land by borehole logging, or by the use of an expanding horizontal surface array. In boreholes, a small probe lowered into the hole provides a continuous record of the resistivity of the material surrounding the probe (Wyllie, 1963). This method has been adapted successfully to marine use by forcing a thin probe into the sea-floor sediments (Bouma et al., 1971; Erchul and Nacci, 1971; Kermabon et al., 1969), as shown schematically in figure 7. The use of a logging probe in marine sediments gives a relatively precise determination of resistivity as a function of depth, but does offer some drawbacks. The depth of measurement is limited to the depth to which the probe can be inserted into the sea floor, which may be small where sediment porosity is low. The

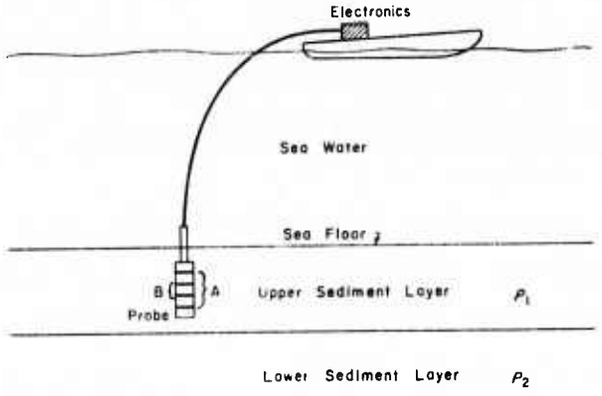

Current I is fed into the sediments through current electrodes A, and causes a voltage ΔV to appear between potential electrodes B. Sediment resistivity ρ is then determined from the formula

$$\rho = K \frac{\Delta V}{I}$$

where K is a factor depending on the geometry of the electrode arrangement.

Figure 7. Well logging probe used to measure resistivity of marine sediments.

volume of bottom material sampled is relatively small for a single insertion of the probe, so interpretation errors may result if the sampled point is not representative of the surrounding area.

Surface-deployed horizontal arrays also are used to measure vertical resistivity profiles on land (Grant and West, 1965; Van Nostrand and Cook, 1966). As shown in figure 8, this method employes two current electrodes to feed low-frequency, commutated direct current into the ground, and two (or more) potential electrodes to measure the potential difference generated at the surface of the earth by the impressed current flow. The potential difference is a function of the electrode configuration and spacing, and of the subsurface resistivity distribution.

For the equispaced Wenner array, shown in figure 8, the "apparent resistivity", ρ_a, of the earth is given by the formula (Van Nostrand and Cook, 1966)

$$\rho_a = 2\pi a \frac{\Delta V}{I} \quad , \tag{14}$$

where

ρ_a = apparent resistivity,
a = electrode spacing,
ΔV = measured potential difference, and
I = impressed current.

By expanding the array, the current is forced to flow deeply into the earth, and the apparent resistivity at larger electrode spacings is indicative of the material at greater depth. The field data is interpreted by plotting measured apparent resistivity ρ_a against electrode separation a, and matching these curves with those contained in standard catalogs of published curves (Mooney and Wetzel, 1956), as shown in figure 9.

The use of an expanding horizontal array for sea-floor resistivity measurements (fig. 10) offers a number of advantages over the use of a probe. The depth below the sea floor to which information may be obtained is limited only by the size of the array and the amount of current available, and the measuring process does not disturb the sediments. Also, it is a simpler operation to deploy an electrode array on the bottom than to

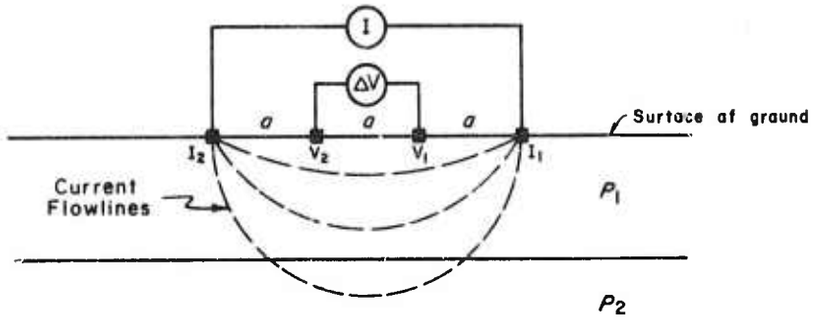

A) Small Separation *a*.

V_1 and V_2 are potential electrodes
I_1 and I_2 are current electrodes

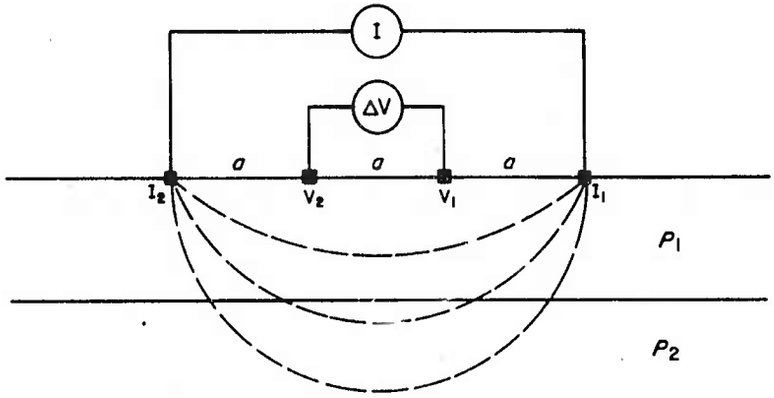

B) Large Separation *a*.

Current I is fed into the ground through the current electrodes I_1 and I_2, creating a potential field on the surface of the ground. The voltage difference, ΔV, between the potential electrodes V_1 and V_2 is a function of the resistivity of the ground below the electrodes. The apparent resistivity of the ground, P_a, is close to P_1 when the separation *a* is small, and approaches P_2 as *a* becomes very large.

Figure 8. Wenner resistivity array.

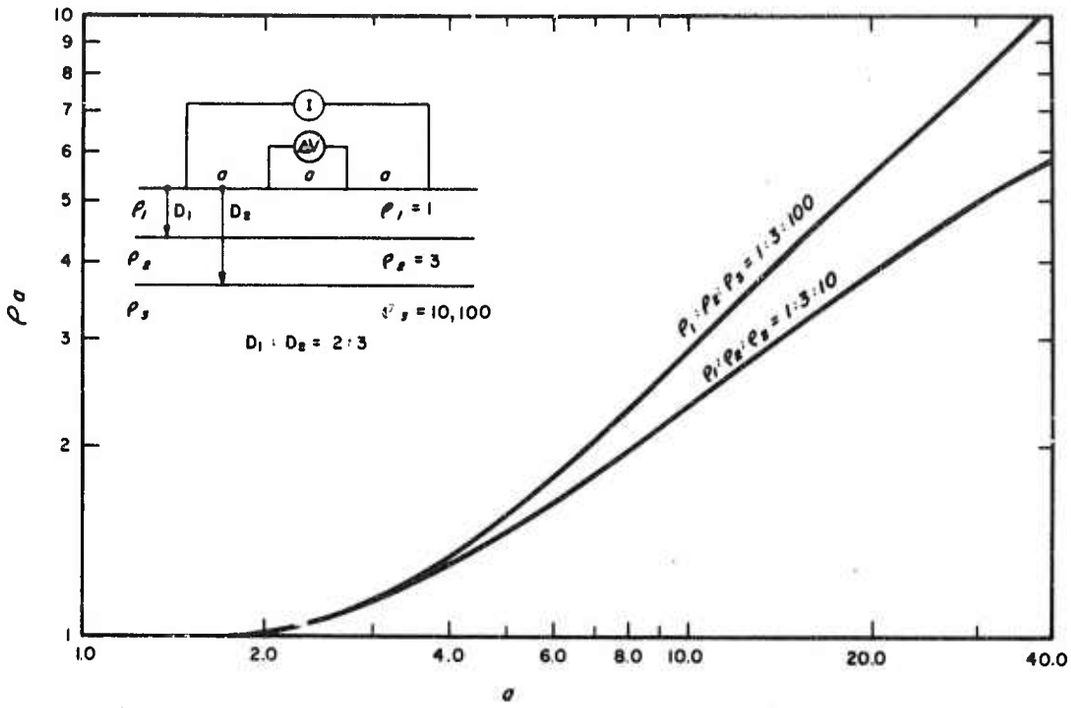

Figure 9. Standard Wenner resistivity curves (after Mooney and Wetzel, 1956).

drive a probe into the sea floor, and a larger volume of material is sampled at each data point. On the other hand, a probe gives a more precise determination of resistivity and structure at a given point. Also, data interpretation is easier and more accurate with a probe because there is no need to match curves to obtain the resistivity-depth relationship from the field data. The probe and horizontal array methods, then, are complimentary, with the probe offering greater precision, and the horizontal array greater penetration and convenience and less sediment disturbance.

For marine use, a horizontal array may be towed over the sea surface or deployed on the sea floor (fig. 11). A surface-towed array provides a fast and convenient method of mapping horizontal changes of average bottom resistivity over large areas. An array deployed on the sea floor, however, provides a more detailed picture of the bottom resistivity distribution at a given location. Both surface-towed and bottom-deployed arrays were tested for this study.

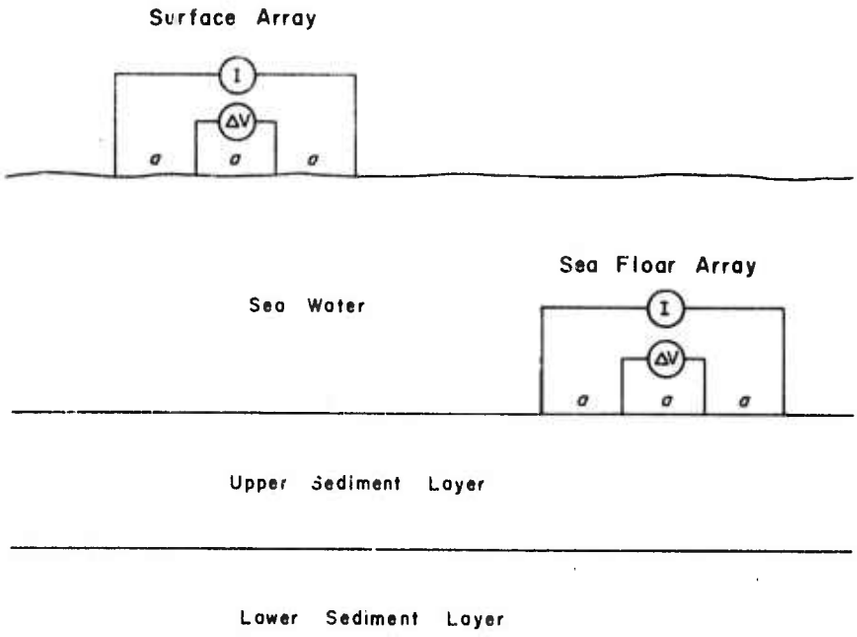

Figure 10. Surface and seafloor resistivity arrays.

4. ELECTRONIC SYSTEMS AND EQUIPMENT

4.1 Reflection Coefficient Mapping Experiment

4.1.1 Acoustic Sources

The types of sources to be used for predicting the geology of the seafloor and its substructure vary depending on the type of sediments and and the problem being examined. For reflectivity measurements it is desirable to cover a broad spectrum containing varying energy levels, band width, pulse width, and beam concentration.

A) Array at Surface.

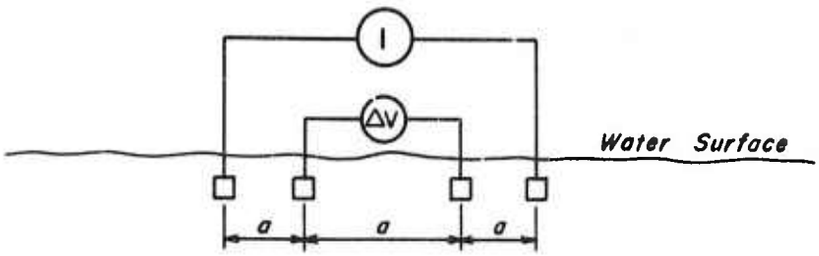

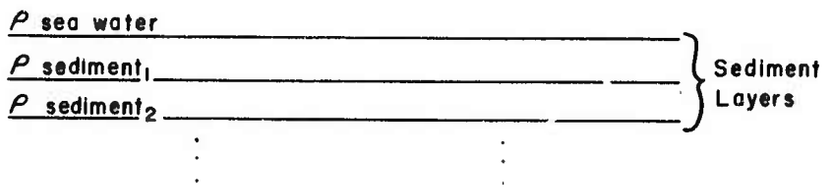

ΔV is relatively insensitive to sediment resistivity.

B) Array on Sea Floor.

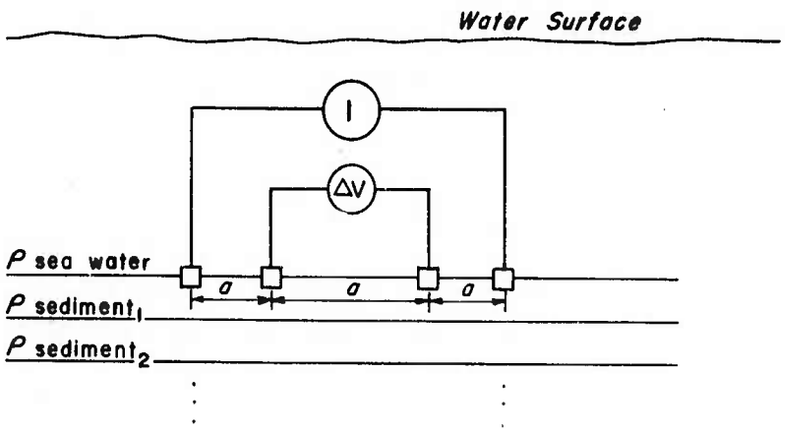

Measurement of ΔV as a function of *a* could resolve thin sediment layers.

Figure 11. Marine resistivity arrays.

In standard sub-bottom profiling techniques, the aim is to get the highest energy level possible in a pulse of fairly short duration. While these requirements are not entirely divorced from frequency considerations, frequency enters into the argument mainly in terms of both discrimination and penetration. It is a common belief that for discrimination a high frequency is needed, while for penetration the converse is true; in fact some sub-bottom profilers now commercially available are designed to operate with a fixed frequency pattern to achieve a desired combination of penetration and discrimination. In general this is a misapplied conception, particularly if one desires to consider application to solving geotechnical problems. A seismic pulse should have a short time duration for resolution and a large energy content to combat noise. Multi-channel stacking is one way of achieving an effective increase in signal energy relative to uncorrelated noise for a given pulse width. Hutchins (1969), accomplished the same effect by using a large time-bandwidth (TW) product signal. The idea behind this appraoch is to generate a long duration signal having a bandwidth appropriate for the required resolution, to obtain more signal energy, and then to effectively time compress the reflected signals by matched filter detection. Such a signal can be band limited random noise, frequency modulated chirp or any other sufficiently complicated sequence. This concept has been applied in transmitting large TW signals used in radar and sonar to get maximum information from a single transmitted pulse. This is clearly necessary when targets are moving and probably taking evasive action.

When using seismic methods to map subsurface geologic structures buried beneath the ocean floor, it is often desirable to be able to control the energy versus frequency spectrum of the sonic pulse (Caulfield, 1962). Sediments have attenuation factors that are frequency dependent (Shumway, 1960). As greater penetration is required, lower frequencies must be used. Since the ability of a sonic system to resolve range differences depends on the wave lengths being employed, it follows there will be some pulse spectrum that provides the best compromise between penetration and resolution.

In this investigation, a discrete frequency wide-beam transducer operating at 12 kHz was selected to obtain a correlation with the values obtained by Breslau (1964), and a broadband multiple-electrode sparker source was tested as an alternate approach using a low frequency, omnidirectional beam.

Pawlowicz (1971) noted the principal differences between the continuous reflection profiling systems and those systems used for echo-sounding of water depth are the requirements of high acoustic power output and, generally, lower frequency. Although penetrations of 90 ft into the seafloor have been obtained with frequencies as high as 14 kHz (Murray, 1967), lower frequencies are more commonly used. A lower limit to the frequency used is set by the resolution desired -- layers thinner than one half the wavelength generally cannot be resolved clearly. Pulse duration is another important factor and must be short for good resolution. In general,

$$2d = v\Delta t, \tag{15}$$

where

d = distance between reflecting layers (m),

v = velocity of sound in water (1500 m/sec), and

Δt = difference between arrival times of the reflected wave fronts.

Thus, when the pulse length becomes comparable with the time of $2d/v$ sec, the two layers may not be resolved.

Each type of reflection equipment, which differs principally in the type of energy source utilized, has its own uses. For a comprehensive discussion of subbottom systems, see Schlank (1968). Briefly, a transducer system operating at frequencies of 1.5 to 12 kHz can show, under favorable circumstances (shallow water, silt and clay sediments), a subbottom structure to depths of 50 m, although penetration of 20 m is more common. This penetration is more than adequate to satisfy the objectives for determining surface sediment properties as done in this investigation.

Problems with fixed frequencies and various sediment types are as those noted by Moore and Kulm (1970), who describe a particular case:

> "No sub-bottom information was obtained with the 3.5 kHz profiler on the Oregon continental shelf. Cores taken off Oregon indicate that thick sand layers cover

> much of the continental shelf and are overlain by only a thin layer of mud (a few cm thick) on the middle and outer shelf. Apparently the signal strength of the 3.5 kHz system is not sufficient to penetrate these sandy deposits."

Our experience with 3.5 kHz, 4.5 kHz, and 12 kHz sources also show little or no penetration in similar sediment even at the shallow depths of area surveyed.

Discounting the need for subsurface structural data and considering only the surface one can say that for reflectivity measurements involving the sea-floor surface material only, it seems that any sound source may be used as long as the measurement of the pulses is proper for the sound source being used; however, for sub-bottom observations it appears that basically a low-frequency with broad-band characteristics is needed to allow both penetration and resolution of the sub-bottom layers. Regarding the high frequency sources (> 4 kHz), it has been acknowledged that standard echo-sounders can offer simple tools for the geologist to use, and with careful interpretation can provide a wealth of data impossible to obtain as simply by any other means. Any conclusion as to the presence of a certain sediment type should only be made after confirming evidence, such as by cores, grab samples, or photographs examined. The experiments conducted in this study, and in previous work (Barnes et al., 1972) with the 12 kHz and 41 kHz sources tend to corroborate this.

Two sources were used in the reflection coefficient mapping experiment described in this report. They consist of a standard 12 kHz transducer and a Directional Multi-Electrode Sparker Sound Source (DMSS) designed and built in this laboratory, and described in Barnes et al. (1972) and by Poston (1972). The two sources were used simultaneously in tests. The 12 kHz pinger transducer produced a pulse length of 1,625 m/sec, and the multi-electrode sparker sound source transmitted a nominal pulse length ranging from .3 to .5 m/sec. The higher frequency source was discrete in bandwidth, but the low frequency source was composed of a nominal 2.5 kHz center frequency with a broad-band width with frequencies ranging from 0 to 5 kHz.

Ten of the twenty-five available electrodes on the DMSS sparker were used during the experiment (fig. 12). This number was selected after extensive testing of impulse output versus bubble pulse output for various numbers of grouped electrodes. For this experiment, 300 joules or 800 joules of output could be selected at the capacitor bank. 800 joules was used during the experiment. Several modifications to the previous system, described in Barnes et al. (1972), have been incorporated in this work. The sparker is mounted on a surface towed vehicle fabricated from a metal frame and 2 surfboards (fig. 13). Adjustment of the mounting bracket and DMSS unit makes it possible to orient the electrodes vertically downward into the water or upward toward the air/sea interface. An upward orientation proved better, since there was less bubble pulse and therefore less ambient noise interference. Vertical adjustment

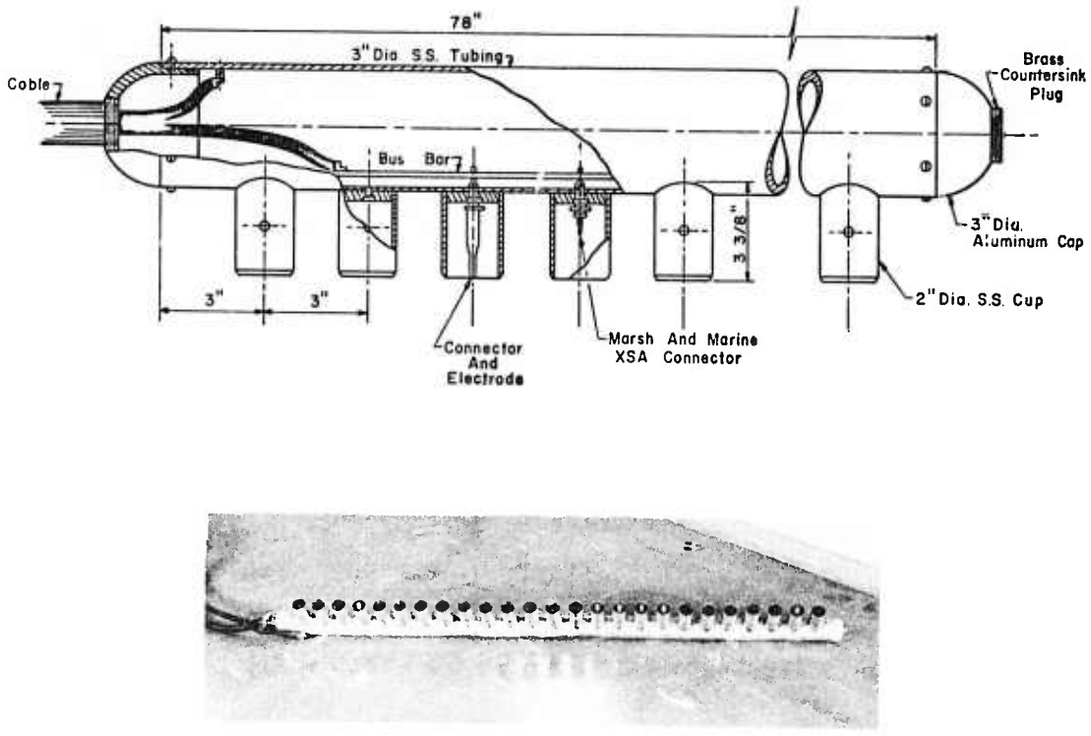

Figure 12. Directional Multiple Electrode Sound Source (DMSS).

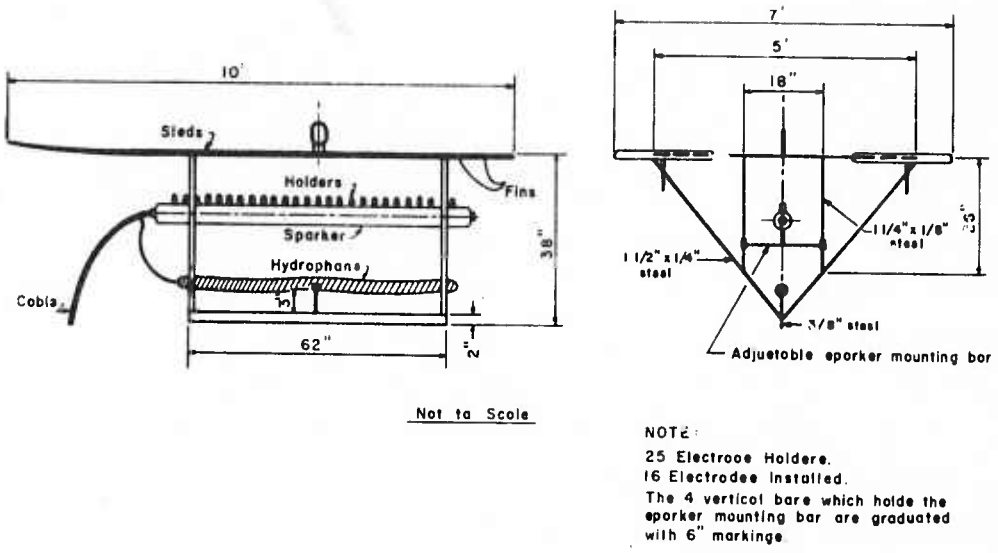

Figure 13. DMSS Unit and Impulse Hydrophone Receiver — Tow Configuration.

of the source also enabled the position of the sparker to be varied relative to depth below the water surface. Tests conducted on various other seismic sources (i.e., the Uni Boom, the 3-electrode sparker manufactured by Egerton Germershausen and Grier, Inc., and a 12 kHz transducer manufactured by Ocean Sonics, Inc.) and other non spark-type discharge sources in this geometrical configuration indicated that the quality of the transmitted pulse could be improved if the source was moved closer to the water surface. This modification in geometry differs from the position used in the previous experiment conducted by Barnes et al. (1972). A marked improvement in the quality of seismic subbottom profiles was noted when the position of the electrode tips was set at about 10 inches below the water surface. In most instances, it was discovered that much more information could be obtained from the broadband frequency source. The

essential requirements of any acoustic source employed for reflection coefficient mapping is that it should provide a broad frequency band acoustic pulse and be capable of analysing any changes produced in this pulse by the effect of the various bottom and sub-bottom reflectors.

Tests of the broad band multi-electrode sparker revealed much the same results as obtained by Li and Taylor-Smith (1969). Their comments about experimenting with a multi-electrode sparker, were, "as the number of sparks in parallel increased so did the efficiency of producing acoustic energy." In the tests conducted by this laboratory, the energy peaked and then decreased after the number of electrodes was increased at a given power level. Also, the duration of the bubble forming period and pulse length decreased, leading to a greater concentration of energy in the higher frequencies. The pulse length and frequency content was also found to be dependent on the spark gap distance. The DMSS gap was normally held constant, except when the electrodes burned too short and arced to the base of the sparker unit, producing a higher frequency output.

The two sources were used simultaneously and were triggered at a 1 sec rate by the recorder. The time base stability of the recorder is specified to be 10 parts per million. It was intended that the 12 kHz pinger source be triggered at a .25 sec rate and the sparker at a 1 sec rate with the use of an external countdown circuit and relay to trigger the capacitor bank, but the triggering operation was too erratic. The addition of a separate power supply and a one-shot multivibration circuit did not produce good results. After many trials the problem was found in the trigger circuit of the recorder. Random pulses caused the two sources to be triggered out of synchronization. A preliminary study of the repetition rate was done on the first tapes made, and it was discovered that a steady rate of 1 sec repetition was more desirable for computer processing efficiency.

4.1.2 Hydrophone Receivers

There were three hydrophones used in conjunction with the sparker signal. The hydrophones monitored the transmitted and reflected signals.

The sled-mounted hydrophone were used to receive the transmitted impulses from the sparker. The two return impulse hydrophones used during the experiment were the streamer hydrophone and a second sled-mounted hydrophone, not shown in figure 13. The receiver hydrophones were identical in electronics, but of different lengths. The streamer hydrophone was approximately 11 ft long with a fluid filled section of 10 ft, 8½ in. The sled-mounted hydrophone was approximately 6 ft long with a fluid filled section of 62 in. The hydrophones including the impulse unit measured 1-5/8 in in diameter. Six hydrophone elements make up each of the streamers. These are wired in parallel to a preamplifier and analog recording devices. The six hydrophone elements are summed for a gain of 15.6 dB, which, added to the basic hydrophone element sensitivity of 96 dB/u/ubar, yields a basic hydrophone sensitivity of 60.4 dB/u/ubar. The hydrophone arrays were calibrated using a Massa Model 115C calibrated hydrophone and a Navy J-9 sound projector. The measured test values were -60.5 dB/u/ubar.

The sled mounted return impulse hydrophone did not produce useable data during the test due to excessive ringing and noise, so all the processed data was obtained from the streamer hydrophone. Various attempts were made to remedy the problem, including the use of a less sensitive hydrophone, but this resulted in insufficient amplitude to tape the return signal.

All three hydrophones are connected to the same amplifier chassis; however, each hydrophone has its separate amplifier circuit and amplitude control. The streamer and return impulse hydrophone signals were at unity gain, the only amplifier being the preamplifier in the hydrophone array. The average effective dynamic range of the hydrophone is 35.4 dB. The low-end sensitivity is limited by the towing noise observed on the records. The nominal operating dynamic range is 66 dB when the low end sensitivity is limited only by ambient noise generated by the electronics. The streamer hydrophone output was also connected to the Ocean Sonics recorder through the rack mounted amplifier which has a gain of 67 or 37 dB.

The location and position of the monitoring hydrophones was also improved by modification of the tow vehicle. A more sensitive receiver hydrophone was installed in addition to the standard unit used in previous

experiments (Barnes et al., 1972). The receiving and impulse hydrophones were placed 27 in and 32 in below the water surface, respectively.

In conjunction with the sparker, an EDO Type 324 (AT/200 A-UQN) transducer array using A.D.P. type crystals was used. The 12 kHz transducer, referred to as the pinger source, was driven by an Ocean Sonics Model GDR-T precision depth recorder. The transmitted pulse is rated at 600 w peak power into the rated 130 ohm load of the transducer, which yields an acoustical power output of 110 dB/v at one yard. The transducer has a beam angle of 35° on the frontal plane. The receiving response is -72 dB/v at one yard (EDO Western Corp.).

The pinger is mounted on the end of a two in diameter pipe which slides up and down in a socket at the end of an A-frame on the port side of the boat. The pipe is locked into position (fig. 14). The depth of the transducer was set at 1.8 ft below the water surface. The distance from the side of the boat to the center of the pinger was 29 in, and the distance from the center of the pinger to the stern was 16½ ft. This location was picked because of the wake characteristics of the boat and convenience of mounting. The A-frame was mounted to the deck with pillow blocks, allowing the transducer to be raised up and inboard, out of the way for portside docking and fast running.

4.1.3 Transmission Measurements

During field tests, the transmission impulses and return impulses were constantly monitored on an oscilloscope. The pulses were visually compared to one another for the reflection measurement and to observe signal/noise ratios. This monitoring is very important since the amplitude of the return pulse is dependent upon: (1) The transmitted amplitude of the acoustic source; (2) the path length of the sound signal to and from the reflecting sea-floor; and (3) the reflecting properties of the sea-floor.

Because the amount of sound energy received is dependent on the amount of energy transmitted, and most echo sounders have no method of displaying the relative energy levels, one cannot assume that the transmitted energy is constant. A variation in the power supply voltage, for

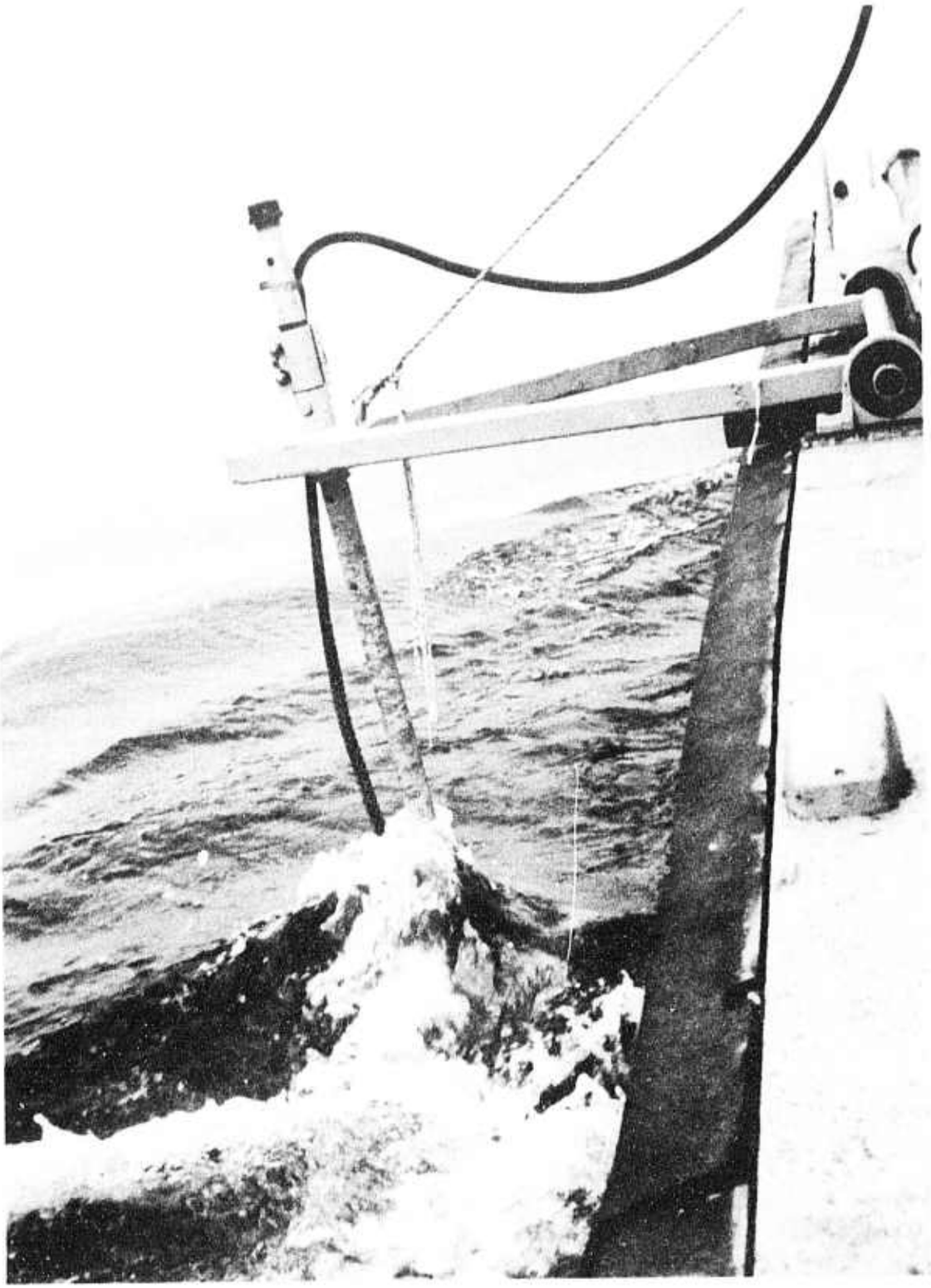

Figure 14. 12 kHz source – tow configuration.

instance, can cause a considerable variation in the electrical power supplied to the transducer. Also, relationships existing between the physical properties of the transducer and those of the surrounding water, such as salinity will affect the output acoustic power even if the electrical power is constant. This is especially true of a sparker device. This has been calculated by Caulfield (1962, p. 342), i.e.,

$$E_{Total} = R_{sp} \frac{B^2}{2b} \frac{(k^2)}{(b^2-k^2)}, \qquad (16)$$

where

E_{Total} = Total energy to spark,

R_{sp} = spark resistance,

B^2 = V_0^2/L^2K^2,

b = $R/2L$,

k = $(R^2/4L^2 - 1/LC)^{\frac{1}{2}}$,

R = Total resistance,

L = Total inductance, and

C = Total storage capacitance.

Equation (16) describes what occurs in the electrical circuit. For example, the spark resistance (R_{sp}) can be affected by the salinity of the water, which can vary from 3.9 mho/cm for a 2 percent salinity solution to 43.9 mho/cm for a 35 percent salinity solution.

If one desires to know acoustical pressure, the equation approximating the first pressure pulse as a function of time is,

$$p = p_0 e^{-mt} \qquad (17)$$

where

p = pressure (dyne/cm^2),

p_0 = peak pressure (dyne/cm^3 at 1 meter),

m = decay constant (determined by experiment), and

t = time.

Then the acoustic energy is expressed as

$$E(t) = \frac{1}{pc} \int_0^\infty 1f(+)1^2 \, dt, \tag{18}$$

where

$f(t) = p_0 e^{-mt}$,

p = density (g/cm^3),

c = velocity of propagation in the medium, and

m = decay constant (determined by experiment).

Caulfield's formula can be correlated to Breslau's (1967, p. 2) formula in terms of peak pressure, i.e.,

$$\int_0^T P_s^2 \, dt = P_s^2 \, (RMS) \, \tau \tag{19}$$

where

P_s = pressure of the source pulse,

τ = duration of the outgoing pulse, and

T = time.

The formula used to obtain the values of the Rayleigh Reflection Coefficient from the digitized values of $V_{SR} + V_{SX}$ may be expressed as;

$$R = .008 \, (4d^2 + 832)^{\frac{1}{2}} \, \frac{V_{SR}}{V_{SX}} \tag{20}$$

(see Appendix A-1),

where

R = Rayleigh Reflection Coefficient,

d = water depth,

V_{SR} = sparker return impulse voltage, and

V_{SX} = sparker transmitted impulse voltage.

The 12 kHz pinger transducer transmitted output was also constantly monitored during field operations. The voltage applied to the transducer was monitored on an oscilloscope while being recorded on an analog magnetic tape recorder. A fixed resistive attenuator network to reduce the high transmitted voltage to a lower voltage was necessary to make the recording level suitable for input to the tape recorder. The return impulse voltage was amplified by the internal amplifier of the recorder, (section 4.1.2) and then connected to the magnetic tape recorder.

Many problems were encountered in calibrating the pinger transducer due to the small physical size of the tanks available for calibration use in the laboratory, and the large amplitude of the transmitted signal. Proper interrogation of the pulse to be used for the computation of the reflection coefficient was threefore difficult. Problems were encountered in obtaining repetitive measurements using a calibrated hydrophone and a sound source in the laboratory tanks. The calibrating hydrophone and source are linear devices, and the pinger transducer is a tuned, or non-linear device; the ratio of the transmitted to received voltages of the transducer itself could have been used to obtain an absolute calibration value, but physical limitations of calibrating in the tank resulted in relying on manufacturer's specifications. Data for obtaining absolute values of the reflection coefficient were taken from the manufacturer's calibration specifications.

Output variations based on reflectivity measurements have been observed by others employing various kinds of sources. Li and Taylor-Smith (1969, pp. 244, 245) noted intensity fluctuations using a sparker source. In their examination of the intensities of sound returned to the surface, both from bottom and sub-bottom reflections, it was thought that the loss in intensity might be attributed to a large number of factors, of which absorption in the medium is only one. They go on to say that, the effect of the unwanted losses may be reduced from a statistical point of view, by a procedure used in spectral analysis, in so doing, it is essential that each set of pulses analysed is taken from single individual transmissions. However, even with this procedure, a fluctuation in the intensity of the reflection can be caused both by the irregularity of the reflecting

boundaries and by the irregular structural pattern of the medium between the bottom and sub-bottom. The effect is mainly one of random scattering, although interference effects probably play an important part as well. Such fluctuations in intensity may be of diagnostic value.

A statistical study of various reflected signals shows that the observed fluctuations appear to correlate with the state of roughness of the reflector (section 3.1, fig. 3). Li and Taylor-Smith (1969) found that, the standard deviation of the intensity fluctuations, expressed as a percentage of the mean peak to peak amplitude, for the signal transmitted directly through the water from a 3-electrode spark is about 4 percent, whereas the figure obtained for a reflection from a sand-covered floor is about 10 percent and from a clay-covered floor 5 percent. While these are isolated results from which general conclusions cannot be drawn, it is certain that scattering due to boundary roughness is an important factor in signal fluctuations. In fact, this property is employed in the attempt to use the oblique asdic (or sideways-looking sonar) to define the sedimentary state of the sea-floor (Chesterman et al., 1967).

Intensity fluctuations were also noted by Porter and Bell (1972) in their reflection studies with 3.5 kHz and 5 kHz electromechanical transducers. A bottom variation of ± 0.85 dB was noted in this experiment, which was conducted with the source mounted in a rigid frame on the bottom of an inland body of water. They found that "the magnitude of the observed variations differed significantly and exceeded the values calculated for the component attributable to source-receiver motion," and "concluded that other error sources such as changes in incident angle and undetected spatial variability in sediment composition exist." They did note that a reduced degree of variability was exhibited in the narrow-band data, which they attributed to an inherently higher signal-to-noise ratio.

4.1.4 Data Acquisition and Display

The shipboard recording equipment consists of a rack-mounted Ampex SP-300, 7-channel magnetic tape recorder. The inputs to the seven

channels are:

Channel 1: Pinger transmitted voltage (fig. 15a)

Channel 2: Sparker received impulse (Streamer Hydrophone) (fig. 16a)

Channel 3: Pinger received impulse (fig. 15b)

Channel 4: Voice

Channel 5: Sparker transmitted impulse (fig. 16b)

Channel 6: Time Code, IRIG B

Channel 7: Sparker received impulse (sled hydrophone).

An Ocean Sonics Series GDR-T precision Sonar recorder and transceiver was used as a visual recorder for the subbottom profile record (fig. 17). The recorder was modified to allow the presentation of either the 12 kHz pinger or the 0.5 kHz sparker seismic returns. The recorder unit also houses the energy source for the 12 kHz pinger transudcer. The output voltage of the transmitter in the recorder to a 35 dB attenuator network to reduce the output voltage to a suitable taping level.

The recorder is also modified so that the amplified output of the received pinger impulse is connected to the tape recorder. The amplifier gain can be changed from a setting of X1, which produced a measured gain of 50, to a setting of X50, which produced a measured gain of 920. Electrical cables from the streamer, and sled-mounted amplifier. The output of the streamer hydrophone was fed from the hydrophone preamplifier to the tape recorder. The streamer hydrophone output was also connected to a Khron-Hite Model 3200 Variable High or Low Pass electronic filter and then to the main hydrophone amplifier. This amplified output was connected to the Ocean Sonics recorder to observe the 2.5 kHz sparker subbottom information. The output from the receiver hydrophone was fed through an attenuator network to the tape recorder. During the survey the attenuation was set at unity. The sparker impulse hydrophone output was fed through an amplifier to the tape recorder. Throughout the survey the amplifier gain was set at unity. The voice channel was used to note the same events noted in the tape roll logs. The time reference for the magnetic tape record was obtained from an IRIG B Time Code generator. The generator and the digital clock used in the navigation system were

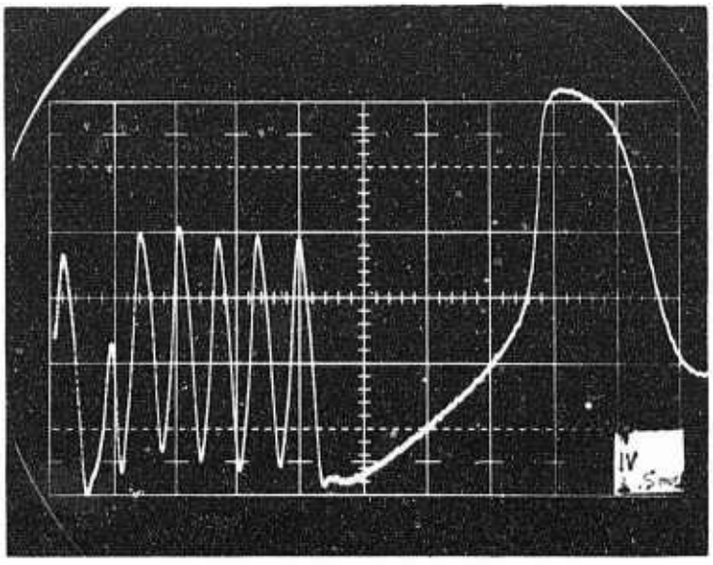

a. 12 kHz transmitted signal.

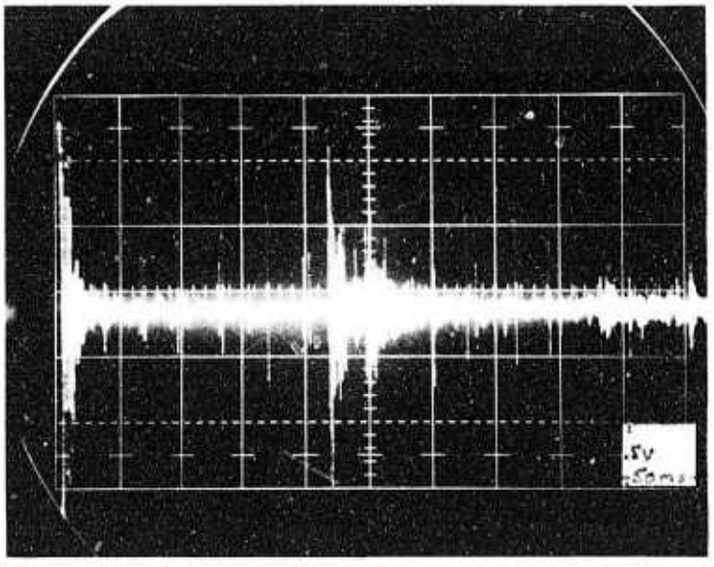

b. 12 kHz received signal.

Figure 15. Pinger (12 kHz) signal wave forms.

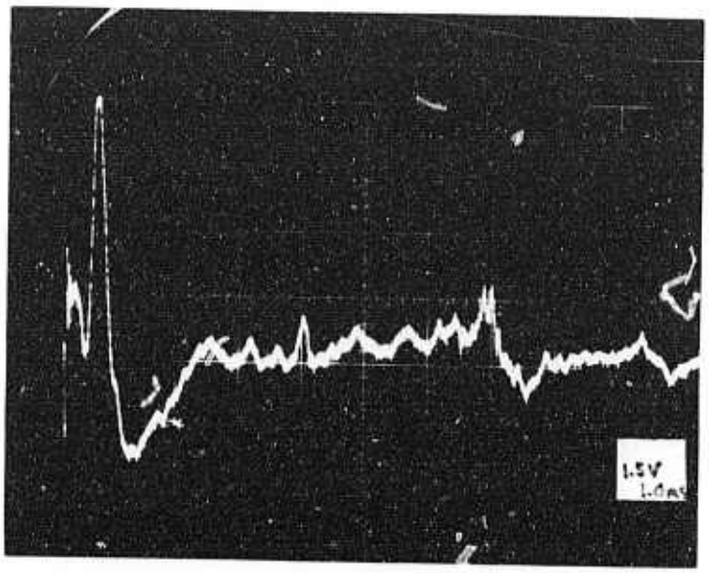

a. 0-5 kHz transmitted signal.

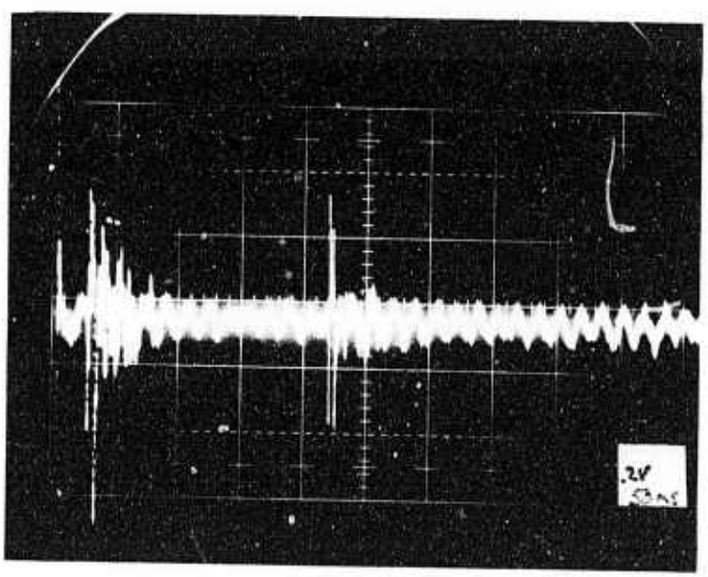

b. 0-5 kHz received signal.

Figure 16. Sparker signal wave forms.

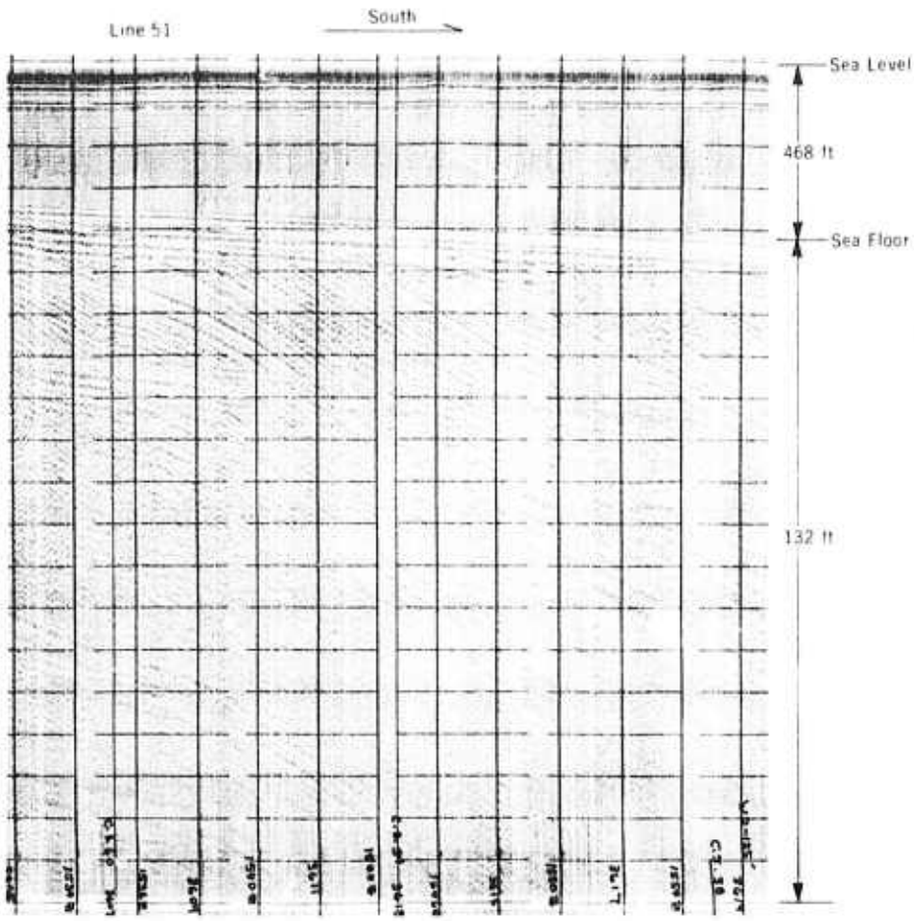

Figure 17. Typical subbottom profile record — Monterey Bay test area.

set together in reference to WWV. The timing lines on the Ocean Sonics recorder were also controlled by the same digital clock marker interface so that the locations of the seismic records could be accurately determined.

4.2 Shear Wave Experiment

4.2.1 Shear Wave Generator

The seismic source needed for the shear wave experiment had to fulfill three important requirements. It had to (1) be rich in shear energy, (2) generate waves of low frequency (as attenuation is proportional to frequency), and (3) discharge its energy below the water-sediment interface. Several sources were considered as to their capability of fulfilling the above requirements. A 3 cubic inch air gun was the final choice as a shear-wave generator.

Attached to the air gun is a probe, a hollow 1 in diameter pipe with a coned point. The energy from the air gun is transported through the probe and then out through an exit port at the base of the probe (fig. 18). By implanting the 0.5 m long probe into sediment, the source energy is discharged below the water-sediment interface.

The exit port is located on the side of the probe to generate shear waves (in particular, S_H-waves). With the probe implanted into the sediment, water and a little sediment fill the hollow probe. When the gun is fired, the water-sediment mixture is forced out, producing a horizontal jet stream. Thus, the basic procedure to detect the direct S_H-wave involves a linear array of transverse geophones with the S_H-source placed at one end of the detector array. The sensitive axis of the geophones and the water stream from the probe are parallel and both are transverse to the direct S_H-ray path. This alignment of horizontal geophones and S_H-source produces maximum response to the direct S_H-wave (fig. 19).

The 3 cubic inch air gun (Rix Industries, Emeryville, California) is cylindrically shaped with a height of 5 in and diameter of 3 in. The high pressure air escapes from a large diameter single opening which provides for a concentration acoustical source. High pressure is supplied to the air gun from a single Scuba diver's tank. Employing a Scuba tank provides a high pressure range from 300 to 2200 psi; however, a high pressure setting of 600-1000 psi is used for tests. The air gun is remotely triggered by a switch which activates a solenoid, which in turn discharges the high pressure air in the piston chamber of the air gun.

There are two inherent disadvantages concerning this S_H-source. One obvious problem is sediment disturbance. Although the water stream from the probe is directed away from the sediment between the source and receivers, the air discharged into the sediment will eventually produce a cavity after several firings. This reduces the efficiency of producing S_H-waves. The second disadvantage arises when the piston of the air gun returns after discharging the air. This draws excessive amounts of sediment into the probe, causing a blockage. The latter problem was rectified by attaching a fine wire mesh across the exit port, allowing only fines to enter the probe.

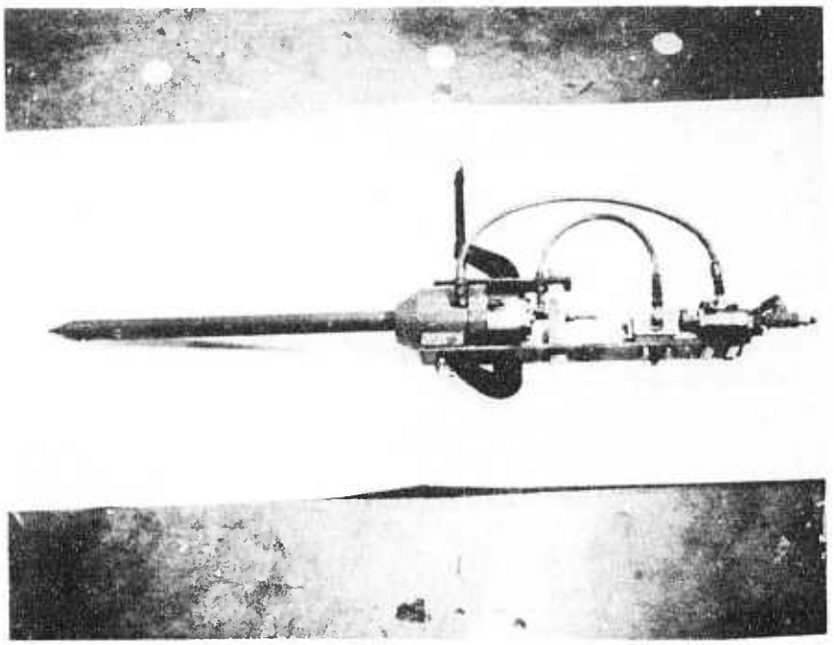

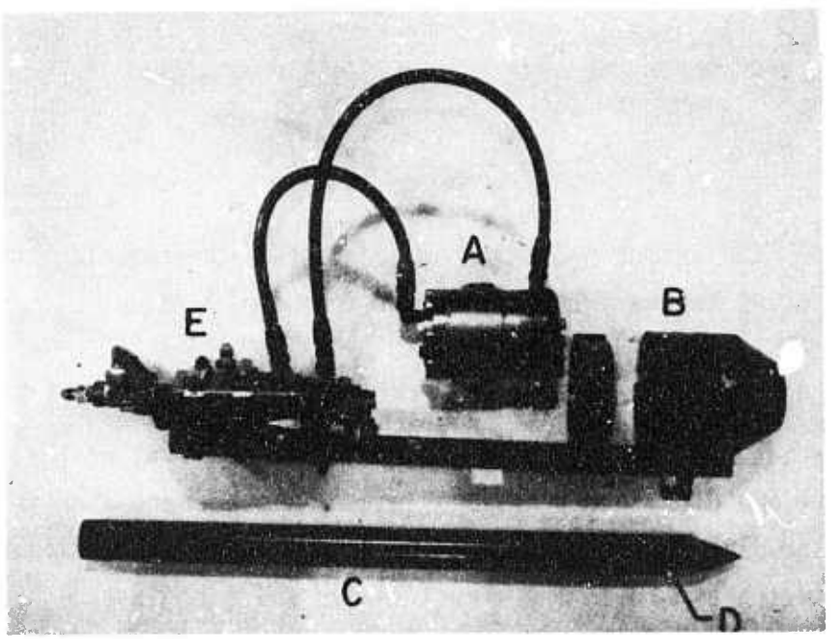

A 3 in.^{3} Air Gun. B Adapter. C Probe (1 1/2').
D Exit Port on Probe. E Solenoid.

Figure 18. Marine S_H-source.

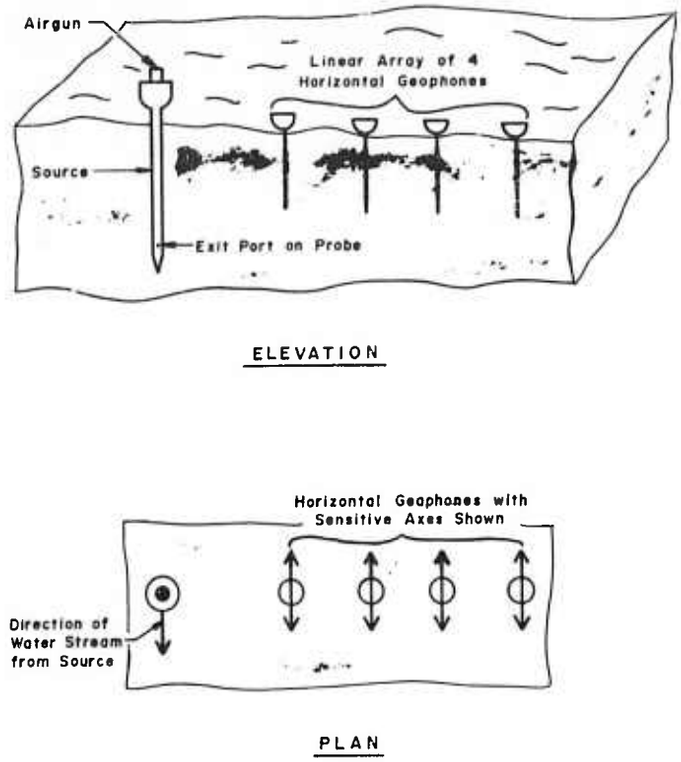

Figure 19. Probe for measurement of shear-wave and compressional-wave velocity.

Altogether, the source proved to be successful in producing low frequency shear waves in the frequency ranges from 80-100 Hz.

4.2.2 Receiver Array

Four geophone units are employed to record the arrival of the direct shear wave and direct compressional wave (denoted hereafter as direct S_H-wave and direct p-wave, respectively). Each unit contains a vertical geophone to respond to the direct p-wave and a horizontal geophone to respond to the direct S_H-wave (receivers manufactured by Geospace, Houston, Texas; HS-5 Model K, standard frequency of 30 Hz). Each geophone unit was equipped with a 1 in brass stake used to implant units.

4.2.3 Signal Processing and Display

The four horizontal geophone outputs are fed into a four channel voltage gain amplifier. The amplified signals are then displayed on a dual beam oscilloscope which was converted to four independent traces with a Tektronix 1A-4 plug-in. The sweep on the oscilloscope is triggered from the same circuit that triggers the solenoid of the air gun. Unfortunately, the air gun has a 52 m/sec delay time between the activation of source trigger switch and the actual firing of the air gun. Thus, it became necessary to delay the sweep on the oscilloscope in order that the signals could be viewed on the oscilloscope screen. The signals are recorded by means of a single exposure oscilloscope camera equipped with Polaroid type 47 film, 3000 ASA speed. The process is repeated by feeding the four vertical geophone outputs into the amplifier and then recording the signals displayed on the oscilloscope with the camera. A functional block diagram of this simple system is shown in figure 20.

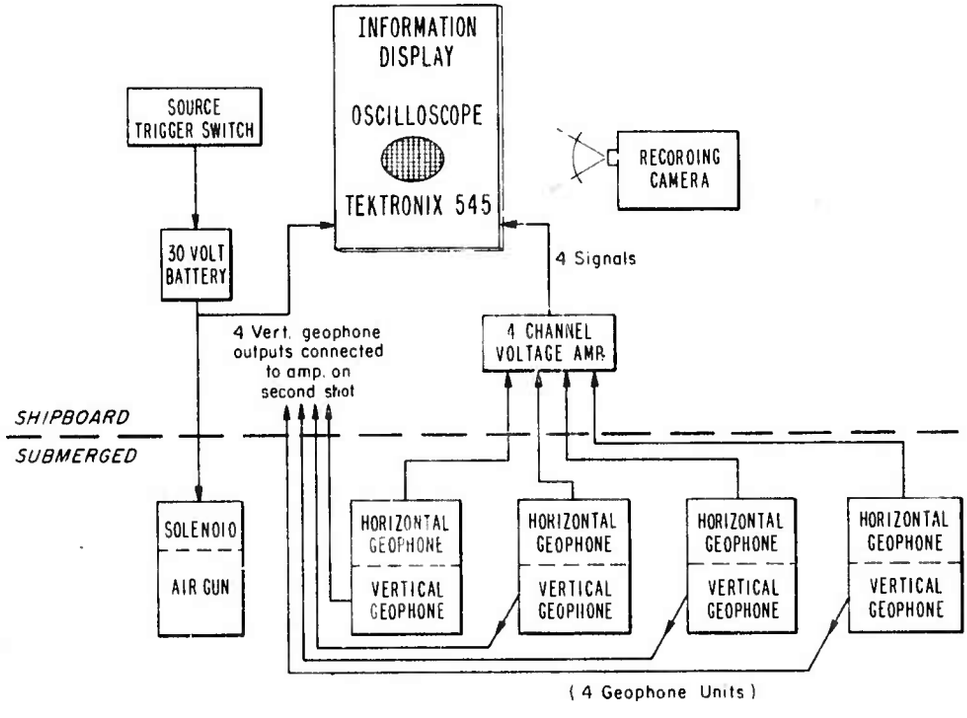

Figure 20. Functional block diagram — S_H-wave data acquisition system.

4.3 Electrical Resistivity System

4.3.1 Expandable Array

The system used to measure bottom resistivity was designed for operation by two Scuba-equipped divers, and consists of separate current and voltage units, a length of line on which electrode separations are marked, and an underwater slate for recording data (fig. 21). The output of the current source is a 10 Hz square wave, with amplitude adjustable between 0 and 500 milliamps in 10 steps. Power is supplied by 16 D-size rechargeable nickel-cadmium batteries, in a series-parallel arrangement which provides a nominal 10 V output. Current electrodes are 1/4 in (0.64 cm) diameter copper rods, 1/2 in (1.27 cm) long.

The voltage unit is a high-impedance (10^6 megohms) rectifying voltmeter, with ranges of 1, 10, 100, 1000, and 10,000 MV full scale, and is powered by mercury batteries. The potential electrodes have a non-polarizing silver-silver chloride element, housed in a 1 in (2.54 cm) outside diameter cylinder of acrylic plastic, and are filled with 2.7 molar potassium chloride saturated with silver chloride. Electrical

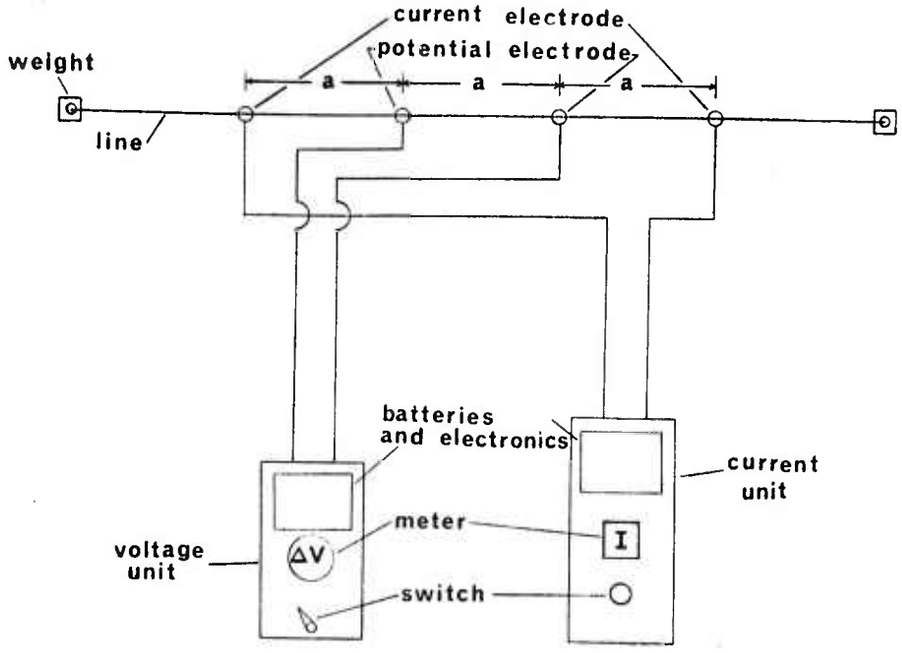

Figure 21. Schematic diagram — diver operated direct current resistivity apparatus.

contact to the sea water is made through a rod of porous ceramic material (Corwin, 1973). Each range of the voltmeter is calibrated by measuring a known voltage across a fixed resistor.

Both current and voltage units are housed in clear acrylic plastic cylinders of 6 in (15.2 cm) inside diameter and 1/4 in (0.64) wall thickness, which allows direct reading of the current and voltage meters. All openings are sealed with O-rings, and the housings are pressurized to a few psi before immersion to check for leaks. The length of the current unit is 12 in (30.5 cm); the voltage unit, 9½ in (24.1 cm). Sufficient cable is provided for an electrode separation a of 300 cm in the Wenner configuration.

In use, a line marked for Wenner electrode spacings of 10, 30, 100, and 300 cm is laid on the bottom with the ends anchored by diving weights. The current and voltage electrodes then are inserted into the sediment at the locations for a = 10 cm and the value of the voltage, ΔV, recorded for several values of the current, I. The electrodes then are moved to the next larger electrode spacing and the procedure repeated. As skin contact resistance is low in salt water, care is taken by the divers not to touch the current electrodes during operation, to avoid the possibility of a dangerous shock.

Electrode spacing, current, voltage, and water depth and temperature are recorded on the slate, and a water sample is taken for later salinity measurement. Although slow and cumbersome to use, especially in water of poor visibility, this prototype system proved reliable in field operation, and yielded data which appears to confirm the feasibility of the sea-floor horizontal array concept.

4.3.2 Surface Towed Array

The equipment used for the towed resistivity array field test is shown schematically in figure 22. A 12 V lead acid automotive storage battery was used as the current source, with current I controlled by the rehostat and monitored on a 0-10 amp ammeter. The switch allows the current to be turned off to monitor the zero level of the potential electrodes, or for polarity reversal. The current electrodes were strips of

zinc-coated pipe hanger strap, 1 in (2.54 cm) wide by about 2 ft (60 cm) long. The potential electrodes were of the silver-silver chloride type described above, and, potential ΔV was read on an Esterline-Angus model T171B battery operated strip chart recorder.

In operation, the current electrodes are energized continuously over areas of interest, and are turned off for about 30 sec every 5 min to check the zero level of the potential electrodes. Typical chart recorder output is shown in figure 23. Current polarity is reversed every so often to equalize electrolytic dissolution of the current electrodes. Although continual reversal of current electrode polarity would have, in effect, doubled the signal-to-noise ratio, it was found that this procedure resulted in a degraded current waveform, with several minutes required for the current to reach a stable value. As the current was not recorded continuously but was read from the meter and noted on the potential record, it was decided to hold current polarity constant as described above.

4.4 Sediment Sampling Equipment

To verify reflectivity measurements, it was necessary to have a core sampler which could rapidly sample the first meter of surface sediments and obtain relatively undisturbed samples. This was required for reliable engineering and mass physical property determinations. A core

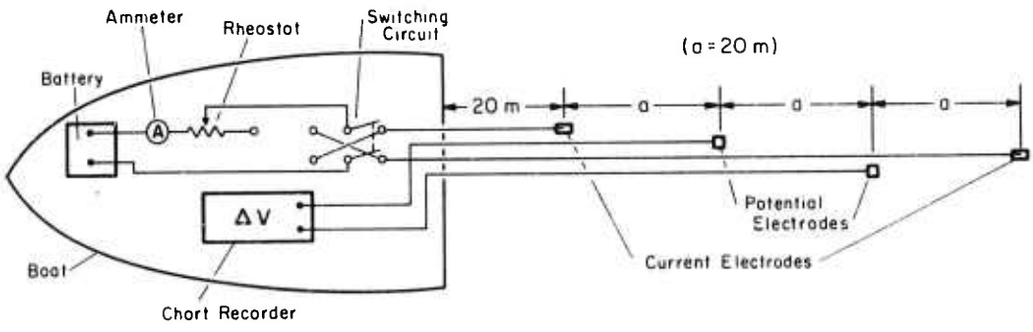

Figure 22. Schematic of towed array — direct current resistivity system.

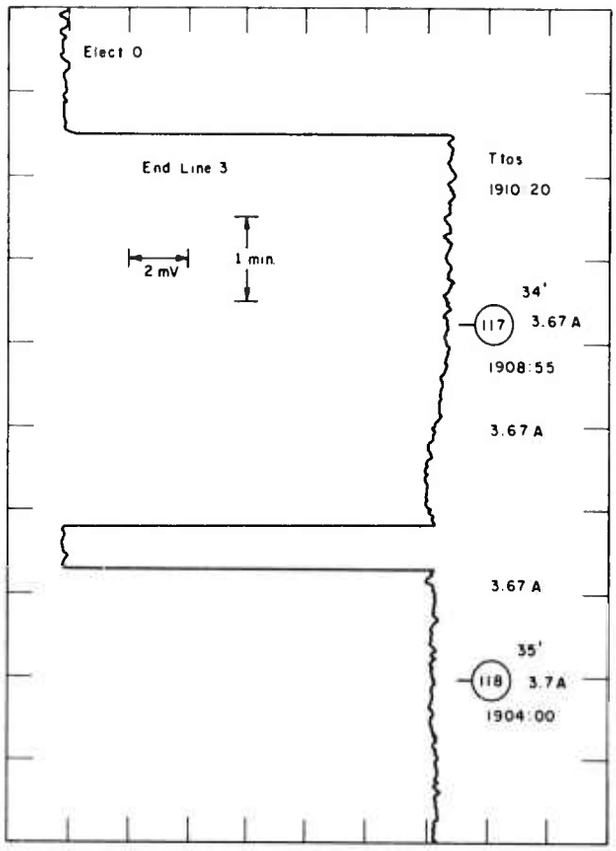

Figure 23. Towed resistivity — chart recorder output.

length ranging from 1 m to 3 m was decided upon because this depth of penetration was within the wave length of either of the two acoustic sources employed for the reflection coefficient mapping experiment (section 4.1.1). This also made it possible to determine to what degree changes in the near surface lithology or small scale structural variations would influence the reflection coefficient. Several samplers of the gravity-type or piston-type gravity corer variety were tested but found unsatisfactory. It was therefore necessary to design, construct, and test coring devices that would provide the desired capability. It was also decided that the energy source for penetration should not be percussion or rotary since these types tend to induce sediment distortion. Therefore, a steady thrust energy produced by pneumatic power

was incorporated in one system for shallow (1 m) penetration, and a vibratory energy system was incorporated in another design to obtain deeper penetration (3 m).

4.4.1 Diver Operated Core Sampler

Simplicity of operation and a minimal number of mechanical-electrical features were other criteria used for design of a shallow penetration corer. A study of figures 24 through 27 gives details of the design and hardware incorporated in the tool. Details covering the laboratory and field test of the diver operated corer are given in a report by Jenkins and Takeyama (1971). The field testing and evaluation of the prototype corer were done in conjunction with the sampling program for the reflectivity experiment conducted in San Francisco Bay (Barnes et al., 1972).

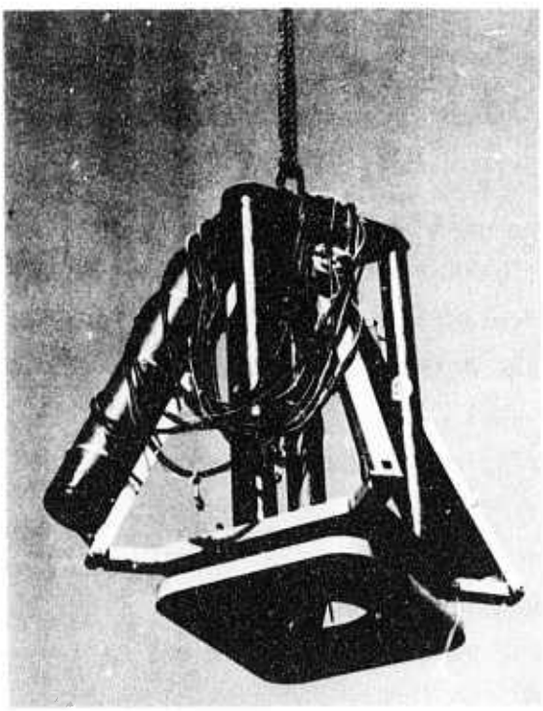

Figure 24. Diver operated sampler (retracted position).

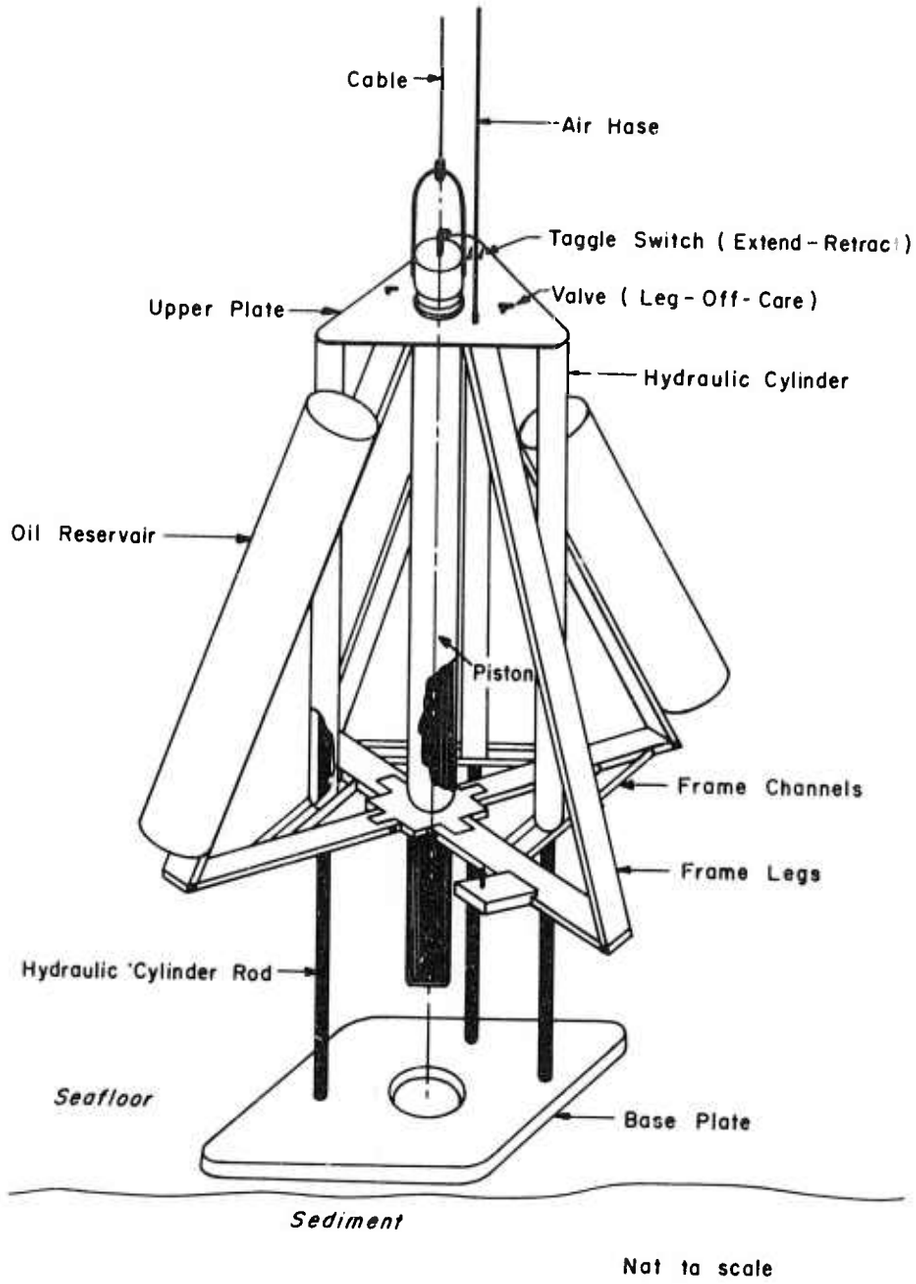

Figure 25. Diver operated sampler (extended position).

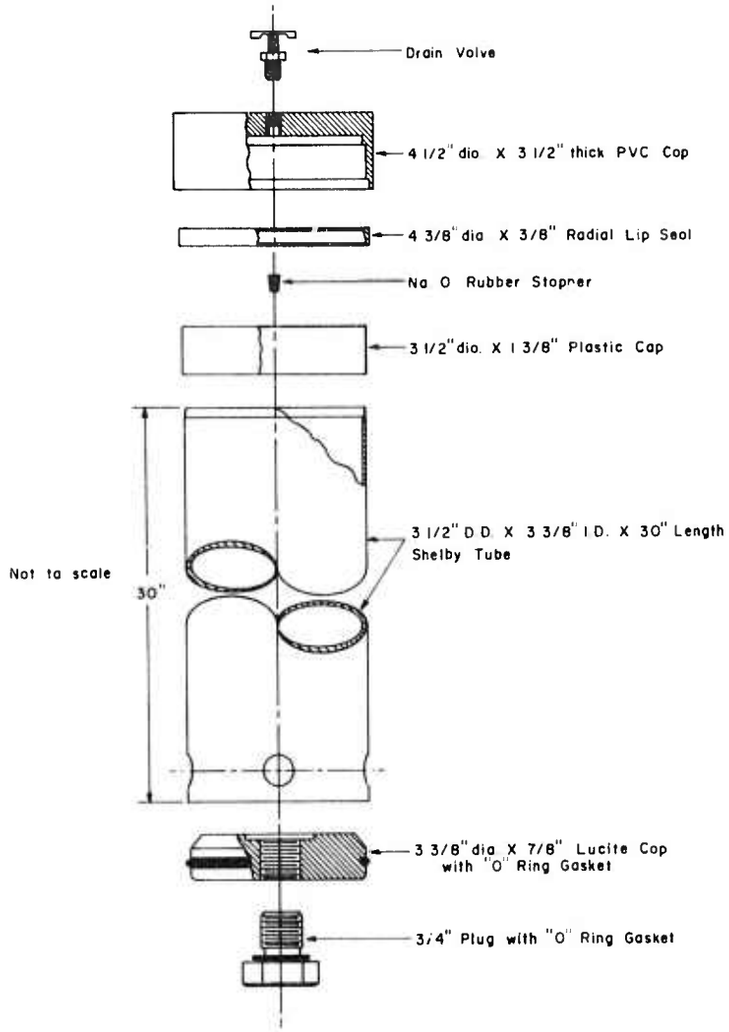

Figure 26. Sample retainer – modified Shelby tube.

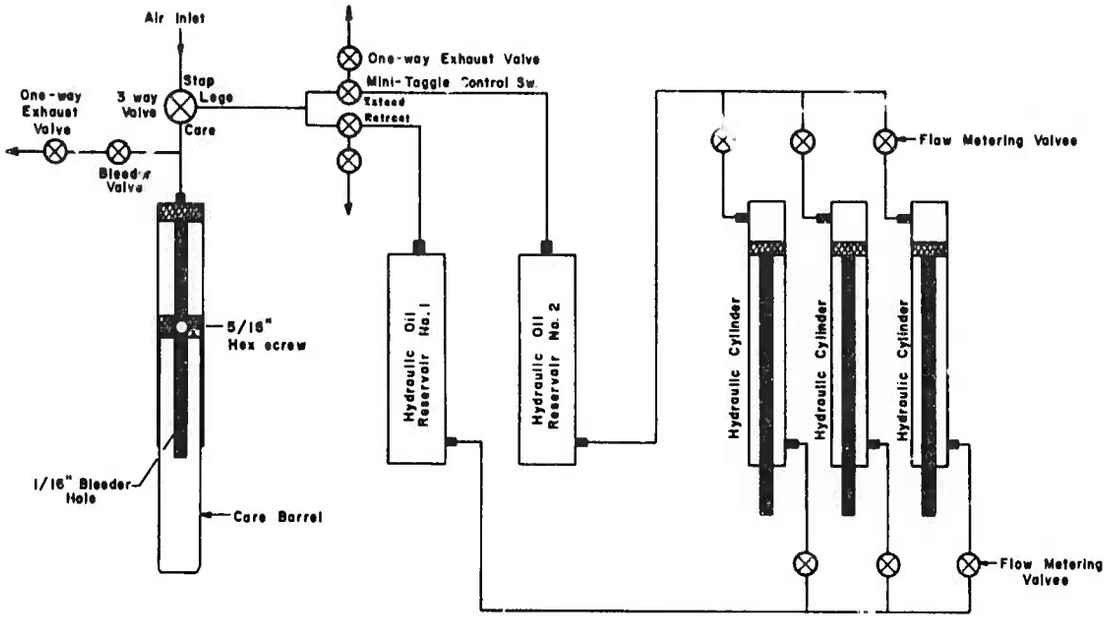

Figure 27. Diver operated sampler piping diagram.

4.4.2 Bottom Sitting Vibracorer

An impact-vibrator hammer and drill pipe mounted in a breakaway tripod (O'Brien and Duley, 1971) was used to sample sediments to depths of 3 m (fig. 28). These samples were tested in the same manner as the diver operated core samples, but their primary purpose was to provide lithologic information beyond the depth capability of the diver core sampler. The energy component of the system was a National Vibrator, Model BH-6. The weight of the vibrator is 350 pounds with an impact force of 240,000-in pounds. It uses 60 cfm of air at 70 psi and has a blow count of 110 blows per min. The exhaust ports are fitted with check valves to prevent water entering the cylinder.

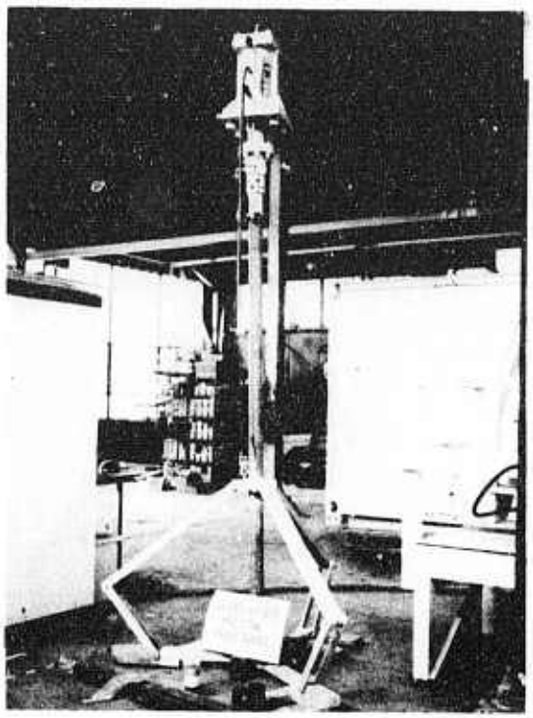

Figure 28. Vibracorer.

The drill pipe is made from round mechanical tubing drawn over a mandrel with a 3.50 in OD, 3.25 in ID, and wall thickness of 0.125 in. The drill bit is made from regular schedule 80 pipe, flush jointed to the pipe, with an OD of 3.50 in, and an ID of 2.875 in. The bit was shaped with a crowd-out relief angle of 15° and is fabricated to permit the installation of polyethylene preloaded cartridge (fig. 29). The cartridge is used as a lining for the drill pipe to reduce wall friction, and because it is collapsible it also serves as a core catcher.

The vibrator and drill pipe are coupled together by a Victaulic coupling. Grooved ends of the coupling are welded to the drill pipe and vibrator.

To provide the support needed for near perpendicular penetration, and to ensure stability, a tripod was designed which supports the drill pipe in the upright position during the initial 1-2 m of penetration. Once penetration has proceded to this point, a coupling on the drill pipe

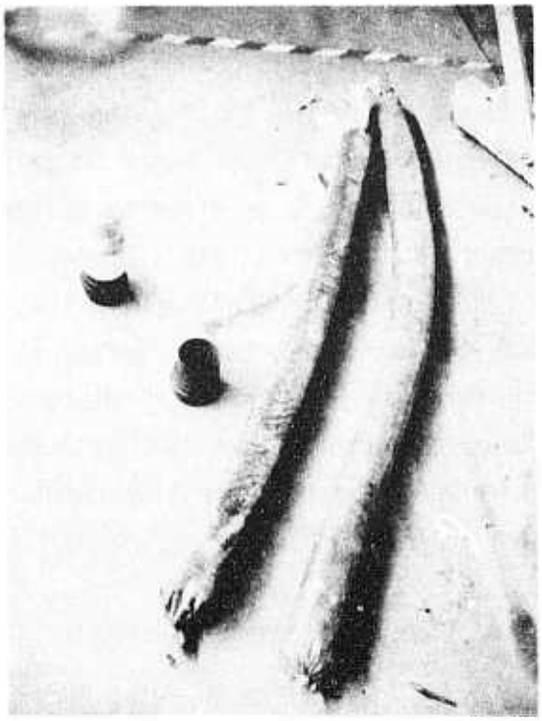

Figure 29. Plastic core retainer for vibracorer samples.

strikes the top of the tripod, causing the tripod to collapse and allows the drill pipe to continue to penetrate to full length. Sea floor slopes greater than 15° could cause the drill to overbalance and fall on its side. Complete details covering the design and fabrication of the tripod are covered by O'Brien and Duley (1971).

The combination of components used in this core sampler make a tool that is light in weight and simple to construct and operate.

4.5 Precision Navigation and Positioning System

A precision radio location system was used in all the field experiments and sampling programs described in this report. The main system, along with a specially designed subsystem, is used in referencing ship's position to geodetic control and for automatic real-time tracking during survey operations. The electronic subsystem enables real-time on-line

digital and graphical conversion of lane identification coordinates to x-y grid coordinates. The subsystem was developed at this laboratory (Barnes and Newman, 1972). The ship's position and track are accurately located to within ± 3 m based on daily repeatability checks of the calibrated value which is fixed by a land survey and represents a geodetic control point at the ship's berth.

Three peripheral input/output units have been added to the system since the work reported in Barnes et al. (1972). These include a digital fathometer, a line follower meter, and a teletype. The programmable calculator/computer allows interface capabilities of these subsystems with the basic navigation-positioning data. A block diagram of the system is shown in figure 30.

4.5.1 Automatic Line Follower

The line-follower meter indicates the position of the vessel; whether it is left or right of the prescribed track line and is calibrated to read how far off track the vessel is, from 0 to 100 ft. The incorporation of the line-follower into the navigation subsystem allows the boat operator to follow a more precise course along the track line, and alleviates constantly monitoring the x-y plotter during survey operations.

4.5.2 Recording and Display

A U-Tech Model 109 digital depth converter was incorporated into the subsystem, along with a teletypewriter. The "red" and "green" lane counts, x-y coordinates, time of print-out, and digital depth is printed out by a digital printer at 2 min intervals on command from the program in the calculator. At the same time, the teletypewriter prints out the time, digital depth, and x-y coordinates. The format of the teletypewriter printout is conducive to quick observation of time, depth and position data. Greenwich Mean Time was used for all recorded events in the navigation and positioning operation and for all magnetic tape recordings of acoustical data.

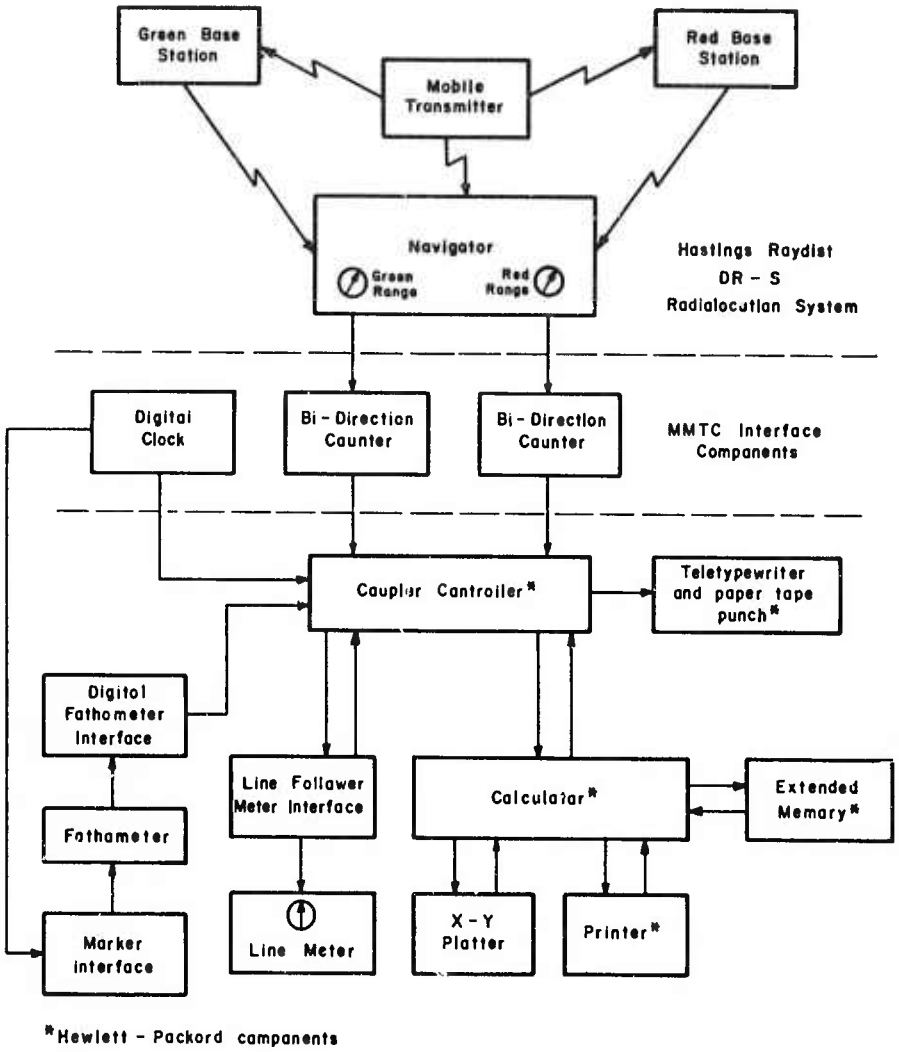

Figure 30. Block diagram of basic navigation system and subsystems.

The track lines of the survey area were pre-plotted on transparent overlays referenced to conventional maps using the California State Grid Coordinate System (Lambert Coordinates). The scale of the overlays was 1 in = 1,000 ft. Each overlay sheet covered an area 15,000 ft by 10,000 ft, with the size of the sheet being limited by the size of the x-y plotter (fig. 31). The boat operator is guided by observing the line meter or the x-y plotter with the appropriate overlay installed. The vessel is thus directed along a desired track line or to pre-designated core sites.

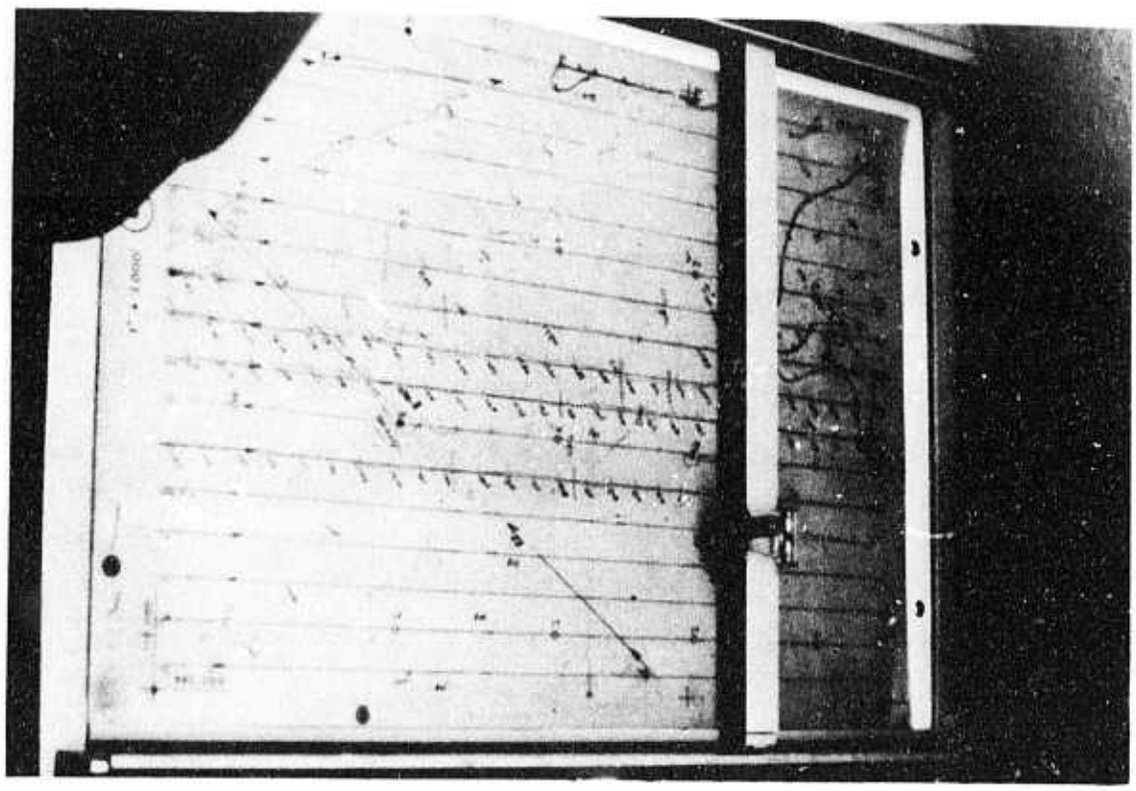

Figure 31. X-y plot for navigation-positioning data.

4.5.3 Indexing

A marker interface which simultaneously marks the records of the fathometer seismic recorder and Raydist strip chart recorder, and which also controls the Raydist digital printer, is activated by a digital clock contained in the subsystem interface. The digital clock gives selectable time outputs ranging from 1 to 30 min. Records are periodically annotated with time and station numbers, referenced to the vessel's location in lane counts which are printed out on the Raydist digital printer. In addition to automatic operation of the marker interface, the marker can also be manually operated to index events such as those that occur during maneuvering, marking of core sites with buoys, and calibration points.

4.5.4 Shore Stations

The two shore station sites required for operating the system were located approximately 15.5 miles apart, southeast of the operations area. The north, or "red", shore station was a 35 ft whip antenna powered by two thermal-electric generators and was located at a site south of Watsonville, California, directly over a USC&GS benchmark designated Holm. This site was at an elevation of 378 ft, and about 6 miles inland from the coast, in line of sight with the calibration point at the ship's berth in Santa Cruz Yacht Harbor. The south or "green" station was also a 35 ft whip antenna but was powered by 110 V ac. This station was located on the Fort Ord military base over a USC&GS benchmark designated Reserve, at an elevation of 485 ft, and approximately 2.6 miles inland from the coast, also in line of sight with the calibration point.

The "red" and "green" lane count — each lane equals 148.2282 ft — from each of the respective shore stations to the vessel is automatically connected to x-y grid coordinates on a Hewlett-Packard Model 7100A programmable calculator. These coordinates are then fed to a Hewlett-Packard 9125A digital plotter to provide a real time, automatic plotting, navigation and positioning system.

Mis-ties of an average of 0.058 lanes (8.59 ft) from the "red" station, and 0.087 lanes (12.89 ft) from the "green" station were noted at the calibrate point. Since the Raydist is a non line-of-sight system using ground wave transmissions, it was felt these mis-ties must be attributed to one or more of 3 causes, namely, (1) changes in the velocity of wave propagation, (2) insufficient warm-up time before commencing operations, and (3) characteristics of the propagation path from both shore stations, taking into consideration the overland distance, soil conductivity, surrounding vegetation, and topography.

5. FIELD OPERATIONS

5.1 Test Sites

5.1.1 Monterey Bay

Following the 1971 San Francisco Bay Study (Barnes et al., 1972), three areas in Monterey Bay, California, were selected for continuing investigations (fig. 32). A program was laid out to conduct several surveys including sampling, subbottom profiling, bathymetry, photo reconnaissance, and tasks associated with the acoustical and electrical resistivity research studies. Only one area (Area A) was surveyed due to time restrictions and limitation of funds. The underwater photo reconnaissance was not attempted because of poor visibility. Actual production on the area selected coincides well with the program intended (fig. 33). Sampling with the diver operated corer was limited to water depths less than 140 ft, thus reducing the number of core sites occupied. Possible hazard of decompression sickness was the main reason for not extending core operations into deeper water.

The bottom sediments in the survey area are of several types, consisting of gravels, medium to fine sands, silts and muds. Hard limestone reefs extend seaward from Point Santa Cruz and Point Soquel, and a generally northeast-southwest trending reef outlier parallels the east edge of the Point Santa Cruz extensions. The bottom topography is generally smooth with a gentle southerly gradient except in the reef areas (fig. 34). The wide variability of sediment/rock type, shallow water and even topography were factors influencing the selection of the area.

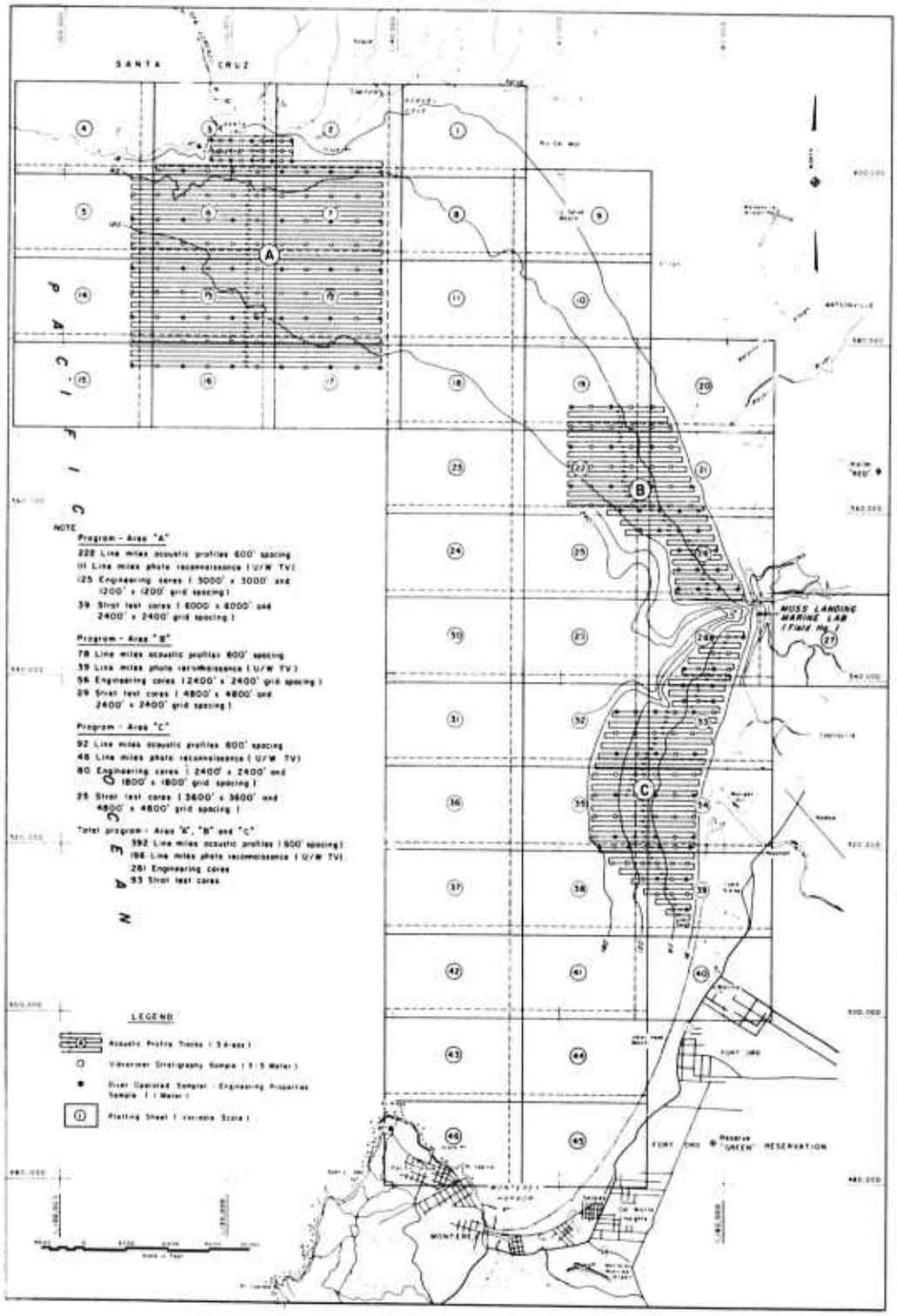

Figure 32. Monterey Bay test site location and program map.

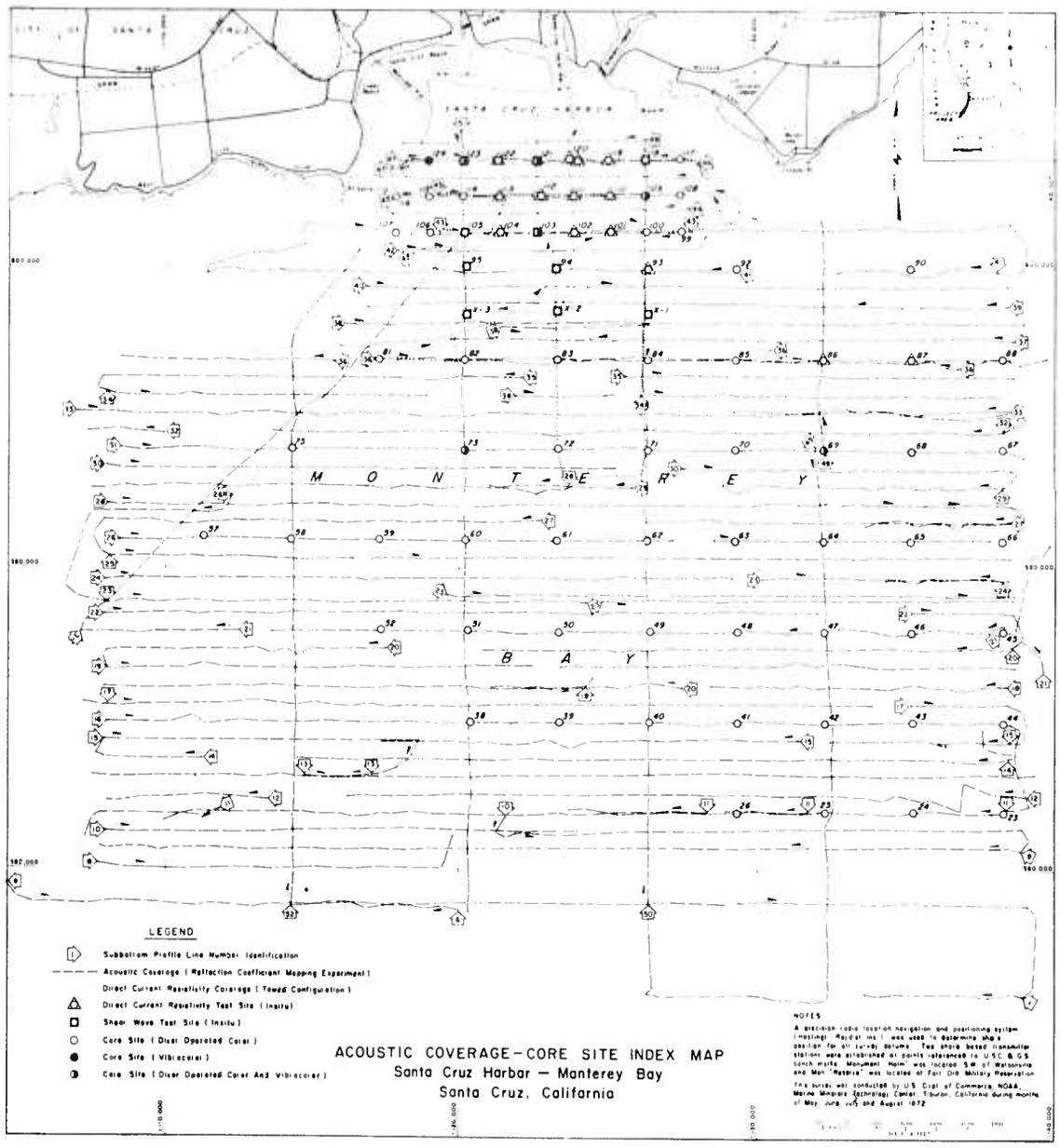

Figure 33. Acoustic and electrical resistivity coverage — core site index map.

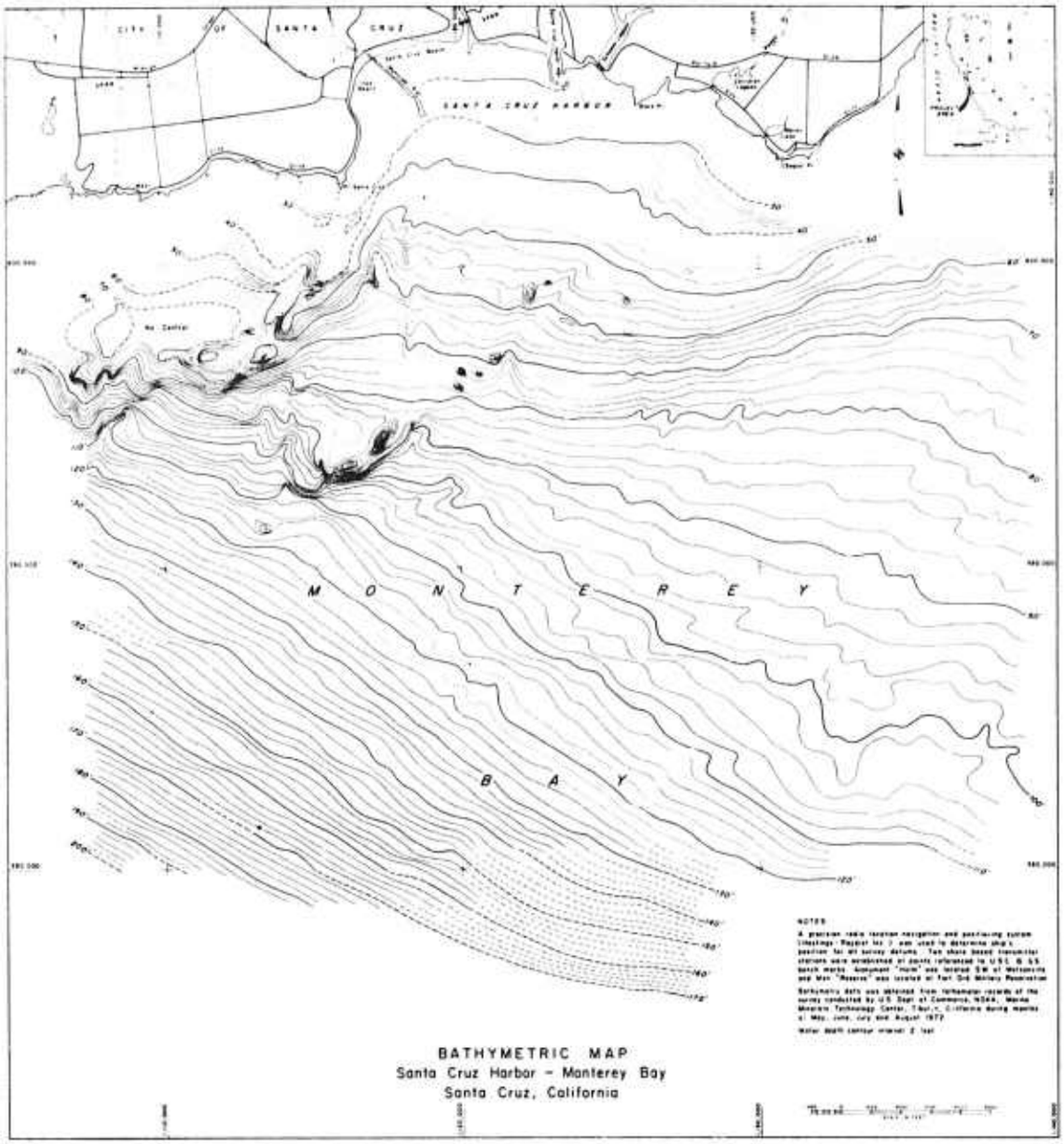

Figure 34. Bathymetric map, Santa Cruz Harbor — Monterey Bay.

The program in Area A comprises 30 square miles and was designed to apply fine grained survey practices. A seismic grid pattern of 600 ft line spacing was laid out for the continuous reflection coefficient mapping survey and towed electrical resistivity survey. Core locations were designated in two densities, the shallow water area grid was laid out with hole spacings of 1,200 ft by 1,200 ft, and the deep water area reflects hole spacings of 3,000 ft by 3,000 ft (fig. 34). Two samplers were used, but the data presented in this study was mostly confined to correlations based on analyses from the 1 m core samples taken using the diver operated corer.

5.1.2 Other Test Sites

Field tests for the shear wave and electrical resistivity experiments were conducted at two other sites besides Monterey Bay. The first test area was located in lake sediments near Fort Cronkite, San Francisco, California. This body of water, which was once open to the ocean, is now separated by a beach of gravelly coarse sand. Shear wave experiments were carried out on the seaward side of the lake in homogeneous beach material. The test site offered the advantages of an unlayered sediment and no hinderance from water wave action and tides. Electrical resistivity tests were conducted at another test site located in a small bay off the Gulf of California, Mexico (section 5.4.1).

Experiments employing both the shear wave generator and electrical resistivity apparatus were conducted in Monterey Bay, California. Shear-wave measurements and core samples were obtained at ten stations (refer to fig. 33 for location of stations 94, 103, 118, 121, 122, 123, X-1, X-2, X-3, and mooring). These stations were selected on the basis of providing a wide variability of sediment type. Although the method of measuring shear-wave was essentially the same at the Fort Cronkite and Monterey Bay test sites, the field procedures were different and will be treated separately. Figure 33 also shows locations and track lines where the direct current resistivity experiments were conducted.

5.2 Reflection Coefficient Mapping Experiment

The reflectivity experiment was performed aboard the *R/V Doodlebug* (fig. 35) with a three man crew, consisting of a navigator, an electronics technician, and a boat operator. The navigator monitored the precision navigation system and attended to operation of subsystems for accurate tracking and position. He also annotated the various location and depth recording printouts, as well as preplotting and selecting the lines to be traveled as indicated on the x-y plotter and by the line follower (fig. 36).

The electronics technician operates, calibrates, and monitors the subbottom and reflectivity measuring and recording apparatus and annotates the subbottom profile records and magnetic recording tape logs (fig. 37).

The first operation of the day was to calibrate and set all the navigation devices while tied up at the berth, which was also the navigation calibration point. The tape recorder, signal generator and ac voltmeter also were turned on and allowed to warm up before commencing operations. The boat then proceeded to the selected track lines and/or core sites for the day. Buoys marking the core sites were numbered in reference to the site number, and track lines were accordingly annotated (fig. 33). Buoys left overnight at a prescribed core site would be rechecked to insure that they were still in position on the site.

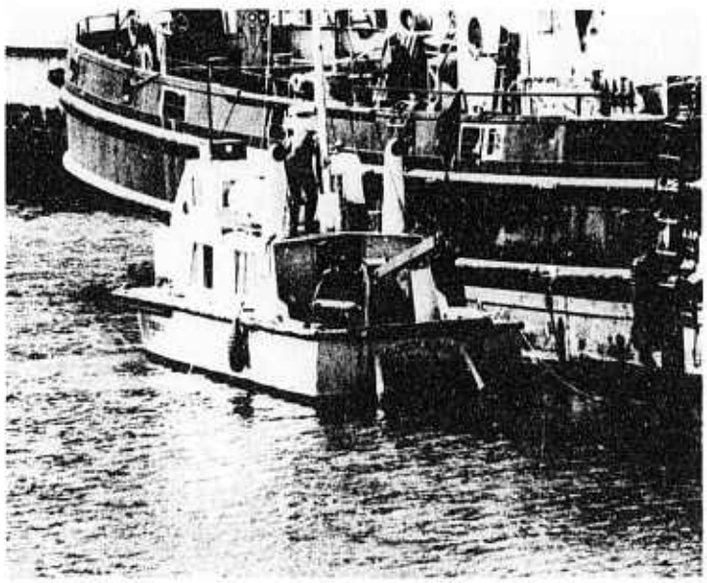

Figure 35. R/V Doodlebug.

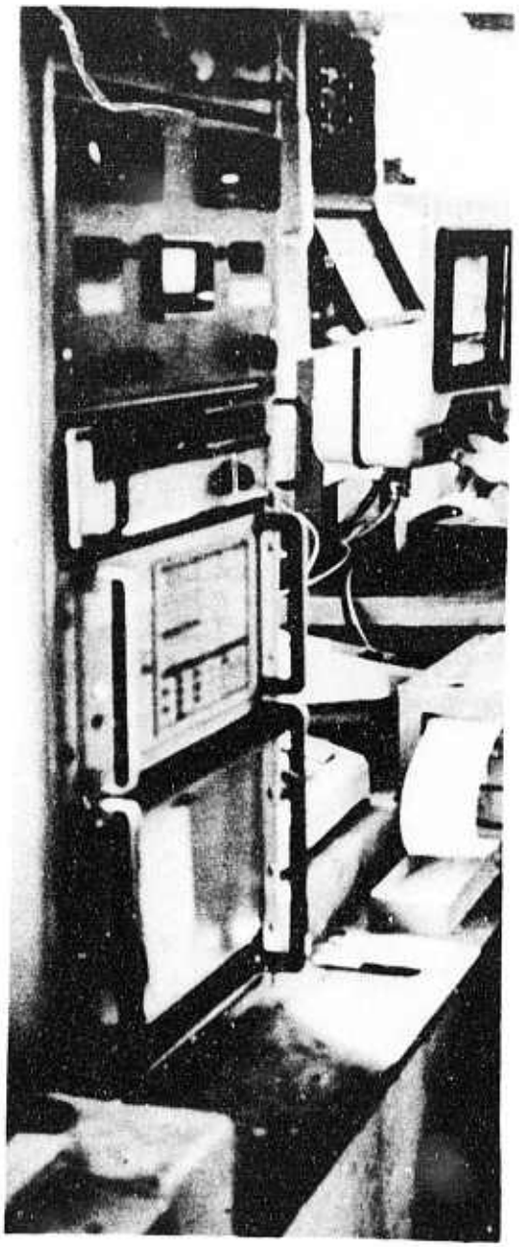

Figure 36. Navigation system — shipboard setup.

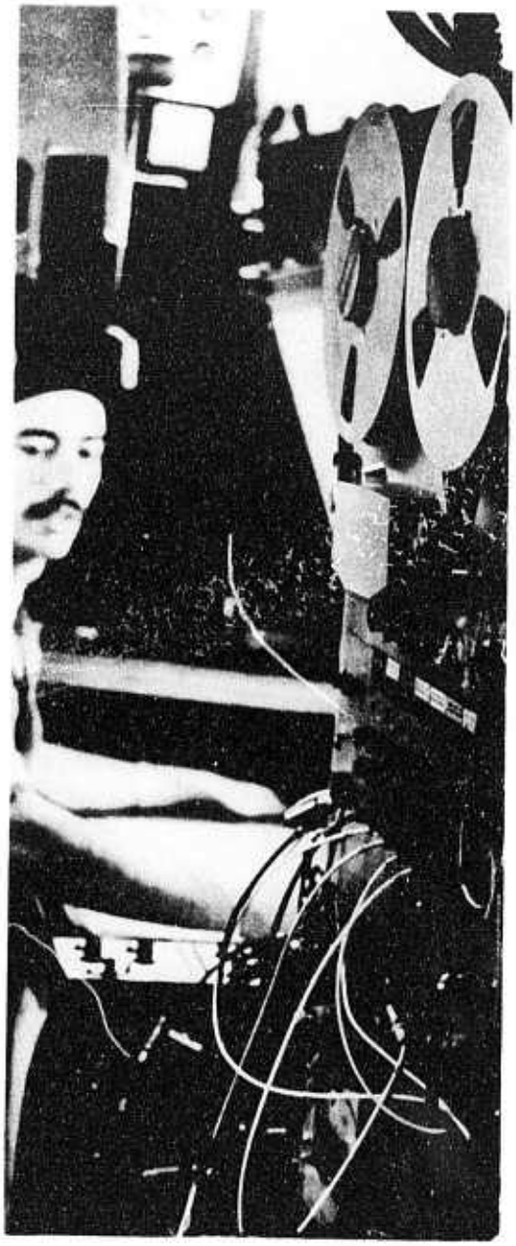

Figure 37. Underway acoustic — shipboard setup.

The seismic and reflectivity operation consisted of loading the tape recorder with a pre-numbered magnetic tape roll. The channels were calibrated and the signal generator set to either 2.5 kHz or 12 kHz and adjusted to a 1 V rms output. The two pinger monitoring channels on the recorder were calibrated. The 12 kHz signal was observed for 60 to 90 sec or more while the tape output level was monitored by the ac voltmeter and oscilloscope. Each tape channel gain control was adjusted for a 1 V rms indication on the voltmeter. The same procedure was used to calibrate the sparker monitoring channels, except that a 2.5 kHz signal was used. The calibration times are noted in a tape log, which was kept constantly for purposes of noting regular gain changes and malfunctions.

Shortly before the line to be profiled was reached, the boat was stopped and the pinger transducer lowered into the water and pinned into position. The sparker sled was lowered from its secured position on the stern with the deck crane and allowed to drift to a position about 50 ft astern of the boat, where it is secured for towing.

The streamer hydrophone was removed from its protective tube and streamed behind the boat until it was about 20 ft astern. An outrigger holding the cable was then extended so the hydrophone was approximately 14 ft from the starboard side of the boat. This aft and side tow positioned the hydrophone outside of the turbulence caused by the boat's wake, thus reducing the noise level.

While the boat headed to the start of the survey line, the precision recorder, power supplies, and capacitor bank are energized. The boat operator then set the throttle to a prescribed rpm for attaining constant boat speed (3-4 knots).

The subbottom profiling record was annotated in selected time measurements of 2-5 min and the record scanned periodically to determine that all was in proper working order. The sound source impulse and receiver waveforms were monitored on the oscilloscope so that all the amplifier gains could be adjusted and logged before the tape recording commences. Upon reaching the starting point of the desired track line, the tape recorder and paper tape punch is started and the time is noted in the tape roll log, as well as on the voice channels of the tape recorder.

During the profiling operation the sparker and pinger transducer receiver-signals were constantly displayed on the dual channel Tektronix Type 422 oscilloscope, except for occasional monitoring of the transmitted impulse waveforms. The monitoring of all these signals was done to insure that the amplitudes were of the proper level for taping and that no distortion was present because of noise or a malfunction of any system. The presence of all signals, including the IRIG B-Time Code and voice, could be observed on the recording level meters on each recording amplifier of the tape recorder.

The tape roll logs and verbal comments on the voice channel included the tape roll number, data, line traveled, direction of travel, calibration times, any change in recording amplitudes, signal source changes, and the start or stopping of the tape recorder or sources. Also noted were sea conditions, and occasionally noting sparker impulse waveforms or any other events the technician thought may influence the waveforms.

5.3 Shear Wave Experiment

5.3.1 Field Procedure — Lake Test Site

The electronics, powered by a portable generator, were stationed on the beach and the probe placed in sediments that were under about 2 ft of water. Both the source probe and receivers were implanted by hand to a depth of approximately 0.43 m (some experiments were conducted with the receivers at a shallower depth). The four geophone units forming the linear receiver array were inserted at predetermined distances from the source through the use of a 1 ft scaled rod. Various geophone unit spacings were employed, but the end geophone unit of the array was never further than 5 ft from the source. The experiments conducted consisted of recording the signals from the four horizontal geophone outputs, the four vertical geophone outputs, or two horizontal and two vertical outputs. Each experiment required 2 to 4 source shots to obtain the correct amplitude, delay time, and time scale settings. After acquiring data for a particular experiment, the source and receivers were relocated to a nearby station of the same sediment type, and a new test was then conducted.

5.3.2 Field Procedure – Monterey Bay Test Site

Because the investigations in Monterey Bay were performed in deeper water, an additional system was required to implant the source probe. The system employed was attached to the diver operated sampler (fig. 38). The system basically includes 3 air operated pistons that displace an inner frame in an up-down vertical motion. The source, attached to the frame moves up or down a track mounted on an outer frame. When on site, the sampler with S_H generator is lowered to the bottom with the inner frame in its highest position (i.e., the pistons are retracted). On the bottom, the divers actuate valves located on the outer frame. This high pressure air released from a scuba tank forces the pistons to move, resulting in the inner frame and the attached source with probe to be forced downward into the sediment. To retract the probes, the valves are reversed causing the pistons to raise the inner frame and source probe from the sediment. No difficulty was experienced in employing this source insertion method, even in gravelly coarse sand.

Before lowering the entire system, the four geophone units were correctly aligned and then clamped into four circular rings on a split bar. With the corer resting on the bottom and after inserting the source probe, a diver removed the split bar from the corer assembly. Two holes on one end of the split bar were positioned over two corresponding vertical rods located on the corer baseplate near the source (fig. 38b). The divers pushed the split bar down over the rods with the simultaneous penetration of the stakes on the geophone units into the sediment. The divers then detached the split bar leaving the geophone units implanted. This procedure provided a linear array of evenly spaced and correctly oriented receivers (1 ft spacings with the end unit 4 ft from source). In some cases the divers implanted the geophones without the split bar.

After inserting the geophone units, the divers surfaced, and acoustical measurements were taken. The first two stations went well, but a current drain into the geophone outputs developed at the third station. This caused the traces on the oscilloscope to wander extensively when recording. The current drain was traced to the 30 V battery triggering the air gun. The problem was partially rectified, although

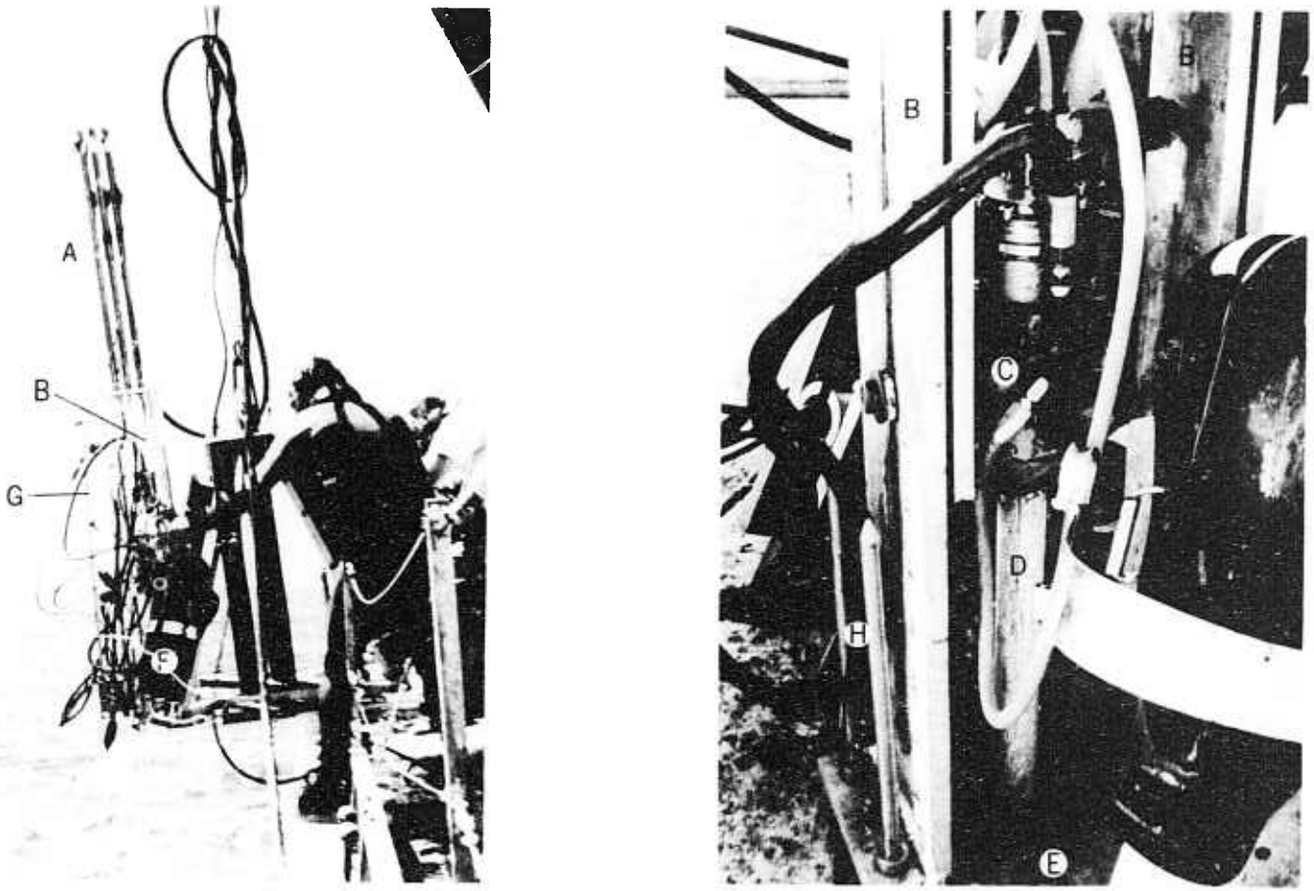

(a) (b)

Figure 38. S_H-wave source adapted to diver operated sampler.

A. Air Operated Pistons
B. Inner and Outer Frame
C. Shear Wave Source
D. Source Probe
E. Hole in Cover Baseplate
F. Scuba Tank
G. Split Bar with Circular Rings
H. Two Vertical Rods

there remained some wandering traces. Several source shots were required to position and focus in on the desired wave arrivals. An average of 24 shots per station were needed to obtain the necessary information on the direct S_H-wave and direct p-wave; therefore, sediment disturbance could be extensive, even though the water stream plus air from the source probe were directed away from the propagation path of the acoustical waves.

Once the data acquisition was completed, the divers submerged, retracted the source, and removed the geophone units. Core samples were then obtained at the site. The complete cycle of positioning the ship, inserting the probes, acquiring acoustical data, removing the probes, and core sampling took between 3 and 4 hours.

5.4 Direct Current Resistivity Experiment

5.4.1 *In Situ* Array

The electrical resistivity system was tested in two locations: a small bay off the Gulf of California at Puerto Escondido, Baja California, Mexico; and Monterey Bay, California. The tests at Puerto Escondido were conducted in warm, clear water over a carbonate sand bottom; those at Santa Cruz were in cold, murky water over a bottom of silty sand. The *in situ* array was tested at both sites.

In actual operation, a line marked for Wenner electrode spacings of 10, 30, 100, and 300 cm, is laid on the bottom, with the ends anchored by diving weights. The current and voltage electrodes then are first inserted into the sediment at the locations for a = 10 cm and the value of the voltage, ΔV, recorded for several values of the current, I. The electrodes then are moved to the next larger electrode spacing and the procedure repeated. As skin contact resistance is low in salt water, care is taken by the divers not to touch both current electrodes at the same time, to avoid the possibility of a dangerous shock.

Electrode spacing, current, voltage, and water depth and temperature are recorded on the slate, and a water sample taken for later salinity measurement. Although slow and cumbersome to use, especially in water

of poor visibility, this prototype system proved reliable in field operation, and yielded data which appears to confirm the feasibility of the sea-floor horizontal array concept (fig. 39).

5.4.2 Surface Towed Array

The simple towed resistivity system described in section 4.3.2 was tested only in Monterey Bay. The purpose of the test was to determine whether data consistent with bottom properties which were measured directly or were determined by other geophysical methods could be obtained by a towed resistivity system. A Wenner array was used, with electrode spacing (a) of 20 m. While it would have been desirable to run several array spacings, extending the array spacing to greater distances proved impractical.

The array was towed from the *R/V Doodlebug* at about 3.5 knots, using the Raydist navigation system described in section 4.5. The track covered is shown in figure 33.

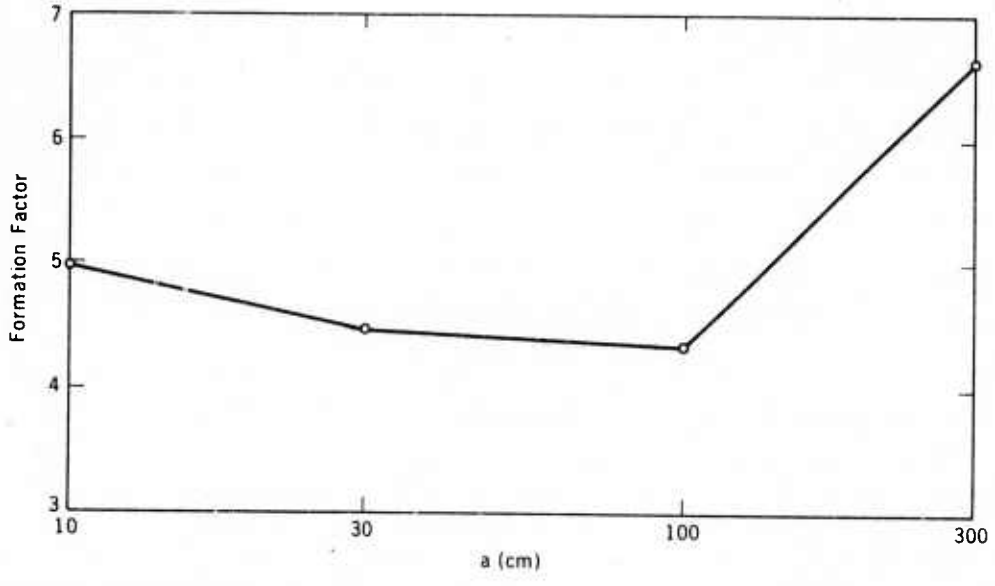

Figure 39. Formation factor vs a-spacing: diver operated Wenner array.

5.5 Sampling Program

The objective of the sampling program was to determine by core analysis, the mass physical and engineering properties of the sediments at the same locations where acoustic reflectivity measurements were made.

The sampling program was conducted aboard the *R/V NOAA's Ark*, a converted LCM6, 56 ft LOA and 14 ft beam (fig. 40). An 8-ton telescoping crane mounted on the bow of the vessel was used to raise and lower equipment over the side. Air for the pneumatic-hydraulic diver-operated sampler and the vibratory sampler was supplied by a compressor delivering 85 cfm of air at 100 psi.

Since the sampling ship did not have an accurate positioning system, the *R/V Doodlebug* would drop marker buoys at each drill site for the projected day's work program. The choice of the mooring used at each location (one or two point anchoring), was dependent upon the water currents, wave action and the velocity and direction of the wind. After anchoring, the sampler to be used at a particular site was prepared and put over the side of the ship.

A vibratory bottom-sitting drive sampler (open type) was used on several occasions. This unit was capable of obtaining a sample 300 cm long and 7.0 cm in diameter. Sampling with this equipment was limited to nine core sites due to operating difficulties (section 4.4.2, fig. 28).

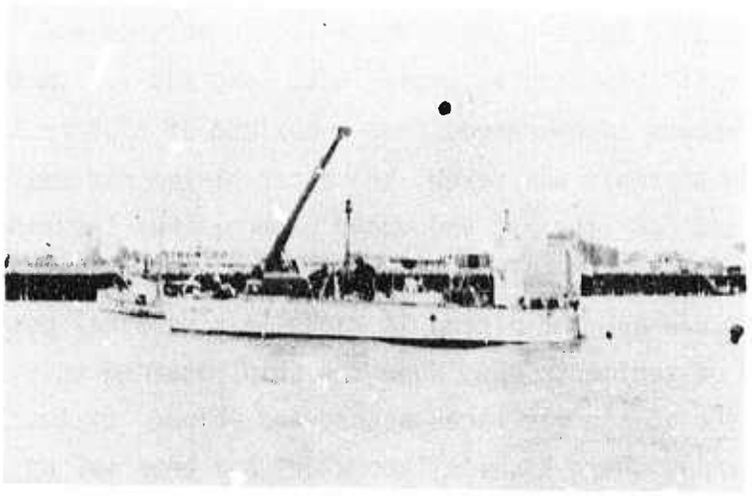

Figure 40. R/V NOAA's Ark.

The procedure for obtaining a core with the vibracorer was to lower the vibracorer and tripod slowly over the side of the vessel until the tripod reached the bottom.

This was indicated by a float attached to the tripod with a length of line the same depth as the water. When the float sank into the water the tripod was on the bottom. At this point, the air was turned on to the impact-vibrator and the winch operator played out the wire rope attached to the upper part of the vibrator. When there was slack in the wire rope it was determined by experience that the drill pipe had penetrated to its maximum depth. The winch operator would then raise the vibrator and tripod slowly onto the deck.

When the diver operated sampler was used, divers were sent down to activate the valves for coring, remove and seal the sample tube, and replace another tube into the sampler. A cycle of operation including anchoring, sampling, retrieving the anchor, and moving to the next sample site would take approximately 1-2 hrs. When wind and water conditions were favorable and malfunctions or equipment breakdown occurred, five sample sites could be cored in one working day. Depth of water and the number of divers available also affected the number of samples taken per day. All dives were made within the U.S. Navy, no decompression limits. At 125 ft a sample could be taken within a total, surface-bottom-surface, time of 6 min.

Most of the samples were obtained with the diver-operated, bottom-sitting drive sampler (piston type) described in section 4.4. The sampler was capable of obtaining a sample 70 cm long and 7.9 cm in diameter. The length of samples taken ranged from a maximum of 65.6 cm to a minimum of 4.5 cm. When a sample was taken, the upper piston was sealed and a plastic cap forced over the bit end under water — thus insuring *in situ* water contents. The tube, with sample, was then handed aboard the research vessel *NOAA's Ark* and placed in racks in a vertical position, oriented with top of sediments up. When the ship returned to its mooring at Santa Cruz, the sample was taken ashore and shipped by truck to Moss Landing, California, where a soils laboratory had been set up.

6. GEOLOGICAL DATA ANALYSIS AND RESULTS

6.1 Laboratory Procedures — Sample Analysis

Generally, there was a 4 to 6 hr interim between actual taking of the sample and the processing in the laboratory. The sample tube was cleaned, and weighed to 0.1 g. The seals were then removed and the excess water was siphoned off, weighed and recorded. Preweighing of all sample tubes facilitated the calculation of the total weight of the sample. The volume of the sample was calculated knowing the cross sectional area of the sample tube and the length of sample retained in the tube. The sample tube was then clamped into a horizontal core-ejector and extrusion of the sample commenced.

Eighty-two samples were collected from the upper Monterey Bay Area with 71 engineering samples obtained by the bottom-sitting drive sampler, piston type, and 9 lithologic samples with the bottom-sitting vibratory sampler, open type. Both types of samplers were designed and developed at MMTC (Jenkins and Takeyama, 1971; O'Brien and Duley, 1971).

Table A-4.1 in Appendix A-4, summarizes the equipment used, corrected depth and other information related to the samples. Mathematical equation used to calculate sample volumes were:

$$C_a = \frac{D_w^2 - D_e^2}{D_e^2} , \tag{21}$$

where C_a is the area ratio, D_w is the maximum outside diameter of the sampler cutter, and D_e is the inside diameter of the sample cutter;

$$C_o = \frac{D_w - D_t}{D_t} , \tag{22}$$

where C_o is the outside clearance ratio controlling outside friction and D_t is the outside diameter of the sample tube;

$$C_i = \frac{D_s - D_e}{D_e} , \tag{23}$$

where C_i is the inside wall friction and D_s is the inside diameter of the sample tube. The gross recovery ratio,

$$R_g = \frac{L_e}{H} , \tag{24}$$

where L_e is the length of the sample obtained and H is the depth of penetration of the sampler. This factor was not determined in the sampling because the sampling equipment was not monitored to determine penetration depth. Table 1 summarizes the parameters and ratios for the two types of samplers used in this project.

6.1.1 Wet Unit Weight, γ_{wet}

Wet unit weight was determined by direct measurements:

$$\gamma_{wet} = \frac{W_{total} - W_{tare}}{V_{total}} \tag{25}$$

where W_{total} is the weight of the sample plus the sample tube and all seals; W_{tare} is the weight of the sample tube and all seals alone, and V_{total} is the volume of the sediments in the sample tube. γ_{wet} represents the in-place unit weight or bulk density.

Wet unit values ranged from a maximum of 2.87 g/cm^3 at core site No. 50, to a minimum of 1.85 g/cm^3 at core site No. 103. Higher values of γ_{wet} were noted in the use of the vibratory drive sampler as compared to the diver operated drive sampler at the same location. This is probably caused by plugging of the sample tube and subsequent compacting of the sediment within the tube.

6.1.2 Specific Gravity of Solids, G_s

A representative sample of approximately 100 g was retained and overdried at 110°C for 10-12 hrs or until a constant weight was observed. This sample was then allowed to cool in a desiccator, then it was split and weighed. The volume of the solids (V_s) was determined directly by a

Table 1. Sampling Equipment Specifications

Type of Sampler	D_e (in)	D_s (in)	D_t (in)	D_w (in)	Area Ratio (C_a)	Clearance Ratio Outside (C_o)	Clearance Ratio Inside (C_i)
Piston-type Drive Sampler (Diver operated)	3.34	3.37	3.44	3.44	5.19	0.0	0.72
Open-type Drive Sampler (Vibracorer)	2.75	3.69	3.75	3.75	86.5	1.7	23.5

Beckman Model 930 Air Comparison pycnometer. The weight of solids (W_s) was determined with a Sartorius balance to 0.01 g.

Specific gravity of the solids, G_s, was determined from

$$G_s = \frac{W_s}{V_s} . \tag{26}$$

Corrections for salt content in the specific gravities were not made. Specific gravities of the solids for over 100 samples ranged from 2.57 to 2.75. The majority of samples were between 2.62 - 2.70 and an average of 2.66.

6.1.3 Water Content, ω; Void Ratio, e; Porosity, ϕ

Water content is a ratio, in percent, of the weight of water in a sediment sample, W_w, to the weight of the over-dried solids, W_s, and is defined as

$$\omega = \frac{W_w}{W_s} \times 100 . \tag{27}$$

In this analysis, determination of water content was found by the calcium carbide gas pressure method and follow AASHO Designation (see T217-67 I, A2-2, ASTM 1970, p. 456-459). Using local soils from Monterey Bay and distilled water, a conversion curve was calculated by regression analysis with a correlation coefficient of .99 and standard error of estimate equal to ± 1.93. Equation 28 was used to calculate water content, ω;

$$\omega = 1.33 \text{ (calcium carbide method)} - 3.34. \tag{28}$$

Another measure for water-saturated sediments is the void ratio, e, which was the ratio of the volume of the void spaces, V_v, to the volume of the solid sediments, V_s, or

$$e = \frac{V_v}{V_s} . \tag{29}$$

Void ratio was calculated in the laboratory from,

$$e = \frac{G_s \gamma_w V}{W_s} - 1 , \tag{30}$$

where γ_w is the unit weight of sea water.

Porosity is the relation expressed in percent of the volume of the voids, V_v, to the total volume, V, which is defined by,

$$\phi = \frac{V_v}{V} \times 100. \tag{31}$$

In this report porosity was computed from other measured parameters and expressed as

$$\phi = \frac{e}{1+e} \times 100 . \tag{32}$$

6.1.4 Grain Size Analysis

A representative sample from any one lithologic zone observed in the core sample was weighed, put into a mixing bowl of water, stirred and allowed to stand for one hour. The sample was wet sieved in a U.S. Standard No. 200 sieve and all material retained was dried overnight at 110°C, or until a constant weight was observed. The wash water was evaporated in the drying oven at 110°C and both fractions were cooled in desiccators. The coarse fraction was sieved using a nest of sieves (openings 12.5, 4.69, 1.981, 1.397, .991, .701, .495 mm) for 7 min and the fraction passing No. 35 (.495 mm) was sieved in a nest of sieves (openings .351, .246, .175, .124, .088, .074 mm) for 10 min in a gyrotating sifting machine. The size fraction finer than No. 200 (.074 mm) was split, and a representative

sample of approximately 35-40 g was used for the determination of the grain size distribution of the fine-grained soil by the hydrometer analysis method. The sample was placed in a beaker with 250 cc of distilled water and 5 cc of a 10 percent by weight solution of sodium hexmetaphosphate (calgon) and hand-mixed. The suspension was transferred to a dispersion cup (ASTM D422-63), and mechanically mixed for 10 min. The dispensed soil suspension was then transferred to a 1000 cc graduated cylinder, distilled water added to increase the volume to 1000 cc, and placed in a constant temperature bath. Approximately 1½-2 hrs in the bath were needed to bring the solid suspension up to test temperature at 25°C. All hydrometer tests were run 4 hrs to find the percentage break-off point of the silt to clay fraction at 5 microns (U.S. Bureau of Soils classification).

Results of sieve and hydrometer analysis were graphed on a cumulative frequency curve by weight from which the mean diameter was selected from average diameter of the 16, 50, and 84 percentiles (Folk and Ward, 1957).

6.1.5 Shear Strength (Penetrometer)

A standard Proctor penetrometer with interchangeable needles was first used by the divers to obtain *in situ* measurements but was discarded as being unmanageable and not enough bottom time. Penetration tests were conducted in the laboratory using a pocket-size penetrometer which was calibrated in T/ft^2 and Kg/cm^2. All measurements were taken as the sample was slowly ejected, but still within the core barrel.

6.1.6 Shear Strength (Vane Shear-Torvane)

Attempts were made to use a hand vane shear tester operated by divers to obtain *in situ* measurements of shear strengths, but this was discarded because of low bottom visibility and consumption of bottom time. Vane shear measurements were made in the laboratory with a hand Torvane device calibrated at 1 rev = 1.0 Kg/cm^2. Here again measurements were taken within the sample tube as the sample was ejected. Most of the measurements were taken when a visual change in lithology was evident.

6.2 Interpretation of Sediment Analyses

Table A-4.3 in Appendix A-4 represents a tabulation in sediment analyses made on approximately 85 core sites contained in Santa Cruz harbor, Monterey Bay (fig. 33). The datums for parameters of mass physical properties, such as, porosity, density, mean grain diameter and sorting coefficient, as well as engineering properties of shear strength, were posted at respective core sites, and contoured interpretations prepared. Figures 41 through 46 show the results of the interpretations. Summary of the parameters datums at each core site and the acoustic values are contained in table A-4.4 in Appendix A-4.

6.2.1 Interrelationship of Sediment Properties

Computer analyses of the parameters representing the mass physical and engineering properties were done using a regression analysis program. Cross-correlations of the parameters resulted in the correlation coefficients given in table 2. The degree of correlation is reflected in percent with a value of 1.000 representing a perfect correlation. The relative interdependence or interrelationship of one parameter to another is reflected in the correlation coefficient. As predicted in other studies cited previously (section 2.1), the correlation of porosity and density (.952) is very good. Also, the correlation of sorting coefficient to mean grain diameter is within reasonable expectations (.830). Evidence of correlation between penetrometer and vane shear measurements (.317) is poor, and may be attributed to the predominance of sand, which has always been an inherent problem in obtaining reliable shear strengths. Other correlations appear to be negligible, thus their significance in diagnosing the interdependence or interrelationship of these parameters appears to be minor.

6.2.2 Sediment Dynamics and Deposition Characteristics

The correlation of acoustical properties to sediment properties is given in section 7.1.3. The value of relating the two measurements in a positive correlation is obvious considering the economics and time involved

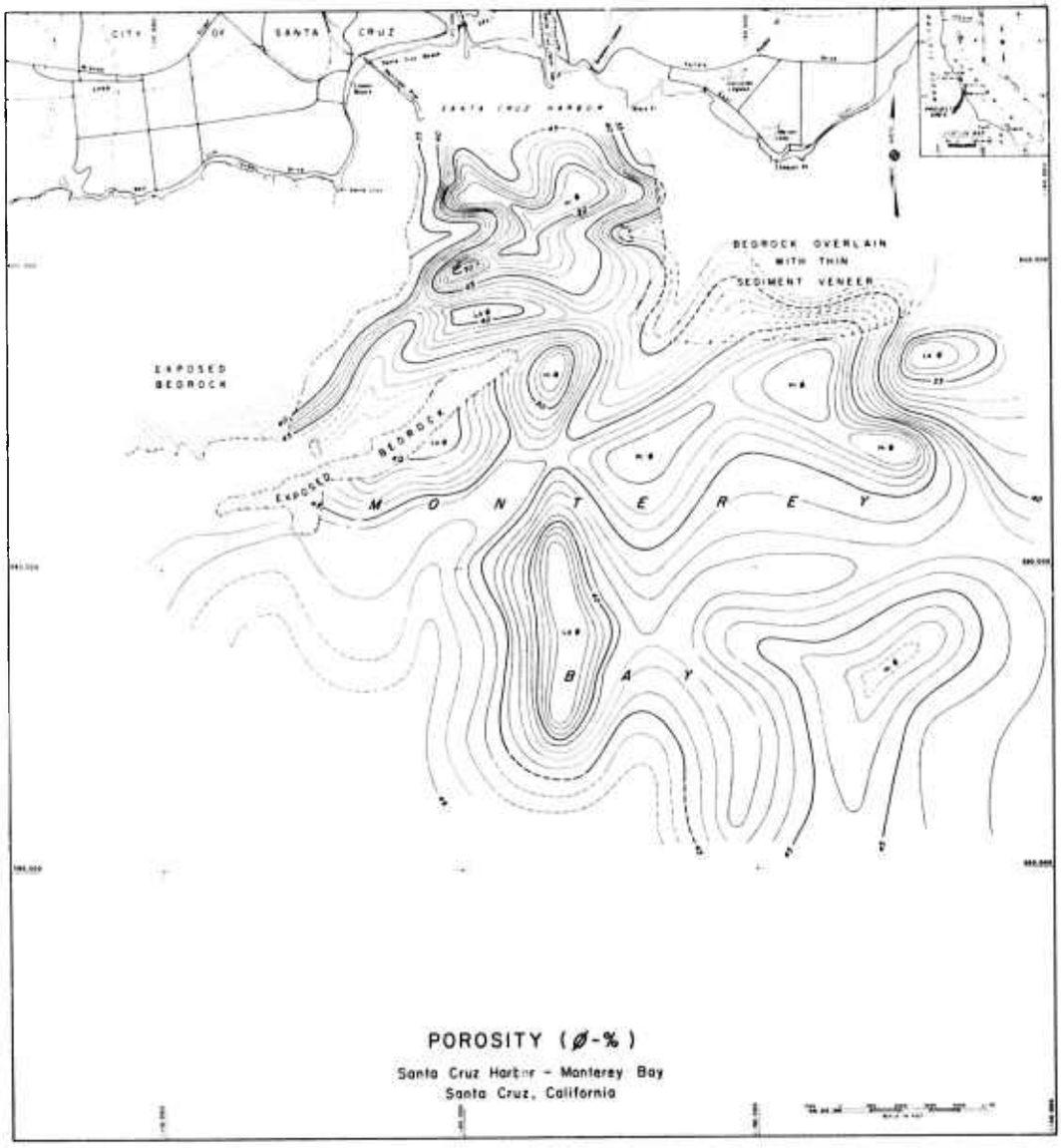

Figure 41. Porosity distribution — Santa Cruz harbor.

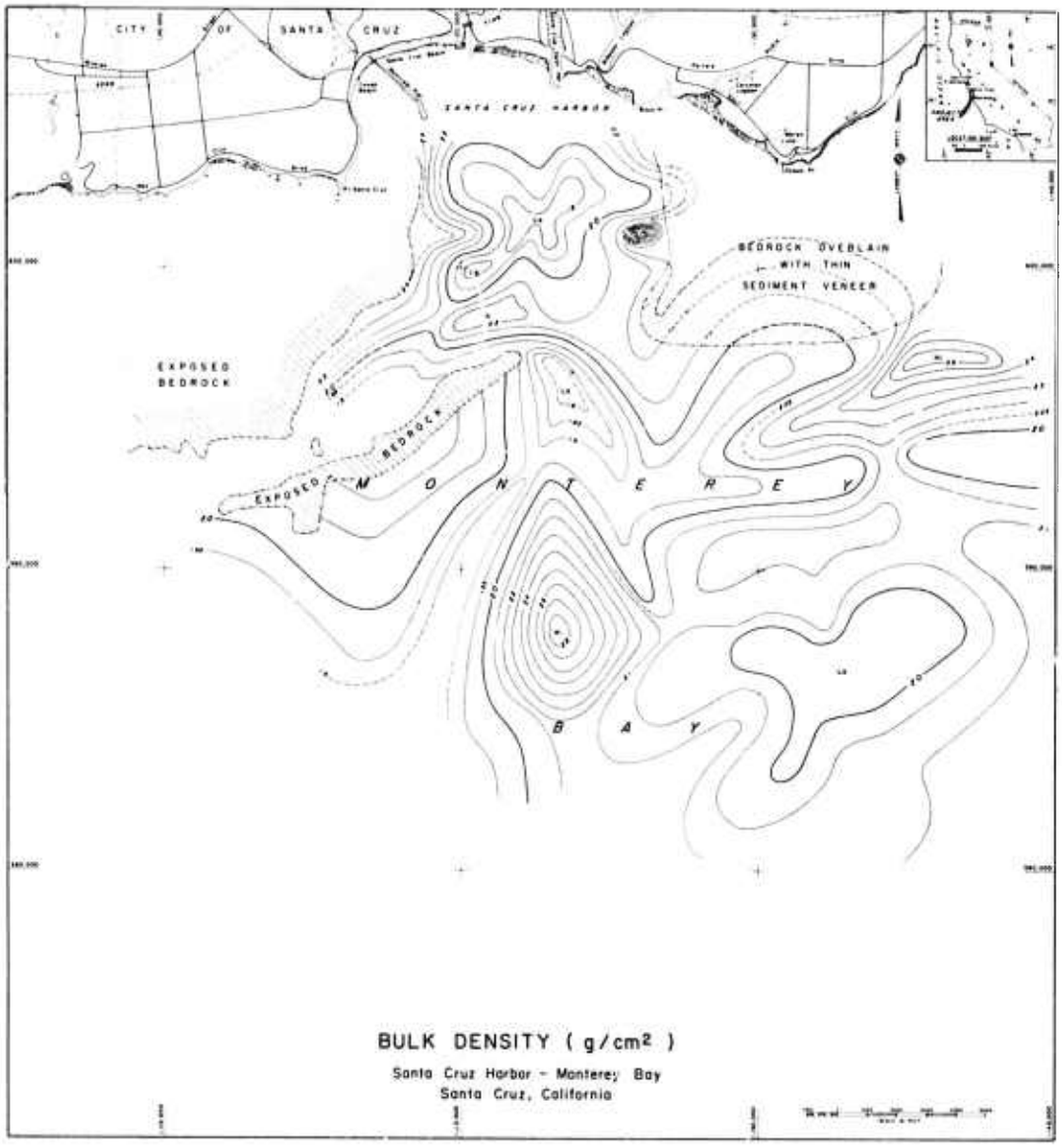

Figure 42. Density distribution — Santa Cruz harbor.

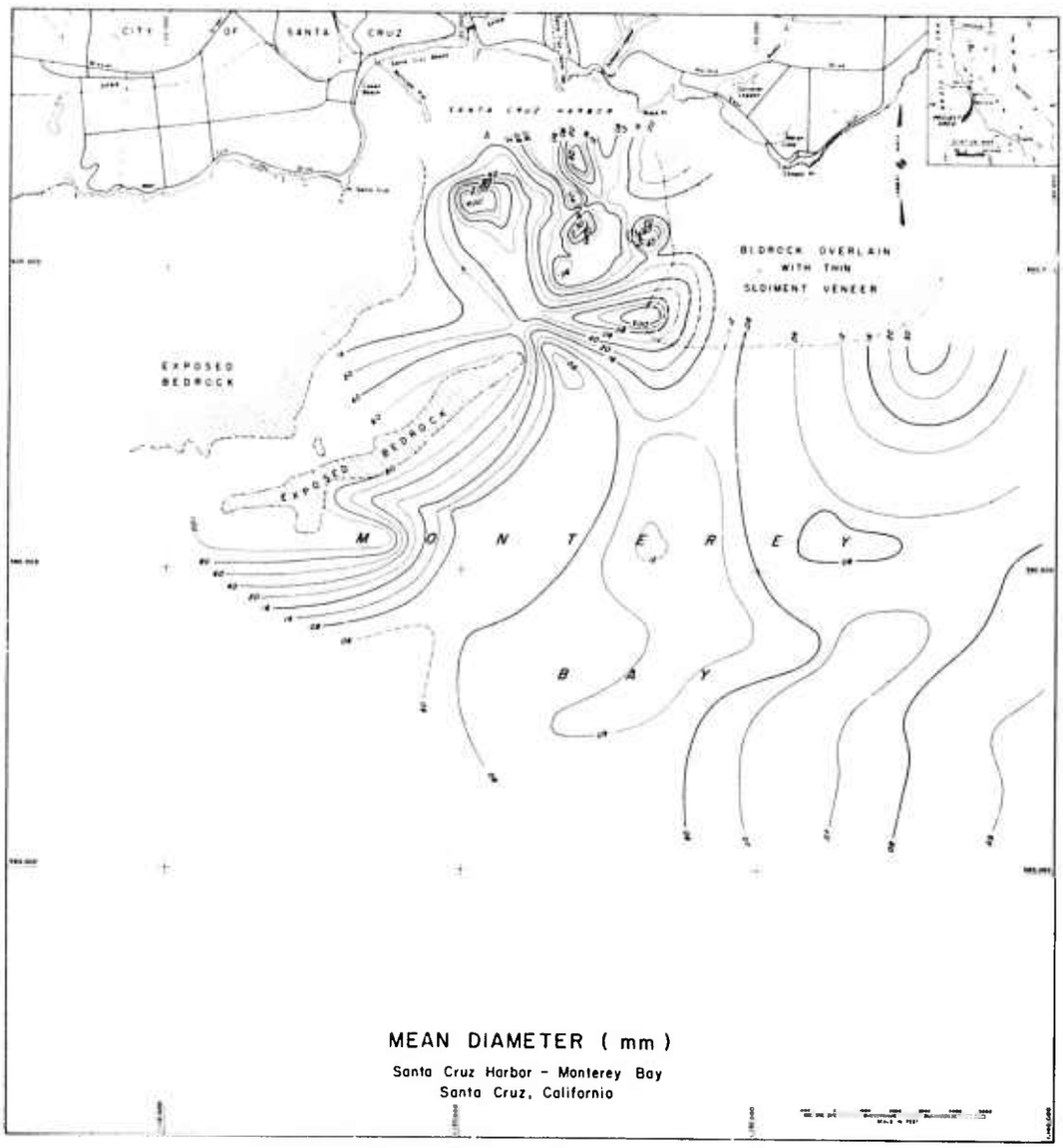

Figure 43. Grain size (mean diameter) distribution — Santa Cruz harbor.

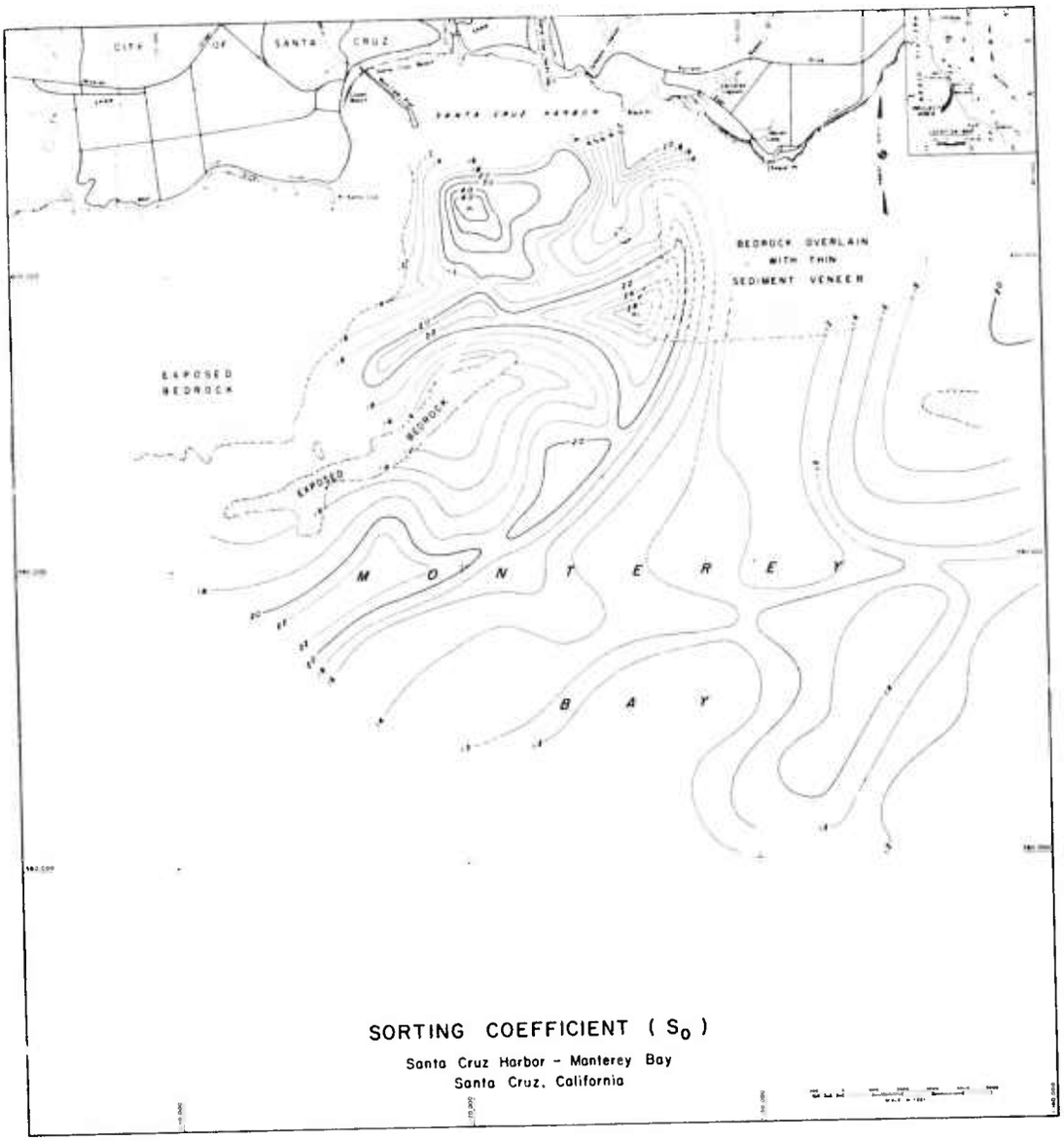

Figure 44. Sorting coefficient distribution — Santa Cruz harbor.

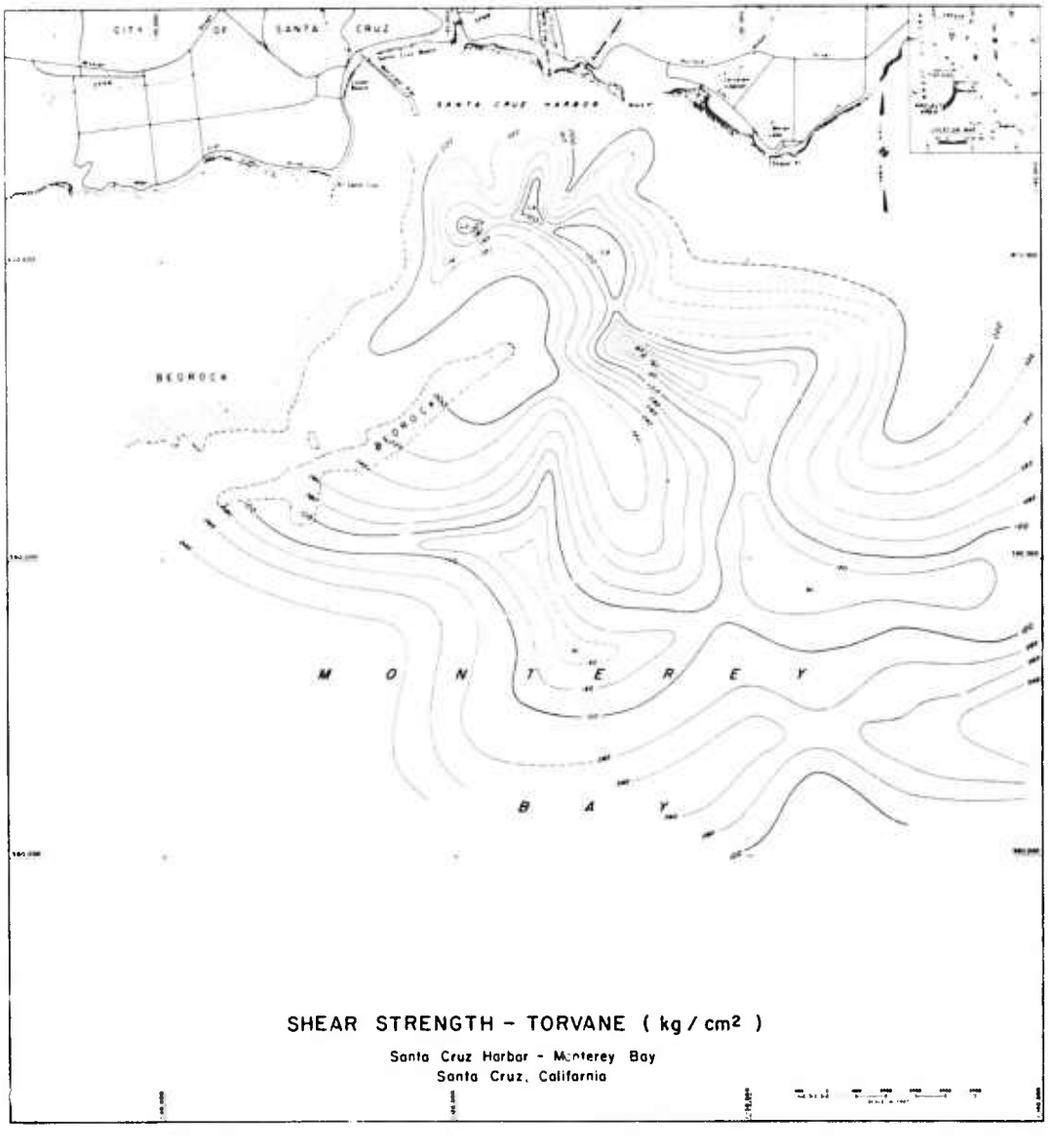

Figure 45. Shear strength (vane shear) distribution — Santa Cruz harbor.

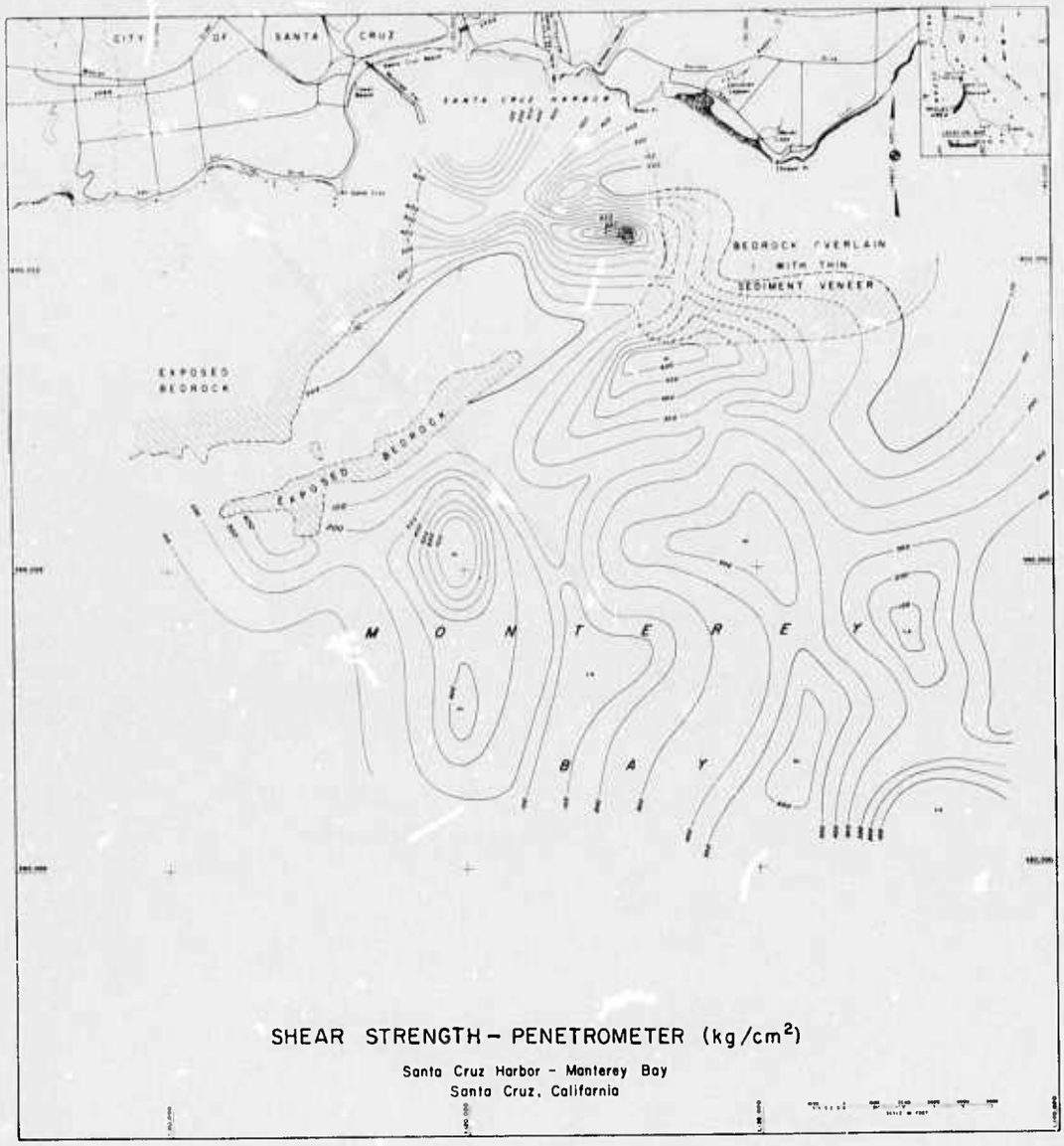

Figure 46. Shear strength (penetrometer) distribution -- Santa Cruz harbor.

Table 2. Correlation Matrix — Sediment Data (Linear Regression Analysis)

Mass Physical and Engineering Properties	Correlation Coefficient	Standard Error of Estimate
Porosity vs:		
Density	0.952	±0.075
Shear Strength (Penetrometer)	0.075	
Shear Strength (Torvane)	0.110	
Grain Size (mean dia)	0.022	
Sorting Coefficient	0.026	
Bulk Density (wet) vs:		
Shear Strength (Penetrometer)	0.117	
Shear Strength (Torvane)	0.091	
Grain Size (mean dia)	0.069	
Sorting Coefficient	0.030	
Shear Strength (Penetrometer) vs:		
Shear Strength (Torvane)	0.317	±0.197
Grain Size (mean dia)	0.082	
Sorting Coefficient	0.005	
Shear Strength (Torvane) vs:		
Grain Size (mean dia)	0.086	
Sorting Coefficient	0.098	
Grain Size (mean diameter) vs:		
Sorting Coefficient	0.830	±0.301

in sampling by core drill from a surface platform at sea. The Monterey Bay study would be incomplete if the sediment dynamics and depositional characteristics were not mentioned. Figure 47 is a map showing the distribution of sediment types in the test area. As can be seen, considerable variation occurs. Figure 48 represents 3-component diagrams of the distribution of sediment types. The distribution was quite different from that found in the San Francisco Bay study (Barnes et al., 1972, p. 125), in which a marked propensity toward finer grained size fractions was noted. Obviously, the forces affecting sediment transport and deposition are different in the two areas. Wolfe (1970), described the effects of the coastal current and swell induced forces on the distribution of sediments in Monterey Bay. The results of his study are shown by vector diagrams that give the direction of major sediment transport in the northern radius. The dominant wave refraction patterns have also been added to provide a complete concept of the dynamics, as shown in figure 49. The deflection of flow by the promontory at Santa Cruz headland

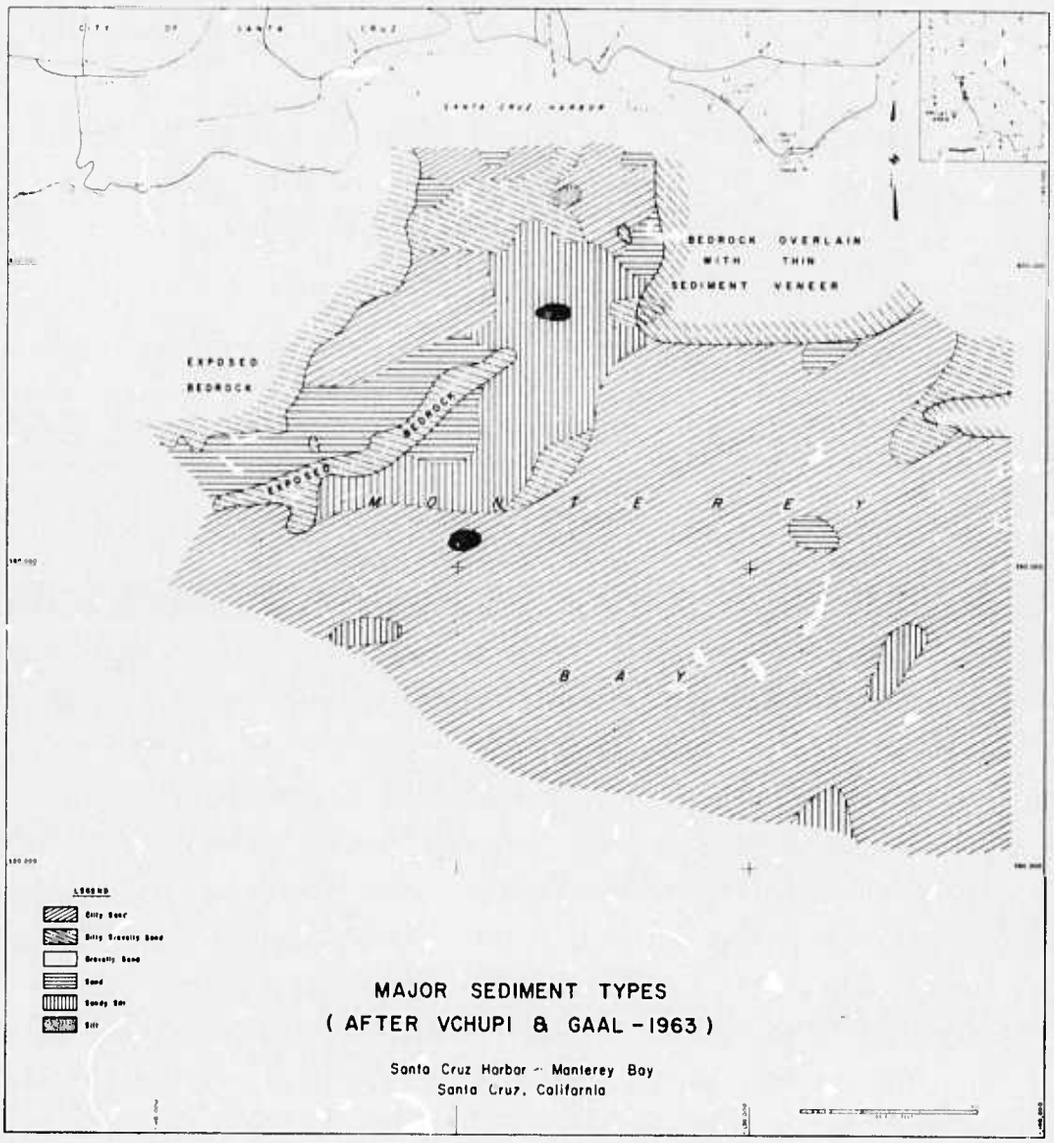

Figure 47. Bottom sediment composition — Santa Cruz harbor.

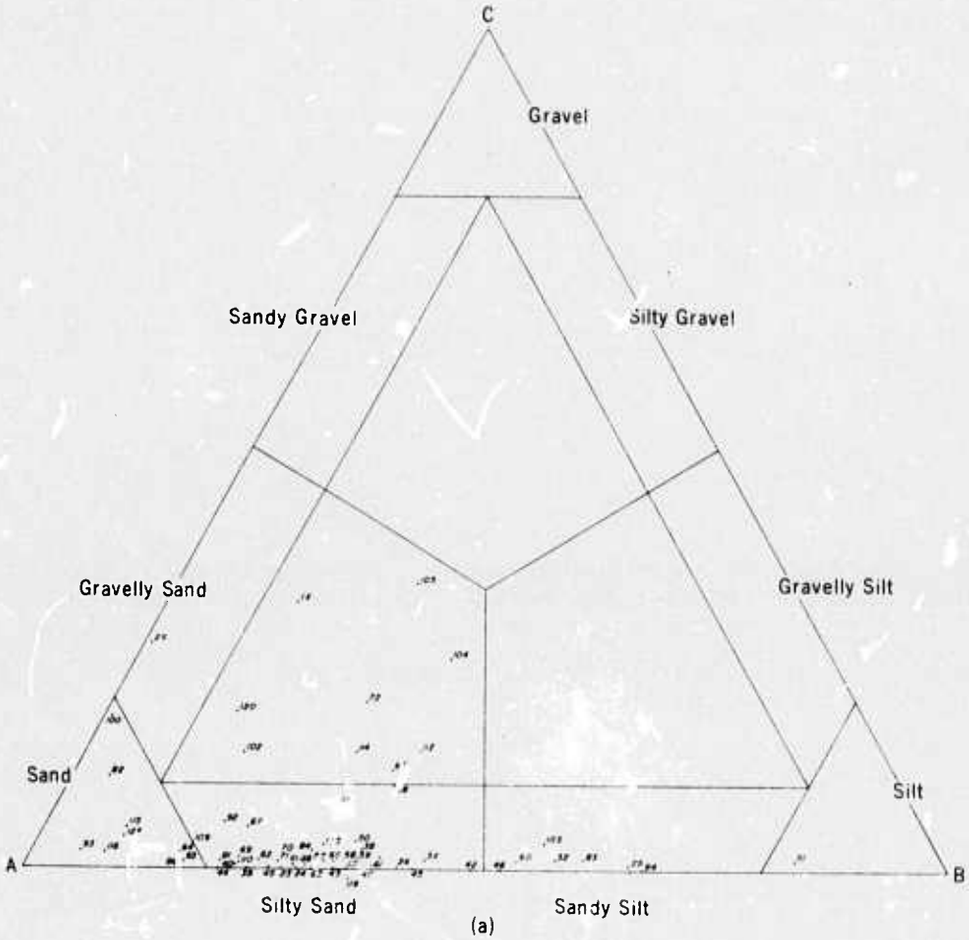

Figure 48. Three-component diagrams sediment types — Santa Cruz harbor.

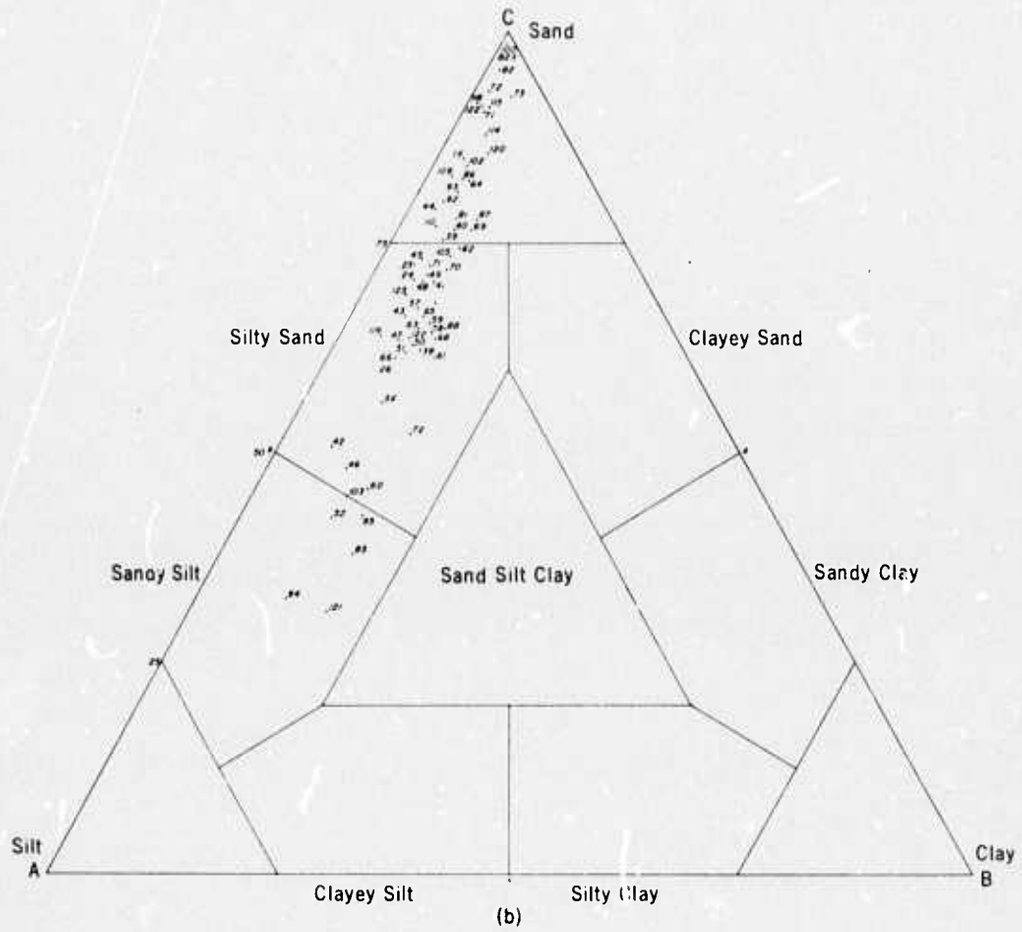

Figure 48. Continued.

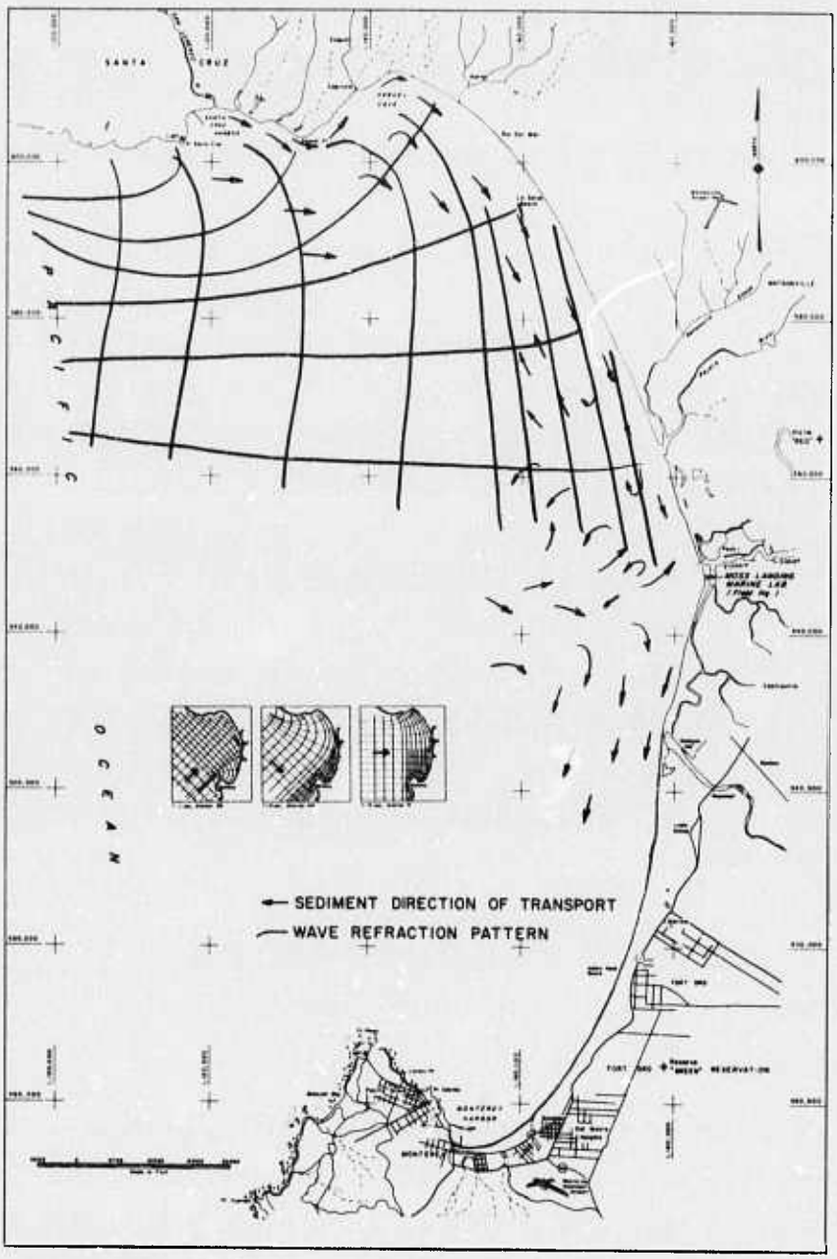

Figure 49. Sediment transport pattern and wave refraction pattern Monterey Bay (after Wolfe, 1970).

coupled with swell-induced bottom currents over submarine topographic obstructions (rock outcrops) have resulted in an erratic distribution of many sediment types in the near shore regions of Santa Cruz harbor. Very poor sorting of sediment grain size combine with a high variability of sediment type. This has resulted in many of the problems of sand deposition in the vicinity of the Yacht Harbor basin entrance (fig. 33), as well as the absence of deposition further south in the beach areas of the city of Capitola.

The area within the 30 ft contour on the bathymetric map (fig. 34) and inward to the shore, could be defined as a secondary circulation cell. It is a type of occurrence more commonly found in estuaries and in closed bays than the offshore areas of the coast. It is only because at the unique set of topographic circumstances, both the marine environment and the shore line that cause such a situation in Santa Cruz harbor. Except for the storm season, very little material is deposited from the rivers that enter the harbor. Nearly all the sediment load is borne in by the longshore current and swell-induced bottom currents. The forces found in the so-called secondary cell existing in the shallow water region, are created out of components of the dominant forces. It is the activity of this subordinate current within the secondary cell that plays the important role in deposition of the sediment load or ultimate transportation to other localized areas along the harbor coastline.

7. GEOPHYSICAL DATA ANALYSIS AND RESULTS

7.1 Continuous Reflection Coefficient Mapping Experiment

7.1.1 Data Reduction Program

Program tasks under a subcontract to the Raytheon Company, Portsmouth, Rhode Island, specified that automatic data processing and reduction be performed on a series of analog acoustic signals acquired in the reflection coefficient mapping experiment. Original specifications of data volume consisted of 222 track miles of acoustic traverse recorded on 7-channel magnetic tape (fig. 32 - Area A). Processing of this data consisted of analyzing sequential sets of 15 acoustic pulses, spaced along a

track line at 600 ft intervals for each of 4 data channels (2 channels of 0-5 kHz signals and 2 channels of 12 kHz signals). Each 4-channel set included therefore, 60 discrete pulses resulting in 2200 sets entailing examination of 132,000 individual pulses (see figs. 50-54).

Statistical analysis also was included on each separate set of data values for the 0-5 kHz and the 12 kHz signals with supporting data involving primarily calculation of water depth, recorder gain variations (acquisition and digital processing gains) and time code indices.

The acoustic data was further processed to yield printout listings and digital tapes delineating the following parameters for each data set:

1. Beginning and ending time code indices.
2. Water depth — 15 individual values with the average range and standard deviation.
3. Computer spherical spreading loss used to compute bottom loss values with the average, range and standard deviation.
4. Sound speed in water column used for depth and spherical spreading loss computations.

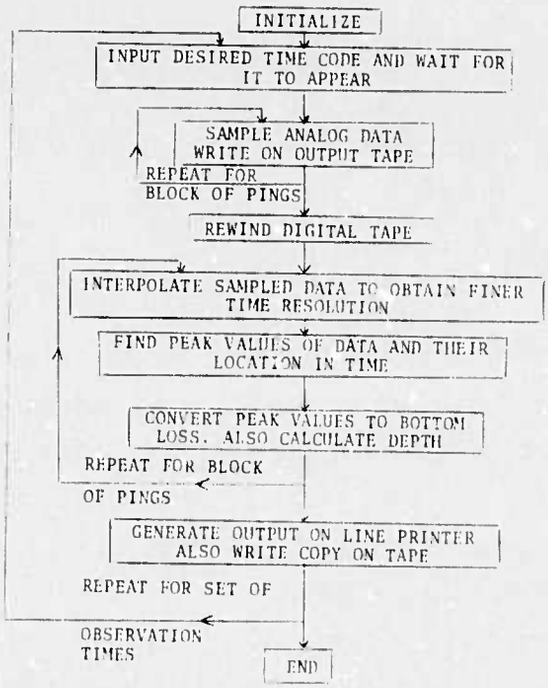

Figure 50. Over-all program flow — computer processing routine.

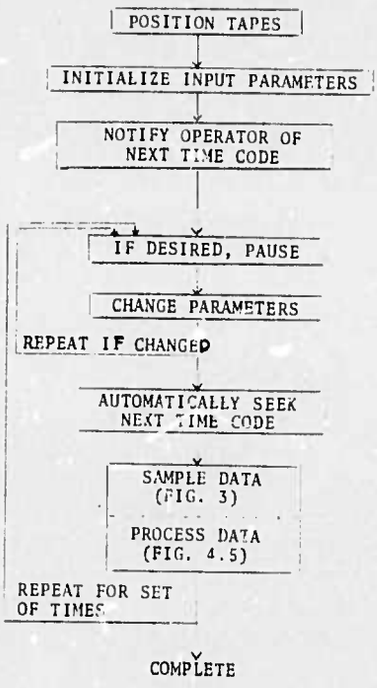

Figure 51. Detail program flow: initialization.

5. Acquisition system gain.
6. Digitizing system gain.
7. Amplitude of individual pulses with the average, range and standard deviation.
8. Bottom loss or reflection coefficient with the average, range and standard deviation.

Initially, processing entailed locating in the seismic wave train, the peak pressure pulse transmitted by the acoustic source and the first seismic reflection event received from the seafloor. The events sampled were located by determining the time interval from transmission to reception of the water path (ray path travel time based on analysis of the 12 kHz wave train) from time domain analysis.

Regarding the quantities, volume, values to be found, and the presentation format, it was mutually agreed with the contractee that due to the experimental nature of the project some flexibility was required. As originally conceived, the analog data acquisition phase was designed to

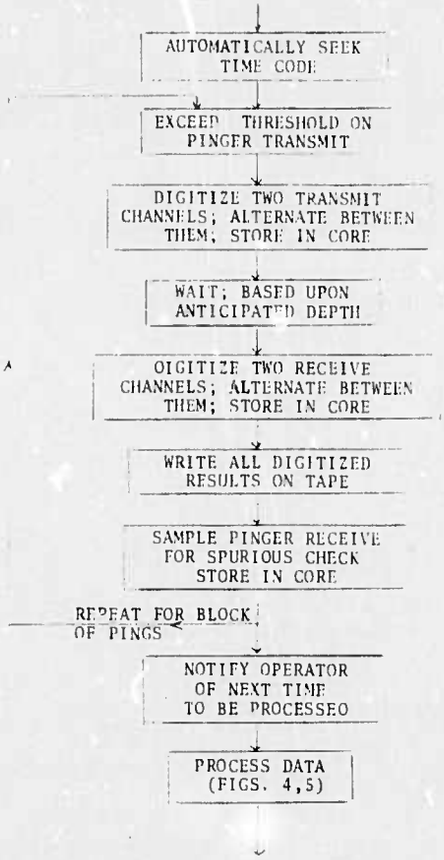

Figure 52. Detail program flow: sample data and save on tape.

acquire simultaneous wave trains (0-5 kHz signals at one per second and 12 kHz signals at 4 per second) with ships speed adjusted in such a manner that a nominal 600 ft track line interval would equal a 1 min processing cycle. Accordingly, machine processing was set to first treat 0-5 kHz signals and then the 12 kHz signal, generating 15 pulse-sets for each, every minute. The actual data acquisition program resulted in both the 0-5 kHz and 12 kHz signals transmitted simultaneously on a one per second basis (section 4.1.3). A slower ships speed also resulted in the 600 ft track line interval being equivalent to a 2 min processing cycle, thus nearly trebling the number of data points acquired.

Further, because of the high variability encountered in the acoustic wave trains and unforeseen problems which resulted from variation in the data acquisition system operation, a preliminary editing cycle on all

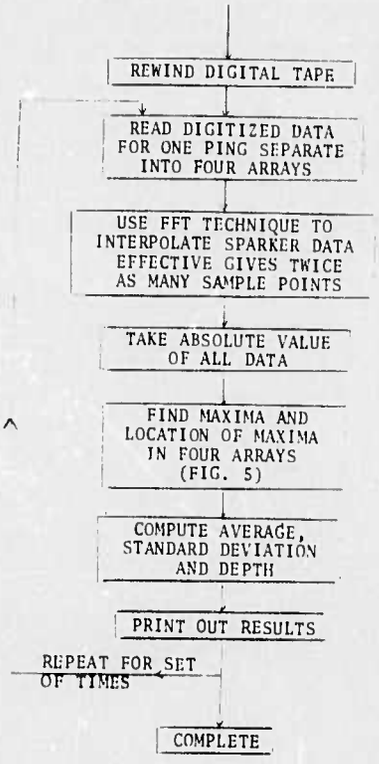

Figure 53. Detail program flow: process data.

data was required. This preliminary editing cycle was necessary to insure that all time intervals specified could in fact be computer processed. Original program scheduling was predicted upon this preliminary editing cycle, having been performed prior to initiation of the processing, but this turned out to be impractical during field operations. The impact of these data acquisition changes resulted in higher cost per processed unit. It was necessary, because of budget limitations, to selectively reduce the volume of data to be processed. Only 40 percent of the total data volume was processed as a result.

An example of the processed data format is presented in table 3. As the volume of processed data in this format is extremely extensive, a data summary was prepared and is included in Appendix A-5.

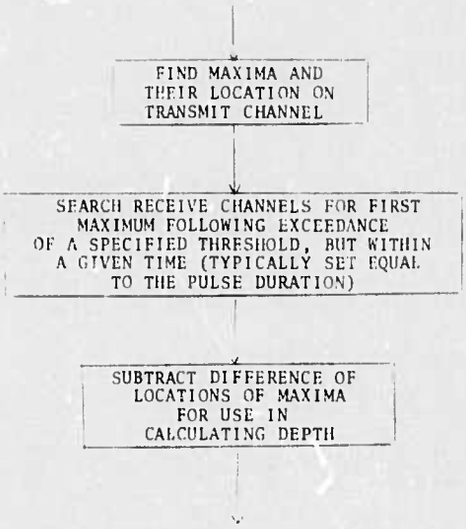

Figure 54. Detail program flow: maxima location.

Digital Processing Objective. Digital processing objectives involved determination for each set of pulse pairs (i.e., i = 1,2 ---15, see table 3) of:

(a) V_{pxi} ≡ peak value of Pinger Transmit,

(b) V_{pri} ≡ peak value of Pinger Receive,

(c) t_i ≡ time difference between Pinger, transmit and Pinger Receive

(d) V_{sxi} ≡ peak value of Sparker Transmit,

(e) V_{sri} ≡ peak value of Sparker Receive,

and calculate

(f) D_i ≡ water depth.

Table 3. Data Format for Computer Processed Acoustic Data — Reflectivity Experiment

ROLL NUMBER 24
DATE 07/25/72
TIME 17.09.53
PINGER REFLECTION COEFFICIENT = .890 (.137)
SPARKER REFLECTION COEFFICIENT = .596 (.091)
WATER DEPTH = 81.4 (.5)
VEL = 4800 FT/SEC
PINGER GAIN = 20X
PINGER DZONE MAX = .33 V

	AVE.	SIGMA	MAX.	MIN.	PULSE NUMBER 1	2	3	4	5	6	7	8	9	10	11	12	13	14	15
PING XMIT	1.08	.05	1.12	.93	1.10	1.04	1.09	1.08	1.10	1.09	1.10	1.11	1.02	1.12	.93	1.10	1.08	1.07	1.11
PING REC	1.13	.16	1.30	.73	1.18	1.23	.84	.98	1.27	1.13	1.30	1.15	.73	1.23	1.24	1.19	1.24	1.23	1.09
PING REFL	.890	.137	1.131	.603	.902	.990	.651	.753	.973	.865	.993	.870	.603	.923	1.131	.924	.978	.961	.829
PING RL	1.1		4.4	-1.1	.9	.1	3.7	2.5	.2	1.3	.1	1.2	4.4	.7	-1.1	.7	.2	.3	1.6
SPKR XMIT	.67	.06	.78	.57	.71	.62	.78	.67	.72	.67	.61	.62	.70	.59	.66	.64	.66	.74	.57
SPKR REC	.30	.03	.35	.24	.30	.35	.27	.24	.34	.28	.32	.30	.28	.26	.28	.33	.30	.27	.31
SPAR REFL	.596	.091	.742	.453	.552	.742	.453	.479	.630	.554	.699	.639	.532	.590	.568	.684	.601	.485	.731
SPKR RL	4.6		6.9	2.6	5.2	2.6	6.9	6.4	4.0	5.1	3.1	3.9	5.5	4.6	4.9	3.3	4.4	6.3	2.7
WATER DPTH	81.4	.5	82.5	80.7	81.4	81.2	81.0	80.7	81.4	81.8	81.5	81.2	81.4	81.4	82.0	82.3	82.5	81.0	81.5

ROLL NUMBER 24
DATE 07/25/72
TIME 17.10.53
PINGER REFLECTION COEFFICIENT = .880 (.101)
SPARKER REFLECTION COEFFICIENT = .619 (.076)
WATER DEPTH = 81.9 (.5)
VEL = 4800 FT/SEC
PINGER GAIN = 20X
PINGER DZONE MAX = .30 V

	AVE.	SIGMA	MAX.	MIN.	PULSE NUMBER 1	2	3	4	5	6	7	8	9	10	11	12	13	14	15
PING XMIT	1.10	.02	1.14	1.06	1.12	1.08	1.10	1.09	1.09	1.08	1.09	1.10	1.11	1.14	1.12	1.10	1.07	1.07	1.06
PING REC	1.14	.13	1.29	.81	1.22	1.23	1.16	1.05	1.11	.81	1.21	1.29	1.28	1.18	.97	1.01	1.21	1.14	1.23
PING REFL	.880	.101	.985	.642	.921	.964	.885	.819	.86	.642	.934	.984	.974	.882	.728	.770	.951	.896	.985
PING RL	1.2		3.8	.1	.7	.3	1.1	1.7	1.	3.8	.6	.1	.2	1.1	2.8	2.3	.4	1.8	.1
SPKR XMIT	.67	.06	.78	.56	70	.71	.66	.68	.66	.75	.67	.62	.68	.56	.78	.70	.58	.65	.69
SPKR REC	.31	.03	.38	.24	30	.31	.30	.24	.29	.30	.32	.28	.30	.31	.34	.38	.31	.31	.37
SPAR REFL	.619	.076	.744	.476	.67	.584	.604	.476	.594	.534	.641	.601	.591	.744	.572	.715	.712	.634	.721
SPKR RL	4.2		6.5	2.6	4.9	4.7	4.4	6.5	4.5	5.5	3.9	4.4	4.6	2.6	4.8	2.9	2.9	4.0	2.8
WATER DPTH	81.9	.5	83.0	81.0	81.8	82.0	81.5	82.0	82.3	83.0	81.8	81.0	81.5	82.3	81.7	81.2	81.5	81.7	82.3

Using these values, perform

(1) Pinger reflection coefficient:

$$G_p(D_i-1.83)(V_{pri}/V_{pxc}), \text{ and} \tag{33}$$

(2) Sparker reflection coefficient, where G_p and G_s are defined as respective system acquisition and digitizing gains:

$$G_s(4D_i^2+832)^{\frac{1}{2}}(V_{sri}/V_{sxi}). \tag{34}$$

In addition calculate:

(3) Pinger Bottom Loss:

$$-20 \text{ Log}_{10} R_{pi}, \text{ and} \tag{35}$$

(4) Sparker Bottom Loss:

$$-20 \text{ Log}_{10} R_{si}. \tag{36}$$

Having completed these determinations, statistically treat each of the resulting nine arrays as follows:

Defining each array as A_j (j array),

$$A_j \quad j = 1,2,\ldots 9$$

and each element within these arrays as a_{ij} (i^{th} element), calculate

$$\bar{A}_j = \frac{1}{15} \sum_{i=1}^{15} a_{ij} \quad \text{(average)}, \tag{37}$$

Maximum and Minimum (range), (38)

$$\sigma A_j = \left(\frac{1}{14} \sum_{i=1}^{15} (a_{ij} - \bar{A}_j)^2\right)^{\frac{1}{2}} \quad \text{(standard deviation)}. \tag{39}$$

For these analyses, a processing cycle time of 1 min was used where the first pulse pair (i=1) occurred 7.0 sec before the listed time code. The results of these determinations and calculations were output in the format presented in table 3.

Digital Processing Techniques. As outlined above, there were 5 basic wave form parameters to be determined for each of the 15 pulse pairs within each pulse set (V_{pxi}, V_{pri}, V_{sxi}, V_{sri}, t_i). Having determined these parameters, a series of subsequent data reduction steps were performed to obtain the remaining arrays of required output information (i.e., D_i, $\bar{D}$, σ_o, R_{pi}, $\bar{R}_p$, $\bar{R}_s$,...etc.)

The general program structure was constructed to process a basic block of 15 pulse pairs per set; each pulse pair was comprised of a transmit pulse and a received pulse from two distinct acoustic systems. For each of the two acoustic systems, (a 0-5 kHz system and a 12 kHz system) we ascertained the maximum value of the transmitted wave forms envelope, the maximum value of the received waveforms envelope, and, in the case of the 12 kHz system, the time difference between these transmit and receive maximums. Having determined these values, the reflection coefficients and bottom losses as defined in equations 33 through 36, were computed.

Data Format. The original analog signal format suggested two acoustic systems transmitting at a repetition rate of 1:4 with the pinger system having the higher repetition rate. Employing this format, the maximum available analog-to-digital conversion rate of 30 kHz could be applied to each of the four waveforms of interest on a non-interfering basis. Specifically, the bandwidth of the 0-5 kHz; is nominally 5 kHz; the 12 kHz approximately 2 kHz. A 30 kHz sampling rate was thus sufficiently above the Nyquist rate to insure individual maxima to be determined with little or no error.

The suggested analog signal acquisition format was not achieved as system design constraints necessitated both systems transmitting synchronously at one per sec repetition rate. As a consequence, the 30 kHz sampling rate had to be alternated between the Pinger and Sparker channels, which resulted in an equivalent 15 kHz sampling rate per channel. For the 12 kHz system that had a 2 kHz bandwidth, the 15 kHz sampling rate still

allowed the maximum to be determined directly. For the 5 kHz system, however, it was necessary to use an FFT interpolation technique to obtain the required degree of time resolution.

As a further complication, the signal of the analog data was difficult to decipher because of either transient noise or multiple reflections. The simple routine of finding the maximum within a given observation window could not be routinely applied. To insure data quality, a modified receive-search procedure was developed in which the received data was scanned in time until a preset threshold value was exceeded, indicating the leading edge of the returning pulse. The procedure then selected the largest value occurring in the next τ sec (τ approximately equal to the transmit pulse deviation), storing this value as the received maximum.

Further, provisions were made to add a small sample of the pinger return during the time it should have negligible amplitude (i.e., during the "off" period). The maximum of these samples, essentially system background noise, also is presented. Large values suggest periods of spurious data.

Processing Parameters. To maintain processing flexibility, attempts were made to make all key parameters detailed selectable at runtime.

Sampling Data — The sample rate, sample size, and onset threshold level are selectable.

Check Data — The check sample size and the channel examined (of the four) can be specified.

Block Size — The number of pings examined can be varied.

Receive Parameters — The onset threshold (within the data acquisition window) and the subsequent time to find a maximum are selectable. This permitted observation of the waveforms on the scope and established a threshold which lies above the noise level yet assures detection of the return.

Anticipated Depth — The receive data observation window must be wide enough to accomodate any depth variations from one block of pulse sets to the next. This window is automatically positioned for the next block of pulse sets by using the previously calculated depth. Its location is held constant for a given block of pulses.

For the initial block, the program accepts the operator's estimate of this initial depth, requiring for input the observed return time as seen on the scope.

Miscellaneous Constants — Also accessible at run-time are several other constants. Included are: the speed of sound; a pinger gain factor related to attenuator settings during record, and a scale constant for each receive channel.

The following parameter values (one exception discussed below) were used during processing:

sample rate	=	30 kHz
sample size	=	256 samples
check sample size	=	15 samples
number of pings	=	15
observe block every	=	1 minute
receive peak sample size	=	10 samples
speed of sound	=	4800 ft/sec.

Occasionally, shallow water required a smaller sample size (128 instead of 256). This was necessary since the transmit observe windows would be of length 1/30,000 (sample rate) by 2 (alternate sampling) by 256 (number of samples) = 17.7 m sec or a depth of 41.5 ft. Thus, one could not begin observing the receive channels until after the primary returns had arrived. By decreasing the sample size to 128, depths as small as 20.8 ft could be processed. Under this condition, however, the observation window is only ± 10.4 ft (as opposed to ± 20.8 ft) so that the depth variations had to be closely monitored.

Detail Program Flow Diagrams. Figures 40 through 44 present a detailed breakdown of the overall program flow presented in figure 40.

7.1.2 Summary of Processing — Comments and Findings

The tables 4 and 5 outline in summary form first the requested times to be processed along with the actual times processed, and second, a copy of the log made out at the time of processing. As a general comment, the actual time required to process any given block of required times varied from 1:1 to 2:1 with a general average of 1.5:1 necessitated by the required preprocessing editing.

Table 4. Processing Specifications

Roll No.	Requested Times	Total	Actual Times Processed	Total	Comments
001	175553-190353	69	175553-190353	69	
002	164753-173553	49			Possibly 10 mins processable
003	173953-180953	31	173953-174453	6	
	183153-190353	33	175253-180953	18	
			183253-184153	10	
			184453-190353	20	
004	153353-162953	55	153353-162953	55	
006	164553-173953	55	165753-173953	43	
	175153-182353	33	175153-182353	33	
017	143753-153653	60	143753-153653	60	
018	162553-164353	19	162953-164353	15	
	174153-175753	17	174153-175753	17	
019	180953-181953	11	180953-181953	11	
020	151753-160153	45	151853-155353	36	
	160753-164553	39	160753-164553	39	
021	152353-162553	63	152353-162553	63	
022	165653-181953	84	165653-181953	84	
023	190353-195753	55	190353-195753	55	
024	162553-170553	41	162553-170553	41	Long Form only
	170953-174753	39	170953-174753	39	
025	180053-181353	14	180053-181353	14	
	160953-165153	43	160953-165153	43	
026	172353-184453	82	172353-184453	82	
027	184753-190753	21	185653-190753	12	
	155753-164153	45	155853-164153	44	
028	165753-174753	51			Inverted Tape
	180753-182153	15			Bad Tape
029	182553-193353	69	183353-193353	61	
030	163153-174153	71	163153-174153	71	
031	174553-181753	33	175153-181753	27	
	192153-201753	57	192153-201753	57	

Table 4. Processing Specifications (Con't)

Roll No.	Requested Times	Total	Actual Times Processed	Total	Comments
032	171753-182153	65	171753-182153	65	
033	182453-184553	22	183153-184553	15	
	185153-200053	70	185153-200053	70	
034	165553-170953	15	165553-170953	15	
035	171153-180353	53	172153-180353	43	
	185153-193153	41	185153-193153	41	
036	193553-195953	25	194053-195953	20	
	174253-175953	18	174253-175953	18	
037	192553-201353	49	192553-201353	49	
038	201753-202753	11	202353-202753	5	
	203553-204153	7	203553-204153	7	
	204953-214353	55	205053-214353	54	
039	171453-180353	50	171453-180353	50	
041	160753-165953	53		0	Sparker channel
042	170953-180353	55		0	Not processable
046	154453-162353	40		0	"
047	163553-170353	29		0	"
	170953-180653	58		0	"
048	181953-185153	33			
	185953-191753	19		0	"
	192353-195753	31			
049	154553-164153	57		0	"
	164653-165553	10			
050	170753-180753	61		0	"
	181553-183553	21			
051	184753-193853	52		0	"
	194753-201553	19			
052	202553-211153	47		0	"
054	182753-183953	13		0	"
055	185153-190553	15			Bad Sparker
	190753-194053	34			
	194353-201753	35			

Table 4. Processing Specifications (Con't)

Roll No.	Requested Times	Total	Actual Times Processed	Total	Comments
058	182153-185353	33	182153-183553	15	
	185753-193553	39	185753-193553	39	
			183753-185353	17	Long Form only
059	194753-202153	35	194753-202153	35	
060	170953-173753	29			Bad Sparker

Data Summary, Short Form. A summary form of all the processed data generated per table 3 is contained in the Appendix A-5. The summary sheets present the numeric values of the average reflection coefficient and one standard deviation for both Pinger and Sparker signal systems, together with the average bottom loss values as a function of data and time code index.

7.1.3 Correlation of Reflectivity to Sediment Properties

Regression analyses were done by computer processing to determine the correlation coefficients for the 12 kHz and 0-5 kHz acoustical data to the sediment data. The Rayleigh Reflection Coefficients and bottom loss values taken over areas circumscribed about each core site were, respectively, averaged for a representative value that was applied to each of the core site locations. The core sites each were thus referenced by respective acoustical and sediment property values or datums. These data were then cross-correlated and correlation coefficients obtained through the regression analyses. The objective was to relate the degree

Table 5. Shipboard Data Analysis and Commentary Log

Roll No.	Findings	Comments
001	Cal's ok. Good data. Few drop-outs. Added -10 dB to pinger channels	Good run with very few few drop-outs.
003	Calibration signals on during time required for processing. Added -10 dB to Pinger channels. Reasonable data.	Segmented Runs: a/. 173953 174433 Cal's 1745 - 1751 b/. 175253 - 180953 c/. 183253 - 184153 Sparker bad 1842, 43 d/. 184453 190353
004	Cal's ok. Deep water, multiple drop-outs. Pinger transmit low. Added -10 dB to Pinger channels	Processed complete run drop-outs could not be picked up due to poor S/N.
006	Calibration signals on during time requested for processing. Not possible under present program configuration. Added -10 dB to Pinger channels. Large interference spiker in Pinger Rec. Sparker Rec. drop-outs.	Segmented Runs: a/. 165753 173953 Cal's 1646 1656 Inter. 1710 1712 b/. 175153 182353 Many data drop-outs.
017	Cal's ok. Reasonable data. Few drop-outs. 10 dB in Pinger channels.	Processed complete run
018	Cal's on during requested times. Time-code drop-outs. Multiple Pinger Rec. drop-outs. Added -4.0 dB to Pinger channels	Segmented Runs: a/. 162953 164353 Cal's on to 1629 b/. 174153 175753 Multiple drop-outs
019	Cal's ok. Reasonable data added -4.0 dB to Pinger channels.	180953 181953
020	Cal's ok. Data starts 150805 Time-Code skip Sparker Transmit funny 155853. End on 155353 Problems after with Sparker. Added -4.0 dB to Pinger channels	151953 155353 Reasonable data. Will review problems at later date.
020	155433-160153 Sparker very erratic. -10 dB in Pinger channel	Unable to auto process
020	160753-164653 Sparker problems. Time Code drop-outs. Very difficult to process -10 dB in Pinger channel	Segmented Runs: a/. 160753 161253 ok b/. Missed 161353-162953 Sparker Transmit and Time Code problems c/. 163053-164653 ok Sparker acting funny
021	Cal's ok. Time Code out 161253, 13. Funnies on tape -10 dB Pinger channels.	Processed complete run

Table 5. Shipboard Data Analysis and Commentary Log (Con't)

Roll No.	Findings	Comments
022	Cal's ok. Pinger transmit loss Sparker low. Added -10 dB Pinger channels.	Processed complete run
023	Cal's ok. Reasonable data. Few drop-outs. -10 dB Pinger channels.	Processed complete run
024	Cal's ok. Reasonable data. Few drop-outs. -10 dB in Pinger channels.	Processed complete run
025	Cal's checked. Pinger Xmit Low (3.0 Vp) Sparker Xmit high (5.0 Vp) 800j source. -10 dB in Pinger channels. Sparker data erratie and multiple drop-outs. Time Code drop-outs.	Segmented Runs: a/. 180053 181353 high sparker, low Pinger b/. 160953 - 165153. Levels ok, but returns erratic. Questionable sparker data run a/.
026	Cal's checked. Both Pinger and Sparker Xmit's low at beginning of run. -10 dB in Pinger ehannels. Pinger Xmit about normal at end of run.	Processed complete run
027	Cal's cheeked. Cal's on during time required to be proeessed. -10 dB Pinger ehannels. Highly variable sparker data Time Code skips. Good levels.	Segmented Runs: a/. 185653 - 190753 Cal's on in beginning b/. 155853 164153 Tape on 155803 variable data, missed 162053, and 162553
028	Tape from net re-wound. Rewound tape. Findings; channels 1. Noise 2. Time Code 3. Noise 5. Pulsed data, but not of the normal form.	Tape to be re-examined later.
029	Cal's eheeked ok. On until 183300 Pinger Xmit low. -10 dB in Pinger ehannels. Time Code Skips 190453.	Segmented Runs: a/. 183353 190353 b/. 190553 193353
030	Cal's ok. Pinger low -10 dB Pinger ehannels	Processed complete run
031	Cal's eheeked but Pinger still low. -10 dB in Pinger ehannels. Cal's on during data. 175153 variable returns	Segmented Runs: a/. 175153 - 181753 b/. 192153 - 201753
032	Cal's cheeked, Pinger low. -10 dB in Pinger ehannels. Very erratic sparker.	Segmented Runs: a/. 171753 - 175253 b/. 175353 - 182153
033	Cal's ehecked. Pinger low. Cal's on during data 183153. Very poor sparker data? Highly variable. Pulse Rep. rate erratic. Time Code skips. Diffieult tape.	Segmented Runs: a/. 183153 - 184553 b/. 185153 - 200053 Difficult Tape!

Table 5. Shipboard Data Analysis and Commentary Log (Con't)

Roll No.	Findings	Comments
034	Cal's checked, Pinger low, Pulse Rep. erratic. -10 dB in Pinger channels.	Completed
035	Cal's checked. Levels wavered in time Ch #1 and #5. Rep. rate erratic. Cal's on during times requested. -10 dB in Pinger.	Completed. Segmented Runs.
036	Cal's checked. -10 dB in Pinger, Cal's on during time requested. Pinger drop-outs	Completed, Segmented runs a/. 194053 - 195953 b/. 174253 - 175953
037	Cal's checked. Erratic Rep. Rate -10 dB Pingers	Processed complete run.
038	Cal's checked. On during time requested. -10 dB Pinger very low Pinger Xmit.	Difficult tape. Segmented runs.
039	Cal's checked. Pinger low. Pinger Xmit 2.0 Vp off tape, Big change 174853. Time Code skips.	Difficult tape. Completed Run.
041	041 052 Sparker Xmit Missing	
054	No Sparker Transmit Total Tape	Pinger channels ok. could process with additional software development.
055	No Sparker Transmit Total Tape	Same as 054
058	Calibration ok. Reasonable data same pinger Rec. drop-outs ≈184000. Pinger Rec. channel too high. Added -10 dB to both Transmit and Receiver data Pinger Gain change at 183700.	Segmented Runs: a/. 185800→193600 Wrong gain factor used, should have been X1. Requires sealing. b/. 182153→183553 Time Zero of processing 000053. c/. 183653→185353 Some Pinger Rec. drop-outs.
059	All channels present with Cal's	Water depth became less than 40'. Required Segmented runs.
060	No Sparker Transmit Total Tape	Same as 054

of correlation between acoustical properties (bottom loss and reflection coefficient) calculated from the peak amplitudes generated in the input-response function of the two sources to parameters measured in the sediment analyses (i.e., porosity, density, mean diameter, sorting coefficient, bearing capacity, and shear strength). No edit of the data was accorded

as to number of samples taken, other than to restrict the area of influence about a core site. This area was defined by drawing circles about each core site to a radius that would produce tangency to circles scribed about adjacent core sites. Since the core hole spacing was uniform in pattern within the high density area and low density area, the areas of influence for the statistical sample were uniformly the same within the two densities. Corrections were made on the acoustic data for obvious wild point values because of errors incurred in the analog to digital conversion. In such cases, the reflection coefficient and corresponding bottom loss values were recomputed.

The correlations obtained from the first analysis, which incorporated the entire area surveyed, are reflected in the correlation matrix given in table 6. Plots of the data represented in the mathematical correlation are shown in figures 55 through 66. One can immediately see the

Table 6. Correlation Matrix — Acoustic and Sediment Properties

VARIABLE NUMBER	1	2	3	4	5	6	7	8	9	10
1	1.000	-.963	.111	-.085	.120	.014	-.006	-.009	-.133	-.131
2		1.000	-.173	.039	-.041	.066	.030	.004	.080	.087
3			1.000	.266	-.114	-.074	-.294	-.088	.138	.145
4				1.000	-.083	-.047	-.051	.142	.046	.067
5					1.000	-.217	-.195	.093	.097	
6						1.000	.141	.129	-.278	-.262
7							1.000	.841	-.657	-.625
8								1.000	-.642	-.620
9									1.000	.989
10										1.000

BMD02R - STEPWISE REGRESSION - VERSION OF APRIL 13, 1965
HEALTH SCIENCES COMPUTING FACILITY, UCLA

PROBLEM CODE	ARPA
NUMBER OF CASES	42
NUMBER OF ORIGINAL VARIABLES	10
NUMBER OF VARIABLES ADDED	0
TOTAL NUMBER OF VARIABLES	10
NUMBER OF SUB-PROBLEMS	24

VARIABLE		MEAN	STANDARD DEVIATION
PROSTY	1	44.03357	4.80310
DENSTY	2	2.08262	.19319
PNITMR	3	.27602	.20130
T-VANE	4	.09076	.10524
M-DIA	5	.20355	.32998
SORT C	6	1.45900	.32749
SKR BL	7	5.42912	.73977
SKR WO	8	5.67864	.85959
PGRRFL	9	1.13074	.22659
PGR WO	10	1.11633	.23224

results show very poor correlations exist. Another representation of the data is given in the contoured maps of bottom loss versus sediment properties in figures 67 and 68. Comparison of the surface distribution of acoustical properties derived from the two sources to any one of the mass physical properties and/or engineering properties again gives little indication of positive correlations. Greater resolution of the acoustical distribution over the entire survey area is shown in figures 69 and 70 for selective comparison to figures 41 - 46.

The results of the correlation represent a marked contrast to the previous results obtained in the San Francisco Bay study (Barnes et al., 1972) and other studies (Breslau, 1964, 1967). Correlation coefficients derived from other studies of acoustics using a pinger acoustic source (12 kHz) and the broad band sparker (0-5 kHz) source are shown in table 7. The difference in the results of previous studies and the Monterey Bay study may be attributed to several causes, each of which bears more data processing of existing data than could be accomplished in the time span of this study. Some of these probable causes can be enumerated as; (1) too large an area was taken for the representative statistical sample; (2) sediment velocity variability in the near shore region may be more severe than assumed; (3) the changing water depth coupled with topography changes over short distances may have altered normal incidence path between source and reflector; (4) stability of the source-receiver systems in a surface towed configuration.

An attempt was made to delve into each of these probable causes. The best explanation of the analysis can be made by drawing an analogy between the San Francisco Bay study and this study. The first of which can be drawn on the basis of size of area surveyed. The previous study encompassed a relatively small area containing approximately 1.5 sq miles (1 mile by 1.5 miles), while this study encompassed nearly 30 sq miles (5 miles by 6 miles). Although the control for navigation-positioning and line density and core site patterns was constant in both stations, variability of sediment type was much greater in Monterey Bay as well as the variability of water depth and the range of water depth. The previous study contained sediments that consisted mainly of fine grained silt and

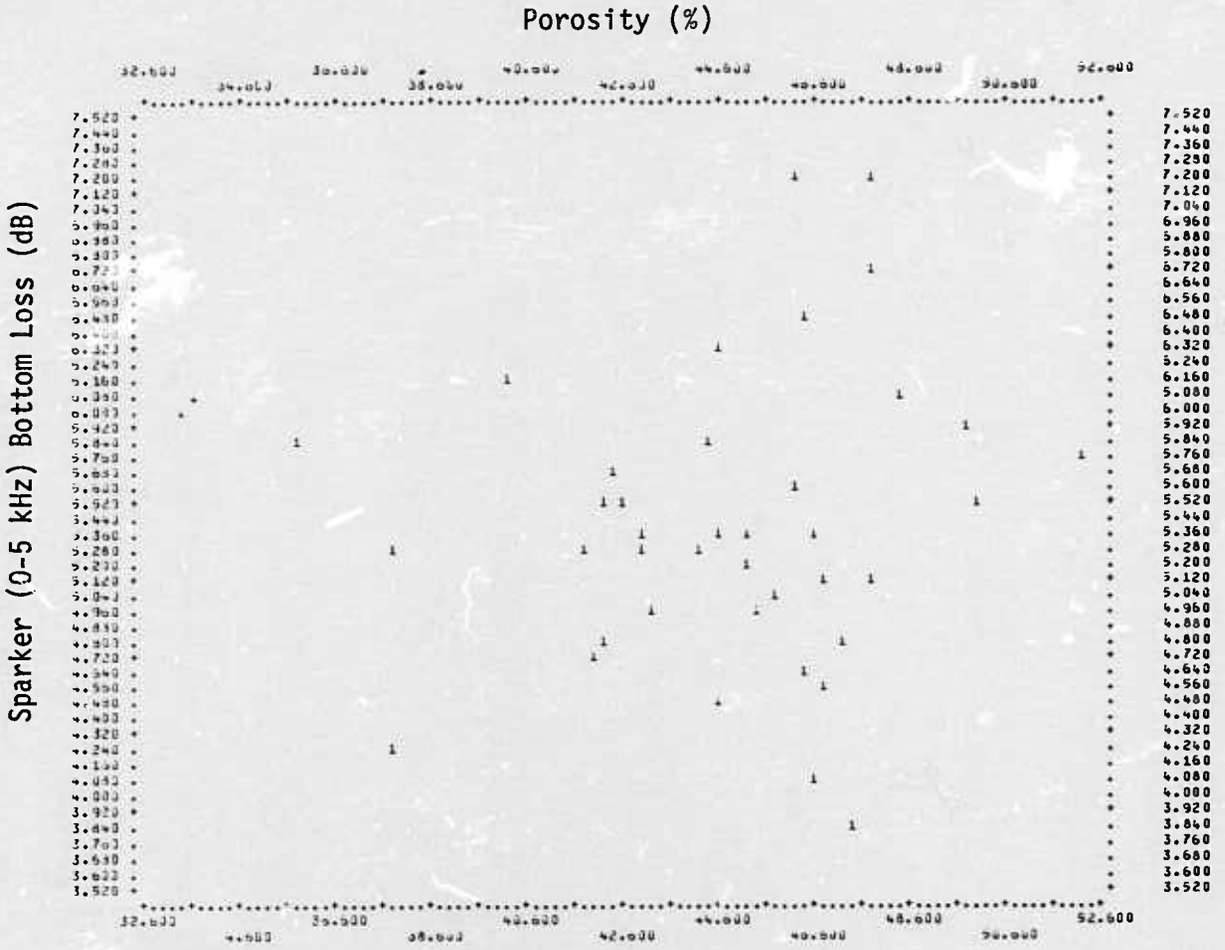

Figure 55. Plot of bottom loss (0-5 kHz) vs porosity.

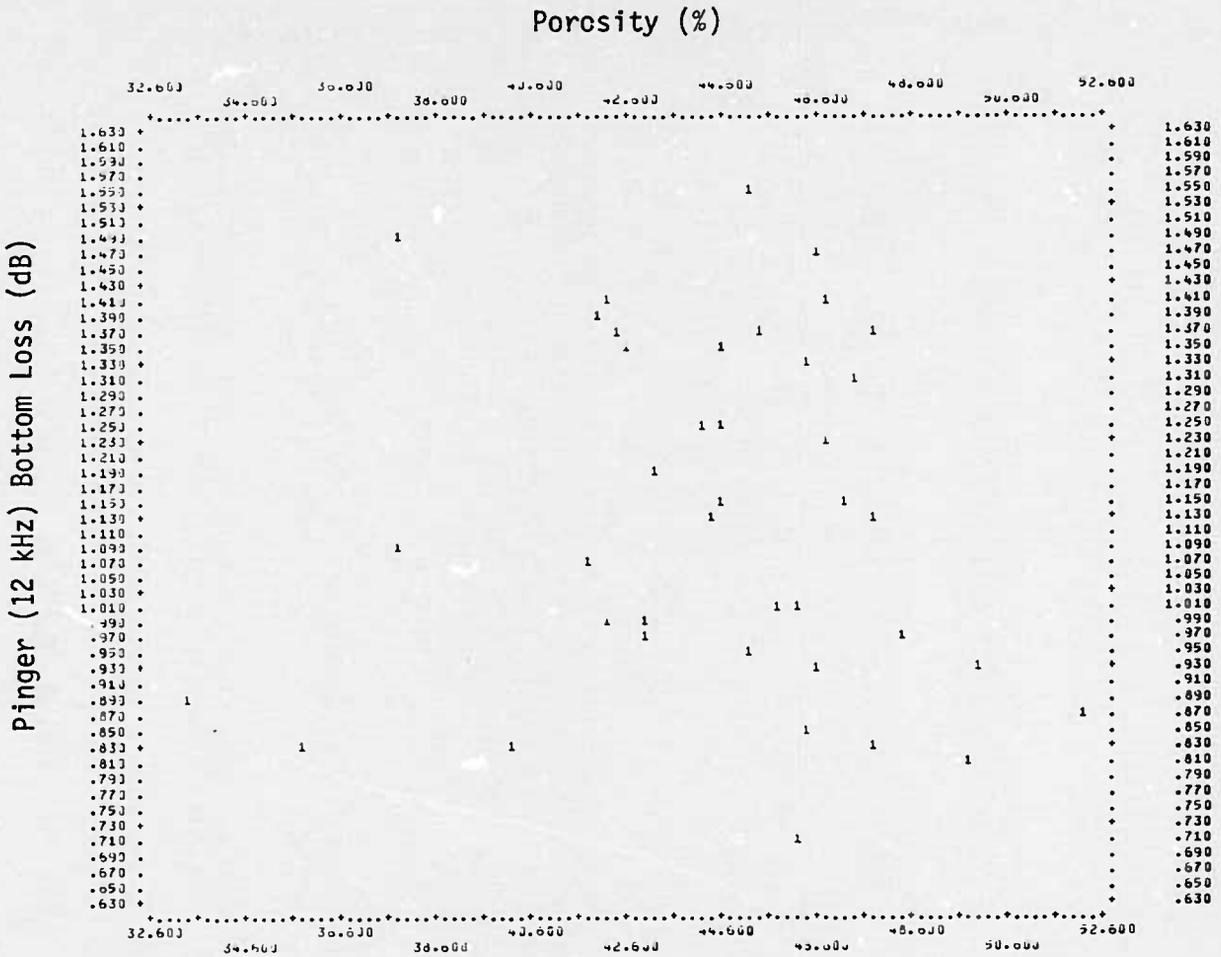

Figure 56. Plot of bottom loss (12 kHz) vs porosity.

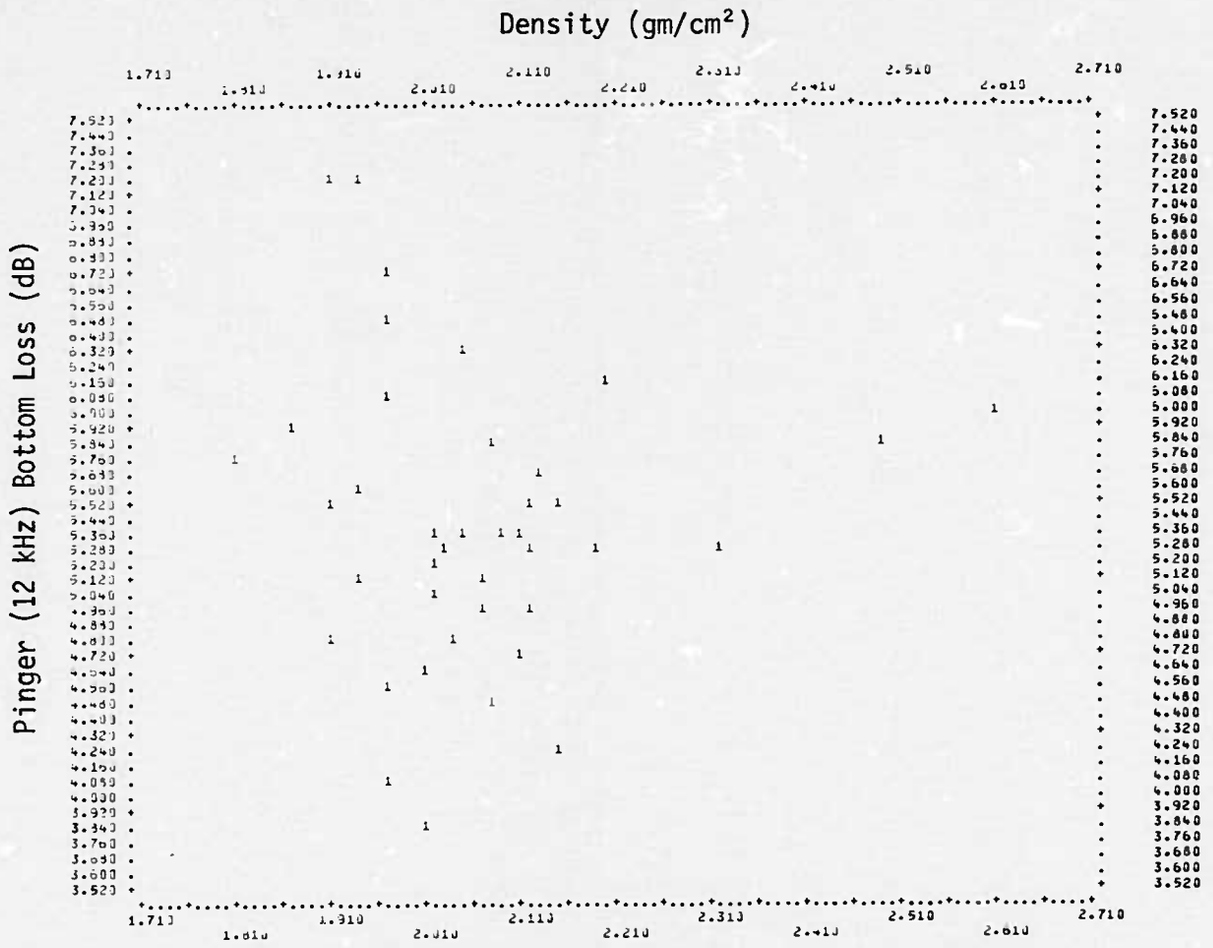

Figure 57. Plot of bottom loss (0-5 kHz) vs density.

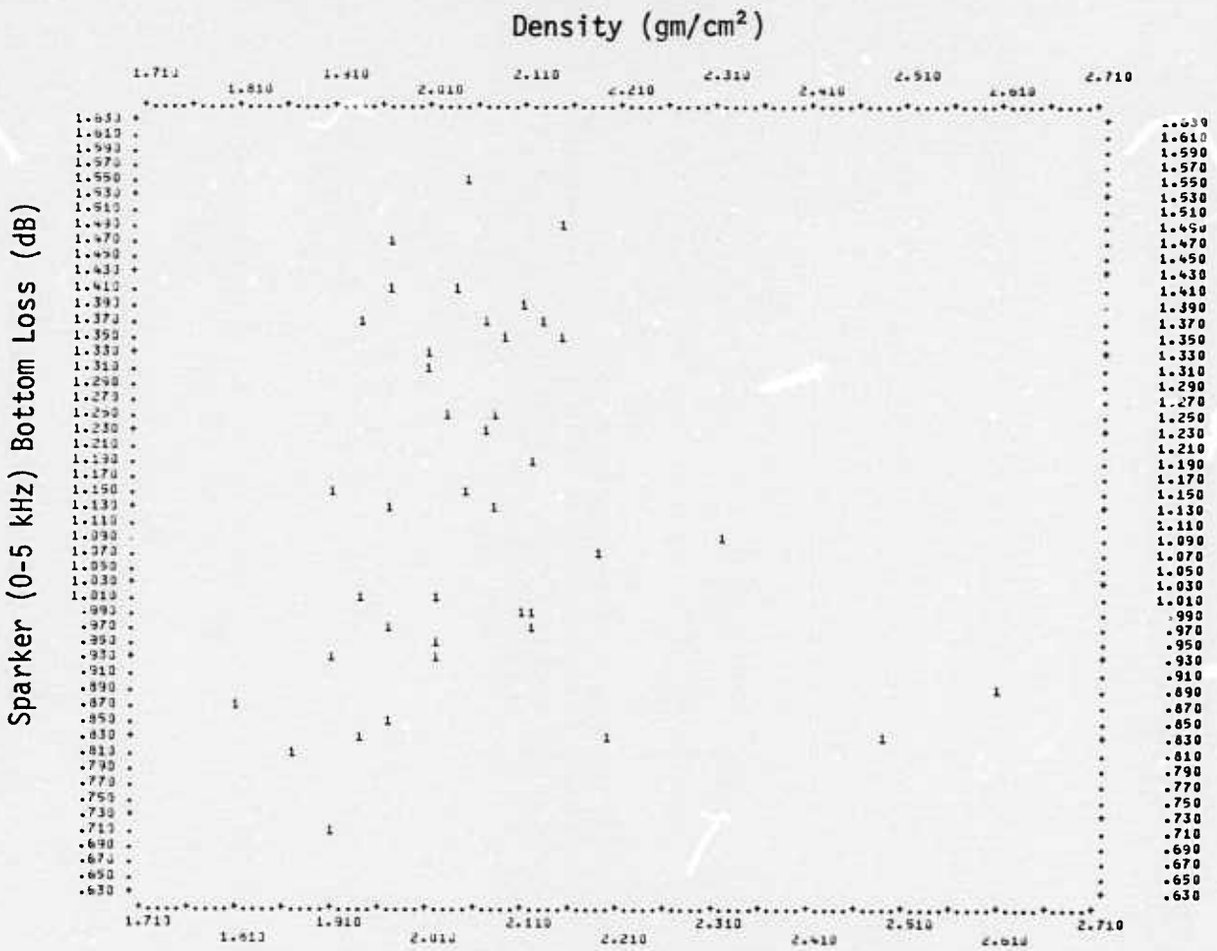

Figure 58. Plot of bottom loss (12 kHz) vs density.

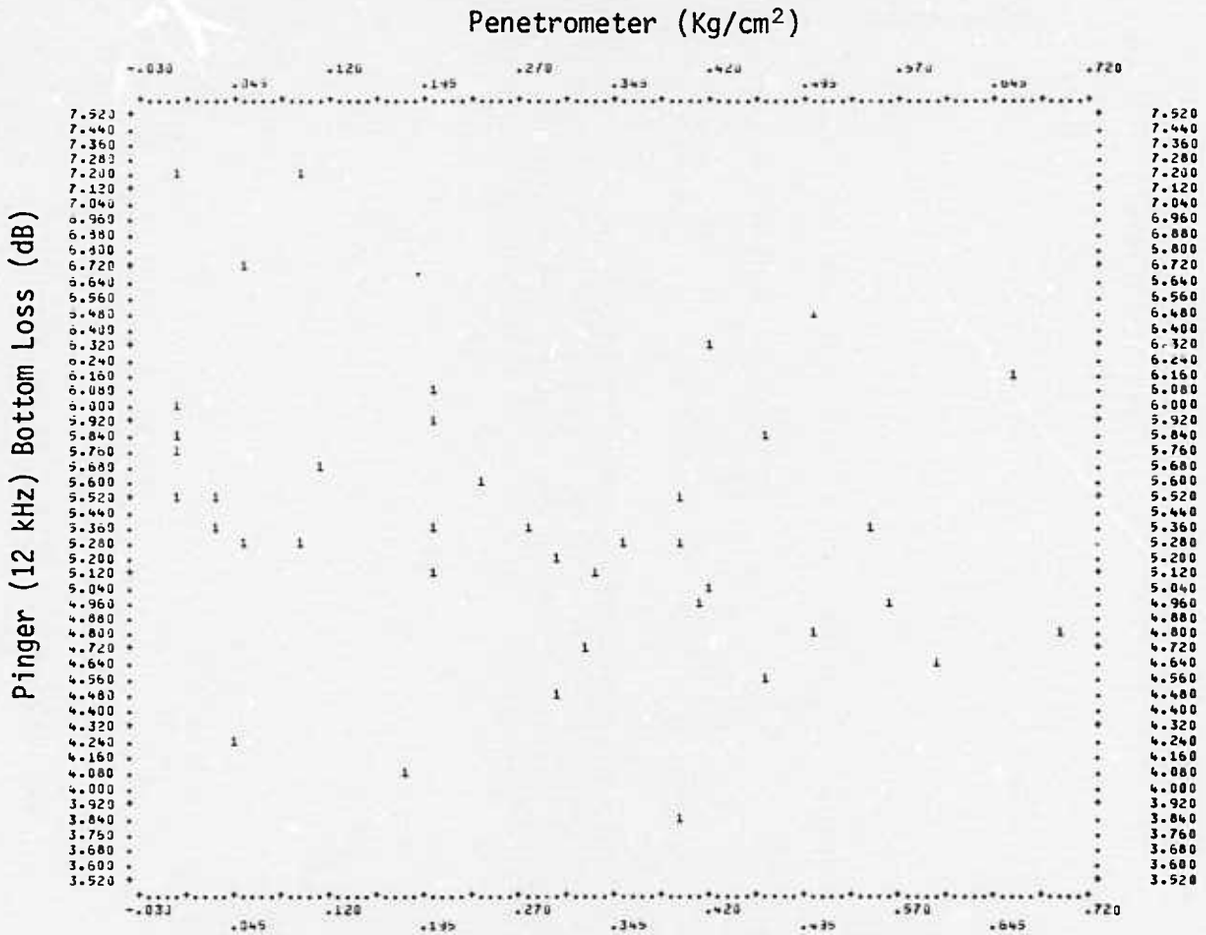

Figure 59. Plot of bottom loss (0-5 kHz) vs penetrometer.

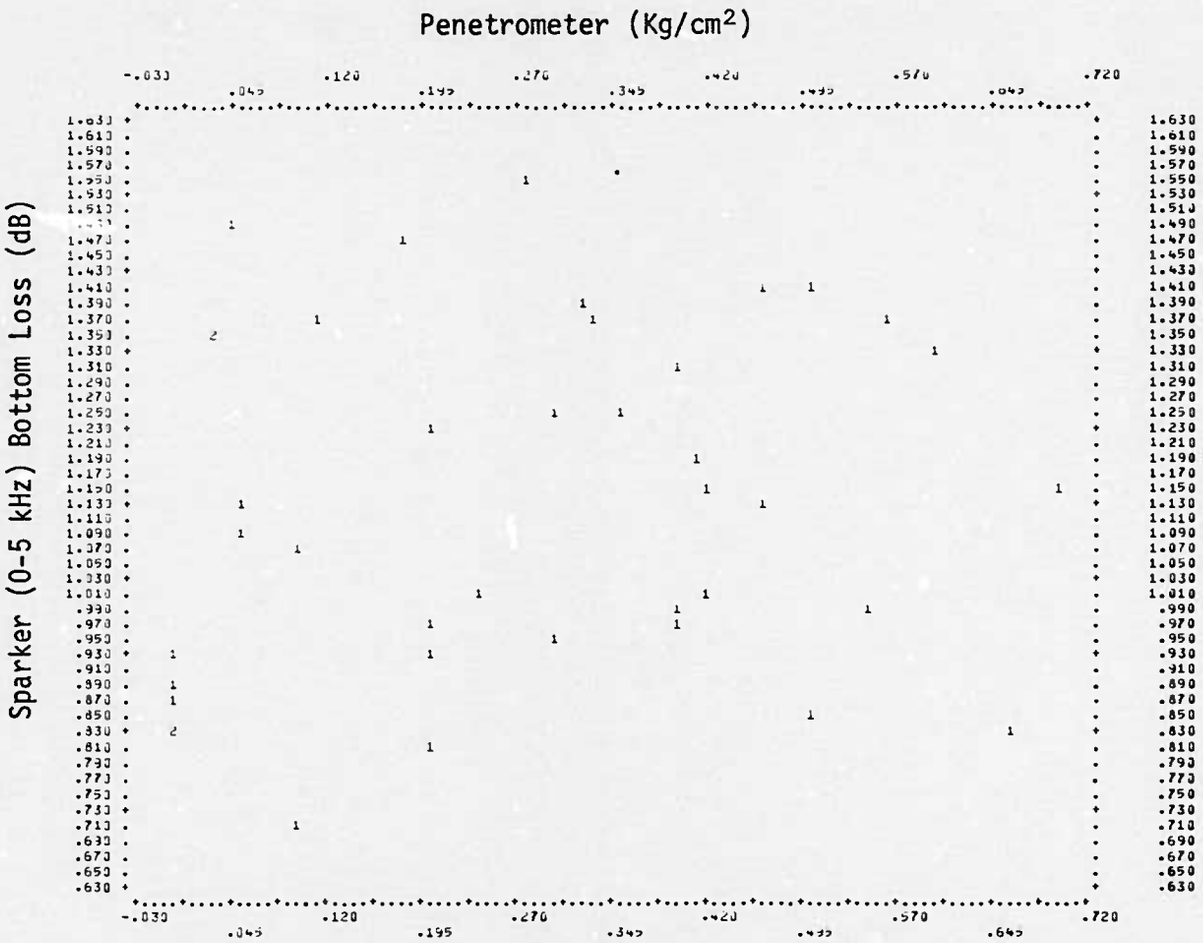

Figure 60. Plot of bottom loss (12 kHz) vs penetrometer.

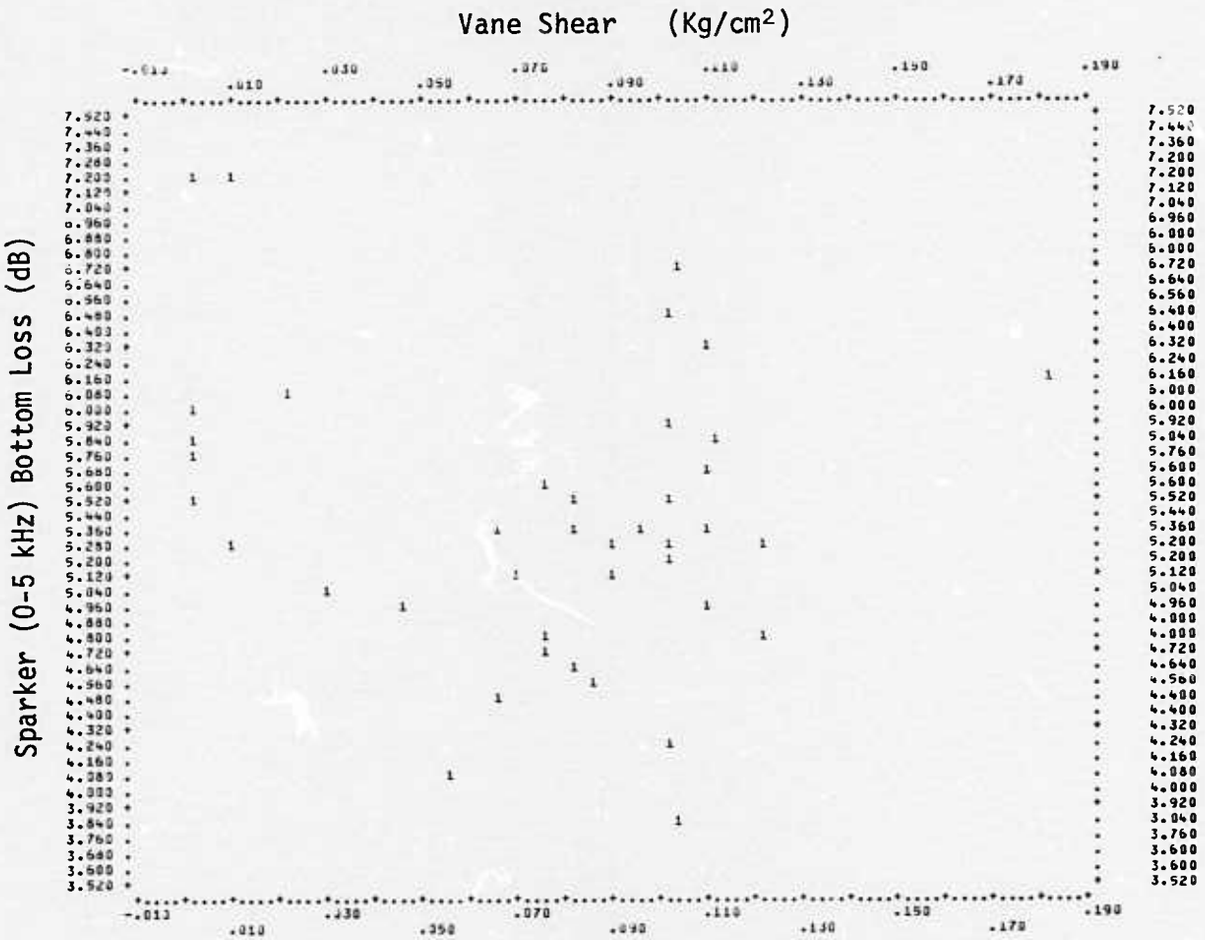

Figure 61. Plot of bottom loss (0-5 kHz) vs vane shear.

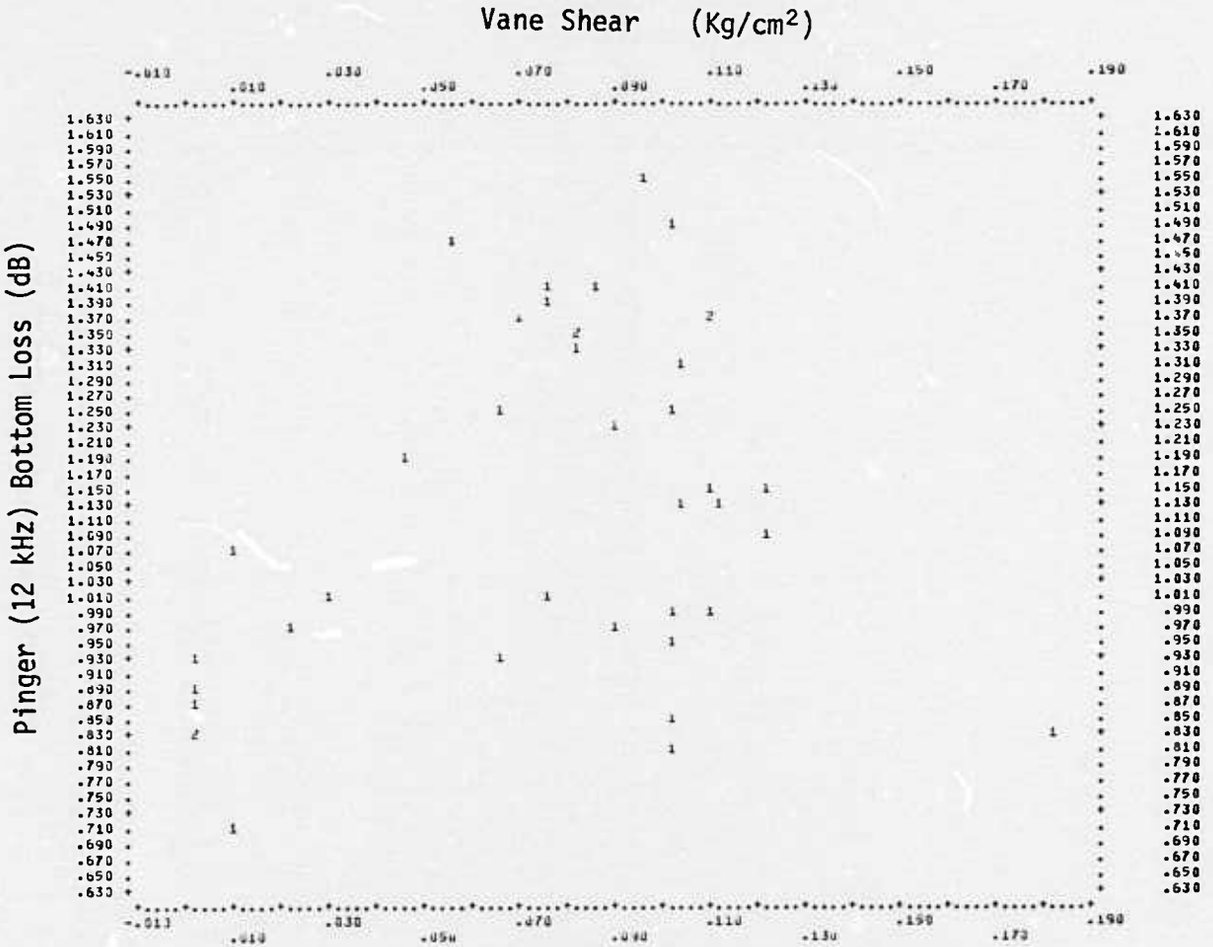

Figure 62. Plot of bottom loss (12 kHz) vs vane shear.

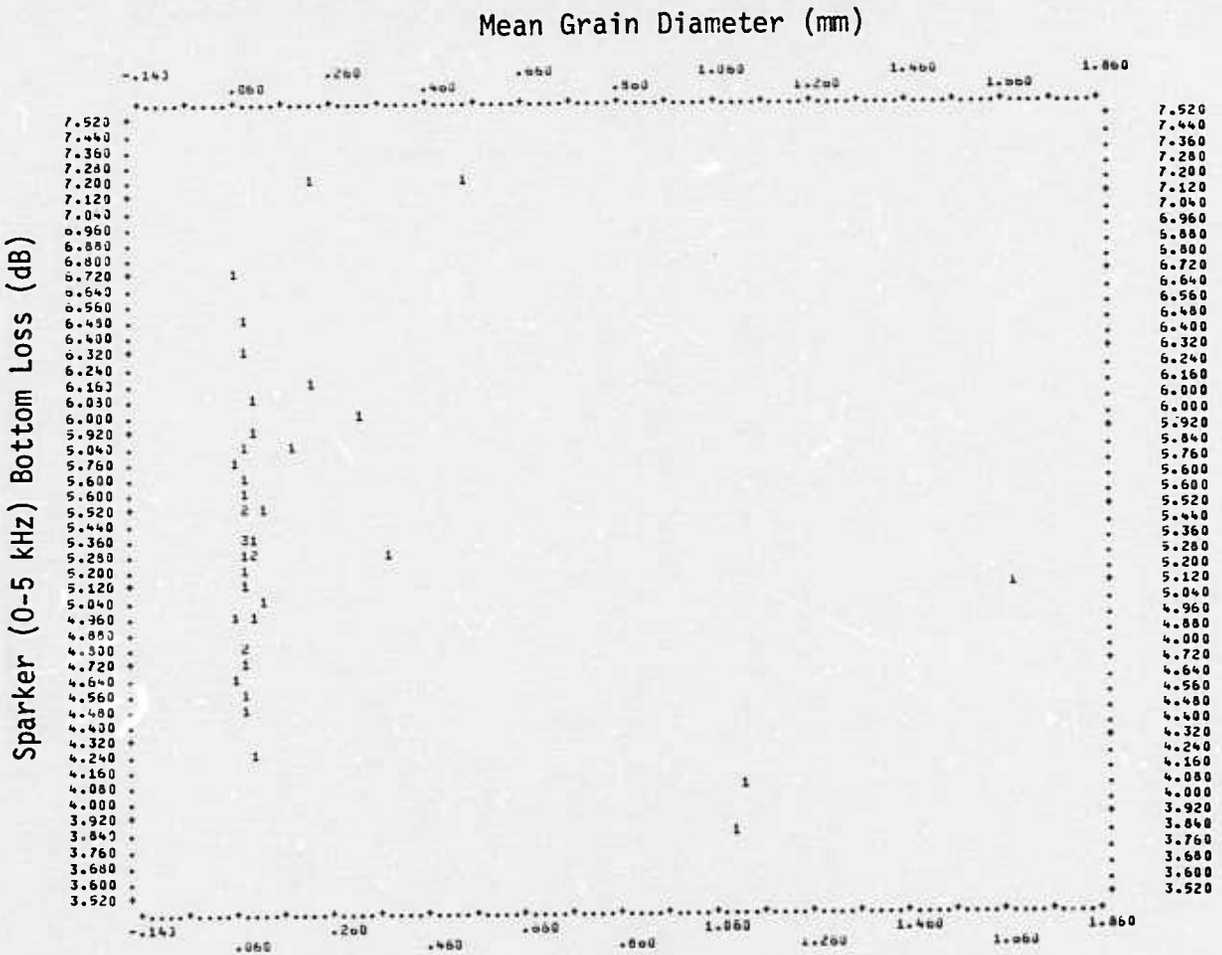

Figure 63. Plot of bottom loss (0-5 kHz) vs mean grain diameter.

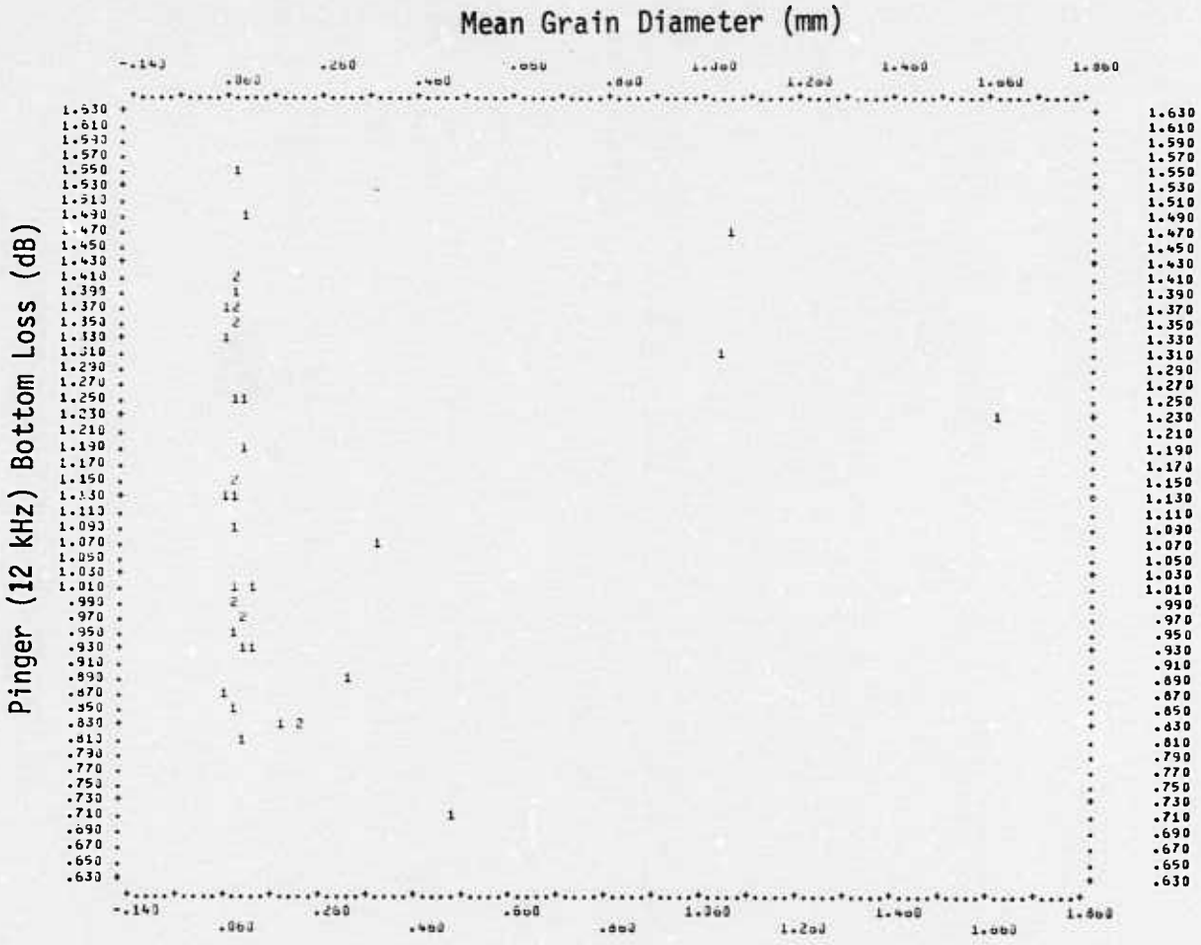

Figure 64. Plot of bottom loss (12 kHz) vs mean grain diameter.

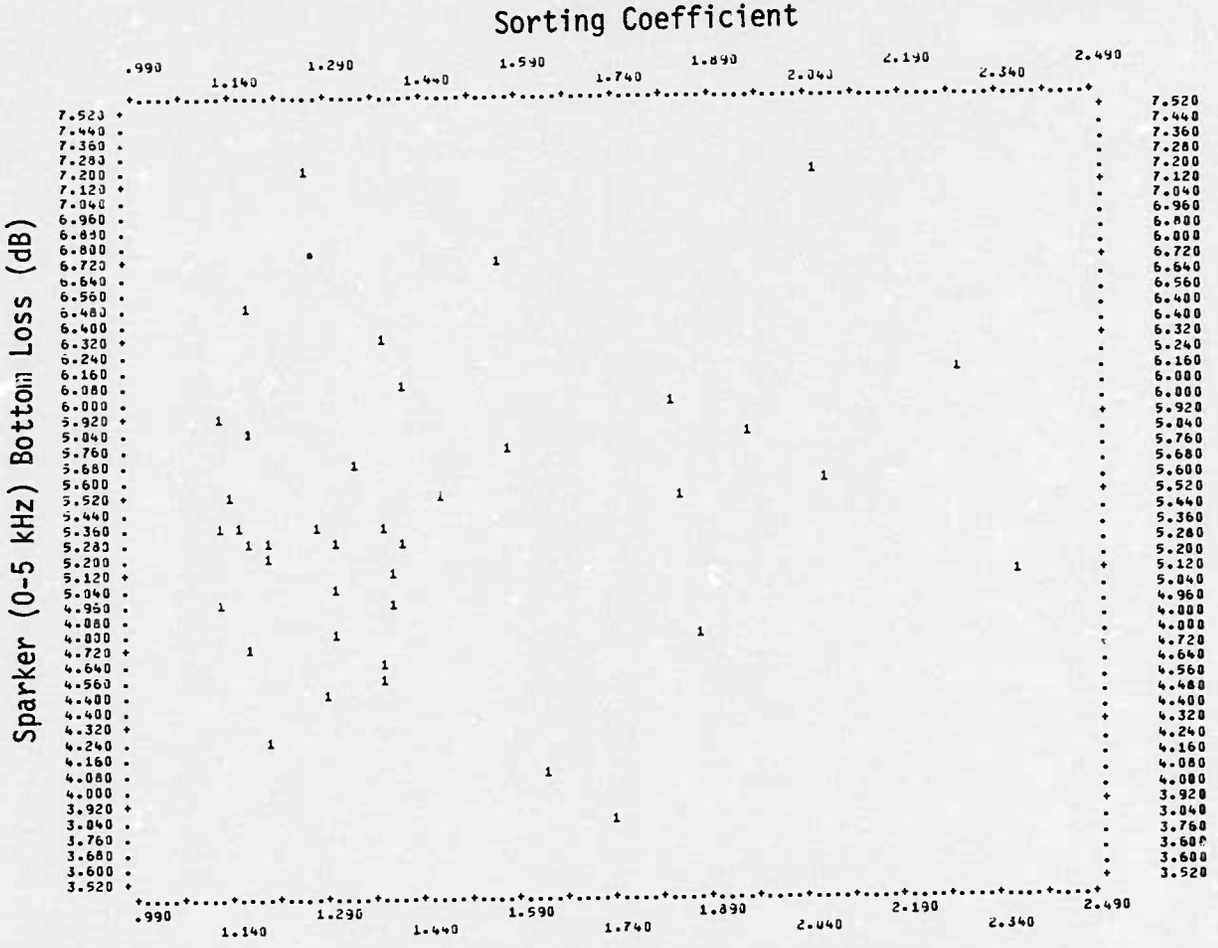

Figure 65. Plot of bottom loss (0-5 kHz) vs sorting coefficient.

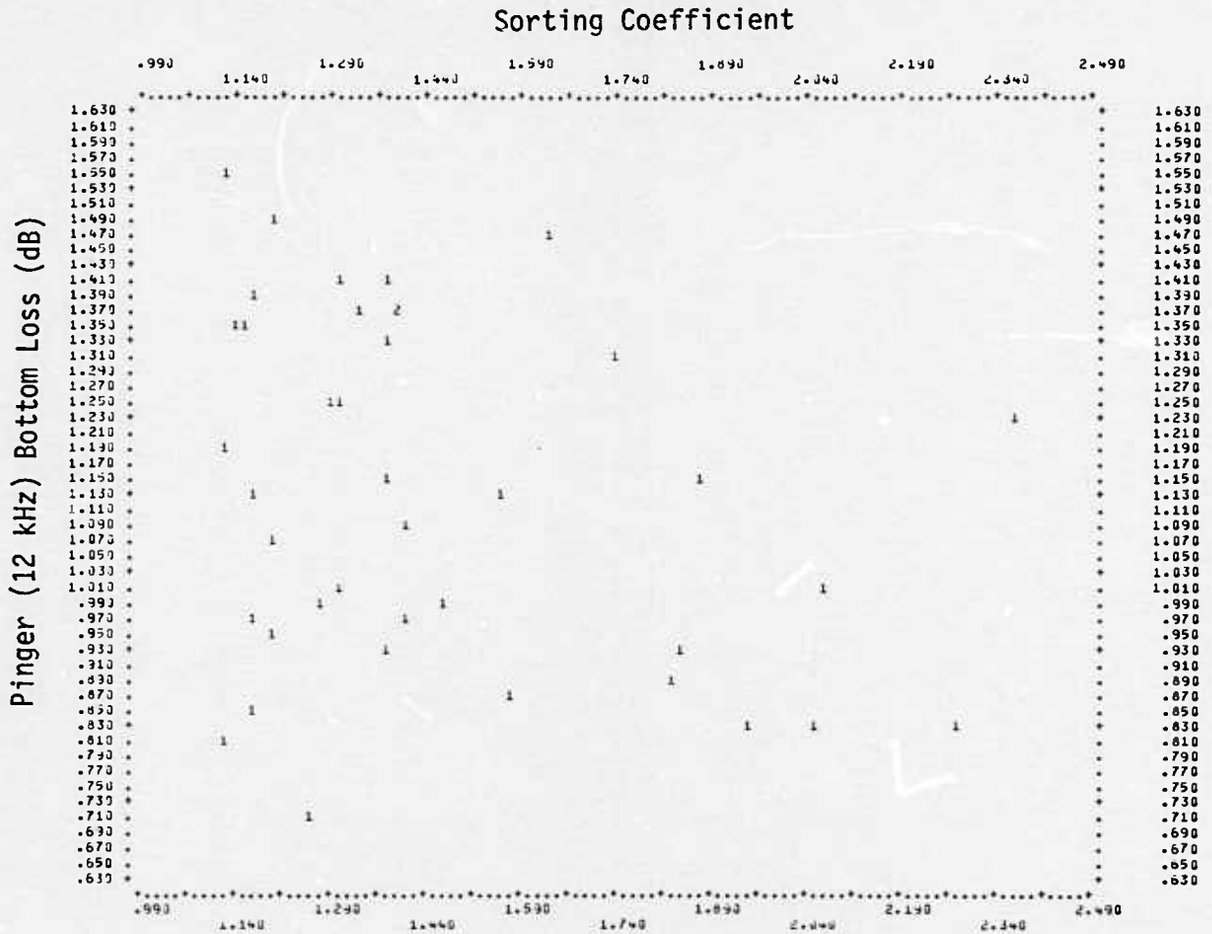

Figure 66. Plot of bottom loss (12 kHz) vs sorting coefficient.

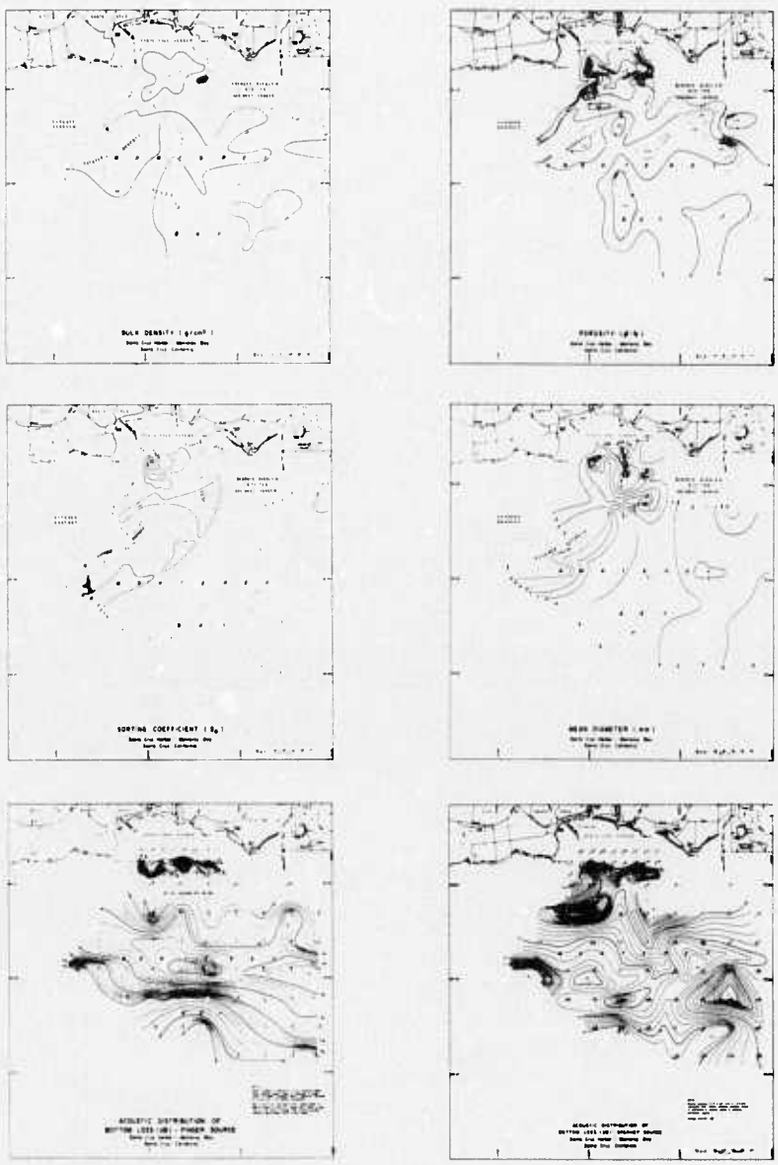

Figure 67. Acoustics vs sediment physical properties Santa Cruz harbor.

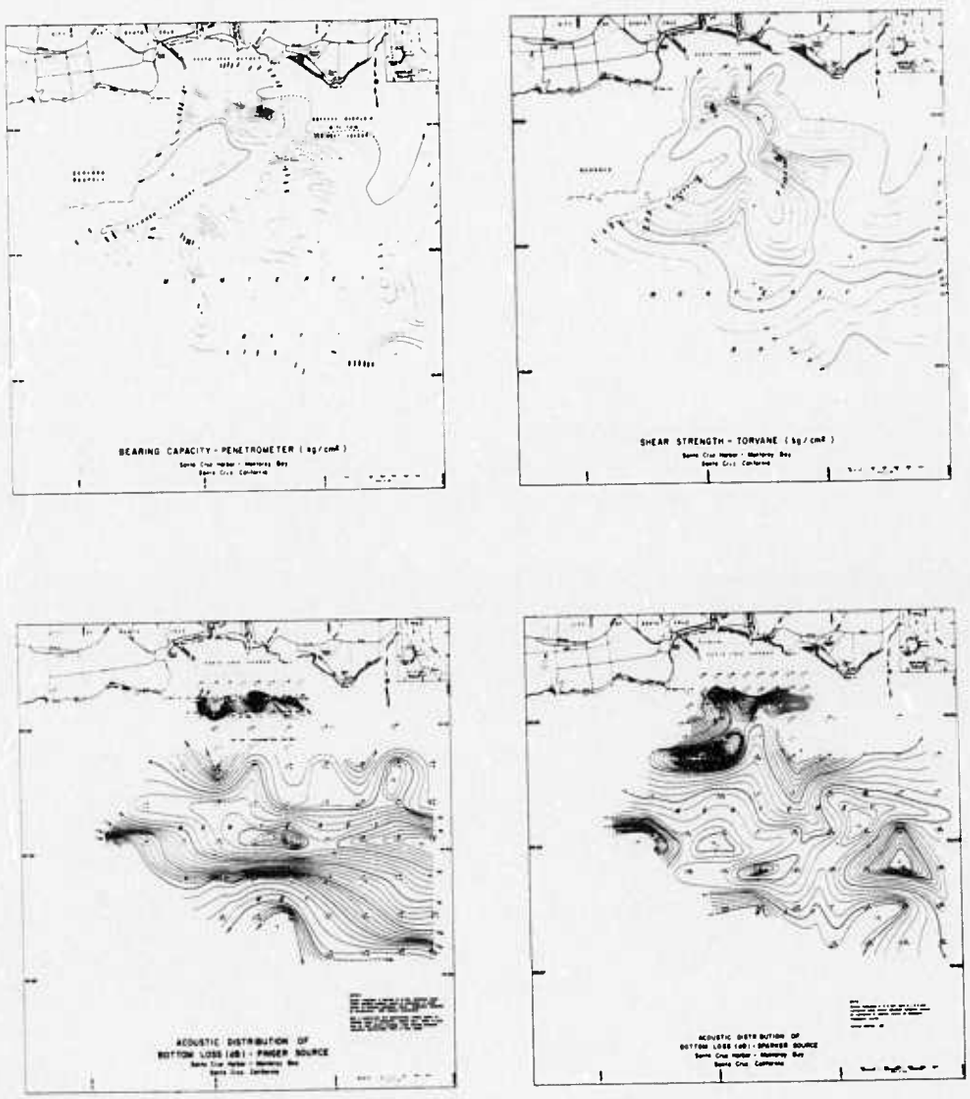

Figure 68. Acoustics vs sediment engineering properties Santa Cruz harbor.

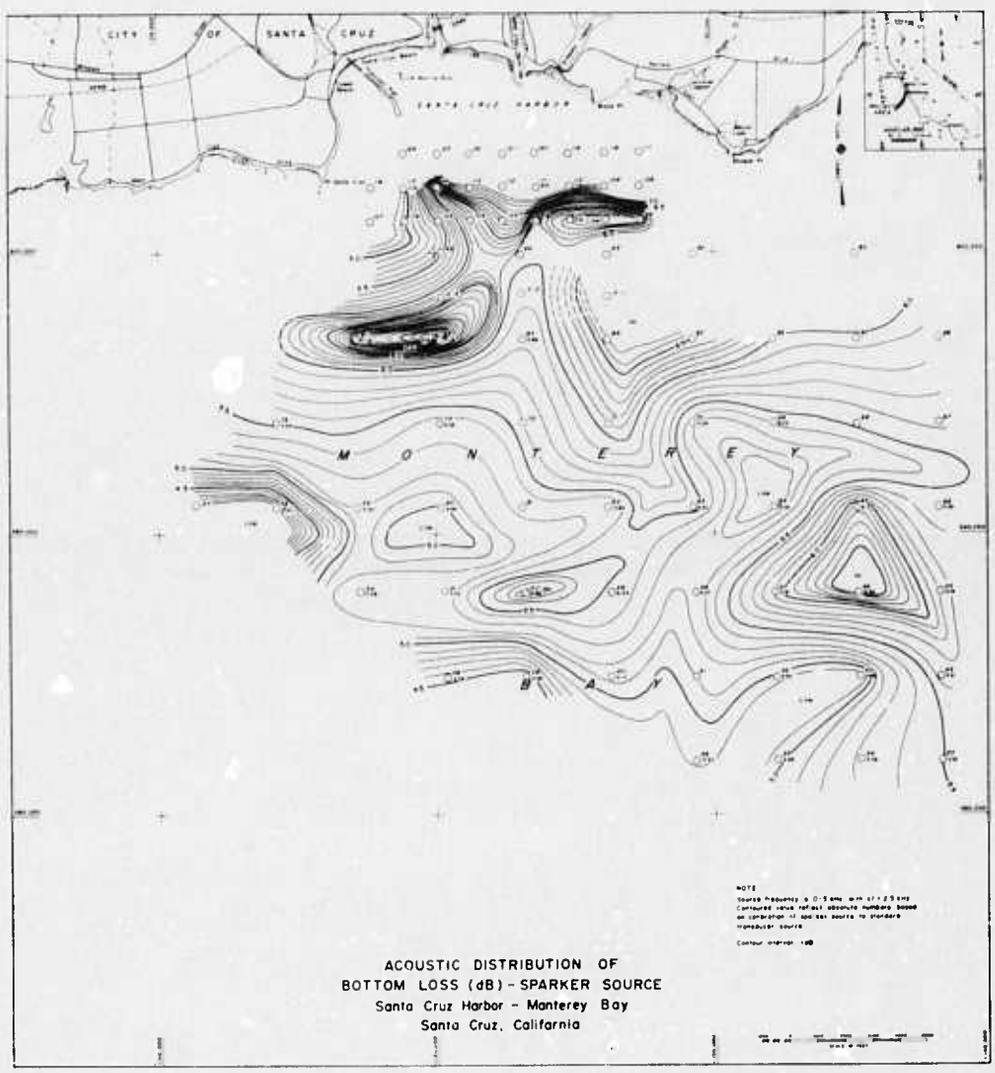

Figure 69. Acoustic distribution of bottom loss (0-5 kHz) Santa Cruz harbor.

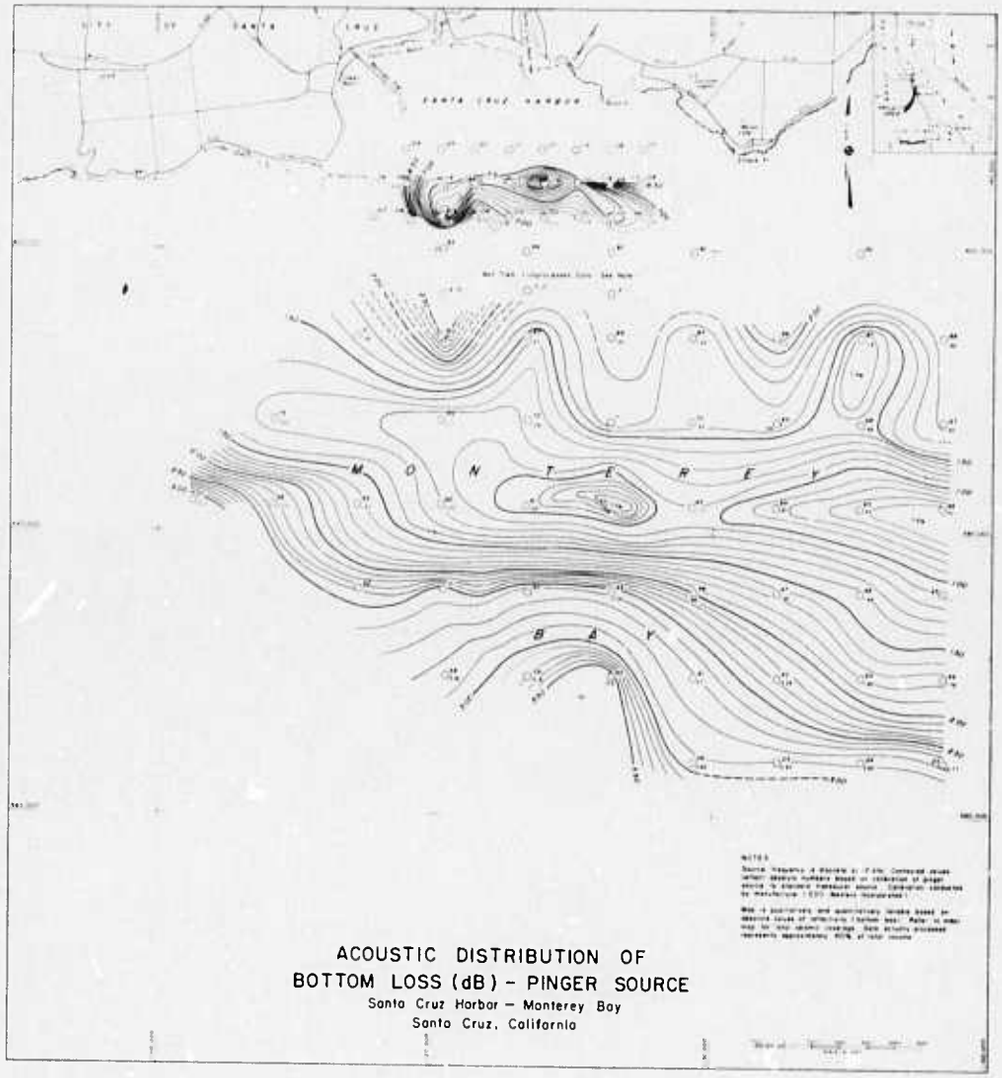

Figure 70. Acoustic distribution of bottom loss (12 kHz) Santa Cruz harbor.

*Table 7. Comparison of Correlative Values of Barnes et al. (1972) vs Breslau (1967)**

	Correlation Coefficient		Standard Error** dB/Unit	
	Barnes et al.	Breslau	Barnes et al.	Breslau
Porosity	.73	.70	±.455	±.039
Grain Size	.92	.646	±.227	±.292
Sorting	.92	.343	±.252	±.660
Fine Material (Silt & Clay)	.89	.786	±.305	±.015

*Bottom loss calculations are based on peak pressure amplitude measurements and Rayleigh Reflection Coefficient determinations.

**The *standard error of estimate* (S) is the standard deviation about a line of average relationship. Assuming a normal distribution, 68 percent of all cases will lie within a range of ±S, 95 percent will fall within ±2S, and 99.7 percent will fall within ±3S. In this instance, the relationship of bottom loss to the other variable is of interest. The values of S are therefore in terms of decibels (dB) per unit of paired variable.

clay fractions with very little material, the Santa Cruz harbor sediments are highly variable ranging in grain size from gravel to silt with admixtures that are poorly sorted and show great diversity in physical properties and engineering properties. According to D. L. Bell (Raytheon Company, Portsmouth, Rhode Island, personal communication), it was learned that such high variability of sediment type can have decided effects on the range of velocity of sound propagation through the sediments. Bell's recent studies of nearshore sediments of the continental shelf off New England, show that sediment velocity changes greatly over short spacial distances and that this has an appreciable influence on corrections applied to acoustic attenuation. Using advanced state-of-the art tools and techniques developed by Raytheon Company, he has been able to accurately measure marine sediment velocities to within 2 percent of the standard velocity for sea water. This accuracy has resulted in obtaining new information on the variability of marine sediment velocities. According to Bell, 40 percent of marine sediments in the nearshore environment range

in velocity within 5 percent below to 2 percent above the standard velocity of sea water. He further believes that sediments can also be categorized into 8 or 9 types through velocity analyses.

Water depths in the San Francisco Bay study area ranged from 25 to 40 ft, as compared to depths ranging from 18 to 250 ft in Monterey Bay. Tests for correlations as a function of water depth were made on the results obtained from the data taken for this study. The results are shown in the correlation matrix given in table 8. Sediment analyses and acoustical data were correlated from core sites along line numbers 16 (sites 38-44); 26 (sites 57-66); 36 (sites 81-88); 43 (sites 100-105); and 45 (sites 109-115) (figs. 33, 34). Figures 71-90 show the cross-sections

Table 8. Correlation of Mass Physical and Engineering Properties vs Acoustics (Linear Regression Analysis).

Mass Physical and Engineering Properties	Correlation Coefficient		Standard Error of Estimate (±)	
	Sparker BL	Pinger BL	Sparker BL	Pinger BL
	Line No. 16 (sites 38-44)			
Porosity	0.393	0.576	0.3472	0.7072
Density	0.602	0.627	0.3771	0.7233
Shear Strength (Penetrometer)	0.554	0.343	0.3694	0.6479
Shear Strength (Torvane)	0.610	0.861	0.3785	0.3117
Mean Grain Diameter	0.582	0.6217	0.3740	0.7217
Sorting Coefficient	0.0618	0.5789	0.3225	0.7082
	Line No. 26 (sites 57-66)			
Porosity	0.506	0.275	0.4814	0.7601
Density	0.3961	0.195	0.5125	0.8061
Shear Strength (Penetrometer)	0.4998	0.394	0.6235	0.8506
Shear Strength (Torvane)	0.304	0.421	0.5834	0.8665
Mean Grain Diameter	0.406	0.8665	0.5102	0.674
Sorting Coefficient	0.271	0.7032	0.5935	0.07882
	Line No. 36 (sites 81-88)			
Porosity	0.485	0.508	0.6219	0.4170
Density	0.570	0.404	0.639	0.4011
Shear Strength (Penetrometer)	0.577	0.545	0.6388	0.4235
Shear Strength (Torvane)	0.559	0.524	0.6339	0.4198
Mean Grain Diameter	0.382	0.217	0.5113	0.3805
Sorting Coefficient	0.571	0.425	0.6370	0.4040
	Line No. 43 (sites 100-105)			
Porosity	0.744	0.534	0.3849	0.5128
Density	0.611	0.489	0.4561	0.5035
Shear Strength (Penetrometer)	0.328	0.779	0.6064	0.5733
Shear Strength (Torvane)	0.925	0.696	0.743	0.696
Mean Grain Diameter	0.288	0.673	0.5518	0.5450
Sorting Coefficient	0.778	0.551	0.7299	0.5163
	Line No. 45 (sites 109-115)			
Porosity	0.837	0.080	0.6270	0.9056
Density	0.914	0.226	0.4643	0.9377
Shear Strength (Penetrometer)	0.289	0.600	0.6759	1.1112
Shear Strength (Torvane)	0.797	0.713	0.8018	1.2802
Mean Grain Diameter	0.618	0.618	1.3458	1.0751
Sorting Coefficient	0.615	0.485	1.3440	1.0163

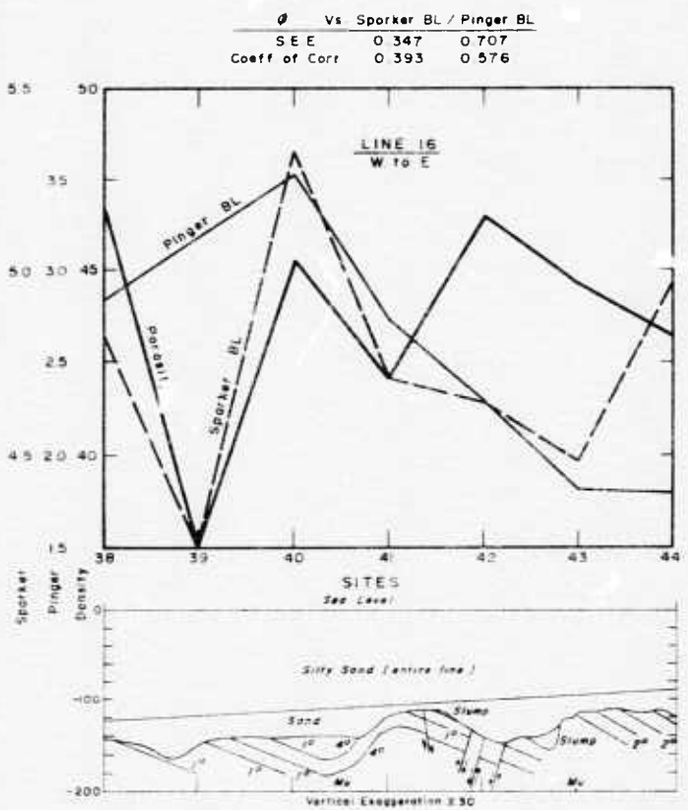

Figure 71. X-section of porosity vs acoustics Line 16.

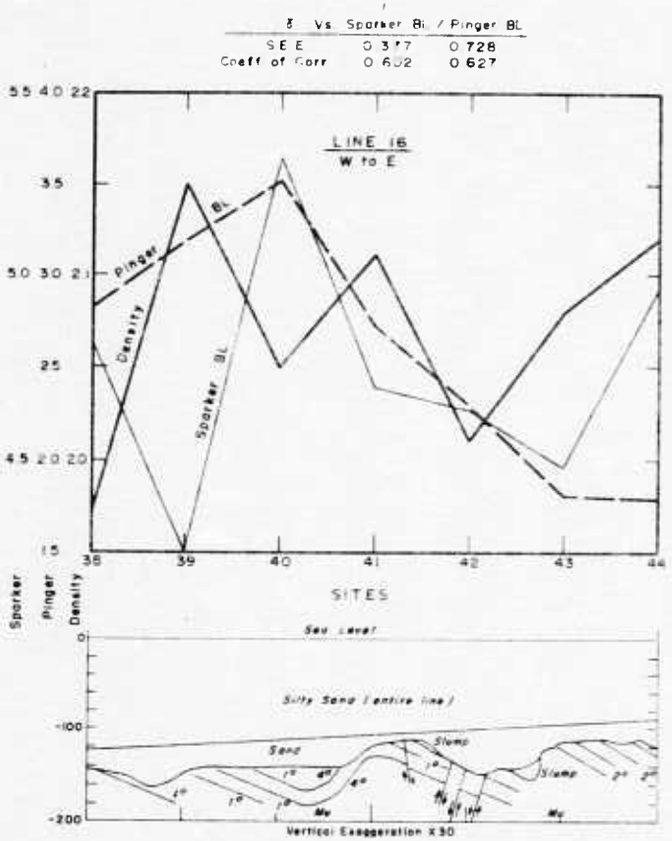

Figure 72. X-section of density vs acoustics Line 16.

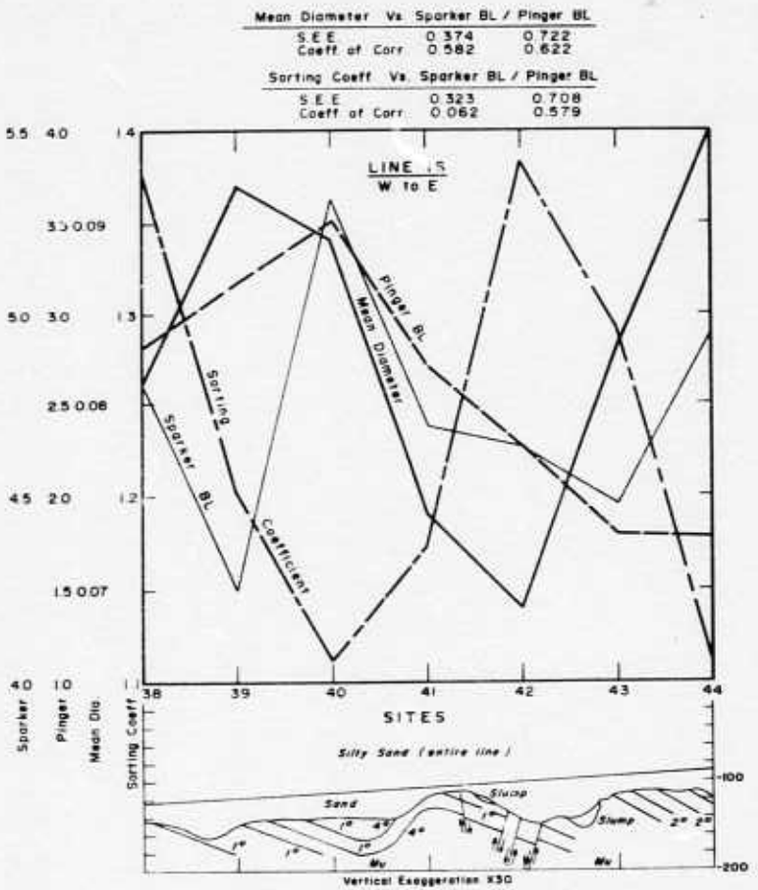

Figure 73. X-section mean diameter and sorting coefficient vs acoustics — Line 16.

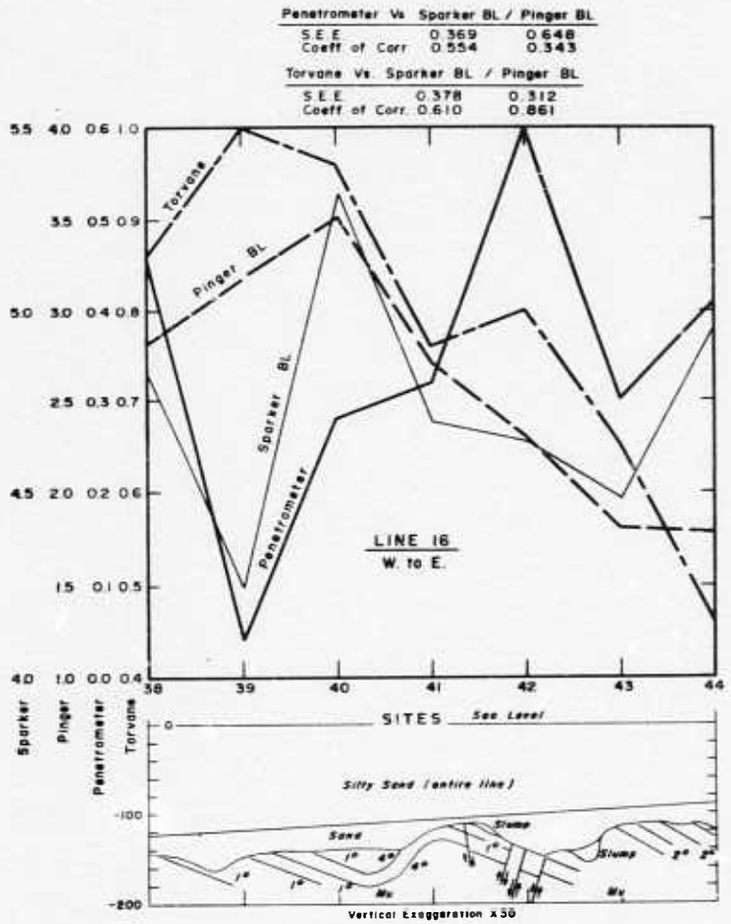

Figure 74. X-section penetrometer and torvane vs acoustics — Line 16.

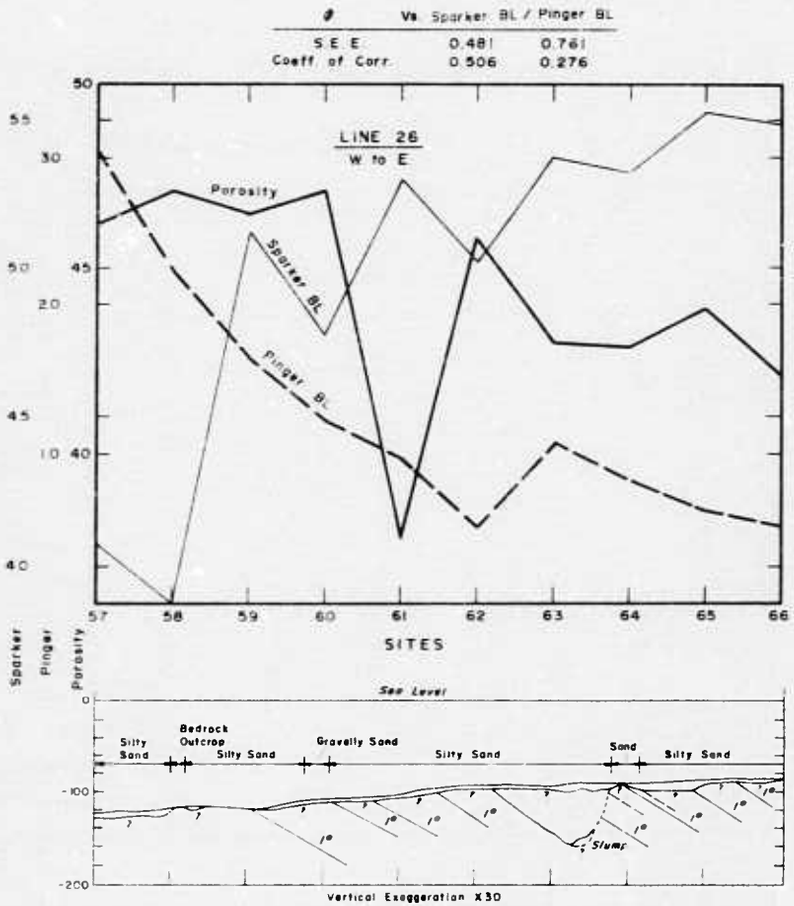

Figure 75. X-section of porosity vs acoustics Line 26.

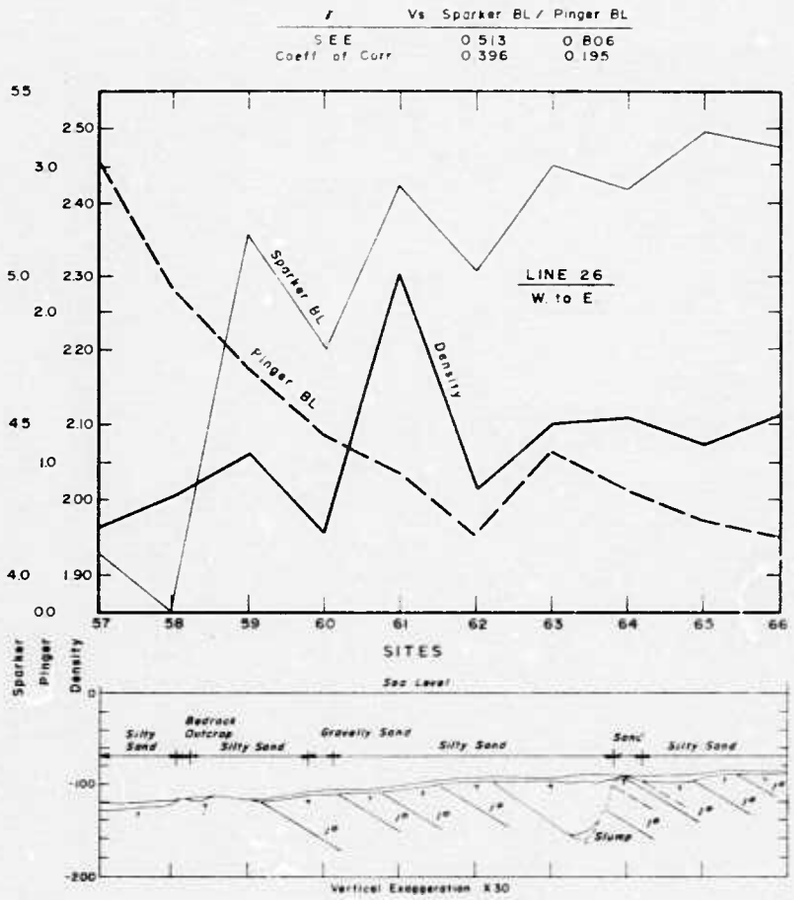

Figure 76. X-section of density vs acoustics Line 26.

Mean Diameter Vs	Sparker BL / Pinger BL
S.E.E	0.510 / 0.703
Coeff of Corr	0.406 / 0.674
Sorting Coeff Vs.	**Sparker BL / Pinger BL**
S.E.E	0.594 / 0.788
Coeff of Corr	0.271 / 0.088

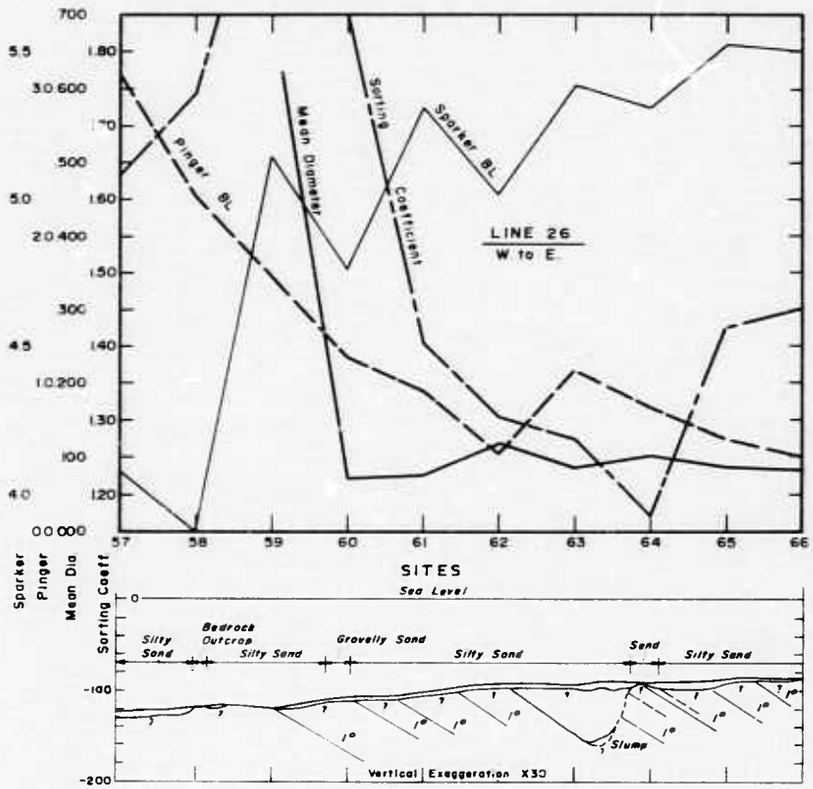

Figure 77. X-section mean diameter and sorting coefficient vs acoustics — Line 26.

Penetrometer Vs	Sparker BL / Pinger BL
S.E.E	0.623 / 0.851
Coeff of Corr	0.500 / 0.394
Torvane Vs	**Sparker BL / Pinger BL**
S.E.E	0.563 / 0.866
Coeff of Corr	0.304 / 0.421

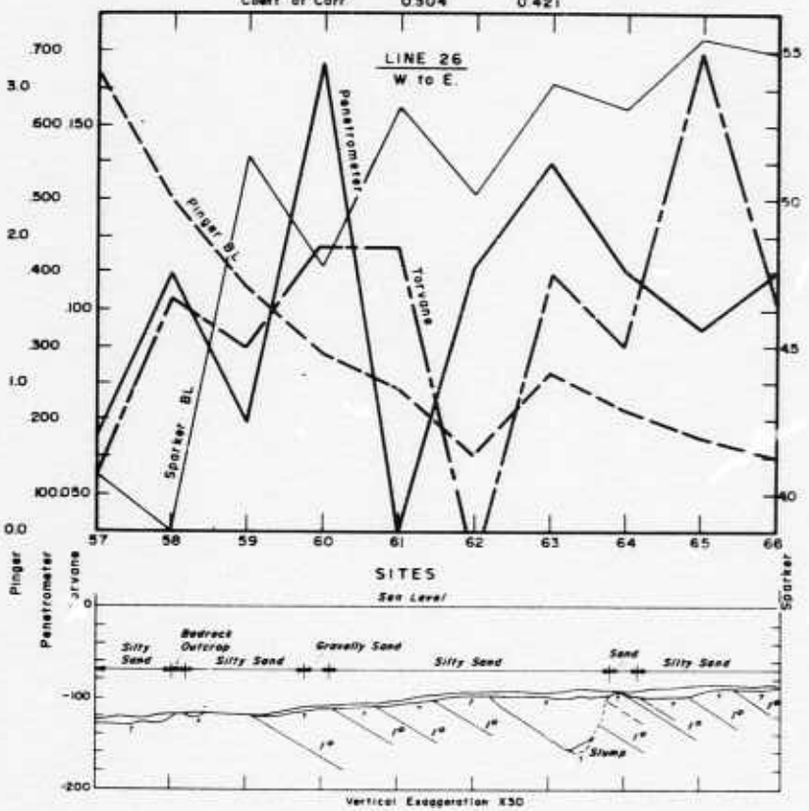

Figure 78. X-section penetrometer and torvane vs acoustics — Line 26.

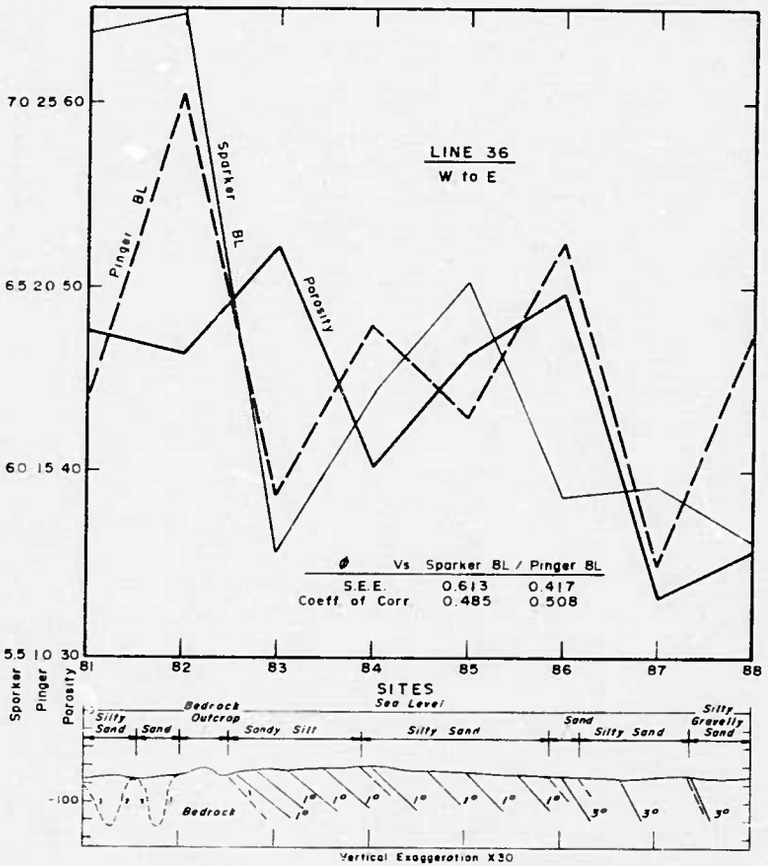

Figure 79. X-section of porosity vs acoustics Line 36.

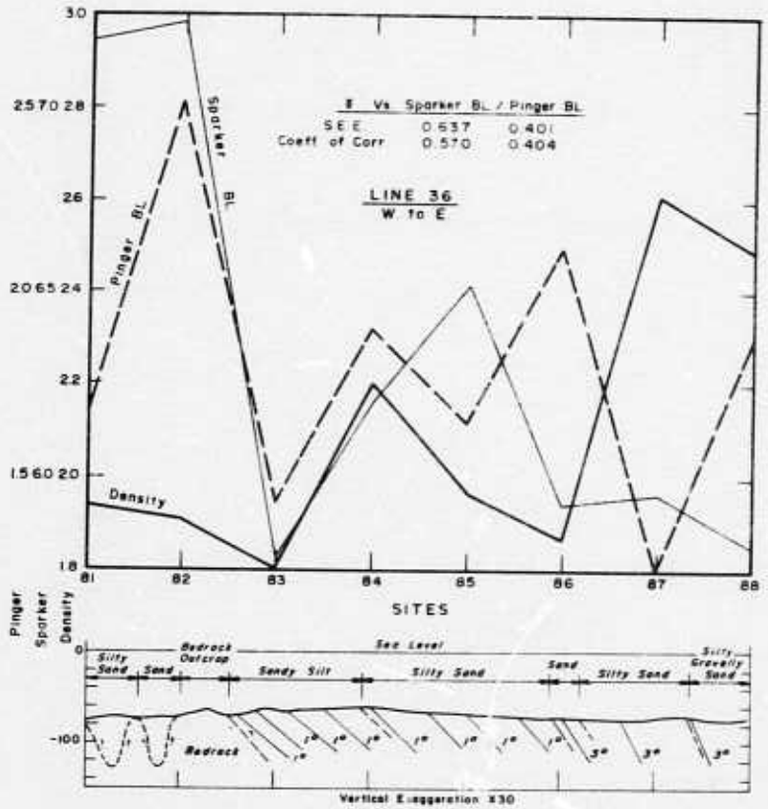

Figure 80. X-section density vs acoustics Line 36.

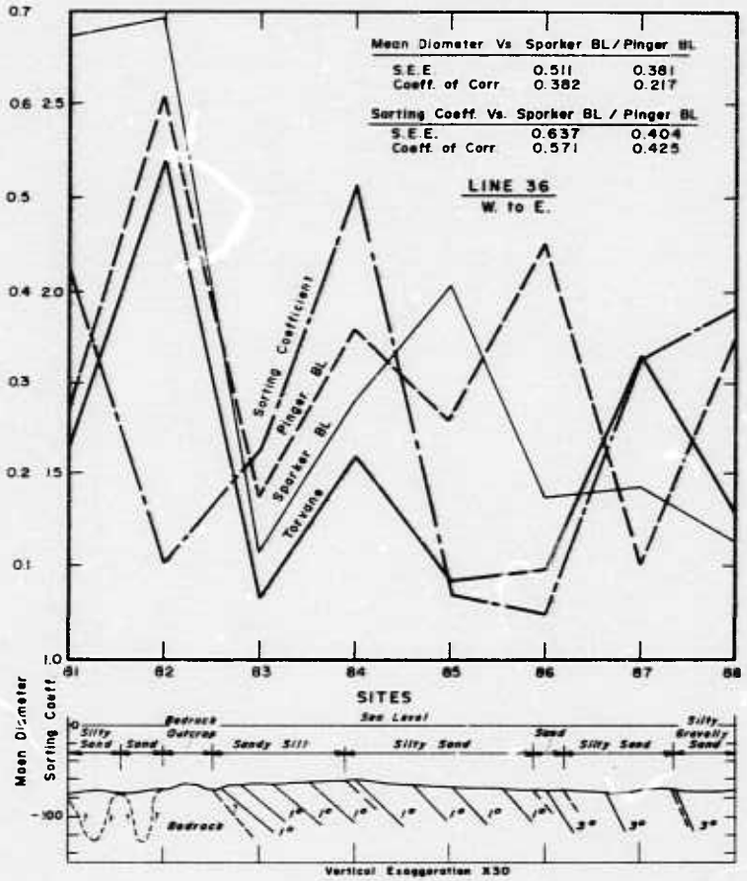

Figure 81. X-section mean diameter and sorting coefficient vs acoustics — Line 36.

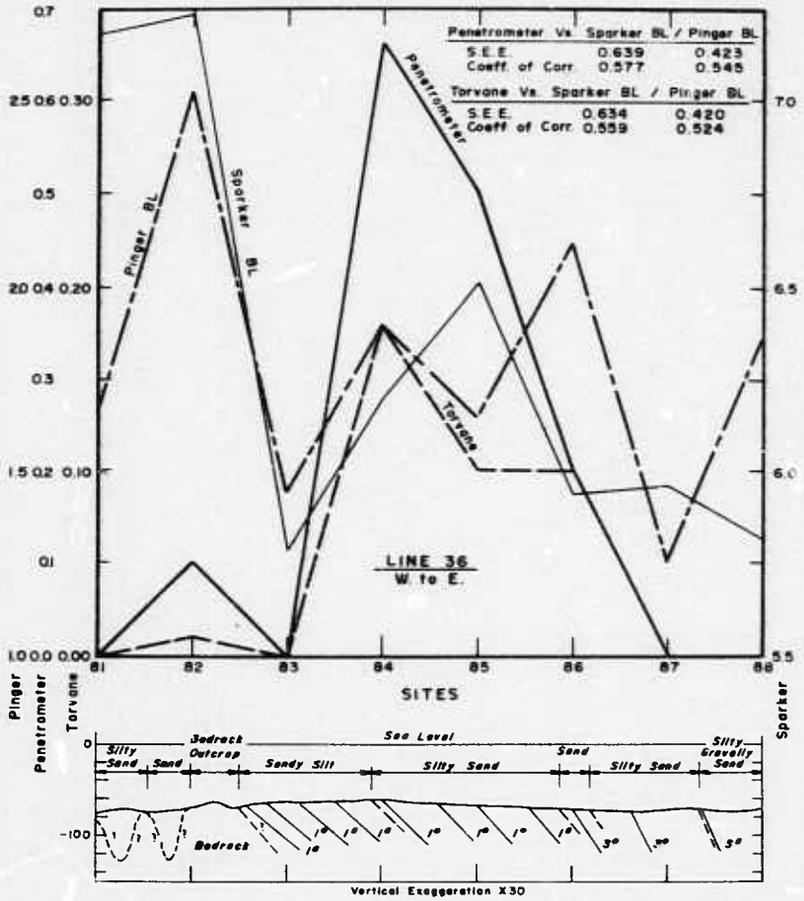

Figure 82. X-section penetrometer and torvane vs acoustics — Line 36.

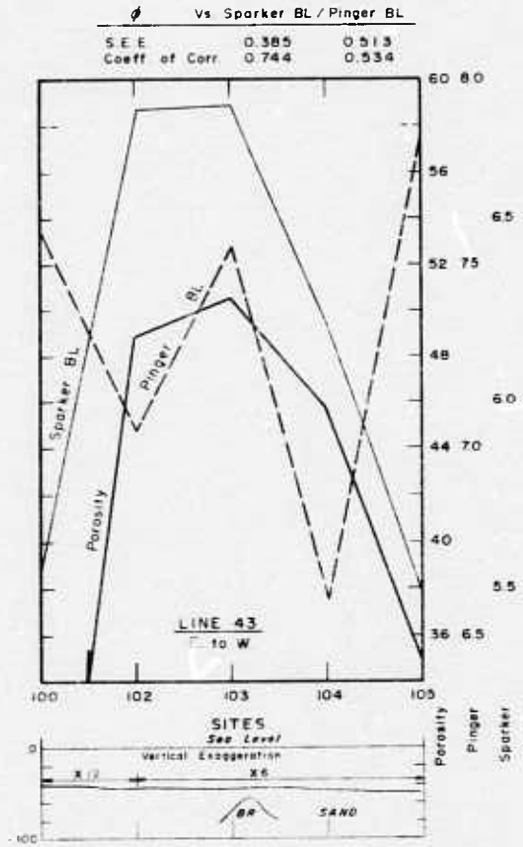

Figure 83. X-section of porosity vs acoustics Line 43.

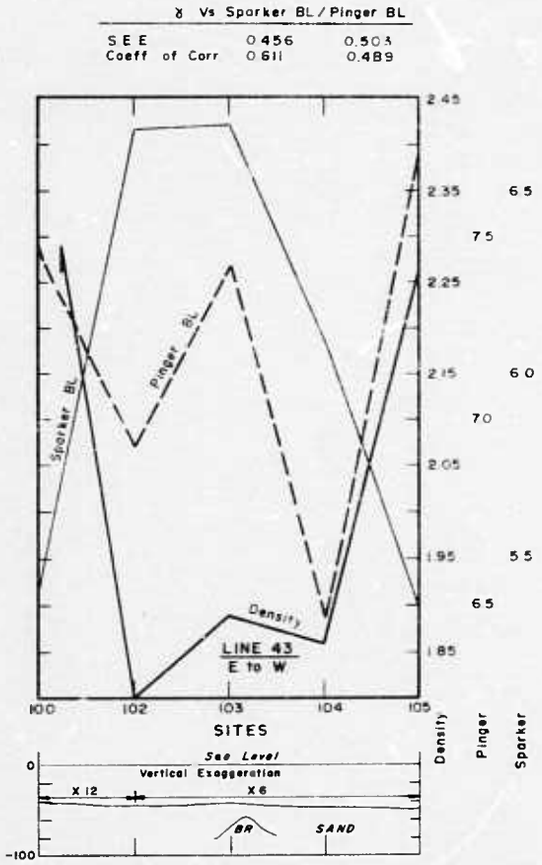

Figure 84. X-section density vs acoustics Line 43.

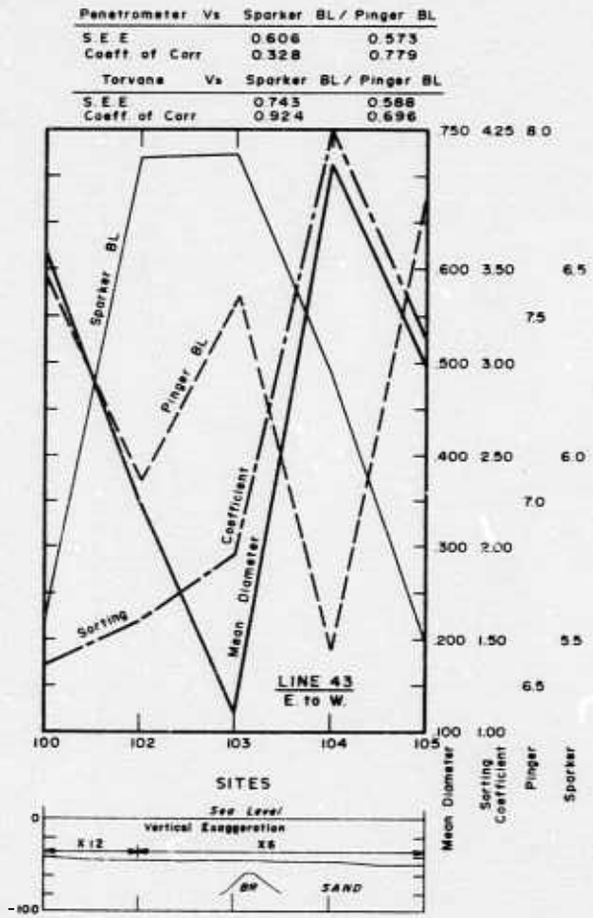

Figure 85. X-section mean diameter and sorting coefficient vs acoustics — Line 43.

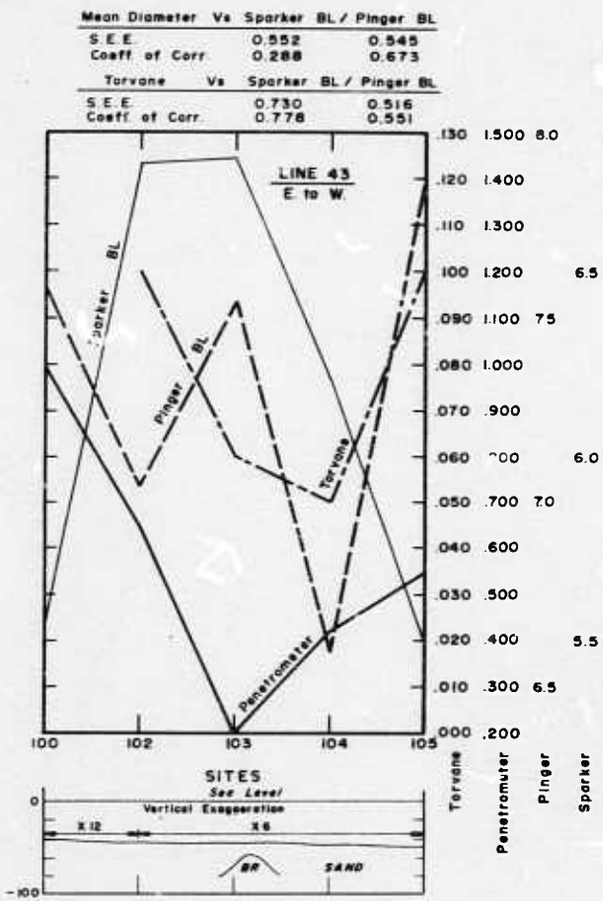

Figure 86. X-section penetrometer and torvane vs acoustics — Line 43.

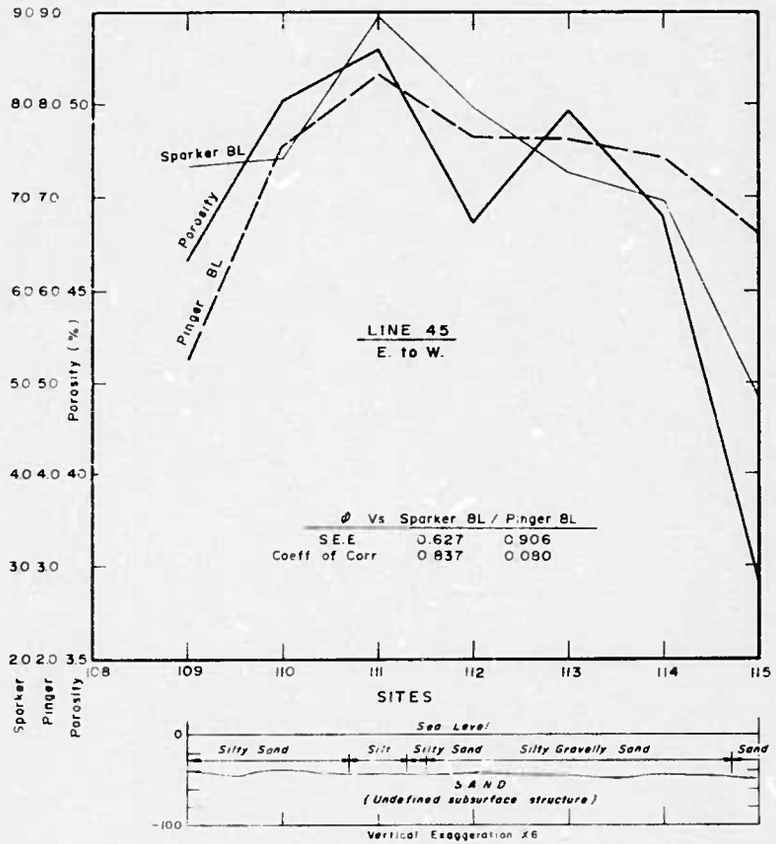

Figure 87. X-section of porosity vs acoustics Line 45.

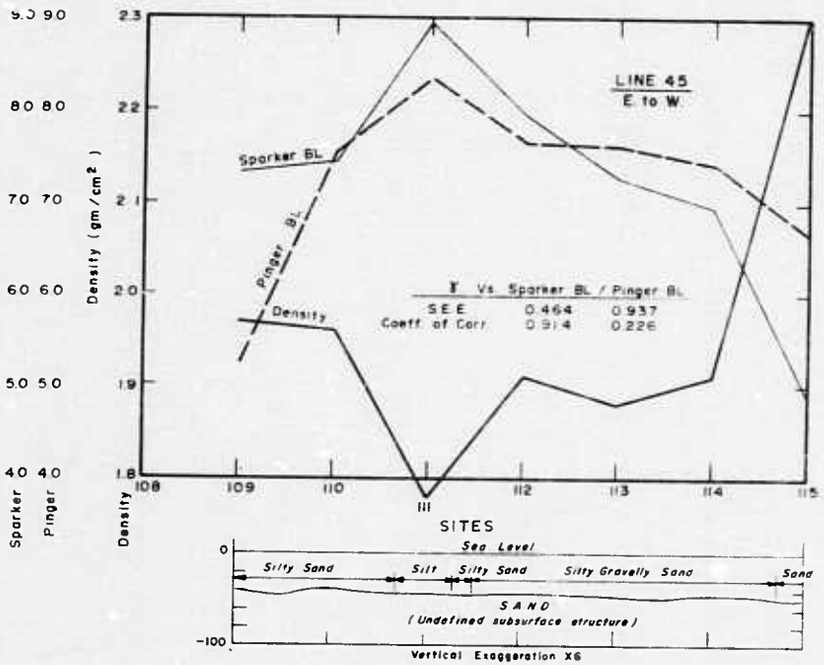

Figure 88. X-section density vs acoustics Line 45.

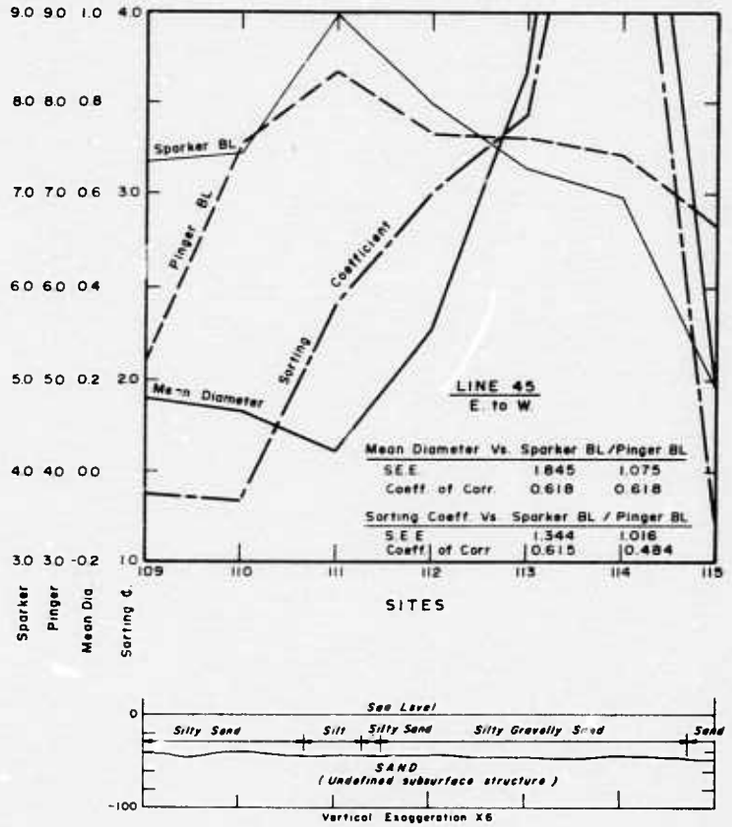

Figure 89. X-section mean diameter and sorting coefficient vs acoustics — Line 45.

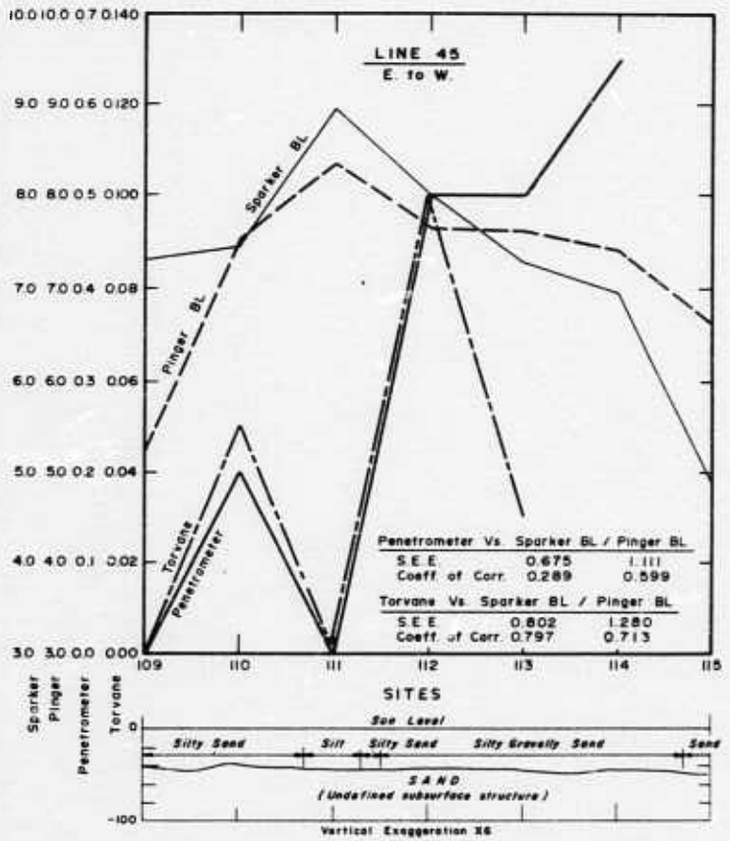

Figure 90. X-section penetrometer and torvane vs acoustics — Line 45.

obtained of the sediment properties and acoustical data, as well as geologic cross-sections along each line. Analyses show no definite trends, except that correlation coefficients seem to run much higher as the statistical sampling number is reduced from the overall area surveyed, to line-by-line, point-to-point sample areas. Geologic structure, such as noted in the exposed bedrock outcrops and thinly covered subcrop are indicated by the seismic subbottom profiles. These profiles and the cross-sections show the influence on the correlations obtained (figs. 17, 41-47, 67 and 68). Such structural variation over short distances may have direct bearing on the results obtained using the high frequency (12 kHz) source as compared to the lower broad band frequency (0-5 kHz) source. It was previously noted in table 6 that the correlation of the input-response functions of the two sources was relatively high (.657) despite their inherently different power and frequency characteristics. As mentioned previously (section 4.1.1), the depth of penetration and resolution of acoustical signal reflected off the bottom and subbottom horizons vary according to the source employed, consequently near surface structural as well as sediment property variations (within the wave length of the signal) can have a decided influence on the reflection coefficient obtained.

Stability of the surface-towed source and receiver systems was not considered a problem. Obviously, sea conditions are a limitation, and should be considered an important factor in obtaining reliable data. The experiments in both the Monterey Bay study and the San Francisco Bay study were conducted under the best prevailing weather conditions with due regard to the adverse circumstances inherent in sea state, swell, wave height and currents.

If the trend analyses, which shows that higher correlation coefficients in shallower water exist as compared to those noted in deeper water, has any validity, it may be concluded that a submerged tow vehicle, which would house the source and receiver systems, could operate with even greater effectiveness. This concept ought to be tested.

7.2 Shear Wave Experiment

From the records, the arrival time of the direct wave was taken to be the point determined from the intersection of the base line and the slope of the waveform. To obtain the shear wave velocity or compressional wave velocity, the time of the first arrival from each of the four traces (produced by either the four vertical geophone outputs or four horizontal geophone outputs) were plotted on a time distance graph.

Before discussing the results, the sources of error inherent in the seismic method should be mentioned. One source of error is in the distance between geophone units. Implanting the receivers by hand could result in an inch of misplacement. For a compressional wave velocity of 1500 m/sec, an error of approximately 8 percent in velocity can result assuming 1 in separation between two receivers, when in fact one receiver is displaced an inch.

Another source of error is in the time scale on the oscilloscope. An appropriate time scale for a wave velocity of 1500 m/sec is .1 m sec/cm; however, 0.5 m sec/cm was the lowest time scale achieved. The possible error that can be introduced using this time scale is 9 percent for a 1500 m/sec wave velocity. On account of the large errors introduced, the error for a particular measurement is not discussed. For the same reason, regression equations were not determined for the acoustical-mass physical property relationship.

It should be mentioned that the primary concern thus far has been to develop an inexpensive tool to investigate the feasibility of detecting S_H-wave in saturated marine sediments. Of secondary importance was construction of a high precision monitoring system. It was felt that if the detection of shear waves was found feasible, a refined system could then be designed.

7.2.1 Results from Lake Sediments

The determined acoustical and mass physical properties are listed in table 9. Figure 91 is an example of the signals received by a geophone implanted 2 in from the source (trace 1, horizontal geophone output; trace

Table 9. Acoustic and Mass Physical Properties at Beach Test Site

Sediment Type	Mass Physical Properties					
	Porosity (%)	Grain Size (mm)		Gravel (%)	Sand (%)	Clay and Silt (%)
		Median	Mean			
gravelly coarse sand	46.2	0.800	0.833	33.7	66	.3

Acoustic Properties (*In situ* Measurements)				
V_p (m/sec)	V_s (m/sec)	e (gm/cm^3)	a_s (m^{-1})	ω (Hz)
1690	125	1.68	.921	604

Computed Properties*						
Q_s^{-1}	μ_R	μ_I	K_R	λ_R	σ	E
0.40	.02	.09	4.77	4.75	.498	.04

*μ, K, λ, and E have units of dynes/cm^2 X 10^{10}.

2 vertical geophone output) and by another geophone unit implanted 4 in from source (trace 3, horizontal geophone output; trace 4, vertical geophone output). The receivers were inserted 1 in into the sediment, whereas the exit port on the source probe was at a depth of 1½ in. Although the voltage gain was high, the signal quality was poor. This is attributed to the high attenuation of the shear wave and to the low response of the vertical geophone to the direct p-wave.

In figure 91, the first arrival detected by each horizontal geophone is assumed to be the direct S_H-wave. The polarity reversal between the first arrival detected by the two horizontal geophones is caused by reversing the sensitive axis of the horizontal geophone, whose output is trace 1, 180° with respect to the other horizontal geophone. The polarity reversal is a necessary condition of an S_H-wave and was used here to aide in the identification of the direct S_H-wave. Presence of the polarity reversal eliminates the first arrival as being a compressional wave, a vertically polarized shear wave, or a Stoneley wave; however, a Love wave will also produce a polarity reversal with the employed geophone orientation, since the Love wave is a low frequency surface wave of the S_H type, formed from the superposition of internal reflections within a surface layer.

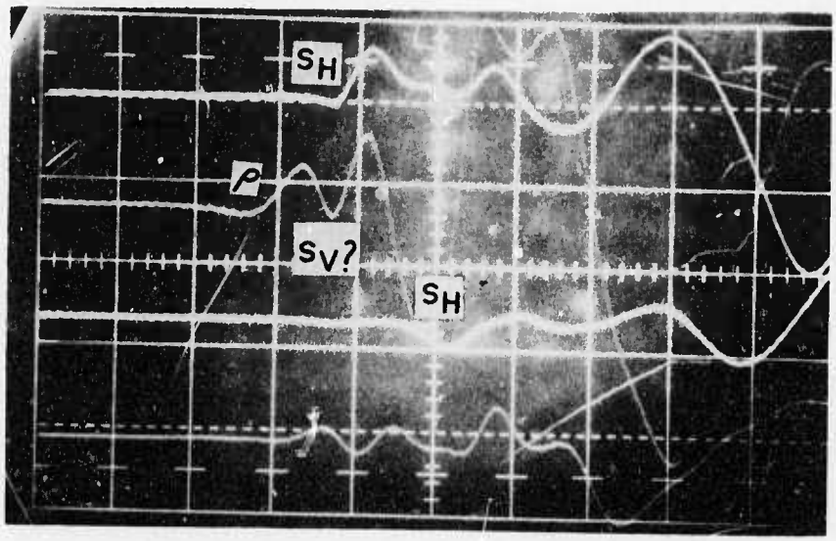

Horizontal Scale : $5 \frac{msec}{cm}$

Vertical Scale : $10 \frac{mv}{cm}$

Figure 91. Signal wave forms, trace 1 and 3: signals from horizontal geophones, 2 in and 4 in from source, trace 2 and 4: signals from vertical geophones, 2 in and 4 in from source (S_H: direct S_H-wave; p direct p-wave; S_V: direct S_V-wave).

A layer over a half space or a velocity gradient produced from vertical inhomogeneities is a necessary condition for the existence of the Love wave. For a source and receiver located in the distance between the source and boundary of the half space, the direct S_H wave will be the first arrival. This is attributed to insufficient time (or distance) for the superposition of reflections to form the Love wave. Beyond the critical distance (the distance at which the direct wave and head wave arrive at the same time), the Love wave will be the first arrival due to the superposition of the head wave with other waves. For the lake sediments, no visible change in the sediment type was observed within the top 1.1 m, with the probes implanted 0.45 m, the next interface below the water-sediment interface is situated at a minimum depth of 0.65 m beneath the probes. The minimum critical distance is thus 1.3 m; therefore, it is reasonable to assume that the direct S_H wave is the first arrival on the traces of horizontal hydrophones shown in figure 92.

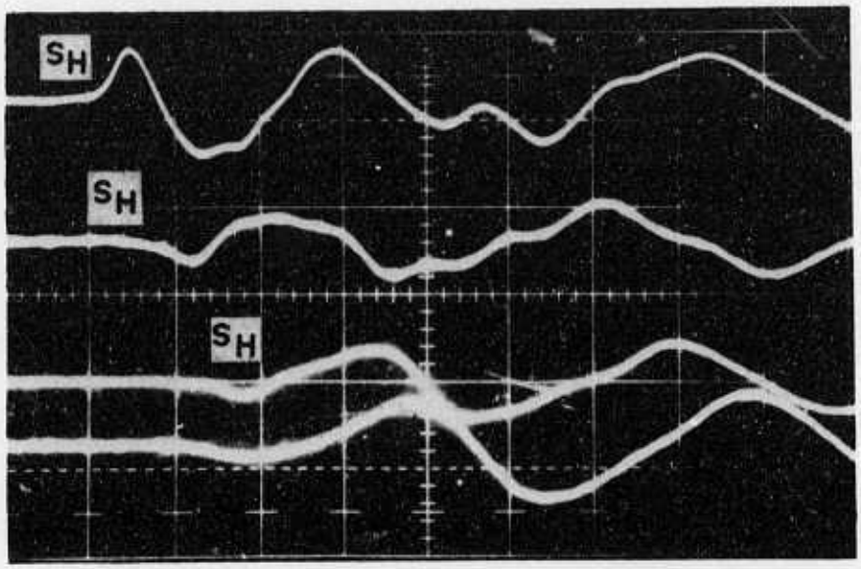

Horizontal Scale : 5 $\frac{msec}{cm}$

Vertical Scale : 10 $\frac{mv}{cm}$

Figure 92. Signals from four horizontal geophones (2', 3', 4', 5' in from source).

In addition to velocity, the attenuation of the direct S_H-wave was measured from records shown in figure 92. Four horizontal geophones at 2, 3, 4, and 5 in from the source were implanted at the same depth as the exit port on the source probe, 1½ in. Note the polarity reversal of trace 1 due to reversing the sensitive axis 180° with respect to the other three geophones. From the measured attenuation, the specific attenuation factor (Q_S^{-1}) was calculated to be 0.40. The error in using the low loss approximations (i.e., Hookean equations of elasticity) for this sediment is approximately 5 percent for the shear velocity.

The arrival of the direct p-wave was difficult to measure. The problem stemmed primarily from the low response of the vertical geophone to the direct p-wave. For a vertical geophone implanted further than 2 in from the source, the actual beginning of the compressional signal was absent. Receivers within 2 in of the source detected the beginning of the

compressional signal until an appropriate oscilloscope time scale was set to measure the arrival time differences. This problem was rectified somewhat by implanting the receivers and source at different depths.

7.2.2 Results from Monterey Bay Sediments

The *in situ* measurements and the calculated properties are listed in table 10. The mass-physical properties of the stations listed are indicated in Appendices A-5 and A-6. The attenuation of the shear wave was not measured because of the previously mentioned difficulties with the geophone probes. The source and receivers were at different depths. As the radiation pattern varies with the angle from the source, attenuation could not be measured, therefore, the low-loss approximation for velocity had to be used in order to determine the calculated values listed in table 10. As discussed earlier, low-loss approximation for the shear velocity could result in errors as high as 43 percent for a sediment with Q_s^{-1} of 2.

Examples of the better quality records obtained are shown in figure 93. Figure 94 illustrates a record of poorer signal quality. The depth of the source and the receivers varied. Generally, the source probe and the receivers were inserted 1½ in and 1 in, respectively. The four geophone units were spaced 1 in apart with the nearest geophone unit 1 in from the source. Distances between the exit port on the source probe and the receivers are noted on the records. Usually, only the two nearest geophone units to the source provided information on the direct waves. The first arrival at the other two geophone units was generally a head wave.

Table 10. In Situ Measured and Calculated Sediment Properties

Core Site	V_s (m/sec)	V_p (m/sec)	ϕ (g/cm³)	dynes/cm² x 10^{10}				σ
				μ	K	λ	E	
Mooring	567	1622	2.06	.66	4.53	4.09	1.91	.431
X1	504	2030	2.24	.57	8.46	8.09	1.66	.467
X2	521	1512	2.08	.57	3.97	3.59	1.62	.433
X3	---	1530	2.23	---	----	----	----	----
94	438	1485	1.99	.38	3.37	3.61	1.11	.452
103	308	1400	1.85	.18	3.39	3.27	.52	.475
118	524	----	2.33	.64	----	----	----	----
121	---	1440	2.03	---	----	----	----	----
122	475	----	2.03	.46	----	----	----	----
123	371	1430	2.09	.31	4.14	3.95	.90	.465

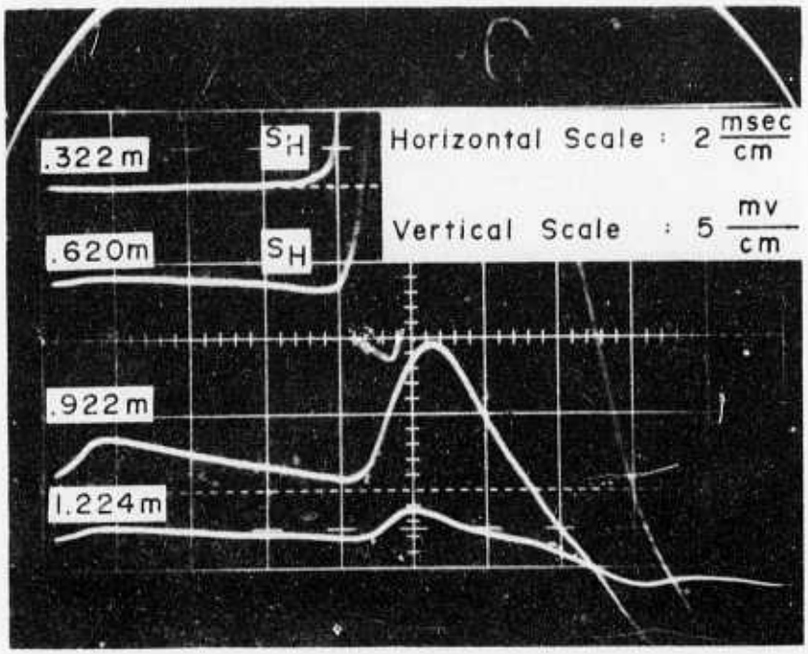

a. Signals from four horizontal geophones.

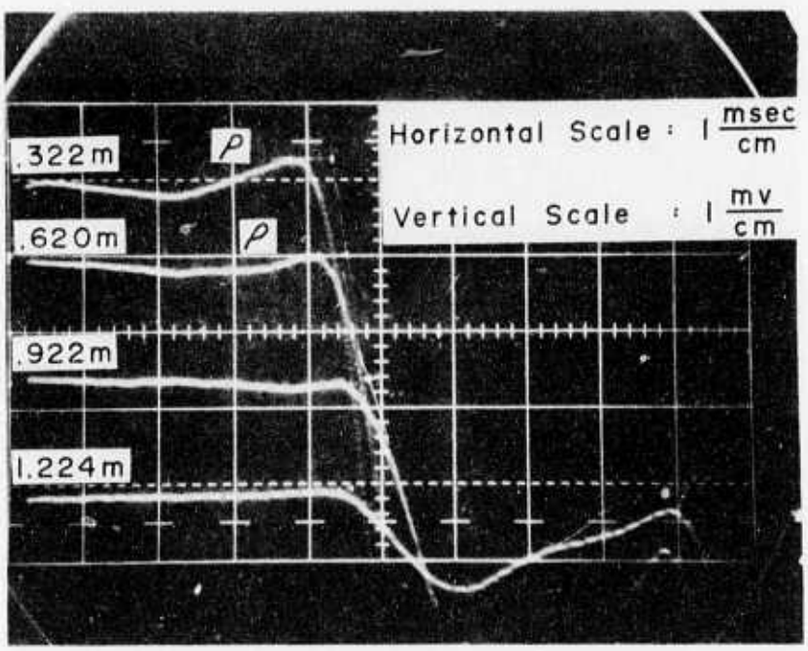

b. Signals from four vertical geophones.

Figure 93. Two records obtained at the mooring site. Distance between exit port on source probe and receiver is provided on the trace.

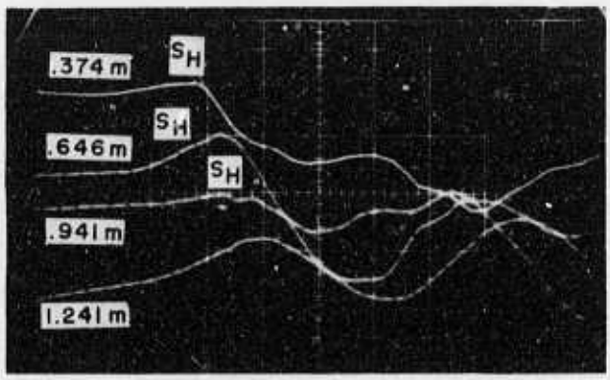

Figure 94. Signals from four horizontal geophones at station 122 (distance between exit port on source probe and receiver is provided on trace).

Difficulty in obtaining the arrival of the direct p-wave also occurred at this test area. The problem stemmed from the absence of a clearly defined first arrival and from information loss when setting the oscilloscope time scale to an appropriate level. A 1 m sec/cm or 0.5 m sec/cm time scale were used in recording the direct p-wave; therefore, significant errors in arrival time differences could have been introduced.

With no knowledge of the attenuation of the first arrival at the horizontal geophone, it is difficult to state whether this first arrival is the direct S_H-wave or the Love wave. The feasibility of being the Love wave was investigated for the sediment at the mooring station. At this station a vibracore was obtained which provided information on the sediment properties in the top 1.7 m. Extending to 0.8 m was a very fine sand density 2.14 g/cm^3 overlaying a dense clayey silt of density 2.4 g/cm^3. As the source probe was implanted 0.45 m, the minimum critical distance is 0.70 m. It is therefore unlikely the first arrival at the nearest two hydrophones (0.3 m and 0.61 m from the source) is the Love wave. At the other stations a core length of less than 0.6 m was taken.

As arrival time measurements were generally made only on the nearest receivers, 1 in and 2 in from the source, the time for the direct S_H wave to propagate to these receivers is very short. Therefore, if the layer thickness is large, the direct S_H wave can arrive before the Love wave. If the layer thickness is small or if there exists a velocity gradient in the surface sediment, the Love wave can arrive first; but the time required to form the Love wave must be short. Consequently, the energy forming the Love wave cannot penetrate further than 2 in from the source. For this case, the Love wave velocity would be comparable to the shear wave velocity. Therefore, it will be assumed that the first arrival is the direct S_H-wave (bearing in mind that further mathematical and experimental investigations are needed to clearly establish the extent to which this can be assumed).

7.2.3 Correlation Between Acoustical and Mass-Physical Properties

Previous investigations by Hamilton (1970b), Horn et al. (1968), Schreiber (1968), and others have found predictable relationships for compressional velocity vs porosity and compressional velocity. Porosity is the ratio of the volume of voids occupied by the water to the total volume. As the rigidity is of low magnitude in saturated sediments, the compressibility of the water largely determines the compressional wave velocity rather than the compressibility of the grains. Therefore, a strong correlation is expected to exist between the compressional wave velocity and porosity. Figure 95 illustrates the relationship obtained between the compressional velocity and porosity.

Also, the compressional velocity is strongly related to the sediment's grain size. This affect is due to the fact that density, porosity, and other sediment porperties are a function of grain size. In marine sediments, a decrease in grain size produces an increase in porosity, and consequently a decrease in compressional velocity. Velocity-mean grain size relationship is shown in figure 96.

In discussing the relationship of the shear wave data with the mass-physical properties, it was more convenient to use rigidity as the shear

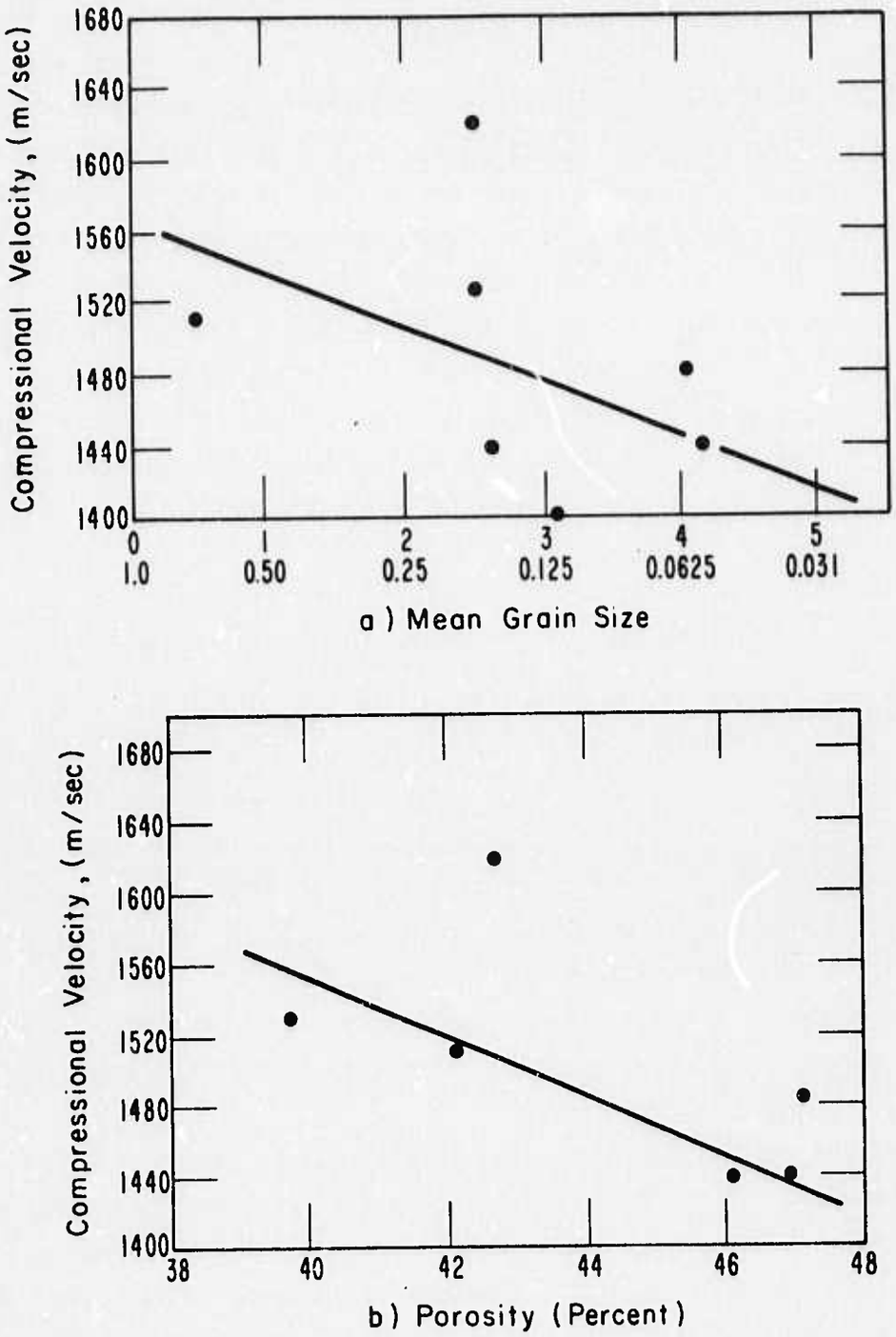

Figure 95. Compressional velocity vs mean grain size and porosity.

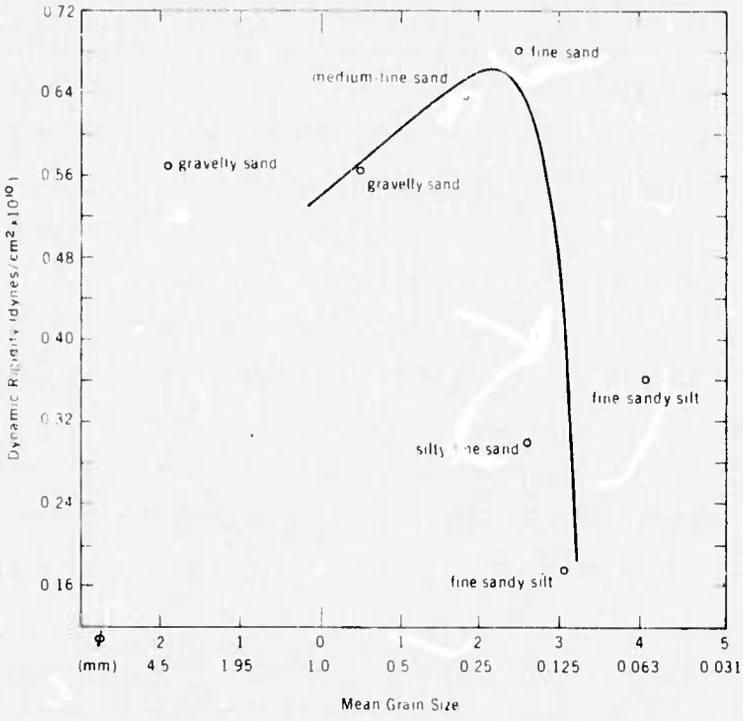

Figure 96. Dynamic rigidity vs mean grain size.

parameter. Hamilton (1971) and Hardin and Richart (1963) give excellent discussions on the correlation of rigidity with other sediment properties such as porosity and grain size. From these reports, the following conclusions were derived for sands:

(1) dynamic rigidity should be a minimum in the coarse sands as they are rounder and possess fewer intergrain contacts;
(2) an increase in porosity will cause a decrease in rigidity for sands of the same grain size and angularity;
(3) although porosity increases as the grain sizes decrease, rigidity may increase as the grains become finer because finer grains have more intergrain contacts and higher angularity;
(4) at some fine sand-silt sizes, the intergrain friction and interlocking will be maximum, and, therefore, rigidity will be maximum for natural uncemented sediments; and
(5) with an increase in amounts of silt and clay, the sand grains are no longer in contact; the intergrain friction and interlocking are no longer effective, and rigidity becomes dependent on the cohesion between finer particles.

As mentioned previously, the determined empirical relationships between rigidity and porosity and between rigidity and mean grain size are illustrated in figures 95 and 96. These relationships generally follow the conclusions of Hamilton (1971) and Hardin and Richart (1963) discussed above. Maximum rigidity occurs for a fine sand of grain size 2.5 phi units (or .24 mm). For the larger grains sizes, the rigidity is less due to fewer intergrain contacts and rounder grains. Moreover, the rigidity decreases rapidly when silt is introduced into the sediment. This phenomenum is better illustrated in figure 97. Included in figure 98 is the variations of rigidity with percent of sand and gravel. As shown, the increase in the amount of silt reduces the rigidity. This is caused by an increase in porosity and a decrease of density.

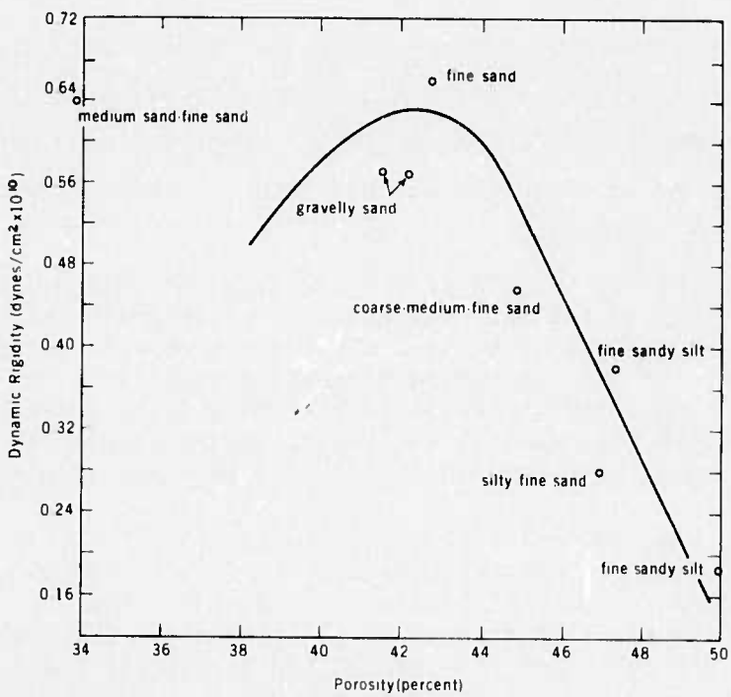

Figure 97. Dynamic rigidity vs porosity.

An additional relationship of rigidity vs Poisson's ratio is shown in figure 99. Poisson's ratio is the ratio of the transverse strain to the longitudinal strain. For a liquid, rigidity is zero, and Poisson's ratio reaches its maximum value, 0.5. Consequently, as rigidity increases, Poisson's ratio will decrease.

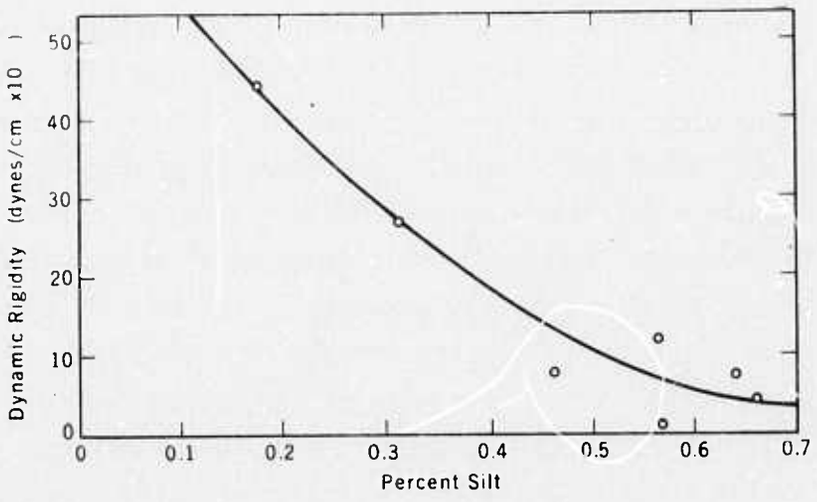

Figure 98. Dynamic rigidity vs percent silt.

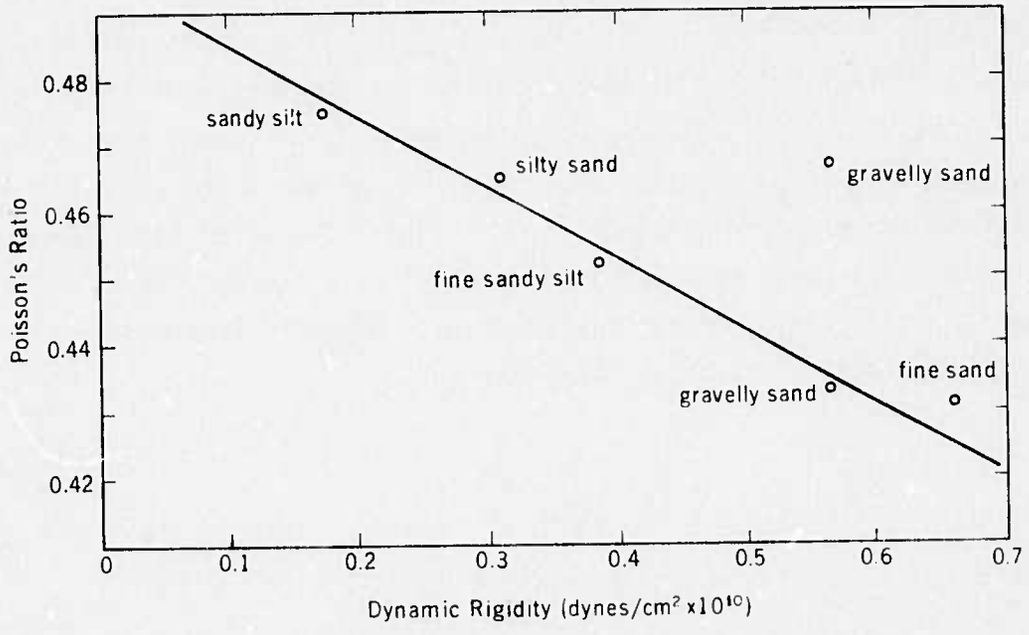

Figure 99. Dynamic rigidity vs Poisson's ratio.

7.3 Direct Current Resistivity Experiment

7.3.1 Data Interpretation

For maximum flexibility in the interpretation of field data, it would be desirable to have available sets of interpretation curves for a seafloor array, similar to those published for land use. Such curves are computed by calculating the potential field generated by a single current electrode placed over a layered medium, with each layer having arbitrary resistivity and thickness. A geometrical factor, depending on the array configuration and spacing, then is used to obtain the voltage difference, ΔV, appearing between the potential electrodes for a given current I[13].

Terekhin (1962a and b) and Van'yan (1956) have examined the theoretical potential generated by a current electrode on a layered sea floor, but their results are not in a form suitable for immediate computation. Other workers in the Soviet Union apparently have published interpretation curves for seafloor arrays, but we have not yet been able to obtain copies of their work. Equations in a form suitable for computer solution are given in Barnes et al. (1972). A simpler, although slightly more time-consuming method of interpreting sea-floor resistivity data has been used for all of our work to date.

For analytical purposes, an array on the sea floor differs from one on land only in that a layer of conductive sea water is present above the array. If the depth and resistivity of the water layer (which are easily measured) are known, the apparent resistivity ρ_ω of the water layer may be obtained from the standard interpretation curves. The water layer then may be considered as a known resistance in parallel with the sea floor, and the true apparent resistivity of the sea floor, ρ_a, obtained from the total measured resistivity ρ_t by using the formula

$$\frac{1}{\rho_a} = \frac{1}{\rho_t} - \frac{1}{\rho_\omega} , \tag{40}$$

where

$$\rho_t = 2\pi a \frac{\Delta V}{I} . \tag{41}$$

Once the value of ρ_a has been calculated, published standard interpretation curves may be used to obtain the true bottom resistivity profile.

The curves of apparent bottom resistivity ρ_a vs electrode separation a obtained in Puerto Escondido are shown in figure 100. Locations B-5a and B-5b were about 30 m apart, in water 12 m deep, and location B-3 was in an area about one km away in water 6 m deep. Bottom water salinity was 32 0/00 in both locations, and temperature ranged between 21 and 23°C.

Figure 101 shows the geologic interpretation obtained by matching the curves of figure 100 against the Wenner interpretation curves published by Mooney and Wetzel (1956a). The resistivity profiles of the two nearby locations, B-5a and B-5b, show no evidence of bedrock. The bottom sediment layers do not, of course, extend to infinity, but the bedrock in this area apparently is too deep to be "seen" with a maximum value of electrode spacing of 300 cm. The presence of bedrock is evident at a depth of 4.8 m at location B-3, which was in shallower water, close to shore. It is significant that even this low-powered array, with relatively small electrode spacings, was able to provide information to a depth of almost 5 m into the sub-bottom.

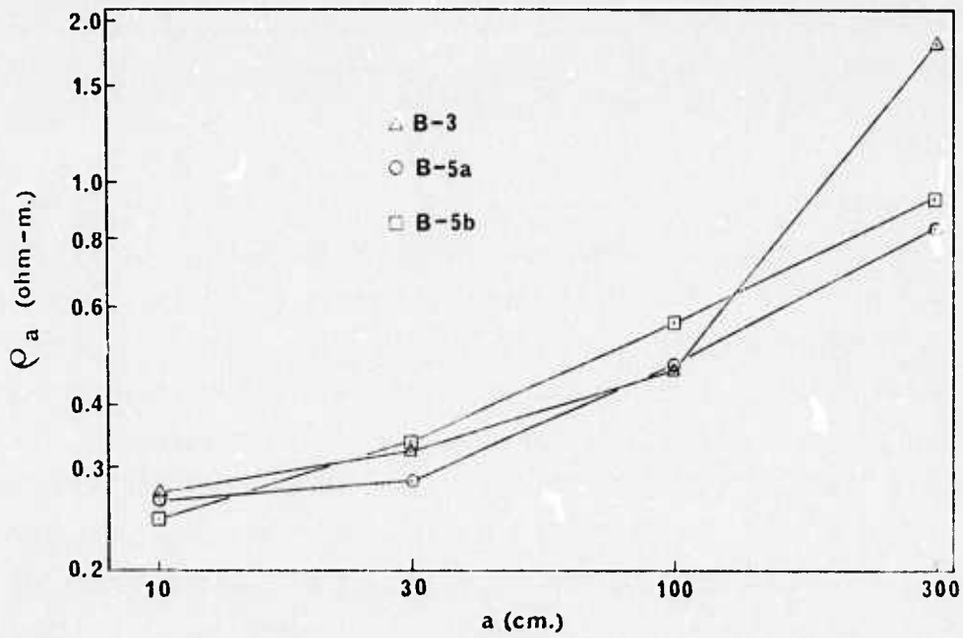

Figure 100. Data from Puerto Escondido, Mexico.

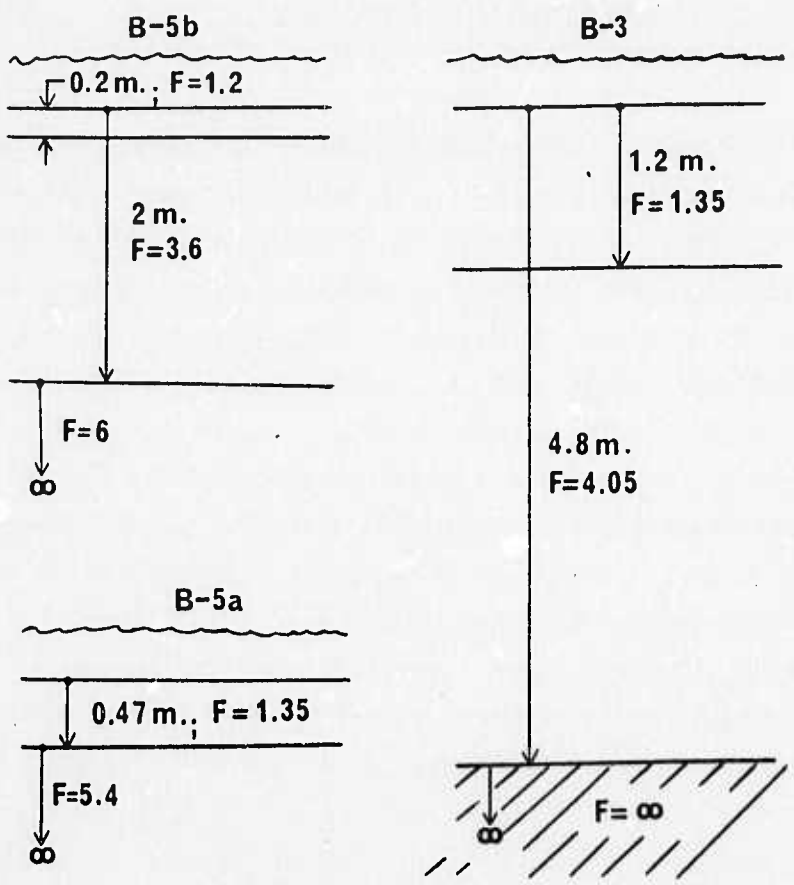

Figure 101. Data interpretation — seafloor array Puerto Escondido test site.

The tests in Monterey Bay using the *in situ* expandable survey were run in water 6 m deep, at a temperature of 15°C and salinity of 34 0/00. The formation factor vs electrode separation curve of figure 39 shows an initial decrease in apparent resistivity with depth. A core (vibracorer) of 1.7 m taken at this location showed compact silty sand overlying a loosely packed layer of sand and gravel beginning 30 cm below the surface. The sand and gravel graded into well compacted sandy silt over the next meter. Unfortunately, the sediment was disturbed considerably during the the process of coring and handling, so no resistivity measurements on the core itself were possible. It is reasonable to assume, however, that the resistivity of the loosely packed sand and gravel was less than that of the fairly compact overlying silty sand, and that of the well-compacted

sandy silt beneath. This interpretation agrees with that obtained by curve matching, shown on figure 9 (section 3.3) and figure 102. The high-resistivity layer at a depth of 1.7 m may have been the cause of the core tube stopping at that depth.

Surface Towed Array. As mentioned in section 3.3, a surface-towed horizontal resistivity array could provide a rapid method of measuring bottom resistivity values over large areas of the seafloor. A surface-towed array cannot offer the resolution of bottom structure available from a bottom-deployed array, but if electrode spacings are large enough to force a sufficient amount of current into the bottom, and if the impressed current is large enough to produce signal levels well above the background noise, considerable information about bottom properties may be obtained.

This is apparent from figures 102 and 103. The ratio $\Delta V/I$ (the voltage appearing between the potential electrodes divided by the impressed current is plotted against the formation factor of the bottom, with the sea floor considered as a single homogeneous layer and the ratio of electrode separation a to water depth d is equal to 4/3. For an impressed current I of 3 amps, a change in sea-floor formation factor from 2 to 3 will result in a change of about 0.7 millivolts in ΔV, and a formation factor change from 9 to 10 gives a change of about 0.2 millivolts in ΔV. A 0.2 millivolt change is detectable in practice, so unit changes in sea-floor formation factor should be distinguishable using this electrode arrangement.

The water was calm near shore, but waves increased to about 5 ft (1.5 cm) in deeper water, resulting in considerable ship motion (which did not impede the profiling operation). Water surface temperature was 15°C, and salinity 34 0/00, over the entire area, giving resistivity ρ_ω of 0.24 ohm-meters. Time, core site, current I, and water depth were noted on the chart recorder output of ΔV (fig. 23).

Previous measurements of resistivity over water-covered areas have been by Schlumberger and Leonardon (1934); Volker and Dijkstra (1955); and Bonlos (1972), but these were done with stationary rather than towed arrays. Unz (1959) discusses some of the theory of water-surface resistivity measurements.

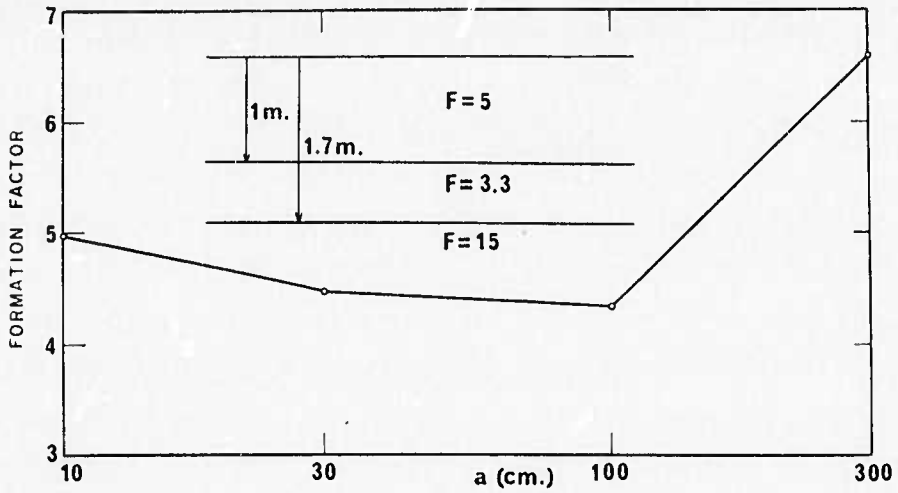

Figure 102. Data interpretation — seafloor array Monterey Bay test site.

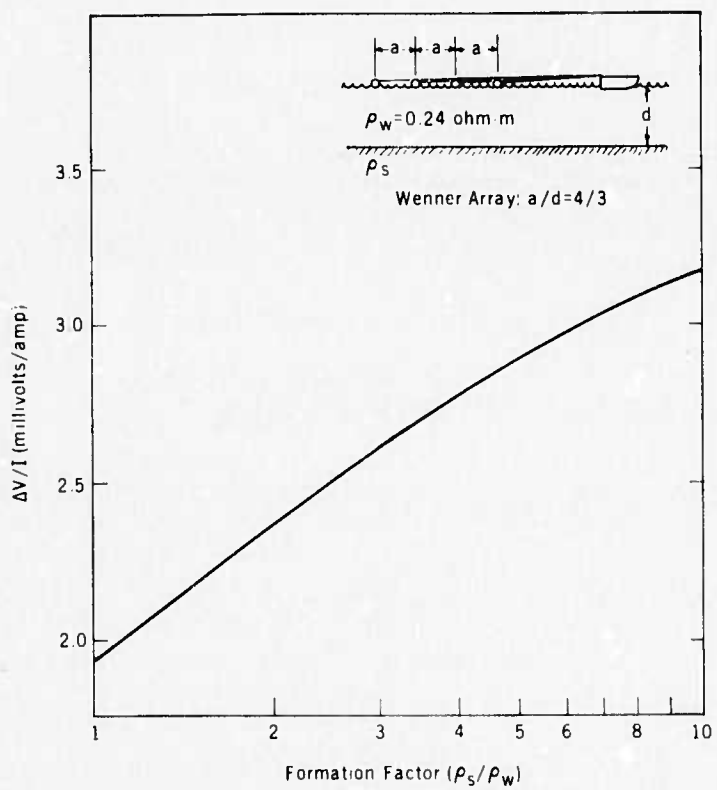

Figure 103. ΔV/I vs formation factor of seafloor sediments.

In contrast to the bottom-deployed array, data obtained from a surface-towed array is handled the same as data obtained from an identical array on land. Differences between the land and marine cases arise mainly during actual application:

(1) Compared to most land situations, the resistivity of the first (salt water) layer in the marine case is very low, so a large fraction of the impressed current will flow through the water layer. Therefore, higher current levels must be used in offshore work to assure that sufficient current will penetrate the seafloor to give accurate readings.

(2) The contact resistance of sea water is much lower than that of most earth materials, so high voltages are not needed to force a large current flow into sea water. While several hundred volts may be required to force one amp into the earth, twelve volts are sufficient to force 10 amps into sea water, using electrodes of the same size.

(3) Noise sources for the land and marine cases are somewhat different in magnitude and origin. While the use of commutated direct current is helpful in removing the effect of dc drift of the potential electrodes on land, excessive changes of dc level often are difficult to compensate. At sea, the drift of the silver-silver chloride potential electrodes is very small, but the effects of waves, currents, and other marine phenomena may be troublesome. Typically, the noise level of a towed electrode pair is less than a few tenths of a millivolt.

(4) In contrast to the onshore situation, the offshore resistivity profile is continuous with every point along the ship's course sampled. Whereas one or more electrodes (usually two or all four) must be dug up and re-implanted for each resistivity measurement on shore, all electrodes are in continuous contact with the water in the offshore case. This allows much faster (and thus more economical) coverage offshore, as a towing speed of at least 3 knots may be maintained in most sea states, with speeds of up to 10 knots feasible in some situations.

7.3.2 Results

The towed resistivity data was analyzed by the following procedure:

(1) The apparent resistivity ρ_a is calculated using the equation

$$\rho_a = 2\pi a \frac{\Delta V}{I} ,$$

where a is the electrode separation (20 m), ΔV is the measured potential difference at the core site, and I is the measured current.

(2) Using the calculated value of ρ_a and the known water depth, the sediment resistivity ρ_s may be found by reference to a standard set of two-layer resistivity curves, such as those given by Mooney and Wetzel (1956a) or Van Nostrand and Cook (1966, p. 91).

(3) The formation factor (F) is calculated by dividing the sediment resistivity ρ_s by the water resistivity ρ_ω (0.24 ohm-m):

$$F = \frac{\rho_s}{\rho_\omega} .$$

The data is summarized in Appendix A-5. The data was recorded continuously (except for short periods when the current was turned off to check the zero level of the potential electrodes). For analysis, however, the data has been tabulated only at individual core sites. The values of formation factor F are considered accurate to ± 10 percent, except at the deepest core sites (71, 71, 83, and 84), where the amount of current penetrating the bottom may have been insufficient for accurate readings.

The surface towed resistivity data shown in table 11 covers the survey area shown in figure 104. The data is shown graphically in figures 105 through 107. Figure 105 shows the formation factor (F) and the porosity (ϕ) measured on core samples for the three east-west traverse lines shown in figure 106. The expected inverse correlation between F and ϕ is readily apparent in lines 124-117 and 107-99, but does not appear on line 116-108. The overall pattern of sediment porosity distribution along the three east-west survey lines is evident in figure 106: soft (high-porosity) sediments toward the center of the area, grading into harder material at the eastern and western boundaries, with a probable bedrock outcrop in the northwestern corner. This pattern also may be seen in the formation factor contour map (fig. 107), which is quite similar in general outline to the porosity contour map (fig. 108).

Table 11. Towed Resistivity Data

Core Site	Depth (m)	I	ΔV	Formation Factor (F)
		Line 1		
107	15.2	3.70	10.2	4.00
106	16.8	3.65	10.0	5.67
105	16.5	3.60	9.7	4.41
104	15.8	3.60	9.5	3.65
103	15.8	3.60	9.5	3.65
102	15.5	3.60	9.7	3.76
101	14.9	3.60	9.9	3.76
100	14.3	3.60	10.5	4.71
99	14.0	3.60	10.6	4.41
		Line 2		
108	12.5	3.80	12.2	5.06
109	12.8	3.75	11.4	4.00
110	13.7	3.72	11.1	4.41
111	13.7	3.70	10.8	4.13
112	13.7	3.67	10.4	3.44
113	14.3	3.70	10.5	4.00
114	14.6	3.68	10.4	4.13
115	15.2	3.70	10.7	5.45
116	13.7	3.70	11.3	5.45
		Line 3		
123	12.8	3.67	12.7	8.52
122	12.2	3.70	11.6	5.90
121	11.3	3.65	12.0	4.13
120	11.6	3.70	11.8	3.88
119	11.3	3.70	12.6	4.88
118	11.3	3.70	12.3	4.26
117	11.0	3.67	12.8	5.25
		Line 4		
118	11.3	3.50	12.4	6.14
109	12.2	3.68	11.2	3.76
100	14.6	3.70	10.5	4.13
93	15.8	3.70	9.8	3.76
X-1	18.3	3.70	9.0	3.35
84	21.0	3.70	8.4	3.00
71	26.8	3.65	7.6	2.33
		Line 5		
72	27.4	3.70	7.4	1.60
83	21.6	3.80	8.5	2.70
X-2	19.5	3.80	9.0	3.26
94	17.1	3.65	9.1	3.08
103	15.2	3.65	9.5	3.08
112	13.4	3.65	10.4	3.44
121	10.4	3.65	11.7	3.44

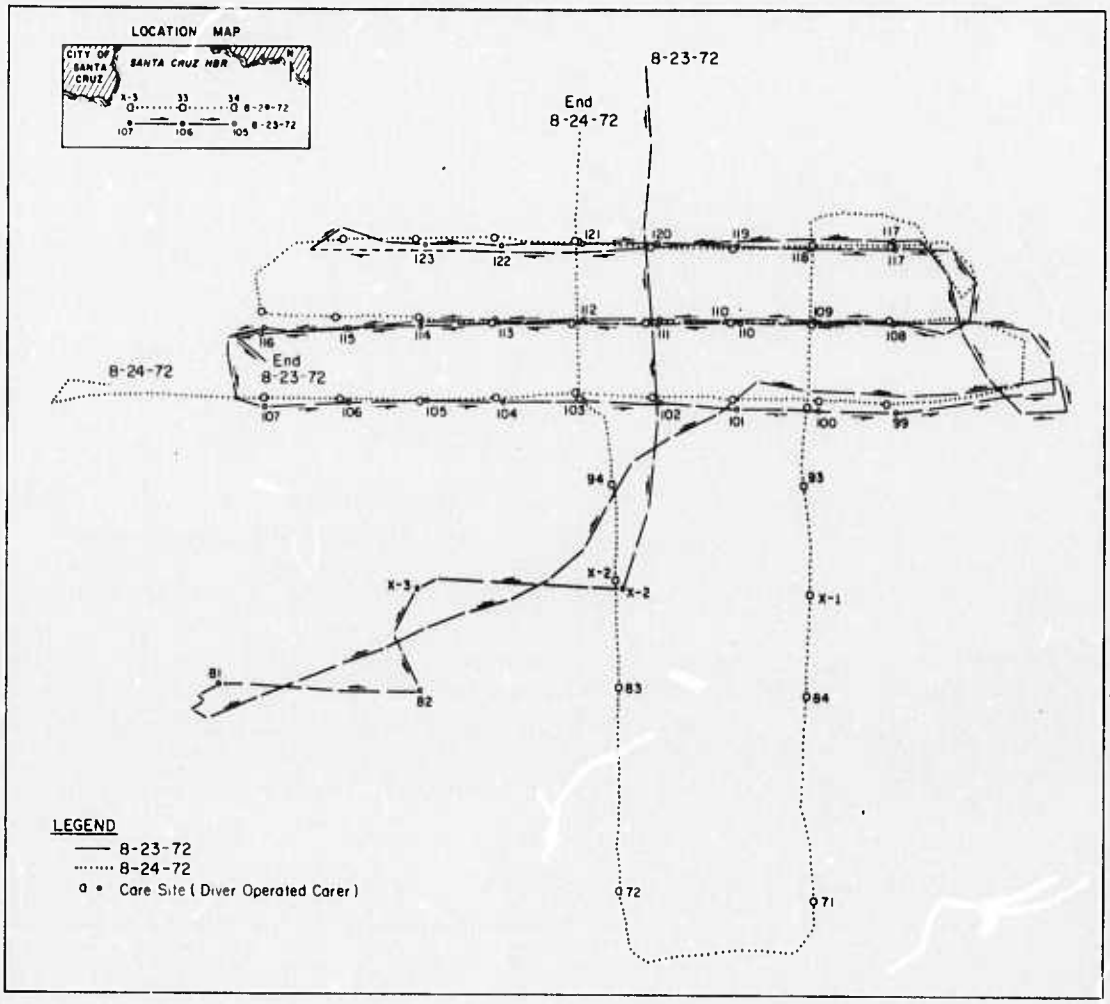

Figure 104. Index map of towed resistivity survey.

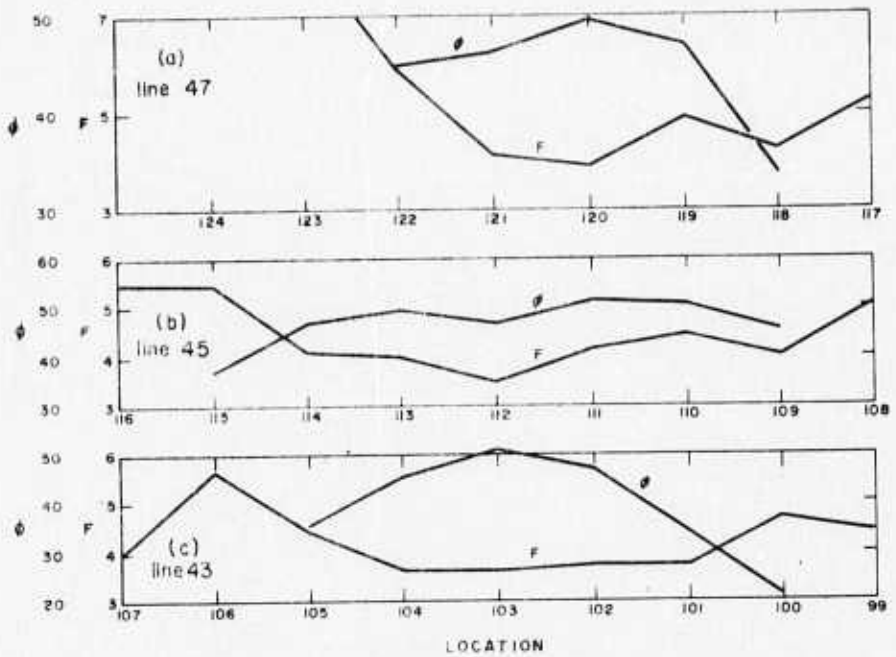

Figure 105. Direct current resistivity test — east-west profil of F vs ϕ.

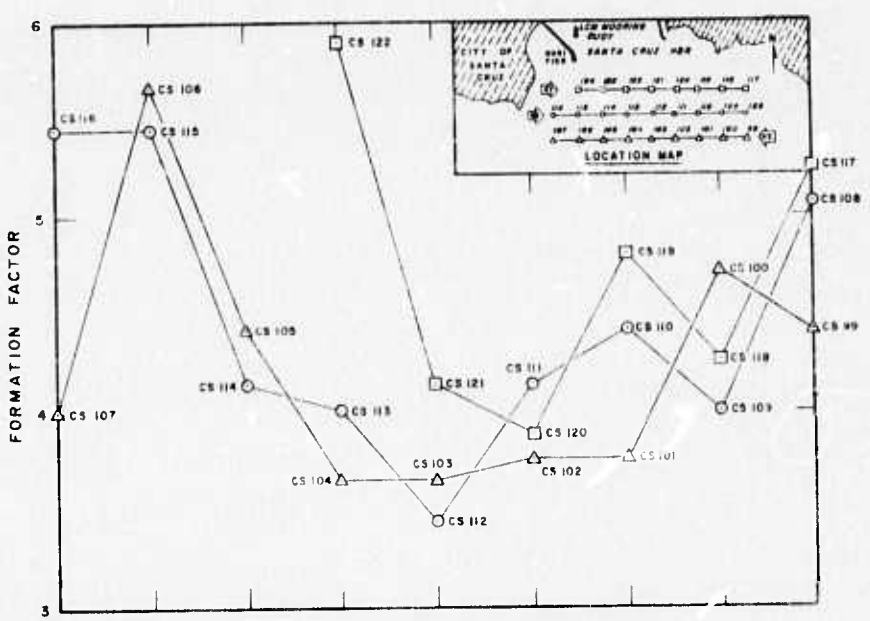

Figure 106. East-west formation factor profiles surface-towed resistivity.

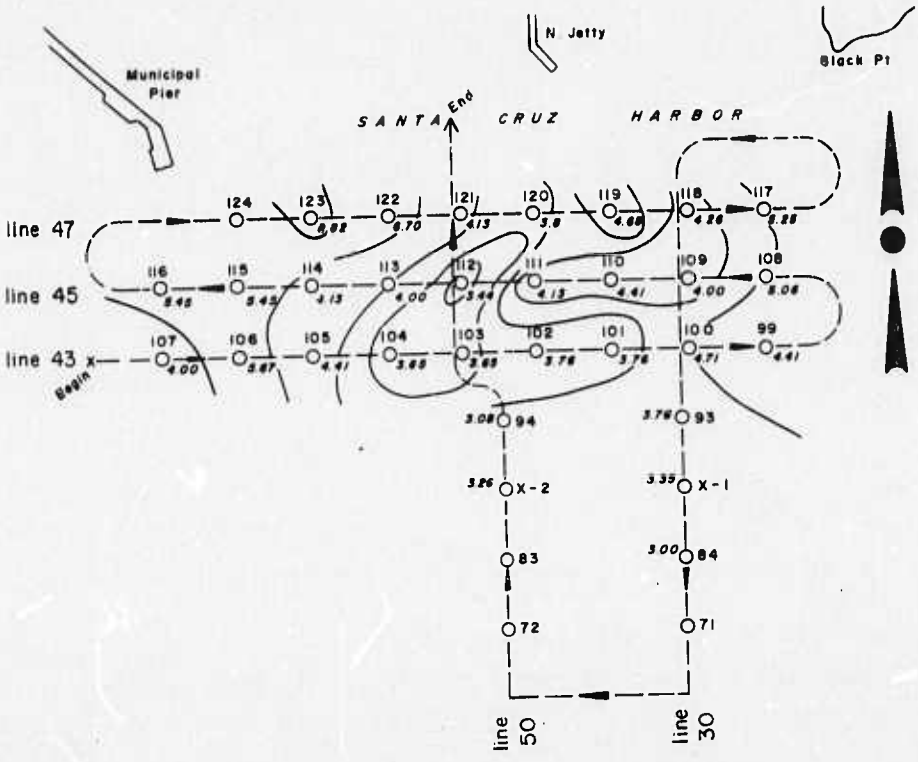

Figure 107. Formation factor contour map.

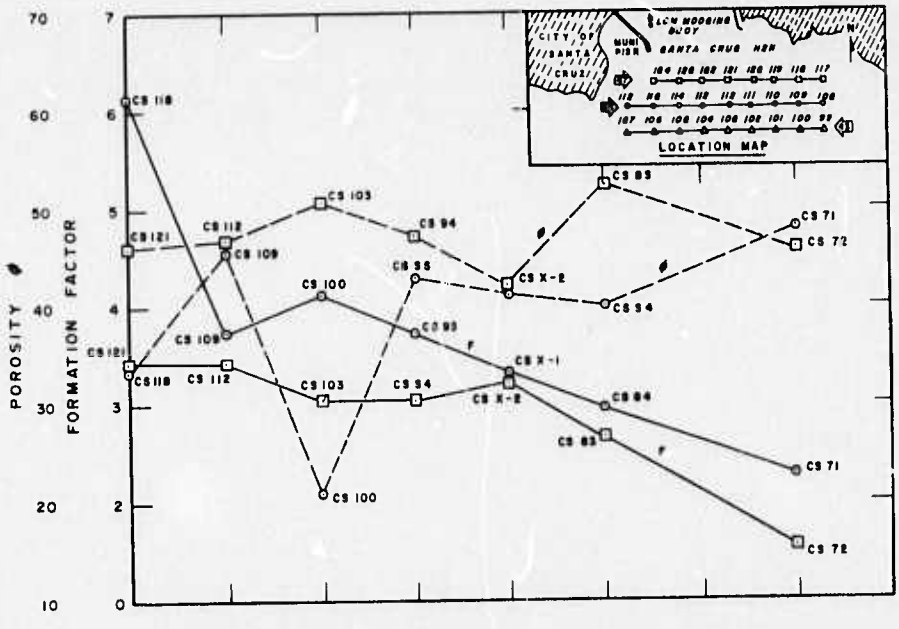

Figure 108. North-south formation factor and porosity profiles surface-towed resistivity.

Formation factor and porosity along the two north-south traverse lines (118-71 and 121-72) are shown in figure 108. The inverse correlation between F and ϕ again is apparent on these profiles, although, as mentioned above, the deep-water values may be somewhat suspect. The low porosity at core site X-2 is reflected as a peak in the formation factor curve at that point. As the depth at X-2 was 64 ft (19.5 m) roughly equal to the electrode separation a, it appears that valid data may be obtained at a water depth at least equal to the electrode separation.

A statistical analysis of formation factor and porosity over the entire survey area showed no mathematical correlation between the two parameters, although reasonable correlation along individual survey lines is evident in figures 105 through 108. There are two possible explanations for the lack of mathematical correlation:

(1) It is quite possible that the porosity measured on some of the cores was not representative of true *in situ* porosity. The sediments are disturbed to some extent when the core is taken, and the degree of disturbance probably varied from core to core. A few "wild points", due to erroneous porosities, could have a strong negative effect on the mathematical correlation coefficient.

(2) The diver-operated coring device has a maximum penetration of 70 cm, and most cores in the survey area did not achieve maximum penetration. The electric current penetrates the bottom to a depth considerably greater than one meter, and so measures sediment properties at depths greater than those sampled by the cores. If sediment porosity changes significantly with depth at a given location, or if bedrock is within a few meters of the sediment surface, this information will be reflected in the towed resistivity values, but may not be evident in the cores.

8. CONCLUSIONS AND RECOMMENDATIONS

8.1 Reflection Coefficient Mapping Experiment

The correlation matrices and other results of this experiment indicate that there is some potential in using remote sensing acoustical apparatus by a ship underway for mapping, at least qualitatively, the mass physical properties of seafloor sediments. Correlations obtained in this study were inconclusive, but in-depth evaluation of the data would provide

information on alternate approaches to the problems involved in data acquisition and analysis. It was obvious from the preliminary analysis of the results that there are many problems in applying surface towed systems to map sediment properties, even with the utmost navigation control and advanced acquisition instrumentation. Improved automatic data processing, using real-time, on-line displays is absolutely essential. It was learned that at least four problems exist which may affect the reliability of the data:

(1) Determining what is a representative statistical sample.
(2) Obtaining accurate near-surface sediment velocity data.
(3) Control of the distance between the source-receiver system and the seafloor to maintain the same differential area that the energy impinges upon.
(4) Maintaining the stability of the sensor package in a horizontal orientation, for attaining normal incidence.

It is recommended that further research be conducted in data processing and analysis procedures, using the data derived from this study. Investigation of all the permutations of data analysis in this study was beyond the capability and funds allotted. Development should be pursued in the engineering design of self-contained submerged tow systems capable of powering and accurately navigating at any depth and at a fixed elevation in a horizontal orientation. This development is particularly desirable in view of the requirements for more information on deep sea sediment properties and the need to obtain these measurements in as rapid and economical manner as possible.

8.2 Shear Wave Experiment

In the past, the detection of the shear wave in saturated marine sediments was accomplished indirectly by measuring the Stoneley wave velocity or employing a viscoelastometer. The high energy losses of the shear wave and the low sediment rigidity prevented direct measurements of the shear wave. It is felt that, on the basis of the data and discussions presented, the described seismic method successfully detected the direct S_H wave in gravelly coarse sand at a lake test site. For most of the stations in the Monterey Bay test area, it could not be clearly established that the detected wave was the shear wave or the Love wave, which has been attributed

to insufficient core lengths to assertain sediment stratigraphy. As drastic changes in the sediment properties and, thus, shear velocities are not generally anticipated, and because the separation distances between source and receivers is small the Love wave, if detected, would have comparable velocity to the shear wave. Therefore it was assumed that the velocity obtained is the shear velocity.

A refined seismic method is planned for future *in situ* tests. A multi-channel magnetic tape recorder will be used instead of the oscilloscope. This will increase the accuracy in time measurements and reduce the number of source shots. Hydrophones will be employed to detect the compressional wave. Moreover, both receivers probes and source probe will be inserted mechanically to obtain accurate distances between probes. A sampler capable of taking longer cores is also a necessary addition.

The source proved adequate in generating shear waves; however, the air gun will introduce air into the sediment. Some air might enter the sediment region between the source and receivers although the source energy is directed away from this sediment. This will reduce the value of compressional wave velocity largely through the reduction in the bulk modulus. Therefore, consideration has been given to develop a new source such as a bi-directional electro-magnetic hammer. Being bi-directional, the new source can produce stacked records to magnify the S_H waves or records showing the polarity reversal of the S_H waves through reversing the direction of the source.

As discussed, the dynamic values of rigidity, bulk modulus, Young's modulus, and Poisson's ratio can be computed from known values of the compressional velocity, shear wave velocity, and density. As the time durations of acoustical stresses last only for a thousandth of a second, the dynamic constants will vary considerably with those determined by conventional static tests in the laboratory. Clearly, *in situ* acoustical measurements can provide useful information about these constants, particularly if acoustical properties can be related with those resulting from static laboratory tests.

Empirical relationships do exist between acoustical and mass physical properties. These relationships can be used in two ways. If porosity,

textural properties, shear strength, bearing capacity, or settlement can be related to the acoustical properties for a particular marine environment (bay, shelf, abyssal plains/hills), one need only secure the acoustical properties and a disturbed core sample to ascertain the sediment type to correlate these relationships and obtain the approximate mass physical and engineering properties of the site. Reversing the procedures, one could obtain the acoustical properties by consulting these relationships if the mass physical properties are measured from an undisturbed core sample. Future work should entail securing these relationships and determining the accuracy that can be expected in using these relationships.

In conclusion, knowledge of the acoustical properties of seafloor sediments, as derived from shear wave analysis, can provide useful information in obtaining the geotechnical variations within the marine environment. This information would be extremely helpful in solving engineering problems related to excavation, tunneling, or for construction of platforms, dams, and bridges in the marine environment.

8.3 Direct Current Resistivity Experiment

From the above discussion of results, it is evident that a towed offshore resistivity array can give information about seafloor properties, even with the use of unsophisticated equipment. Several improvements in equipment and data handling could result in even more rapid, more accurate, and less expensive resistivity data acquisition:

(1) Other electrode arrays, such as the Schlumberger and Anipole, should be investigated theoretically in the field. It should be possible to optimize array configuration and electrode spacing for expected water depths and bottom properties.
(2) The use of a multiple electrode array would enable multiple-layer interpretations of bottom geology to be made. Electrodes could be switched sequentially to vary their spacing, or arrays could be devised in which a single pair current electrodes is continuously energized and the signal between multiple potential electrode pairs recorded.
(3) Improved accuracy and speed would result from electronic processing of the data, with the current signal divided electronically into the filtered potential signal. This information could be stored on tape, along with water depth, temperature, and salinity, for automatic processing of the data.

In summary, the results of this study indicate that a towed offshore resistivity system can, especially when used in conjunction with other geophysical techniques, provide valuable data about seafloor properties. System improvements, such as those suggested above, could make the technique even more accurate and economical.

9. ACKNOWLEDGMENTS

This research was supported in part by the Department of Defense, Advanced Research Projects Agency and was monitored by the Bureau of Mines, Department of Interior under contract H0220019. The authors are grateful to the supporting services of the Marine Minerals Technology Center and the advisory services of the Department of Engineering Geoscience of the University of California, Berkeley, particularly the technical assistance of Professors Thomas McEvilly, Patrick Wilde and consultant Dr. Peter Rogers.

The credits for the fine line drawings and art work go to Mr. Yok S. Gee, Cartographer for the Center.

Our appreciation also goes to the operators of the *R/V Doodlebug* and *R/V NOAA's Ark*, Captain Peter Sheppard and John Brown and engineer Herb Price.

10. REFERENCES

Albers, Vernon M. (1969), Underwater acoustics instrumentation, *Instrument Soc. of America*, 72-75.

Anderson, O. L., and P. C. Liebermann (1968), Sound velocities in rocks and minerals: Experimental methods, extrapolations to very high pressures and results in physical acoustics, principals and methods, ed. W. P. Mason (Academic Press, New York, N.Y.).

Archie, G. E. (1942), The electrical resistivity log as an aid in determining some reservoir characteristics, *AIME* 146:54-62.

Barnes, B. B., R. F. Corwin, J. H. Beyer, Jr., and T. G. Hildenbrand (1972), Geologic Prediction: Developing tools and techniques for the geophysical identification and classification of sea-floor sediments, NOAA Tech. Rept. ERL 224-MMTC 2, 163 pp.

Barnes, B. B., and R. Newman (1971), A subsystem for electronic positioning and navigation at sea, *Proc. of the IEEE Conf. on Engineering in the Ocean Environment*, 121-146.

Bieda, G. E. (1970), Measurement of the visco elastic and related mass physical properties of some continental terrace sediments, M.S. Thesis, U.S. Naval Postgraduate School, Monterey, Calif.

Biot, M. A. (1962), Mechanics of deformation and acoustic propagation in porous media, *J. Appl. Phys.*, 33:1482-1498.

Birch, F., V. F. Schairer and H. C. Spicer (1942), Handbook of physical constants, *Geol. Soc. America Special Paper* 36, 325 pp.

Bobber, Robert J. (1970), Underwater electroacoustic measurements, Naval Res. Labs., pp. 11-15, 17-45 and 193-273.

Bodholt, H. (1969), Scientific echo sounding systems — measuring target strength and backscattering strength, *SIMRAD Tech. Bull.* No. 5, SIMRAD, Inc., Kew Gardens, N.Y., 11 pp.

Borcherdt, Roger D. (1971), Inhomogeneous body and surface plane waves in a generalized viscoelastic half space, Ph.D. Thesis (Nov).

Boulas, F. K. (1972), Electrical sounding on the water surface at Khor Kundi El-Bahari in Egypt, *Geophysical Prospecting* 20(2):304-316.

Bouma, A. H., W. E. Sweet, F. B. Chmelik and G. L. Huebmer (1971), Shipboard and *in situ* electrical resistivity logging of unconsolidated marine sediments, *Proc. Third Annual Offshore Technology Conf.*, 1(1351):253-368, Houston, Texas.

Boyce, R. E. (1968), Electrical resistivity of modern marine sediments from the Bering Sea, *J. Geophys. Res.* 73(14):4759-4766.

Boyce, R. E. (1967), Electrical resistivity logging of modern marine sediments from the Bering Sea, M.S. Thesis, San Diego State College, Calif., 172 pp.

Breslau, L. R. (1967), The normally incident reflectivity of the sea floor at 12 KC and its correlation with physical and geological properties of naturally occurring sediments, Woods Hole Oceanographic Institution Reference No. 67-16, 131 pp.

Breslau, L. R. (1964), Classification of sea floor sediments with a shipborne acoustic system, Woods Hole Oceanographic Contribution No. 1678 in *Le Petrole et Mer*, Sec. 1, No. 132 (printed in French-English transl.), 9 pp. (Also in *La Revue Petroliere*, 1965 reprint).

Buchan, S., F. C. D. Dewes, D. M. McCann and D. Taylor-Smith (1967), Measurements of the acoustic and geotechnical properties of marine sediment cores, in Marine Geotechnique, ed. Richards (Univ. of Illinois Press, Urbana, Ill.), pp. 65-92.

Bucker, H. P. (1964), Normal mode sound propagation in shallow water, *J. Acoust. Soc. Am.* 36:251-258.

Caulfield, David D. (1962), Predicting sonic pulse shapes of underwater spook discharges, Woods Hole Oceanographic Institution Rept. No. 1270 (ONR-sponsored research).

Chesterman, W. D., J. M. P. St. Quinton, Y. Chan and H. R. Matthews (1967), Acoustic surveys of the sea floor near Hong Kong, *Internatl. Hydro. Rev.* 44(I):35-54.

Coggon, J. H., and H. F. Morrison (1970), Electromagnetic investigation of the sea floor, *Geophys.* 35(3):476-489.

Cohen, S. R. (1968), Measurement of the visoelastic properties of water-saturated clay sediments, M.S. Thesis, U.S. Naval Postgraduate School, Monterey, Calif.

Connors, D. N., and K. Park (1967), The partial equivalent conductances of electrolytes in seawater, revised, *Deep-Sea Res.* 14:481-484.

Cooley, J., P. Lewis and P. Welch (1967), Historical notes on the FFT, *IEEE Trans. on Audio and Electroacoustics* AV-15(2):76-79.

Corwin, R. F. (1973), Application of self-potential to offshore prospecting, Ph.D. Thesis, Univ. of California, Berkeley, Calif.

Corwin and Conty, A rugged silver-silver chloride electrode for field use, *Rev. Sci. Instru.* (to be published).

Dakhnov, V. N. (1959), Geophysical well logging, *Colo. School of Mines Quarterly* 57(2):445 pp.

Davies, D. (1965), Dispersed Stoneley waves on the ocean bottom, *Bull. Seismol. Soc. Am.* 55:903-918.

Dunlop, H. F., and C. H. Johnson (1958), Research and progress in exploration, *Geophysics* 23(2):267-284.

Erchul, R. A., and V. A. Nacci (1971), The use of electrical resistivity measurements to predict porosity of marine sediments, Proc. Interntl. Symp. on Engineering Properties of Sea-Floor Soils and their Geophysical Identification, Seattle Wash., pp. 296-308.

Ewing, W. M., W. S. Jardetzky and F. Press (1957), Elastic Waves in Layered Media (McGraw-Hill, New York, N.Y.) 380 pp.

Faas, R. W. (1969), Analysis of the relationship between acoustic reflectivity and sediment porosity, *Geophysics* 34(4):549-553.

Flügge, W. (1967), Viscoelasticity (Blaisdell Press,).

Folk, R., and W. Ward (1957), Soils analysis, *J. Sedim. Pet.* 27:3-26.

Fung, Y. C. (1965), Foundations of Solid Mechanics (Prentice-Hall, Inc., New York, N.Y.).

Garrels, R. M., and M. E. Thompson (1962), A chemical model for sea water at 25°C and one atmosphere total pressure, *Am. J. Sci.* 260:57-66.

Grant, F. S., and G. F. West (1965), Interpretation Theory in Applied Geophysics (McGraw-Hill, New York, N.Y.), 584 pp.

Griffiths, D. H., and R. King (1965), Applied Geophysics for Engineers and Geologists (Pergamon Press, Oxford), 78-82.

Hamilton, E. L. (1972), Compressional wave attenuation in marine sediments, *Geophys.* 37(4):p. 620.

Hamilton, E. L. (1971), Elastic properties of marine sediments, *J. Geophys. Res.* 76:579-603.

Hamilton, E. L. (1970), Sound velocity and related properties of marine sediments, North Pacific, *J. Geophys. Res.* 75(23):4423-4444.

Hamilton, E. L. (1970), Reflection coefficients and bottom losses at normal incidence computed from Pacific sediment properties, *Geophys.* 35:995-1004.

Hamilton, E. L. (1969), Sound velocity, elasticity and related properties of marine sediments, North Pacific, Part I: Sediment Properties, Environmental Control and Empirical Relationships, Naval Undersea Res. Dev. Center Tech. Publ. 143.

Hamilton, E. L., and H. W. Menard (1956), Density and porosity of seafloor surface sediments off San Diego, *Bull. Am. Assoc. Petrol. Geol.* 40:754-761.

Hamilton, E. L., H. P. Bucker and D. L. Kein (1970), Velocities of compressional and shear waves in marine sediments determined *in situ* from a research submersible, *J. Geophys. Res.* 75:4039-4049.

Hardin, B. O., and L. E. Richart, Jr. (1963), Elastic wave velocities in granular soils, *J. Soil. Mech. and Foundations Div., Chem. Soc. Civil Engr.* SM 1, pp. 33-65; and discussions, SM 5, pp. 103-118.

Harvey, H. W. (1960), The Chemistry and Fertility of Sea Waters (Cambridge Univ. Press, Cambridge, Mass), p. 4.

Hirowaka, M. C. (1966), Engineering properties of marine sediments near San Miguel Island, USN Civ. Engrg. Lab. Tech. Rept. R-503, Port Hueneme, Calif.

Horn, D. R., B. M. Horn and M. N. Delacy (1968), Correlation between acoustical and other physical properties of deep sea coves, *J. Geophys. Res.* 73:1939-1957.

Humphrey, Burton, and William J. Gunman (1967), Study of a pulsed underwater sound projector, PC 088 R000Z, FHR 2229-5, PCD-TR-67-16, pp. 3, 9-11 (Dec.).

Hutchins, Roger W. (1969), Broadband electro-acoustic sources for high resolution sub-bottom profiling, *presentation at Internatl. Oceanology Conf.*

I. C. Logic Handbook (1972), Published by Data Scan, pp. 79-80.

Internatl. Oceanog. Tables (1966), Natl. Inst. Oceanography of Great Britain and UNESCO.

Jenkins, R., and W. Takeyama (1971), Bottom-sitting diver-operated core sampler, NOAA Rept. ERL-MMTC Tech. Memo., 13 pp.

Jones, J. L., C. B. Leslie and L. E. Burton (1964), Acoustic characteristics of underwater bottoms, *J. Acos. Soc. of Am.* 36:154-163.

Jones, R. (1958), *In situ* measurement of the dynamic properties of soil by vibration methods, *Geotech.* 8:1-21.

Keller, G. H. (1965), Deep sea nuclear sediment density probe, *Deep Sea Res.* 12:373-376.

Keller, G. H. (1964), Investigation of the application of standard soil mechanic techniques and principles to buy sediments, *Proc. First Symp. Military Oceanography*, p. 329.

Kesser, G. H., and F. C. Frischknecht (1966), Electrical Methods in Geophysical Prospecting (Pergamon Press, Oxford), 519 pp.

Kermabon, A. C., C. Gehin and P. Blavier (1969), A deep-sea electrical resistivity probe for measuring porosity and density of unconsolidated sediments, *Geophys.* 34(4):554-571.

Knepoff, L., and G. J. F. MacDonald (1960), Models for acoustic loss in solids, *J. Geophys. Res.* 65:2191-2197.

Knepoff, L., and G. J. F. MacDonald (1958), Attenuation of small amplitude stress waves in solids, *Rev. Modern Phys.* 30:1178-1192.

Laughton, A. S. (1957), Sound propagation in compacted ocean sediments, *Geophys.* 22:233-260.

Levy, J. D. (1961), Viscoelastic Properties of Polymers (John Wiley & Sons, New York, N.Y.).

Lewis, L. (1971), An investigation of ocean sediments using the deep ocean sediment probe, Ph.D. Thesis, Dept. of Ocean Engrg., Univ. of Rhode Island, 76 pp.

Lewis, L., V. A. Nacci and J. Gallagher (1970), *In situ* investigations of ocean sediments, *Offshore Technol. Conf. Paper No. 1290.*

Li, W. N., and D. Taylor-Smith (1968), Identification of seafloor sediments using underway acoustics, *Geophys. Prospecting* 17(3):pp 234, 239-249.

Li, W. N., and D. Taylor-Smith (1966), Identification of seafloor sediments by a ship underway, *Geophys. Prospecting* 19(1):45-47.

Lieberman, L. N. (1948), Reflection of sound from coastal sea bottoms, *J. Acous. Soc. of Am.* 20:305-309.

Longsworth, L. G. (1932), Transference numbers of aqueous solutions of potassium chloride, sodium chloride, lithiam chloride and hydrochloric acid at 25°C by the moving boundary method, *J. Am. Chem. Soc.* 54:2751-2758.

Lyman, J., and R. H. Fleming (1940), Composition of sea water, *J. Marine Res.*, 3:134-146.

MacKenzie, K. V. (1960), Reflection of sound from coastal bottoms, *J. Acous. Soc. Am.* 32:221-231.

Marke, P. A. B. (1965), The development and use of offshore mineral exploration techniques, Ph.D. Thesis, Geophys. Dept., Imperial College, London, S.W. 7, 166-278.

McCann, C., Theory of propagation of compressional waves in marine sediments, Mar. Sci. Lab. Geol. Rept. No. 66-5 (unpublished).

McKinney, C. M., and C. D. Anderson (1964), Measurements of backscattering of sound from the ocean bottom, *J. Acous. Soc. Am.* 36:158-163.

Mooney, H. M., and W. W. Wetzel (1956), The Potential About a Point Electrode Resistivity Curves for a Two- Three- and Four-Layered Earth (Univ. of Minn. Press, St. Paul, Minn.). (Available from University Microfilms, A Xerox Company, Ann Arbor, Mich.).

Moore, D., and G. Shumway (1959), Sediment thickness and physical properties, Pigen Pt., Calif., *J. Geophys. Res.* 64(3):p. 367.

Moore, T. C., and L. D. Kulm (1970), A high-resolution sub-bottom profiling system for use in ocean basins, Reprint from *Marine Res.* 28(2): pp. 271, 272, 279.

Murray, H. W. (1967), Topography of the Gulf of Maine field season of 1940, *Geol. Soc. Am. Bull.* 22(3):523-552.

Nafe, J. E., and C. L. Drake (1963), Physical properties of marine sediments, in The Sea (John Wiley & Sons, New York, N.Y.), M. N. Hill, ed.

Nafe, J. E., and C. L. Drake (1957), Variation with depth in shallow and deep water marine sediments of porosity, density, and velocities of compressional and shear waves, *Geophys.* 22:523-552.

Noorany, I. (1972), Underwater soil sampling and testing, a state-of-the-art review, ASTM-STP 501.

Officer, C. B. (1958), Introduction to the Theory of Sound Transmission (McGraw-Hill, New York, N.Y.), 284 pp.

Parasnis, D. S. (1962), Principles of Applied Geophysics (Methuen, London; John Wiley & Sons, New York, N.Y.).

Park, K. (1964), Parial equivalent conductance of electrolytes in seawater, *Deep Sea Res.* 11:729-736.

Pawlowicz, E. F. (1971), Ocean engineering significance of marine seismic reflection profiling technology, Tech. Note N-1157, Port Hueneme, Calif., pp. 1, 7, 8, 22 (May).

Physics of Sound in the Sea, Part I (1946), Transmission, Summary Tech. Rept. of the Natl. Defense Res. Committee, section on sound transmission studies.

Porter, W. J., and D. L. Bell, Variability of bottom reflected sound and its influence on sediment prediction models, (unpublished).

Poston, A. (1973), Patent application, Serial No. 033453, for invention of a directional multiple electrode acoustic source.

Preiss, K. (1968), *In situ* measurement of sediment density by gamma radiation, *Deep Sea Res.* 15:637-641.

Preiss, K. (1967), Nondestructive measurement of the water content and density of sediment using radiosotopes, in Marine Geotechnique (Univ. Illinois Press, Urbana, Ill.), 307-318.

Rayleigh, J. W. S. (1945), The Theory of Sound, 2 (Dover Publ., New York, N.Y.).

Rechtin, E. L., J. Steele, R. Scales (1957), Engineering problems related to design of offshore mobile platforms, Paper No. 10, *Annual meeting Soc. Naval Architects and Marine Engineers.*

Richards, A. F. (1967), Marine Geotechniques (Univ. of Ill. Press, Urbana, Ill.).

Richards, A. F. (1962), Investigations of deep sea sediment cores, Part II, Mass physical properties, U.S. Navy Hydrographic Office, Tech. Rept. TR-106, 146 pp.

Rijkswaterstaat, The Netherlands (1969), Standard graphs of resistivity prospecting, European Assoc. of Exploration Geophysicists.

Rose, V. C., and J. R. Ronsy (1971), A nuclear gage for in-place measurement of sediment density, *Offshore Technology Conf. Paper No. 1290.*

Sarmiento, R., and R. A. Kirby (1962), Recent sediments of Lake Maracaibo, *J. Sed. Petrol.* 32:698-724.

Schlank, J. J. (1968), Sub-bottom Sounding: A survey for naval applications, M.S. Thesis, Naval Postgraduate School, Monterey, Calif.

Schlumberger, C. M., and E. G. Leonardon (1934), Electrical exploration of water – covered areas, Trans. *AIME Geophysical Prospecting* 110.

Schopper, J. (1966), A theoretical investigation of formation factor/permeability/porosity relationship using a network model, *Geophys. Prospect.* 14:301-341.

Schreiber, B. D. (1968), Sound velocity in deep sea sediments, *J. Geophys. Res.* 73:1259-1268.

Shumway, G. (1960), Sound speed and absorption studies of marine sediments by a resonance method, Parts I and II, *Geophys.* 25:451-467, 659-682.

Smith, R. J. (1962), Engineering properties of ocean floor soils, ASTM Spec. Tech. Publ. No. 322, 280-302.

Stoneley, W. C., and W. G. Harris (1968), Acoustic sea bottom classifier, Navy Mines Defense Lab. Rept. NSRDC 2739, Panama City, Fla. (July-AD 835600).

Strick, E., and A. S. Ginzberg (1956), Stoneley-wave velocities for a fluid solid interface, *Bull. Seis. Soc. Am.* 46:281-292.

Sutton, G. H., H. Berkheimer and J. E. Nafe (1957), Physical analysis of deep sea sediments, *Geophys.* 22:779-812.

Taylor-Smith, D. (1968), Physics and sea floor minerals, *Contemp. Phys.* 9(6):565-585.

Taylor-Smith, D., and W. N. Li (1966), Echo sounding and sea floor sediments, *Marine Geol.* (Elsevier Publ. Co., Amsterdam), 4:353-364.

Taylor-Smith, D., and W. N. Li (1966), Identification of sea-bottom sediments by ship underway, Reprint from *Geophys. Prospect.* 24(1):45-47.

Terekhin, E. I. (1962), Theoretical basis of electrical probing with an apparatus immersed in water, in Applied Geophysics in U.S.S.R., ed. N. Rast (Pergamon Press, New York, N.Y.), 169-195.

Unz, M. (1959), Interpretation methods for geophysical exploration of resources, *Geophys.* 24(1):109-141.

Urick, R. J. (1954), The backscattering of sound from a harbour bottom, *J. Acous. Soc. Am.* 26:231-235.

Urick, R. J., and D. S. Saling (1962), Backscattering of explosive sound from the deep sea bed, *J. Acous. Soc. Am.* 34:1721-1724.

Van Nostrand, R. G., and K. L. Cook (1966), Interpretation of resistivity data, *Geol. Survey Professional Paper 499*, U.S. Government Printing Office, Washington, D.C., 310 pp.

Van'yan, L. L. (1956), Theoretical curves for electrical sea probing with a sea bottom apparatus, *Appl. Geophys.* No. 50, Gostoptekhizdat.

Vees, E., and H. F. Winterkorn (1967), Engineering properties of several pure clays as functions of mineral type, exchange ions, and phase composition, Highway Res. Board No. 198, 68-70.

Volker, A., and J. Dijkatra (1955), "Determination des salinites des eaux dans le sous sol du Zuiderzee par Prospection Geophysique, *Geophys. Prospect.* 3(2):111-125.

Von Arx, W. X. (1962), Introduction to Physical Oceanography (Addison-Wesley, Reading, Mass.), 422 pp.

White, J. E. (1965), Seismic Waves; Radiation, Transmission and Attenuation (McGraw-Hill, New York, N.Y.), 302 pp.

Wilde, P. (1969), Tables of formalities and p ion in sea water of total Cl, Na, K, Mg, Ca, Sr, Br, and SO_4 for the salinity range of 28 to 40 percent assuming dittmarian conservancy, Univ. of Calif., Berkeley, Calif., 62-63.

Wilson, E., and E. L. Hamilton (1970), Sound velocities and related properties of marine sediment, North Pacific, *J. Geophys. Res.* 75:4423-4446.

Wolfe, S. C. (1970), Coastal currents and mass transport of surface sediments over the shelf of Monterey Bay, Calif, *Marine Geol.* 8:321-336.

Wood, A. B. (1941), A Textbook of Sound (G. Bell, London), 578 pp.

Wyllie, M. R. J. (1963), The Fundamentals of Well Log Interpretation (Academic Press, New York, N.Y.), 238 pp.

Wyllie, M. P. J., and A. R. Gregory (1953), Formation factors of unsolidated porous media: Influence of particle shape and effect of cementation, *Petrol. Trans.* 198:103-110.

APPENDIX A.1. CALCULATIONS FOR UNDERWAY ACOUSTICS EXPERIMENT

APPENDIX A.1. CALCULATIONS FOR UNDERWAY ACOUSTICS EXPERIMENT

A.1.1 Calculation of Reflection Coefficient (R) for Sparker (0-5 kHz Source)

t = time

α = Sound velocity

u = Particle motion amplitude or pressure

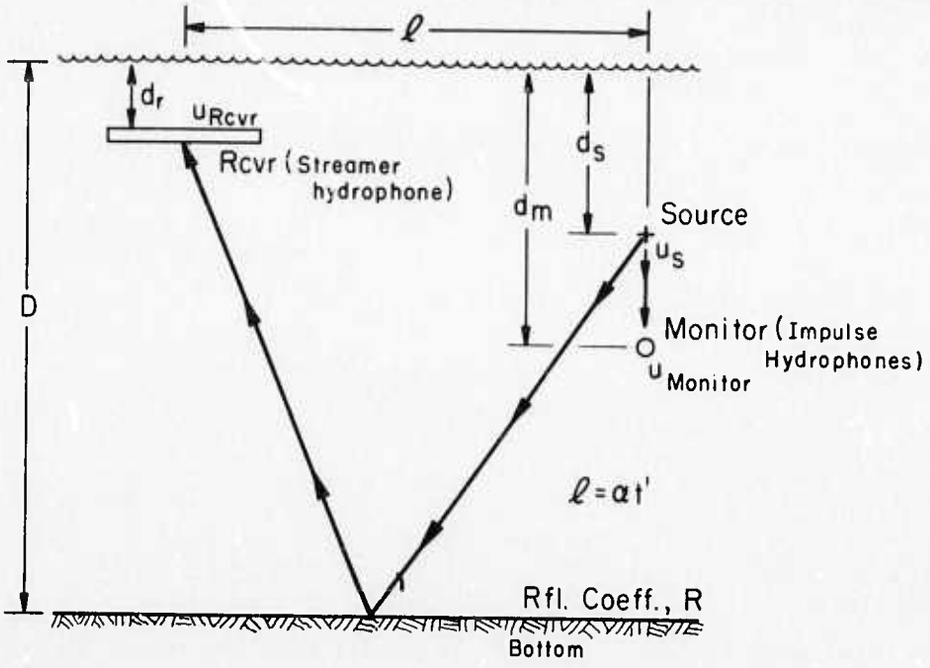

Streamer hydro signal

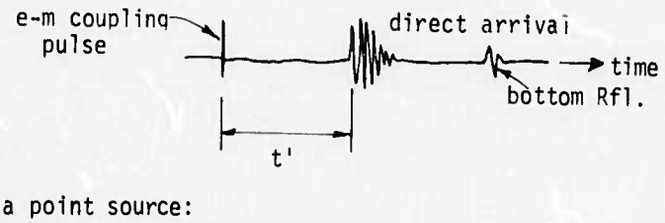

Assuming a point source:

$$u_{monitor} = u_{source} \cdot \frac{const.}{d_m - d_s} \quad . \qquad (A\text{-}2)$$

Assume d_s and d_r << D so source to receiver reflector path length is approximate

$$\sqrt{(D-d_s)^2 + (\ell/2)^2} + \sqrt{(D-d_r)^2 + (\ell/2)^2} = \text{reflection path.}$$

So almost exactly

$$\text{reflector path} = 2\sqrt{(D-d_s)^2 = (\ell/2)^2}$$

$$= \sqrt{4(D-d_s)^2 + \ell^2}$$

Note: In deeper water $\ell << D$ so reflector path $\simeq$ $2D - (d_s + d_r)$.

Now

$$u_{rcvr} = u_{source} \cdot \frac{\text{Const.}}{\sqrt{4(D-d_s)^2 + \ell^2}} \cdot R \ . \qquad \text{(A-3)}$$

Eliminating u_{source} between (1) and (2)

$$\frac{u_{monitor}}{u_{rcvr}} = \frac{1}{R} \cdot \frac{\sqrt{4(D-d_s)^2 + \ell^2}}{d_m - d_s} \ . \qquad \text{(A-4)}$$

Solving for R,

$$R = \frac{\sqrt{4(D-d_s)^2 + \ell^2}}{d_m - d_s} \cdot \frac{u_{rcvr}}{u_{monitor}} \qquad \text{(A-5)}$$

$$e_{monitor} = u_{monitor} \cdot G_{impulse\ hydro} \cdot$$

$$e_{rcvr} = u_{rcvr} \cdot G_{streamer\ hydrophone}$$

$$\therefore \frac{u_{rcvr}}{u_{monitor}} = \frac{e_{rcvr}}{e_{monitor}} \cdot \frac{G_{imp.\ hyd.}}{G_{sta.\ hyd.}} \ . \qquad \text{(A-6)}$$

Eliminating $u_{rcvr}/u_{monitor}$ between (A-5) and (A-6) we have for R for the sparker system:

$$R = \underbrace{\frac{\sqrt{4(D-d_s)^2 + \ell^2}}{d_m - d_s}}_{\text{geometrical factor}} \cdot \underbrace{\frac{G_{imp.\ hydro.}}{G_{streamer\ hydro}}}_{\text{hydrophone gain ratio}} \cdot \underbrace{\frac{e_{rcvr}}{e_{monitor}}}_{\text{ratio of VoHages recorded on Mag. tape, i.e., } S_r/S_x} \ . \qquad \text{(A-7)}$$

Substituting the numerical data from below we have:

$$R = .532 \sqrt{4D^2 + 832} \cdot (.0233) \cdot \frac{e_{str.\ rcv}}{e_{imp.\ hyd}} \qquad \text{(A-8)}$$

$$\boxed{R = .0124 \sqrt{4D^2 + 832} \cdot \frac{e_{str.\ rcv}}{e_{imp.\ hyd}}} \ . \qquad \text{(A-9)}$$

Numerical Data:

Sparker:

d_s = 10" = .832'

d_m = 2' 8½" = 2.71'

d_r = 15".

Pinger:

d = 22"

Constants: V = 4.66 ft/m-sec t = 6.2 m-sec

$\therefore \ell = vt = 28.8'$

$$\frac{G_{\text{imp. hyd.}}}{G_{\text{streamer hyd.}}} = .0233$$

$$\text{Geometrical Factor} = \frac{\sqrt{4(D-.832)^2 + (28.8)^2}}{2.71 - .832} \qquad \text{(A-10)}$$

$$= .532\sqrt{4D^2 + 832} \ . \qquad \text{(A-11)}$$

Streamer Calibration Flow Chart:

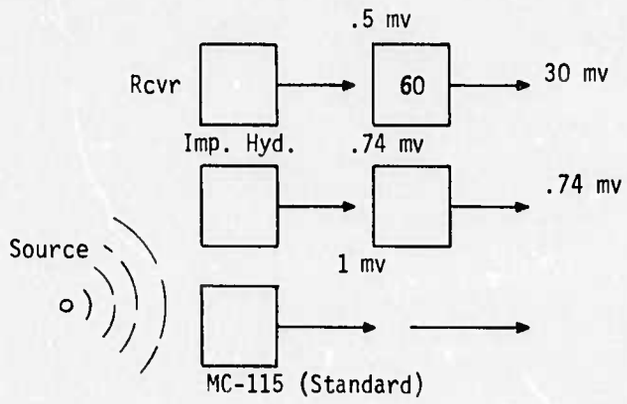

$$\frac{G_{\text{imp. hydro.}}}{G_{\text{streamer hyd.}}} = \frac{.7 \text{ mv}}{30 \text{ mv}} = .0233 \ . \qquad \text{(A-12)}$$

A.1.2 Calculation of Reflection Coefficient for Pinger (12 kHz Source)

u = particle amplitude or pressure

In the pinger, unlike the sparker, the source and receiver are the same transducer; however, to aid analysis assume they are two separate transducers.

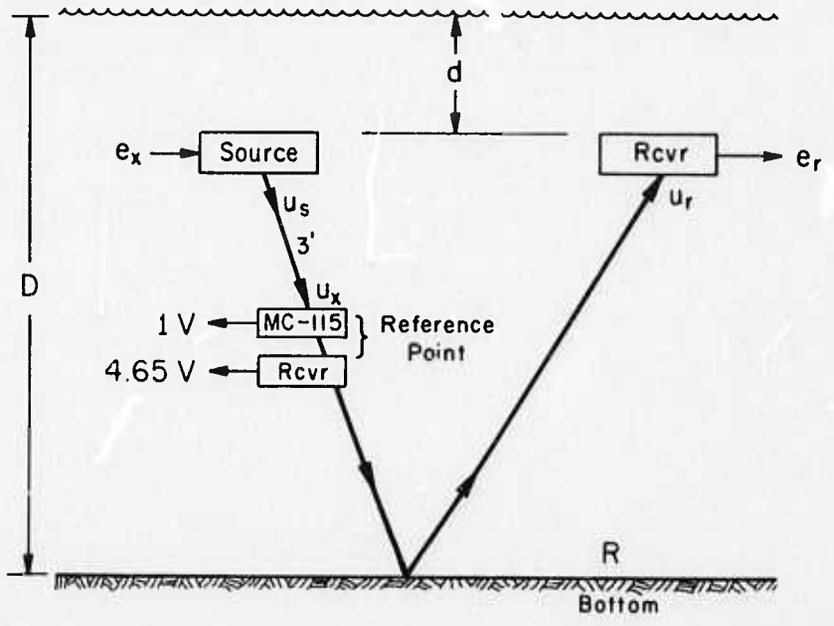

Also assume that the calibrated hydrophone, MC-115, is located at the reference point 3 feet below the pinger. From previous tank calibrations, when e_x = 183 v., the MC-115 develops 1v. The pinger receiver in the same location would develop 4.65.

Assuming a point source,

$$u_x = c\,\frac{u_s}{3} \tag{A-13}$$

$$u_r = c\,\frac{u_s}{2(D-d)}\,R\,. \tag{A-14}$$

Eliminating $c\,u_s$

$$u_r = u_x\,\frac{3}{2(D-d)}\cdot R\,. \tag{A-15}$$

Let $u_r = e_r/4.65$ and $u_x = e_x/183$.

Then

$$e_r = \left[\frac{e_x}{183}\right]\left[\frac{3}{2(D-d)}\right]\ 4.65\ R. \tag{A-16}$$

APPENDIX A.2 DERIVATION OF BASIC EQUATIONS OF LINEAR VISCOELASTICITY
(after Borcherdt, R. D., 1972)

APPENDIX A.2 DERIVATION OF BASIC EQUATIONS OF LINEAR VISCOELASTICITY
(after Borcherdt, R. D., 1972)

A.2.1 Body Waves in a Linear Viscoelastic Medium

This section is included for completeness, although a detailed study will not be given. The development of the basic equations will follow the approach given by Borcherdt (1972), and the reader is referred to that thesis for a more comprehensive study.

Viscoelasticity is a property of solids and liquids which exhibit both viscous and elastic behavior under deformation. The dissipation and storage of mechanical energy is observed from this behavior. In addition, the constant that links stress and strain in the theory of elasticity becomes a time dependent function in the constitutive equation of viscoelastic theory. For sufficiently small strains, the behavior of a viscoelastic material can be described by the linear theory of elasticity. Employing the superposition principal, the stress strain relation can be written as follows:

$$P_{ij}(t) = \int_{-\infty}^{\infty} r_{ijk\ell}(t-\tau)\, de_{k\ell}(\tau) \qquad \text{(A-19)}$$

where $P_{ij}(t) \equiv$ components of the 2^{nd} order time dependent stress tensor,

$e_{ij}(t) \equiv$ components of the 2^{nd} order time dependent strain tensor, and

$r_{ijk\ell} \equiv$ components of the 4^{th} order time dependent relaxation function.

This equation can be written in a more condensed form as a convolution:

$$P_{ij} = r_{ijk\ell} \quad de_{k\ell} \,. \qquad \text{(A-20)}$$

If the material is isotropic, a further simplification can be made:

$$P'_{ij} = r_s \quad de'_{ij} \qquad i \neq j \qquad \text{(A-21)}$$

$$P_{kk} = r_k \quad de_{kk} \qquad \text{(A-22)}$$

where $r_s \equiv$ relaxation function describing shear behavior and

$r_k \equiv$ relaxation function describing bulk behavior.

The primes denote the deviator components of stress and strain:

$$P'_{ij} = P_{ij} - \tfrac{1}{3}\,\delta_{ij}\,P_{kk} \qquad \text{(A-23)}$$

$$e'_{ij} = e_{ij} - \tfrac{1}{3}\,\delta_{ij}\,e_{kk}. \qquad \text{(A-24)}$$

It would be convenient to simplify these stress strain relationships by considering the steady state problem. Moreover, it will be assumed sufficient time has elapsed so initial conditions may be neglected. Let $P_{ij} = \underline{P}_{ij} e^{i\omega t}$ and $e_{ij} = E_{ij} e^{i\omega t}$ where $\underline{P}_{ij}$ and E_{ij} are complex constants independent of time. Equations (A-21) and (A-22) can now be written as

$$\underline{P}'_{ij} = i\omega R_s(i\omega) E'_{ij} \qquad i \neq j \tag{A-25}$$

$$\underline{P}_{kk} = i\omega R_k(i\omega) E_{kk} \tag{A-26}$$

where R_s and R_k represent the Fourier transforms of the shear and bulk relaxation functions, respectively. These quantities, R_s and R_k, can be formulated into a more familiar form:

$$\mu \equiv \frac{i\omega R_s}{2} \tag{A-27}$$

$$\kappa \equiv \frac{i\omega R_k}{3} \tag{A-28}$$

$$\lambda \equiv \frac{i\omega\left(R_k - R_s\right)}{3} . \tag{A-29}$$

It follows

$$\underline{P}'_{ij} = 2\mu^3 E'_{ij} \qquad i \neq j \tag{A-30a}$$

$$\underline{P}_{kk} = 3\kappa E_{kk} . \tag{A-30b}$$

Other useful relationships are

$$\underline{P}_{ij} = \delta_{ij} \lambda E_{kk} + 2\mu E_{ij} \tag{A-31}$$

and

$$\underline{P}_{ij} = \delta_{ij} \left(\kappa - \frac{2}{3}\mu\right) E_{kk} + 2\mu E_{ij} . \tag{A-32}$$

Attention will now be focused on the equation of motion and strain tensor. From the conservation of linear momentum, the equation of motion is:

$$P_{ij,j} + f_i = \phi \frac{\partial^2 u_i}{\partial t^2} \tag{A-33}$$

where $f_i \equiv$ body force per unit volume,
$\phi \equiv$ mass density, and
$u_i \equiv$ component of the displacement vector.

The strain tensor, assuming infinitesimal displacement is given by

$$e_{ij} = \frac{1}{2}\left(u_{i,j} + u_{j,i}\right) . \tag{A-34}$$

Steady state simplification will be employed again. Let $u_i = U_i e^{i\omega t}$ where U_i is a complex constant independent of time. Therefore, the equation of motion and strain tensor simplify to

$$P_{ij,j} + \Phi\, \omega\, U_i = 0 \tag{A-35}$$

and

$$E_{ij} = \frac{1}{2}\left(U_{i,j} + U_{j,i}\right) \tag{A-36}$$

(where body forces have been neglected). Using (A-36) and (A-32) the equation of motion, (A-35), can be written in terms of u_i (in vector form):

$$\left(\kappa + \frac{4}{3}\mu\right)\nabla\,\theta - \mu\,\nabla\,x(\nabla x u) + \Phi\,\omega^2\,u = 0 \tag{A-37}$$

where

$$\theta \equiv \nabla\, u\ .$$

Note that this equation is equivalent to the equation of motion for an elastic medium except for the Lamé constants which may now be complex (i.e., $\mu = \mu_R + i\mu_I$ and $\kappa = \kappa_R + i\kappa_I$). Also, the expression for the time rate of energy and 2nd law at thermodynamics reveal that μ_I and κ_I are non-negative (Borcherdt, 1972, p. 43).

By taking the divergence and the curl of the equation of motion, (A-37), one can obtain, respectively, the equations for dilatational and rotational waves:

$$\nabla^2\theta + \frac{\omega^2}{\alpha^2}\,\theta = 0 \tag{A-38}$$

and

$$\nabla^2\left(\frac{\nabla x u}{2}\right) + \frac{\omega^2}{\beta^2}\left(\frac{\nabla x u}{2}\right) = 0, \tag{A-39}$$

where the complex compressional velocity (α) and the complex shear velocity (β) are given by

$$\alpha \equiv \text{P.V.}\left(\frac{\kappa + \frac{4}{3}\mu}{\Phi}\right)^{\frac{1}{2}}, \tag{A-40}$$

$$\beta \equiv \text{P.V.}\left(\frac{\mu}{\Phi}\right)^{\frac{1}{2}} . \tag{A-41}$$

(P.V. represents the principal value). The respective velocities of the shear and compressional wave in homogeneous isotropic linear viscoelastic medium are

$$V_p = \left[\text{Re}\left(\frac{1}{\alpha}\right)\right]^{-1}, \tag{A-42}$$

$$V_s = \left[\text{Re}\left(\frac{1}{\beta}\right)\right]^{-1}. \tag{A-43}$$

The absorption coefficient of these two waves are

$$a_p = -\omega\, I_m\left(\frac{1}{\alpha}\right), \tag{A-44}$$

$$a_s = -\omega\, I_m\left(\frac{1}{\beta}\right). \tag{A-45}$$

Little will be said concerning the quantity Q^{-1} except to define Q_κ^{-1}, Q_s^{-1}, and Q_p^{-1}. The specific attenuation factor in bulk will be denoted as Q_κ^{-1} and is expressed as

$$Q_\kappa^{-1} = \frac{\kappa_I}{\kappa_R} \quad . \tag{A-46}$$

Similarly, the attenuation factor for general dilatation and shear is given respectively as

$$Q_p^{-1} = \frac{\kappa_I + \frac{4}{3}\mu_I}{\kappa_R + \frac{4}{3}\mu_R} \tag{A-47}$$

and

$$Q_s^{-1} = \frac{\mu_I}{\mu_R} \quad . \tag{A-48}$$

It is convenient to express the compressional and shear velocity in terms of Q_p^{-1} or Q_s^{-1}. From (A-43)

$$\frac{1}{V_s} = \mathrm{Re}\sqrt{\frac{\phi}{\mu}} = \frac{\sqrt{\phi}}{|\mu|}\,\mathrm{Re}(\sqrt{\mu}) \tag{A-49}$$

or

$$\frac{1}{V_s} = \frac{\sqrt{\phi}}{|\mu|}\,\mathrm{Re}\sqrt{\frac{|\mu| + \mathrm{Re}(\mu)}{2}} + i\sqrt{\frac{|\mu| - \mathrm{Re}(\mu)}{2}} \quad . \tag{A-50}$$

Further reduction using (A-48) yields

$$V_s = \sqrt{\frac{\mu_R}{\phi}}\sqrt{\frac{2(1 + Q_s^{-2})}{\sqrt{1 + Q_s^{-2}} + 1}} = q_s\sqrt{\frac{\mu_R}{\phi}} \tag{A-51}$$

similarly,

$$V_p = \sqrt{\frac{\kappa_R + \frac{4}{3}\mu_R}{\phi}}\sqrt{\frac{2(1 + Q_p^{-2})}{\sqrt{1 + Q_p^{-2}} + 1}} = q_p\sqrt{\frac{\kappa_R + \frac{4}{3}\mu_R}{\phi}} \quad . \tag{A-52}$$

This concludes the discussion on the basic equations of body waves in linear viscoelastic medium. For further discussions, refer to Borcherdt (1972).

We can check the correctness of the formula from the following consideration. The term 2(D-d) is the distance from source to receiver. If we move the receiver to the reference point as shown this term equals 3' and there is no reflection (R=1). Then (A-16) becomes:

$$e_r = \left[\frac{e_x}{183}\right]\left[\frac{3}{3}\right] 4.65, \qquad \text{(A-17)}$$

for e_x = 183v. This yields e_r = 4.65 volts which is the value from tank measurements. Solving for R with d = 22" = 1.83'

$$\boxed{R = 26.2\ (D' - 1.83')\ \frac{e_{rcvr}}{c_{xmtr}}} \ . \qquad \text{(A-18)}$$

Tank Calibrations of Pinger — Block Diagram:

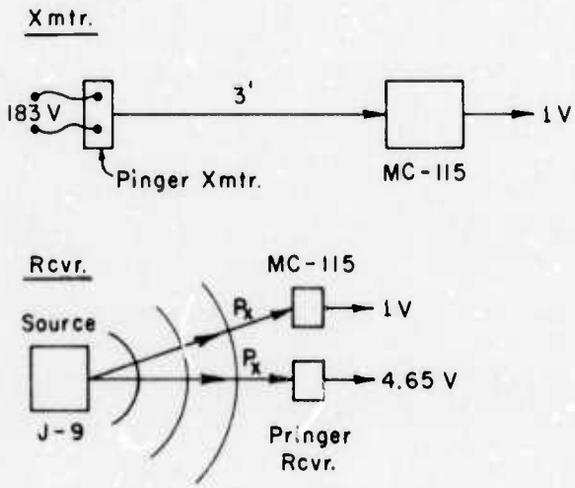

APPENDIX A.3 SEDIMENT PROPERTY EQUATIONS

APPENDIX A.3 SEDIMENT PROPERTY EQUATIONS

Property	Symbol	Method of Calculation
Shear-wave dissipation function	Q_s^{-1}	$Q_s^{-1} = \frac{2 V_s a_s}{\omega} \Big/ \left[1 - \frac{V_s a_s}{\omega} \right]^2$
Rigidity representing elastic response	μ_R	$\mu_R = \phi \left(\frac{V_s}{q_s} \right)^2$
Rigidity representing wave energy damping	μ_I	$\mu_I = \mu_R Q_s^{-1}$
Bulk modulus representing elastic response	K_R	$K_R = \phi V_p^2 - \frac{4}{3} \mu_R$
Lamé constant representing elastic response	λ_R	$\lambda_R = K_R - \frac{2}{3} \mu_R$
Poisson's ratio	σ	$\sigma = \left[\frac{(V_p q_s / V_s)^2 - 2}{2(V_p q_s / V_s)^2 - 2} \right]$
Young's modulus	E	$E = \mu_R (1+\sigma)$

A-3.2 Notation Summary

Symbol	Description
a_s	Shear-wave attenuation coefficient
a_p	Compressional-wave attenuation coefficient
E	Young's modulus
K_I	Bulk modulus representing wave energy damping
K_R	Bulk modulus representing elastic response
q_p	$= \sqrt{2(1+Q_p^{-2})}/\sqrt{1+Q_p^{-2}} + 1$
q_s	$= \sqrt{2(1+Q_s^{-2})}/\sqrt{1+Q_s^{-2}} + 1$
Q_s^{-1}	Shear-wave dissipation function
Q_p^{-1}	Compressional-wave dissipation function
V_s	Snear-wave velocity
V_p	Compressional-wave velocity
ϕ	Bulk density
λ_I	Lamé constant representing wave energy damping
λ_R	Lamé constant representing elastic response
μ_I	Rigidity representing wave energy damping
μ_R	Rigidity representing elastic response
σ	Poisson's ratio
ω	Angular frequency

APPENDIX A.4 SUMMARY OF SAMPLING PROGRAM

Site No	Corrected Water Depth (ft)	Core Length (cm)	Predominant Sediment Type	Corer Type Driver Sampler: Piston type-P Open type-O
23	102	60.4	silty-sand	P
24	106	43.8	silty-sand	P
25	106	63.2	sandy-silt	P
26	113	65.1	silty-sand	P
38	124	61.7	silty-sand	P
39	117	62.2	silty-sand	P
40	111	65.6	silty-sand	P
41	105	60.9	silty-sand	P
42	99	65.0	silty-sand	P
43	100	62.9	silty-sand	P
44	97	63.6	silty-sand	P
45	92	64.0	silty-sand	P
46	92	65.4	silty-sand	P
47	95	63.3	silty-sand	P
48	96	61.7	silty-sand	P
49	102	62.0	silty-sand	P
50	105	27.9	silty-sand	P
51	114	54.5	silty-sand	P
52	121	47.9	sandy-silt	P
57	123	42.2	silty-sand	P
58	118	55.6	silty-sand	P
59	111	62.3	silty-sand	P
60	105	64.4	silty-sand/sandy-silt	P
61	96	65.2	silty-sand	P
62	93	62.9	silty-sand	P
63	91	62.3	silty-sand	P
64	89	40.2	silty-sand	P
65	87	60.9	silty-sand	P
66	85	51.1	silty-sand	P
68	83	13.8	silty-sand	P
69	83	45.2	silty-sand	P
69	83	90.2	silty-sand	O
70	83	62.6	silty-sand	P
71	84	63.8	silty-sand	P
72	85	63.2	silty-sand	P
73	90	54.5	silty-sand	P
73	90	104.0	silty-gravelly sand	O
81	73	6.3	silty-sand	P
82	70	32.6	silty-sand	P
83	68	4.5	sandy-silt	P
84	65	54.2	silty-sand	P
85	69	63.7	silty-sand	P
86	73	52.2	silty-sand	P
87	75	10.4	silty-sand	P
88	73	11.0	silty-sand	P
92	45	9.0	silty-sand	P
93	48	63.9	silty-sand	P
94	53	59.7	sandy-silt	P
95A	56	38.7	sandy-silt	P
95B	56	5.1	sandy-silt	P

Site No	Corrected Water Depth (ft)	Core Length (cm)	Predominant Sediment Type	Corer Type Driver Sampler: Piston type-P Open type-O
100	43	34.1	gravelly-sand	P
102	47	39.9	silty-sand/sandy-silt	P
103	48	51.0	sandy-silt	P
103	48	38.1	sandy-silt	O
104	49	63.0	silty-gravelly sand	P
105	49	41.2	silty-gravelly sand	P
109	38	54.3	silty-sand	P
109	38	36.3	silty-sand	O
110	40	51.2	silty-sand	P
111	42	23.7	sandy-silt	P
112	42	41.7	silty-sand	P
113	43	59.7	silty-gravelly sand	P
114	45	51.7	silty-sandy gravel	P
115	46	6.0	silty-sand	P
118(1)	32	47.2	silty-sand	P
118(2)	32	56.8	silty-sand	P
119	33	14.9	silty-sand	P
120	34	22.4	silty-sand	P
121	34	54.9	silty-sand	P
121	34	31.4	silty-sand	O
122	36	55.8	silty-sand	P
123	39	52.7	silty-sand	P
123	39	34.3	silty-sand	O
124	38	24.1	silty-sand	O
1X	56	15.2	silty-sand	P
2X	60	31.2	silty-sand	P
3X	63	6.0	silty-sand	P
T.H.1	17	64.6	silty-sand	P
T.H.2	17	62.8	silty-sand	P
S.C. Buoy	17	62.0	gravelly-silty sand and sandy-silt	P
S.C. Buoy 7/10	17	259.0	gravelly-silty sand	O
S.C. Buoy 8/28	17	170.2	silty-gravelly sand	O

APPENDIX A.5 SUMMARY OF ACOUSTIC, ELECTRICAL RESISTIVITY AND SEDIMENT ANALYSES DATA

Preceding page blank

Site No	Porosity	Density	Penetrometer	Torvane	Mean Diameter	Sorting Coefficient	Resistivity	Pinger		Sparker	
								Corrected	Observed	Corrected	Observed
23	42.53	2.15	0.030	0.080	0.090	1.1408		1.353		5.522	
24	44.63	2.09	0.030	0.080	0.086	1.1547		1.357		5.363	
25	45.41	2.07	0.560	0.110	0.066	1.3964		1.367		4.956	
26	42.28	2.04	0.500	0.076	0.072	1.3031		1.410		4.833	
38	46.78	1.97	0.460	0.086	0.081	1.3771		1.402	1.385	4.582	
39	37.89	2.15	0.043	0.100	0.092	1.2030		1.496	1.428	4.250	4.468
40	45.27	2.05	0.280	0.096	0.089	1.1180		1.558	1.512	5.324	
41	42.10	2.11	0.320	0.076	0.074	1.1734		1.395	1.351	4.688	5.520
42	46.49	2.01	0.600	0.080	0.069	1.3838		1.327	1.294	4.638	5.259
43	44.66	2.08	0.300	0.065	0.083	1.2910		1.252		4.481	5.282
44	43.18	2.12	0.410	0.046	0.095	1.1180		1.198		4.971	6.263
45	44.32	2.08	0.460	0.113	0.086	1.1748		1.121		5.850	6.753
46	47.80	1.96	0.050	0.103	0.066	1.5644		1.121	1.217	6.694	6.945
47	44.66	2.05	0.420	0.110	0.078	1.3608		1.142	1.187	6.318	5.500
48	44.13	2.03	0.350	0.100	0.092	1.3000		1.245		5.257	5.709
49	42.30	2.13	0.110	0.110	0.090	1.3284		1.379	1.372	5.704	5.459
50	24.64	2.87	0.220	0.130	0.084	1.4384		1.361	1.363	5.832	5.935
51	47.70	1.94	0.330	0.070	0.080	1.4015		1.369	1.355	5.145	5.300
52	47.17	1.97	0.140	0.040	0.065	1.5359		1.341	1.315		
57	46.55	1.97	0.180	0.056	1.120	1.6366		1.462		4.083	
58	47.48	2.01	0.400	0.103	1.110	1.7423		1.303		3.850	4.093
59	46.81	2.07	0.200	0.090	1.680	2.3774		1.229		5.150	5.250
60	47.17	1.91	0.700	0.120	0.074	1.8787		1.152		4.768	5.144
61	37.69	2.32	0.050	0.120	0.075	1.4142		1.081		5.308	
62	45.74	2.02	0.420	0.030	0.123	1.3093		1.012		5.018	5.675
63	42.95	2.11	0.550	0.110	0.088	1.2813		0.980		5.383	5.685
64	42.92	2.12	0.400	0.090	0.102	1.1744		0.979		5.310	4.872
65	43.76	2.08	0.330	0.700	0.085	1.4261		0.989		5.541	6.805
66	42.23	2.12	0.400	0.100	0.085	1.4686		0.997		5.496	5.604
67								0.907	0.824		
68	49.97	1.91	0.000	0.000	0.118	1.8451		0.937		5.535	
69	46.64	2.06	0.200	0.066	0.091	1.3801		0.929	0.863	5.341	5.548
70	45.24	2.02	0.300	0.100	0.083	1.1978		0.941	0.858	5.219	5.485
71	48.32	1.96	0.200	0.020	0.097	1.4142	2.23	0.969	0.865	6.083	
72	46.12	1.94	0.230	0.076	0.076	2.0701	1.50	1.007	0.943	5.590	
73	41.72	2.19	0.100	0.010	0.357	1.1972		1.062	0.990	5.293	5.357
81	47.59	1.94	0.000	0.000	0.227	2.0622		0.834	0.801	7.188	
82	46.29	1.91	0.100	0.010	0.540	1.2566		0.719	0.683	7.233	8.333
83	52.17	1.81	0.000	0.000	0.067	1.5683	2.77	0.862		5.790	5.931
84	40.26	2.20	0.660	0.180	0.217	2.2856	3.08	0.823	0.793	6.200	7.725

Site No	Porosity	Density	Penetrometer	Torvane	Mean Diameter	Sorting Coefficient	Resistivity	Pinger		Sparker	
								Corrected	Observed	Corrected	Observed
85	46.38	1.97	0.500	0.100	0.081	1.1704		0.840		6.520	
86	49.57	1.87	0.200	0.100	0.096	1.1244		0.815	0.799	5.933	
87	33.33	2.61	0.000	0.000	0.330	1.8150		0.881	0.866	5.965	
88	35.77	2.49	0.000	0.000	0.154	1.9570		0.835		5.818	
92	39.87	2.22	0.000	0.000	0.133	1.2759					
93	43.08	2.17	0.330	0.086	0.233	2.0054	3.44				
94	47.17	1.99	0.250	0.040	0.061	1.7321	3.00				
95	50.52	1.86	0.000	0.020	0.357	1.8257					
99								2.378		5.500	
100	21.14	2.93	1.000	ND	0.620	1.3693	4.41	2.423		5.557	
101								2.331		5.640	5.714
102	46.89	1.94	0.650	0.100	0.353	1.5811	3.76	23.94		6.800	6.086
103	50.69	1.85	0.200	0.060	0.123	1.9695	3.88	2.188	2.064	6.814	
104	45.80	1.91	0.420	0.050	0.713	4.2517	3.88	2.587		6.200	
105	34.85	2.31	0.550	0.100	0.499	3.1192	4.26	2.634		5.483	
106								2.321		4.975	
108								2.097		8.775	
109	45.83	1.97	0.000	0.000	0.160	1.3744	4.88	1.900		7.350	
110	50.15	1.96	0.200	0.050	0.130	1.3693	4.13	2.409		7.433	
111	51.43	1.78	0.000	0.000	0.043	2.4121	4.00	2.631		8.950	8.267
112	46.78	1.91	0.500	0.100	0.311	3.0064	3.65	2.417		7.975	
113	49.88	1.88	0.500	0.030	0.871	3.4473	4.00	2.424		7.275	
114	46.98	1.91	0.650	ND	4.870	6.6771	4.00	2.360		6.975	
115	36.99	2.31	ND	ND	0.178	1.2247	5.45	2.156		4.875	
118	33.82	2.33	0.100	0.020	0.285	2.0736	4.41				
119	47.06	2.01	ND	ND	0.093	1.2813	4.88				
120	49.62	1.90	0.500	0.050	0.490	2.4403	4.00				
121	46.09	2.03	0.500	0.050	0.056	1.8081	4.13				
122	44.81	1.96	0.100	0.030	0.340	1.5652	3.76				
123	46.89	1.93	0.100	0.020	0.145	1.6514	(9.00)				
X-1	41.49	2.24	0.100	0.050	3.730	8.0623	3.08				
X-2	42.06	2.08	0.000	0.000	0.717	2.5641	2.64				
X-3	39.72	2.23	ND	ND	0.174	2.2650					

APPENDIX A.6 SEDIMENT ANALYSES

Site No	Sample Wt. (gm)	Sample Vol. (cc)	Density (Wet) Sample Interval (cm)	Density (Wet) Interval Wet (gm/cm)	Ave Wet	Spec. Grav. (G_s)	Water Content W(%)	Void Ratio (e)	Porosity ϕ(%)	Size Analysis (%)	Coef. of Uniform. (C_u)	Engineering Properties	Grain Size Distribution (mm)	Sorting Coefficient (So)
23	7168.8	3337.7	0-60.4	2.15		2.68	36.0	0.751	42.53	0.03 G[1] 0.04 CS[2] 0.36 MS[3] 71.81 FS[4] 24.05 S[5] 3.71 C[6]	2.25	0.080 T* 0.30 P†	0.09 md** 0.095 Q_{75} 0.073 Q_{25} 0.011 QOa	1.1408 QOg 0.1317 Ln
24	5049.1	2420.4	0-43.8	2.09		2.66	38.2	.806	44.63	0.02 CS .19 MS 70.47 FS 24.50 S 4.82 C	2.81	0.080 T 0.30 P	0.086 md 0.096 Q_{75} .072 Q_{25} .012 QOa	1.547 QOg .1438 Ln
25	7237.8	3492.4	0-63.2	2.07		2.68	37.7	.832	45.41	.01 G .01 CS .22 MO 34.45 FS 58.74 S 6.57 C	3.30	.110 T .56 P	0.066 md .078 Q_{75} .040 Q_{25} .019 QOa	1.3964 QOg .3339 Ln
26	734.3	3597.4	0-65.1	2.04		2.59	38.3	.795	42.28	.04 G .09 CS .16 MO 59.60 FS 34.27 S 5.84 C	3.07	.076 T .50 P	0.072 md .090 Q_{75} .053 Q_{25} .018 QOa	1.3031 QOg .2647 Ln
38	6706.9	3409.5	0-61.7	1.97		2.62	37.5	.879	46.78	2.32 G .18 CS .48 MS 61.72 FS 28.01 S 7.29 C	10.00	.086 T .46 P	0.081 md .11 Q_{75} .058 Q_{25} .026 QOa	1.3771 QOg .3200 Ln
39	7384.4	3437.2	0.62.2	2.15		2.66	37.1	.610	37.89	.09 G .07 CS .87 MO 74.65 FS 19.06 S 5.26 C	3.57	.10 T .043 P	0.092 md .10 Q_{75} .076 Q_{25} .017 QOa	1.2030 QOg .1849 Ln

[1]Gravel [2]Coarse Sand [3]Medium Sand [4]Fine Sand [5]Silt [6]Clay

*Torvane (kg/cm^2) †Penetrometer (kg/cm^2)

**mean diameter

NOTE: T-M, M-B, T-B } equals { Top-Middle, Middle-Bottom, Top-Bottom

Site No	Sample Wt. (gm)	Sample Vol. (cc)	Density (Wet) Sample Interval (cm)	Density (Wet) Interval Wet (gm/cm)	Ave Wet	Spec. Grav. (G_s)	Water Content W(%)	Void Ratio (e)	Porosity ϕ(%)	Size Analysis (%)	Coef. of Uniform. (C_u)	Engineering Properties	Grain Size Distribution (mm)	Sorting Coefficient (So)
40	7436.2	3625.1	0.65.6	2.05		2.67	36.4	.826	45.24	.46 G .18 CS .45 MS 75.89 FS 17 47 S 5.55 C	3.59	.096 T .28 P	0.089 md .10 Q_{75} .080 Q_{25} .010 QDa	1.1180 QDg .1116 Ln
41	7111.4	3365.3	0-60.9	2.11		2.66	33.5	.727	42.10	.20 G .06 CS .33 MS 69.91 FS 23.11 S 6.39 C	3.33	.076 T .32 P	.074 md .095 Q_{75} .069 Q_{25} .013 QDa	1.1734 QDg .1599 Ln
42	7228.0	3591.9	0-65.0	2.01		2.66	37.8	.869	46.49	.04 G .03 CS .29 MS 51.02 FS 43.68 S 4.94 C	2.86	.08 T .60 P	0.069 md .090 Q_{75} .047 Q_{25} .021 QDa	1.3838 QDg .3248 Ln
43	7213.7	3475.9	0-62.9	2.08		2.66	37.7	.807	44.66	.01 G .01 CS .46 MS 66.29 FS 27.29 S 5.94 C	3.41	.065 T .30 P	.083 md .10 Q_{75} .060 Q_{25} .020 QDa	1.2910 QDg .2554 Ln
44	7442.2	3514.5	0-63.6	2.12		2.66	37.2	.760	43.18	.01 G .00 CS .24 MS 78.70 FS 18.06 S 2.99 C	1.90	.046 T .41 P	.095 md .10 Q_{75} .080 Q_{25} .010 QDa	1.1180 QDg .1116 Ln
45	7352.0	3536.6	0-64.0	2.08		2.68	36.2	.796	44.32	.15 G .15 CS .99 MS 71.98 FS 22.16 S 4.57 C	2.32	.113 T .46 P	.086 md .098 Q_{75} .071 Q_{25} .013 QDa	1.1748 QDg .1611 Ln

Site No	Sample Wt. (gm)	Sample Vol. (cc)	Density (Wet) Sample Interval (cm)	Density (Wet) Interval Wet (gm/cm)	Ave Wet	Spec. Grav. (G_s)	Water Content W(%)	Void Ratio (e)	Porosity ±(%)	Size Analysis (%)	Coef. of Uniform. (C_u)	Engineering Properties	Grain Size Distribution (mm)	Sorting Coefficient (So)
46	7096.5	3614.0	0-65.4	1.96		2.69	36.3	.916	47.80	.14 G .34 CS .72 MS 47.47 FS 42.63 S 8.70 C	9.00	.103 T .50 P	.066 md .093 Q_{7s} .038 Q_{2s} .027 QDa	1.5664 QDg .4475 Ln
47	6835.1	3332.2	0-63.3	2.05		2.66	35.4	.807	44.66	.41 G .11 CS .83 MS 62.48 FS 30.01 S 6.16 C	4.75	.11 T .42 P	.078 md .10 Q_{7s} .054 Q_{2s} .023 QDa	1.3608 QDg .3081 Ln
48	6935.7	3409.5	0-61.7	2.03		2.67	33.1	.790	44.13	1.08 G .32 CS .50 MS 69.41 FS 23.04 S 5.65 C	3.55	.10 T .35 P	.092 md .12 Q_{7s} .071 Q_{2s} .024 QDa	1.3000 QDg .2624 Ln
49	7285.6	3426.1	0-62.0	2.13		2.67	35.1	.733	42.30	.29 G .37 CS .51 MS 69.67 FS 23.28 S 5.88 C	4.35	.11 T .11 P	.090 md .12 Q_{7s} .068 Q_{2s} .026 QDa	1.3284 QDg .2840 Ln
50	4425.0	1541.7	0-27.9	2.87		2.68	38.3	.327	24.64	3.22 G .17 CS .43 MS 62.35 FS 28.06 S 5.77 C	3.48	.13 T .22 P	.084 md .11 Q_{7s} .058 Q_{2s} .031 QDa	1.4384 QDg .3635 Ln
51	5848.5	3011.7	0-54.5	1.94		2.61	38.9	.912	47.70	.47 G .14 CS .55 MS 61.42 FS 29.89 S 7.53 C	5.55	.07 T .33 P	.080 md .11 Q_{7s} .056 Q_{2s} .027 QDa	1.4015 QDg .3376 Ln

Site No	Sample Wt. (gm)	Sample Vol. (cc)	Density (Wet) Sample Interval (cm)	Density (Wet) Interval Wet (gm/cm)	Ave Wet	Spec. Grav. (G_s)	Water Content W(%)	Void Ratio (e)	Porosity ϕ(%)	Size Analysis (%)	Coef. of Uniform. (C_u)	Engineering Prooerties	Grain Size Distribution (mm)	Sorting Coefficient (So)
52	5214.5	2646.7	0-47.9	1.97		2.64	37.9	.893	47.17	.24 G .16 CS .64 MS 41.43 FS 47.73 S 9.75 C	15 40	.04 T .14 P	.065 md .092 Q_{7s} .039 Q_{2s} .026 QDa	1.5359 QDg .4291 Ln
57	4602.7	2331.9	0-42.2	1.97		2.59	38.9	.871	46.55	.18 G 1.46 CS 1.74 MS 64.30 FS 26.56 S 5.76 C	5.80	.056 T .18 P	1.12 md .15 Q_{7s} .056 Q_{2s} .047 QDa	1.6366 QDg .4926 Ln
58	6178.3	3072.5	0-55.6	2.01		2.71	3.81	.904	47.48	.35 G 1.63 CS 3.30 MS 59.79 FS 25.29 S 9.64 C	30.00	.103 T .40 P	1.11 md .17 Q_{7s} .056 Q_{2s} .057 QDa	1.7423 QDg .5552 Ln
59	7137.8	3442.7	0-62.3	2.07		2.75	38.1	.880	46.81	.50 G 5.10 CS 20.91 MS 39.21 FS 25.28 S 9.00 C	29.17	.09 T .20 P	1.68 md .26 Q_{7s} .046 Q_{2s} .107 QDa	2.3774 QDg .8660 Ln
60	7068.9	3558.7	0-64.4			2.63	37.4	.835	45.50					
Top	3947.4	2066.7	0-37.4	1.91		2.64	34.0	.893	47.17	.15 G .35 CS 4.22 MS 41.95 FS 41.06 S 12.27 C	45.0	.12 T .70 P	.074 md .12 Q_{7s} .034 Q_{2s} .043 QDa	1.8787 QDg .6306 Ln
Bottom	2805.0	1492.0	37.4-64.4	1.88		2.63	36.1	.955	48.85	4.31 G 1.01 CS 7.23 MS 43.89 FS 33.89 S 9.89 C	20.00	.06 T .32 P	.093 md .12 Q_{7s} .045 Q_{2s} .037 QDa	1.6330 QDg .4904 Ln
T-8					1.90									

Site No	Sample Wt. (gm)	Sample Vol. (cc)	Density (Wet) Sample Interval (cm)	Density (Wet) Interval Wet (gm/cm)	Ave Wet	Spec. Grav. (G_s)	Water Content W(%)	Void Ratio (e)	Porosity ¢(%)	Size Analysis (%)	Coef. of Uniform. (C_u)	Engineering Properties	Grain Size Distribution (mm)	Sorting Coefficient (So)
61	7033.4	3029.9	0-65.2	2.32		2.66	36.4	.605	37.69	.54 G .23 CS 1.74 MS 59.73 FS 27.99 S 9.77 C	18.40	.12 T .50 P	.075 md .096 Q_{75} .048 Q_{25} .024 QDa	1.4142 QOg .3466 Ln
62	7039.4	3475.8	0-62.9	2.02		2.66	36.7	.843	45.74	.11 G .16 CS .77 MS 73.17 FS 18.02 S 7.77 C	7.33	.03 T .42 P	.123 md .12 Q_{75} .070 Q_{25} .025 QDa	1.3093 QDg .2695 Ln
63	7258.6	3442.7	0-62.3	2.11		2.65	35.9	.753	42.95	.48 G .32 CS 1.07 MS 63.66 FS 27.03 S 7.44 C	11.29	.11 T .55 P	.088 md .11 Q_{75} .067 Q_{25} .022 QDa	1.2813 QDg .2479 Ln
64	4714.8	2221.4	0-40.2	2.12		2.63	37.7	.752	42.92	.95 G .38 CS 2.02 MS 79.72 FS 13.25 S 3.68 C	2.16	.09 T .40 P	.102 md .12 Q_{75} .087 Q_{25} .017 QDa	1.1744 QDg .1608 Ln
65	6989.1	3365.3	0-60.9	2.08		2.67	37.4	.778	43.76	.83 G .57 CS 1.98 MS 63.14 FS 25.94 S 7.54 C	6.71	.70 T .33 P	.085 md .12 Q_{75} .059 Q_{25} .031 QDa	1.4261 QDg .3550 Ln
66	5993.1	2823.8	0-51.1	2.12		2.65	35.1	.731	42.23	.44 G 1.18 CS 2.73 MS 57.53 FS 31.64 S 6.48 C	3.96	.10 T .40 P	.085 md .11 Q_{75} .051 Q_{25} .030 QDa	1.4686 QDg .3843 Ln

Site No	Sample Wt. (gm)	Sample Vol. (cc)	Density (Wet) Sample Interval (cm)	Density (Wet) Interval Wet (gm/cm)	Ave Wet	Spec. Grav. (G_s)	Water Content W(%)	Void Ratio (e)	Porosity ¢(%)	Size Analysis (%)	Coef. of Uniform. (C_u)	Engineering Properties	Grain Size Distribution (mm)	Sorting Coefficient (So)
68	1454.3	762.6	0-13.8	1.91		2.67	34.3	.999	49.97	9.01 G 3.73 CS 5.47 MS 45.79 FS 25.67 S 10.33 C	26.19	.00 T .00 P	.118 md .16 Q_{7s} .047 Q_{2s} .056 QDa	1.8451 QDg .6125 Ln
69	5042.0	2497.7	0-45.2	2.02		2.65	39.0	.874	46.64	49 G .88 CS 2.57 MS 73.15 FS 15.57 S 7.34 C	7.14	.066 T .20 P	.091 md .12 Q_{7s} .063 Q_{2s} .028 QDa	1.3801 QDg .3222 Ln
69V	8222.0	3779.4	0-92.2			2.66								
Top	768.1	406.4	0-9.2	1.89		2.63	35.7	.901	47.40	.16 G .41 CS 3.04 MS 72.96 FS 17.84 S 5.59 C	3.44	.10 T .35 P	.096 md .12 Q_{7s} .080 Q_{2s} .020 QDa	1.2247 QDg .2027 Ln
Middle	5807.3	2933.0	9.7-79.7	1.99		2.68	30.3	.808	44.69	43.84 G 3.10 CS 7.45 MS 31.37 FS 10.30 S 5.59 C	33.02	.10 T 1.00 P	.096 md .12 Q_{7s} .080 Q_{2s}	
Bottom	915.0	439.9	79.7-90.2	2.08		2.69	24.0	.642	39.09	1.43 G .84 CS 3.96 MS 81.80 FS 6.36 S 5.61 C	4.09	.30 T 2.50 P	.163 md .19 Q_{7s} .15 Q_{2s} .020 QDa	1.1255 QDg .1182 Ln
T-M M-B T-B					1.94 2.03 1.99									
70	6983.0	3459.3	0-62.6	2.02		2.67	34.8	.826	45.24	.54 G .36 CS 1.90 MS 69.57 FS 20.73 S 6.90 C	5.47	.10 T .30 P	.083 md .099 Q_{7s} .069 Q_{2s} .015 QDa	1.1978 QDg .1805 Ln

Site No	Sample Wt. (gm)	Sample Vol. (cc)	Density (Wet) Sample Interval (cm)	Density (Wet) Interval Wet (gm/cm)	Ave Wet	Spec. Grav. (G_s)	Water Content W(%)	Void Ratio (e)	Porosity e(%)	Size Analysis (%)	Coef. of Uniform. (C_u)	Engineering Properties	Grain Size Distribution (mm)	Sorting Coefficient (So)
71	6925.6	3525.6	0-63.8	1.96		2.66	39.1	.935	48.32	.12 G .08 CS 1.50 MS 70.86 FS 22.52 S 4.92 C	2.58	.02 T .20 P	.097 md .11 Q_{7s} .055 Q_{2s} .027 QDa	1.4142 QDg .3466 Ln
72	6765.3	3492.4	0-63.2	1.94		2.66	33.6	.856	46.12	.40 G .63 CS 2.07 MS 49.89 FS 34.45 S 12.56 C	21.13	.076 T .23 P	.076 md .12 Q_{7s} .028 Q_{2s} .046 QDa	2.0701 QDg .7276 Ln
73	6598.0	3011.7	0-54.5	2.19		2.66	37.4	.716	47.72	1.52 G 11.21 CS 69.15 MS 12.51 FS 3.83 S 1.78 C	2.66	.01 T .10 P	.357 md .43 Q_{7s} .3[illegible] Q_{2s} .065 QDa	1.1972 QDg 1.0942 Ln
73V	9761.0	4357.6	0-104.0			2.66								
Top	6999.0	3645.3	0-87.0	1.92		2.68	34.8	.936	48.34	16.44 G 10.06 CS 38.63 MS 15.49 FS 14.28 S 5.10 C	20.00	.10 T .10 P	.438 md .53 Q_{7s} .13 Q_{2s} .200 QDa	2.0191 QDg .7027 Ln
Bottom	1481.6	712.3	87.0-104.0	2.08		2.65	23.1	.608	37.81	26.90 G 19.54 CS 17.14 MS 25.37 FS 8.90 S 2.15 C	10.30	.10 T 1.00 P	.736 md .98 Q_{7s} .084 Q_{2s} .448 QDa	3.4157 QDg 1.2284 Ln
T-8					2.00									
81	674.2	348.1	0-06.3	1.94		2.66	35.6	.908	47.59	.67 G 9.05 CS 33.66 MS 35.49 FS 16.49 S 4.64 C	6.75	.0 T .0 P	.227 md .37 Q_{7s} .087 Q_{2s} .141 QDa	2.0622 QDg .7238 Ln

Site No	Sample Wt. (gm)	Sample Vol. (cc)	Density (Wet) Sample Interval (cm)	Density (Wet) Interval Wet (gm/cm)	Ave Wet	Spec. Grav. (G_s)	Water Content W(%)	Void Ratio (e)	Porosity ϕ(%)	Size Analysis (%)	Coef. of Uniform. (C_u)	Engineering Properties	Grain Size Distribution (mm)	Sorting Coefficient (So)
82	3446.5	1801.5	0-32.6	1.91		2.67	29.8	.862	46.29	11.60 G 32.18 CS 47.88 MS 4.65 FS 2.56 S 1.13 C	1.88	.01 T .10 P	.54 md .60 Q_{75} .38 Q_{25} .110 QDa	1.2566 QDg .2284 Ln
83	450.7	193.41	0-04.5	1.81		2.65	39.4	1.091	52.17	.33 G .64 CS 4.30 MS 33.66 FS 47.72 S 13.35 C	33.33	.00 T .00 P	.067 md .091 Q_{75} .037 Q_{25} .027 QDa	1.5683 QDg .4450 Ln
84	6594.7	2995.1	0-54.2	2.20		2.71	32.2	.674	40.26	2.11 G 7.50 CS 33.21 MS 27.39 FS 23.88 S 5.91 C	7.10	.18 T .66 P	.217 md .35 Q_{75} .067 Q_{25} .141 QDa	2.2856 QDg .8266 Ln
85	6934.0	3520.1	0-63.7	1.97		2.60	38.1	.865	46.38	.20 G .13 CS 2.58 MS 67.07 FS 22.60 S 8.42 C	14.00	.10 T .50 P	.081 md .10 Q_{75} .073 Q_{25} .014 QDa	1.1704 QDg .1574 Ln
86	5792.8	2884.6	0-52.2			2.65								
Top	3972.4	2028.0	0-36.7	1.87		2.63	37.2	.983	49.57	.14 G .31 CS 1.37 MS 81.56 FS 13.47 S 3.45 C	1.77	.10 T .20 P	.096 md .11 Q_{75} .087 Q_{25} .011 QDa	1.1244 QDg .1173 Ln
Bottom	1635.9	856.5	36.7-52.2	1.91		2.66	34.8	.921	47.94	17.56 G 5.06 CS 4.06 MS 25.40 FS 36.38 S 11.54 C	31.58	.10 T .60 P	.530 md .35 Q_{75} .04 Q_{25} .155 QDa	2.9580 QDg 1.0845 Ln
T-B					1.89									

Site No	Sample Wt. (gm)	Sample Vol. (cc)	Density (Wet) Sample Interval (cm)	Density (Wet) Interval Wet (gm/cm)	Ave Wet	Spec. Grav. (G_s)	Water Content W(%)	Void Ratio (e)	Porosity ϕ(%)	Size Analysis (%)	Coef. of Uniform. (C_u)	Engineering Properties	Grain Size Distribution (mm)	Sorting Coefficient (So)
87	1432.5	547.7	0-10.4	2.61		2.72	40.5	.500	33.33	4.47 G 6.12 CS 18.31 MS 49.10 FS 14.14 S 7.86 C	18.33	.00 T .00 P	.330 md .28 Q_{75} .085 Q_{25} .097 QDa	1.8150 QDg .5961 Ln
88	1511.3	607.9	0-11.0	2.49		2.70	39.5	.557	35.77	11.49 G 1.23 CS 6.11 MS 46.92 FS 24.13 S 10.12 C	34.15	.00 T .00 P	.154 md .18 Q_{75} .047 Q_{25} .066 QDa	1.9570 QDg .6714 Ln
92	1107.3	4973.4	0-09.0	2.22		2.66	35.4	.663	39.87	6.10 G .89 CS 9.08 MS 64.96 FS 16.75 S 2.22 C	1.89	.00 T .00 P	.133 md .14 Q_{75} .086 Q_{25} .027 QDa	1.2759 QDg .2436 Ln
93	7674.0	3531.1	0-63.9	2.17		2.69	38.3	.757	43.08	.98 G 6.29 CS 39.71 MS 35.58 FS 14.28 S 3.16 C	5.60	.086 T .33 P	.233 md .37 Q_{75} .092 Q_{25} .1390 QDa	2.0054 QDg .6959 Ln
94	6557.7	3299.0	0-59.7	1.99		2.64	39.0	.893	47.17	.11 G .74 CS 6.28 MS 26.20 FS 57.22 S 9.45 C	15.00	.04 T .25 P	.061 md .090 Q_{75} .030 Q_{25} .030 QDa	1.7321 QDg .5493 Ln
95A	4131.8	2138.6	0-38.7			2.63								
Top	2230.3	1199.1	0-21.7	1.86		2.64	38.9	1.021	50.52	2.40 G 4.36 CS 11.55 MS 25.68 FS 43.74 S 12.27 C	62.14	.02 T .00 P	.357 md .11 Q_{75} .033 Q_{25} .038 QDa	1.8257 QDg .6020 Ln
Bottom	1747.3	939.4	21.7-38.7	1.86		2.63	38.2	.998	49.95	22.48 G 11.38 CS 11.49 MS 13.27 FS 32.71 S 8.67 C	50.66	.07 T .25 P	.548 md .80 Q_{75} .045 Q_{25} .377 QDa	4.2184 QDg 1.4390 Ln
T-8					1.86									

Site No	Sample Wt. (gm)	Sample Vol. (cc)	Density (Wet) Sample Interval (cm)	Density (Wet) Interval Wet (gm/cm)	Ave Wet	Spec. Grav. (G_s)	Water Content W(%)	Void Ratio (e)	Porosity ϕ(%)	Size Analysis (%)	Coef. of Uniform. (C_u)	Engineering Properties	Grain Size Distribution (mm)	Sorting Coefficient (So)
95B	576.9	281.8	0-05.1	2.05		2.64	39.1	.842	45.71	.11 G .60 CS 7.22 MS 25.58 FS 51.99 S 14.50 C	46.25		.058 md .088 Q_{7s} .025 Q_{2s} .031 QDa	1.8752 QD_g .6292 Ln
100	5524.8	1884.4	0-34.1	2.93		2.72	33.3	.268	21.14	17.67 G 37.89 CS 39.65 MS 3.93 FS .86 S	1.93	1.0 P	.62 md .75 Q_{7s} .40 Q_{2s} .175 QDa	1.3693 QD_g .3143 Ln
102	4580.0	2204.9	0-39.9			2.68								
Top	1715.3	884.2	0-16.0	1.94		2.68	32.6	.883	46.89	14.19 G 3.67 CS 44.12 MS 21.12 FS 13.03 S 3.87 C	9.43	.10 T .65 P	.353 md .40 Q_{7s} .16 Q_{2s} .120 QDa	1.5811 QD_g .4581 Ln
Bottom	2628.2	1320.7	16.0-39.9	1.99		2.69	29.9	.803	44.54	.52 G 1.21 CS 7.71 MS 33.68 FS 50.04 S 6.84 C	3.39	.05 T .30 P	.085 md .11 Q_{7s} .038 Q_{2s} .036 QDa	1.7014 QD_g .5314 Ln
T-B					1.97									
103	5220.8	2829.3	0-51.2	1.85		2.63	39.3	1.028	50.69	3.12 G 4.32 CS 9.49 MS 27.86 FS 44.51 S 10.70 C	23.16	.06 T .20 P	.123 md .12 Q_{7s} .031 Q_{2s} .044 QDa	1.9695 QD_g .6768 Ln
103V	2990.0	1596.4	0-38.1	1.55		2.65	40.0	1.448	59.15	.27 G .70 CS 3.99 MS 21.78 FS 57.92 S 15.34 C		.045 T .75 P	.055 md .080 Q_{7s} .018 Q_{2s} .031 QDa	2.0182 QD_g .7458 Ln

Site No	Sample Wt. (gm)	Sample Vol. (cc)	Density (Wet) Sample Interval (cm)	Density (Wet) Interval Wet (gm/cm)	Ave Wet	Spec. Grav. (G_s)	Water Content W(%)	Void Ratio (e)	Porosity ¢(%)	Size Analysis (%)	Coef. of Uniform. (C_u)	Engineering Properties	Grain Size Distribution (mm)	Sorting Coefficient (So)
104	7056.1	3481.4	0-63.0			2.61								
Top	3694.1	1934.1	0-35.0	1.91		2.59	32.3	.845	45.80	25.58 G 13.83 CS 14.33 MS 13.30 FS 25.16 S 8.70 C	51.06	.05 T .42 P	.713 md .94 Q_{75} .052 Q_{25} .444 QDa	4.2517 QDg 1.4473 Ln
Bottom	3017.2	1547.3	35.0-63.0	1.95		2.62	30.6	.803	44.54	1.75 G 5.54 CS 11.41 MS 26.42 FS 42.59 S 12.29 C	34.78	.05 T .25 P	.115 md .15 Q_{75} .027 Q_{25} .061 QDa	2.3570 QDg .8574 Ln
T-B					1.93									
105	5272.5	2276.7	0-41.2	2.31		2.62	31.7	.535	34.85	18.65 G 16.31 CS 24.19 MS 14.55 FS 19.37 S 6.93 C	28.66	.10 T .55 P	.499 md .72 Q_{75} .074 Q_{25} .233 QDa	3.1192 QDg 1.1376 Ln
109	6221.1	3000.6	0-54.3			2.70								
Top	4278.3	2171.7	0-39.3	1.97		2.70	31.6	.846	45.83	3.45 G 5.03 CS 15.94 MS 58.63 FS 14.41 S 2.50 C	1.86	.00 T .00 P	.160 md .17 Q_{75} .090 Q_{25} .040 QDa	1.3744 QDg .3180 Ln
Bottom	1649.5	828.9	39.3-54.3	1.99		2.70	29.9	.810	44.75	21.89 G 21.25 CS 21.79 MS 27.21 FS 7.14 S .72 C	5.93	.00 T .00 P	.603 md .80 Q_{75} .120 Q_{25} .340 QDa	2.5820 QDg .9486 Ln
T-B					1.98									

Site No	Sample Wt. (gm)	Sample Vol. (cc)	Density (Wet) Sample Interval (cm)	Density (Wet) Interval Wet (gm/cm)	Ave Wet	Spec. Grav. (G_s)	Water Content W(%)	Void Ratio (e)	Porosity ϕ(%)	Size Analysis (%)	Coef. of Uniform. (C_u)	Engineering Properties	Grain Size Distribution (mm)	Sorting Coefficient (So)
109V	3346.0	1520.9	0-36.3			2.71	32.5							
Top	1786.2	879.9	0-21.0	2.03		2.72	28.0	.754	42.99	9.22 G 9.89 CS 23.62 MS 39.36 FS 14.69 S 2.50 C	4.33	.00 T .00 P	.268 md .40 Q_{75} .090 Q_{25} .155 QDa	2.1082 QDg .7458 Ln
Bottom	1352.7	641.1	21.0-36.3	2.11		2.71	23.0	.616	38.12	.61 G 1.62 CS 8.05 MS 64.50 FS 21.72 S 3.50 C	1.81	.10 T .10 P	.103 md .12 Q_{75} .018 Q_{25} .051 QDa	2.5820 QDg .9486 Ln
T-B					2.07									
110	5550.0	2829.3	0-51.2	1.96		2.64	45.4	1.006	50.15	1.32 G 2.45 CS 12.60 MS 60.81 FS 19.02 S 3.80 C	2.90	.05 T .20 P	.130 md .15 Q_{75} .080 Q_{25} .0350 QDa	1.3693 QDg .3143 Ln
111	2335.1	1309.7	0-23.7	1.78		2.57	39.4	1.059	51.43	1.36 G 1.16 CS 4.33 MS 10.20 FS 65.38 S 17.48 C		.00 T .00 P	.043 md .064 Q_{75} .011 Q_{25} .026 QDa	2.4121 QDg .8805 Ln
112	4686.7	2304.3	0-41.7			2.62								
Top		1420.2	0-25.7	1.91		2.62	33.7	.879	46.78	12.39 G 12.30 CS 15.65 MS 23.47 FS 28.92 S 7.27 C	23.33	.10 T .50 P	.311 md .47 Q_{75} .052 Q_{25} .209 QDa	3.0064 QDg 1.1007 Ln
Bottom		884.2	25.7-41.7	1.92		2.62	32.6	.853	46.03	2.64 G 9.43 CS 14.72 MS 33.10 FS 33.19 S 6.92 C	6.25	.03 T .15 P	.187 md .25 Q_{75} .050 Q_{25} .100 QDa	2.2361 QDg .8047 Ln
T-B					1.91									

Site No	Sample Wt. (gm)	Sample Vol. (cc)	Density (Wet) Sample Interval (cm)	Density (Wet) Interval Wet (gm/cm)	Ave Wet	Spec. Grav. (G_s)	Water Content W(%)	Void Ratio (e)	Porosity ϕ(%)	Size Analysis (%)	Coef. of Uniform. (C_u)	Engineering Properties	Grain Size Distribution (mm)	Sorting Coefficient (So)
113	6399.4	3299.0	0-59.7			2.63								
Top	3116.7	1657.8	0-30.0	1.88		2.63	35.9	.995	49.88	24.67 G 6.85 CS 12.84 MS 27.87 FS 20.53 S 7.24 C	30.00	.03 T .05 P	.871 md .82 Q_{75} .069 Q_{25} .376 QDa	2.4473 QDg 1.2376 Ln
Bottom	3134.7	1641.2	30.0-59.7	1.91		2.63	33.1	.886	46.98	17.35 G 4.41 CS 13.14 MS 31.71 FS 26.05 S 7.34 C	11.67	.03 T	.554 md .42 Q_{75} .068 Q_{25} .176 QDa	2.4852 QDg .9104 Ln
T-B					1.90									
114	5850.0	2856.9	0-51.7			2.63								
Top	2427.6	1271.0	0-23.0	1.91		2.63	33.7	.886	46.98	58.99 G 6.98 CS 7.02 MS 14.70 FS 8.60 S 3.71 C	105.45	.10 P	4.87 md 1D.7 Q_{75} .24D Q_{25} 5.23 QDa	6.6771 QDg 1.8987 Ln
Bottom	3076.6	1585.9	23.0-51.7	1.94		2.63	31.3	.823	45.15	4.29 G 11.19 CS 16.97 MS 41.88 FS 19.76 S 5.91 C	8.25	.05 T .10 P	.218 md .30 Q_{75} .073 Q_{25} .113 QDa	2.0272 QDg .7067 Ln
T-B					1.93									
115	765.9	331.56	0-06.0	2.31		2.63	36.0	.587	36.99	5.25 G 3.55 CS 9.95 MS 72.69 FS 6.45 S 2.11 C	1.73		.178 md .18 Q_{75} .120 Q_{25} .0300 QDa	1.2247 QDg .2027 Ln

Site No	Sample Wt. (gm)	Sample Vol. (cc)	Density (Wet) Sample Interval (cm)	Density (Wet) Interval Wet (gm/cm)	Ave Wet	Spec. Grav. (G_s)	Water Content W(%)	Void Ratio (e)	Porosity ϕ(%)	Size Analysis (%)	Coef. of Uniform. (C_u)	Engineering Properties	Grain Size Distribution (mm)	Sorting Coefficient (So)
118 (1)	5941.7	2608.3	0-47.2	2.28		2.68	37.7	.656	39.61	3.56 G 10.32 CS 27.11 MS 46.46 FS 10.53 S 2.02 C	3.57	.00 T .00 P	.234 md .28 Q_{75} 100 Q_{25} .1400 QDa	1.9493 QDg .6675 Ln
118 (2)	7306.3	3138.8	0-56.8	2.33		2.71	26.3	.511	33.82	1.43 G 13.04 CS 40.17 MS 37.12 FS 7.41 S .83 C	4.37	.02 T 0.1 P	.285 md .43 Q_{75} .1 Q_{25} .165 QDa	2.0736 QDg .7293 Ln
119	1653.6	823.37	0-14.9	2.01		2.67	38.9	.889	47.06	.16 G .80 CS 6.79 MS 58.19 FS 31.48 S 4.58 C	2.83		.093 md .11 Q_{75} .067 Q_{25} .021 QDa	1.2813 QDg .2479 Ln
120 Top	1574.9	828.92	0-15.0	1.90		2.69	36.7	.985	49.62	18.79 G 7.00 CS 11.55 MS 48.18 FS 9.48 S 5.00 C	4.42	.05 T .50 P	.490 md .530 Q_{75} .089 Q_{25} .220 QDa	2.4403 QDg .8921 Ln
120 Bottom	801.4	408.9	15.0-22.4	1.96		2.69	31.7	.852	46.00	8.29 G 1.52 CS 2.41 MS 41.95 FS 37.26 S 8.57 C	15.00	.00 T .00 P	.090 md .115 Q_{75} .089 Q_{25} .035 QDa	.8906 QDg -.1159 Ln
T-8					1.93									
121	6147.3	3033.8	0-54.9	2.03		2.64	38.6	.855	46.09	.16 G .12 CS 1.08 MS 30.00 FS 53.73 S 14.91 C	22.66	.05 T 0.5 P	.056 md .085 Q_{75} .026 Q_{25} .029 QDa	1.8081 QDg .5923 Ln

Site No	Sample Wt. (gm)	Sample Vol. (cc)	Density (Wet) Sample Interval (cm)	Density (Wet) Interval Wet (gm/cm)	Ave Wet	Spec. Grav. (G_s)	Water Content W(%)	Void Ratio (e)	Porosity ϕ(%)	Size Analysis (%)	Coef. of Uniform. (C_u)	Engineering Properties	Grain Size Distribution (mm)	Sorting Coefficient (So)
121V	3050.0	1315.7	0-31.4	2.31		2.72	39.7	.691	40.83	10.23 G 1.55 CS 5.20 MS 49.72 FS 26.60 S 6.70 C	5.60	.036 T .18 P	.144 md .185 Q_{75} .064 Q_{25} .061 QDa	1.7002 QDg .5307 Ln
122	6251.1	3083.5	0-55.8			2.63								
Top	4419.0	2254.6	0-40.8	1.96		2.65	30.8	.812	44.81	4.02 G 21.72 CS 45.14 MS 20.51 FS 7.20 S 1.41 C	4.94	.03 T .10 P	.340 md .49 Q_{75} .2 Q_{25} .145 QDa	1.5652 QDg .4480 Ln
Bottom	1660.5	828.9	40.8-55.8	2.00		2.63	27.0	.718	41.79	31.68 G 15.89 CS 23.46 MS 18.26 FS 8.47 S 2.24 C	7.38	.05 T .25 P	.132 md 1.5 Q_{75} .20 Q_{25} .650 QDa	2.7386 QDg 1.0074 Ln
T-B					1.98									
123	5906.6	2912.2	0-52.7			2.62								
Top	4224.3	2193.8	0-39.7	1.93		2.61	32.0	.883	46.89	2.80 G 6.08 CS 10.05 MS 49.75 FS 26.45 S 4.87 C	3.53	.02 T .10 P	.145 md .18 Q_{75} .066 Q_{25} .057 QDa	1.6514 QDg .5016 Ln
Bottom	1451.0	718.4	39.7-52.7	2.02		2.62	25.6	.669	40.08	50.29 G 8.51 CS 8.08 MS 19.16 FS 11.04 S 2.92 C	38.00	.01 T .75 P	3.9 md 5.1 Q_{75} .13 Q_{25} 2.485 QDa	6.2634 QDg 1.8347 Ln
T-B					1.98									
123V	2924.6	1437.2	0-34.3	2.03		2.72	37.0	.885	46.95	6.60 G 3.03 CS 8.94 MS 47.32 FS 18.25 S 15.86 C			.133 md .19 Q_{75} .018 Q_{25} .086 QDa	3.2489 QDg 1.1783 Ln

Site No	Sample Wt. (gm)	Sample Vol. (cc)	Density (Wet) Sample Interval (cm)	Density (Wet) Interval Wet (gm/cm)	Ave Wet	Spec. Grav. (G_s)	Water Content W(%)	Void Ratio (e)	Porosity ϕ(%)	Size Analysis (%)	Coef. of Uniform. (C_u)	Engineering Properties	Grain Size Distribution (mm)	Sorting Coefficient (So)
124V	1905.0	1009.8	0-24.1	1.88		2.67	37.2	.988	49.70	5.98 G 2.92 CS 7.49 MS 80.53 FS 2.47 S .61 C	1.94	.06 T .25 P	.173 md .19 Q_{75} .13 Q_{25} .0300 QDa	1.2089 QDg .1897 Ln
X-1	1877.7	839.9	0-15.2	2.24		2.70	38.3	.709	41.49	31.54 G 5.78 CS 19.01 MS 28.79 FS 11.94 S 2.94 C	7.24	.05 T .10 P	3.73 md 6.50 Q_{75} .10 Q_{25} 3.20 QDa	8.0623 QDg 2.0872 Ln
X-2	3583.4	1724.1	0-31.2	2.08		2.71	29.1	.726	42.06	26.99 G 34.66 CS 32.10 MS 4.99 FS .95 S .31 C	2.53	.00 T .00 P	.717 md 1.00 Q_{75} .39 Q_{25} .305 QDa	2.5641 QDg .9416 Ln
X-3	739.9	331.6	0-06.0	2.23		2.62	37.9	.659	39.72	.52 G 6.70 CS 26.53 MS 22.71 FS 35.42 S 8.12 C	9.61		.174 md .33 Q_{75} .059 Q_{25} .135 QDa	2.2650 QDg .8608 Ln
TH#1	7160.0	3569.8	0-64.6	2.01		2.66	28.2	.744	42.66	.44 G .74 CS 7.76 MS 81.84 FS 7.27 S 1.95 C	2.19	.05 T .40 P	.167 md .21 Q_{75} .125 Q_{25} .042 QDa	1.2961 QDg .2594 Ln
TH#2	7136.0	3470.3	0-62.8	2.06		2.67	34.3	.745	42.69	.59 G 1.30 CS 12.14 MS 79.28 FS 5.46 S 1.23 C	2.02	.05 T .70 P	.176 md .22 Q_{75} .13 Q_{25} .045 QDa	1.3009 QDg .2630 Ln
						S. C. Buoy divers (7/10/72)								
	7341.8	3426.1	0-62.0	2.11		2.67	36.8	.778	43.75	11.14 G 1.78 CS 8.02 MS 71.90 FS 5.80 S 1.36 C	1.99	.05 T .40 P	.213 md .22 Q_{75} .125 Q_{25} .047 QDa	1.3266 QDg .2827 Ln

Site No	Sample Wt. (gm)	Sample Vol. (cc)	Density (Wet) Sample Interval (cm)	Density (Wet) Interval Wet (gm/cm)	Ave Wet	Spec. Grav. (G_s)	Water Content W(%)	Void Ratio (e)	Porosity ϕ(%)	Size Analysis (%)	Coef. of Uniform. (C_u)	Engineering Properties	Grain Size Distribution (mm)	Sorting Coefficient (So)
							S. C. Buoy (7/10/72)							
	7173.3	3352.0	0-80.0			2.67	36.7	.768	42.43					
Top	5869.4	2849.2	80.0-148.0	2.60		2.66	38.1	.568	36.22	.51 G .09 CS 1.26 MS 22.09 FS 48.84 S 27.21 C		.17 T .50 P	.040 md .074 Q_{75} .0045 Q_{25} .035 Q0a	4.0551 QDg 1.4000 Ln
Middle	188.0	125.7	148-151	1.50		2.66	32.6	1.414	58.57	.41 G .40 CS .47 MS 18.32 FS 51.32 S 29.05 C		.25 T .20 P	.035 md .060 Q_{75} .0027 Q_{25} .029 Q0a	4.7140 Q0g 1.5505 Ln
Bottom	9774.4	4525.2	151-259	2.16		2.66	39.4	.760	43.18	.19 G .16 CS .91 MS 22.34 FS 49.82 S 26.58 C		.15 T .60 P	.035 md .073 Q_{75} .0045 Q_{25} .034 Q0a	4.0277 Q0g 1.3932 Ln
T-M					2.08									
M-8					1.78									
T-8					1.83									
							S. C. Buoy (8/28/72)							
	14293.1	7131.4	0-170.2											
Top	2364.2	1244.3	0-29.7	1.90		2.67	36.0	.956	48.87	.53 G 1.29 CS 10.93 MS 82.48 FS 3.90 S .87 C	1.90	.15 T .10 P	.175 md .22 Q_{75} .13 Q_{25} .045 Q0a	1.3009 Q0g .2630 Ln
Middle	3641.0	1906.4	29.7-75.2	1.91		2.67	35.3	.939	48.42	19.82 G 1.76 CS 5.77 MS 53.10 FS 14.59 S 4.96 C	5.50	.05 T .30 P	.833 md .29 Q_{75} .09 Q_{25} .100 Q0a	1.7951 Q0g .5850 Ln
Bottom	7602.8	3980.5	75.2-170.2	1.91		2.67	35.0	.935	48.32	.18 G .15 CS 1.79 MS 23.62 FS 46.57 S 21.29 C		.23 T .75 P	.048 md .09 Q_{75} .0064 Q_{25} .042 Q0a	3.7500 Q0g 1.3218 Ln
T-M					1.90									
M-8					1.91									
T-8					1.90									

APPENDIX A.7 DATA SUMMARY SHEETS — REFLECTION COEFFICIENT MAPPING EXPERIMENT

DATE 6/[illegible]/77 ROLL 0 1

TIME	PINGER CHANNEL AVE	SIGMA	B-LOSS	SPARKER CHANNEL AVE	SIGMA	B-LOSS	WATER DEPTH AVE	SIGMA
18.06.00	.445	.064	7.1	.185	.098	15.6	73.7	1.1
18.07.00	.537	.055	5.5	.408	.150	8.5	84.3	1.1
18.08.00	.565	.078	5.0	.486	.222	7.3	93.0	1.5
18.09.00	.507	.105	4.6	.573	.270	5.7	94.5	.7
18.10.00	.562	.048	4.8	.615	.191	4.6	93.5	.5
18.11.00	.640	.021	3.9	.440	.101	7.4	91.9	.3
18.12.00	.512	.105	4.8	.498	.082	6.2	91.3	.7
18.13.00	.555	.092	5.2	.527	.128	5.9	91.1	.7
18.14.00	.621	.057	4.2	.566	.070	5.0	89.6	.7
18.15.00	.540	.054	4.7	.502	.066	6.1	90.0	.4
18.16.00	.624	.039	4.1	.506	.060	6.0	90.3	.2
18.17.00	.671	.157	3.6	.415	.082	7.6	89.8	.2
18.18.00	.622	.035	4.2	.428	.103	7.6	89.4	.4
18.19.00	.617	.012	4.3	.417	.062	7.7	88.8	.6
18.20.00	.617	.019	4.2	.428	.083	7.5	88.4	.3
18.21.00	.614	.011	4.3	.452	.037	6.9	87.7	.3
18.22.00	.611	.013	4.4	.432	.081	7.4	87.3	.3
18.23.00	.577	.059	4.7	.438	.102	7.4	86.9	.3
18.24.00	.544	.063	5.0	.426	.098	7.7	86.4	.4
18.25.00	.587	.041	4.6	.445	.083	7.2	86.3	.4
18.26.00	.556	.065	5.2	.441	.060	7.2	86.0	.4
18.27.00	.594	.056	4.6	.464	.060	6.8	85.6	.5
18.28.00	.543	.063	5.0	.475	.060	6.5	85.3	.3
18.29.00	.530	.081	5.5	.452	.072	7.0	85.6	.4
18.30.00	.544	.045	5.3	.421	.106	7.9	85.3	.4
18.31.00	.540	.073	5.3	.453	.062	7.0	85.3	.5
18.32.00	.540	.071	5.4	.429	.087	7.5	85.2	.5
18.33.00	.538	.073	5.6	.445	.117	7.4	85.1	.6
18.34.00	.555	.061	5.2	.450	.092	7.1	84.9	.3
18.35.00	.535	.060	5.5	.465	.071	6.8	84.7	.4
18.36.00	.550	.051	5.2	.428	.081	7.5	84.6	.3
18.37.00	.554	.030	5.1	.476	.046	6.5	84.5	.3
18.38.00	.520	.053	5.6	.461	.046	6.8	84.3	.5
18.39.00	.533	.061	5.1	.429	.110	7.7	84.2	.3
18.40.00	.543	.070	4.5	.462	.068	6.8	84.1	.3
18.41.00	.542	.071	5.3	.482	.051	6.4	84.1	.4
18.42.00	.546	.033	5.0	.474	.047	6.5	83.9	.3
18.43.00	.503	.048	5.2	.471	.075	6.7	83.9	.5
18.44.00	.534	.037	5.1	.481	.041	6.4	83.9	.6
18.45.00	.534	.050	5.1	.451	.075	7.1	83.8	.5
18.46.00	.550	.024	5.2	.448	.057	7.0	83.8	.3
18.47.00	.513	.107	6.1	.462	.064	6.8	84.0	.7
18.48.00	.533	.056	5.1	.429	.053	7.4	83.9	.3
18.49.00	.492	.062	6.3	.440	.041	7.2	83.8	.3
18.50.00	.527	.043	5.7	.437	.077	7.3	83.9	.3
18.51.00	.543	.026	5.3	.445	.068	7.1	84.0	.3
18.52.00	.542	.011	5.3	.422	.038	7.5	83.8	.4
18.53.00	.510	.001	6.0	.493	.094	6.3	83.9	.5
18.54.00	.537	.037	5.5	.410	.062	7.8	83.6	.5
18.55.00	.524	.044	5.6	.528	.163	5.8	83.0	.5

DATE 6/2[illegible]

TIME	PINGER CHANNEL			SPARKER CHANNEL			WATER DEPTH	
	AVE	SIGMA	B-LOSS	AVE	SIGMA	B-LOSS	AVE	SIGMA
18.56.00	.519	.054	5.9	.500	.067	6.1	82.7	.2
18.57.00	.519	.020	5.7	.511	.056	5.9	82.3	.5
18.58.00	.527	.017	5.6	.477	.065	6.5	81.7	.4
18.59.00	.49[illegible]	.060	6.1	.432	.037	6.9	81.5	.2
19.00.00	.4[illegible]5	.[illegible]93	6.4	.433	.072	7.4	80.5	1.5
19.01.00	.5[illegible]2	.035	6.0	.462	.054	6.8	80.5	.3
19.02.00	.4[illegible]4	.030	6.3	.461	.059	6.8	80.0	.4
19.03.00	.5[illegible]7	.036	6.1	.506	.068	6.0	79.7	.4
19.04.00	.4[illegible]8	.174	6.5	.411	.143	6.9	77.2	7.4

DATE 06/29/72 ROLL NO 2

TIME	PINGER CHANNEL			SPARKER CHANNEL			WATER DEPTH	
	AVE	SIGMA	B-LOSS	AVE	SIGMA	B-LOSS	AVE	SIGMA
17.16.53	.878	.108	1.2	.530	.286	6.4	102.3	.6
17.17.53	.694	.043	3.2	.798	.342	2.6	101.6	.4
17.18.53	.713	.081	3.0	.997	.715	1.3	101.0	.4
17.19.53	.760	.093	2.8	.841	.641	3.3	100.0	.5
17.20.53	.771	.088	2.3	.572	.180	5.3	99.1	.6
17.21.53	.820	.124	1.8	.574	.259	5.8	98.4	.6
17.22.53	.680	.095	3.4	.531	.203	6.2	97.6	.5
17.23.53	.678	.029	3.4	.541	.182	5.8	96.9	.3

DATE 06/29/72 PILOT 3

TIME	PINGER CHANNEL			SPARKER CHANNEL			WATER DEPTH	
	AVE	SIGMA	B-LOSS	AVE	SIGMA	B-LOSS	AVE	SIGMA
17.52.53	.584	.036	4.7	.511	.068	5.9	88.7	.5
17.53.53	.565	.065	5.0	.453	.114	7.3	88.6	.5
17.54.53	.551	.051	5.2	.518	.039	5.7	88.4	.3
17.55.53	.569	.032	4.9	.503	.038	6.0	88.3	.4
17.56.53	.563	.038	5.0	.475	.059	6.5	88.1	.4
17.57.53	.538	.070	5.5	.479	.086	6.5	87.8	.6
17.58.53	.565	.033	5.0	.455	.089	7.0	87.5	.8
17.59.53	.556	.044	5.1	.470	.075	6.7	87.4	.4
18.00.53	.529	.057	5.6	.446	.083	7.2	87.4	.4
18.01.53	.553	.060	5.2	.484	.066	6.4	86.9	.5
18.02.53	.530	.040	5.5	.472	.044	6.6	86.8	.2
18.03.53	.534	.077	5.5	.501	.067	6.2	86.4	.5
18.04.53	.532	.039	5.5	.483	.086	6.5	86.2	.8
18.05.53	.535	.060	5.5	.488	.065	6.3	85.9	.6
18.06.53	.556	.046	5.1	.481	.061	6.4	85.6	.5
18.07.53	.535	.030	5.4	.463	.126	7.3	85.2	.5
18.08.53	.514	.062	5.8	.520	.100	5.9	84.8	.6
18.09.53	.537	.034	5.4	.457	.113	7.3	84.7	.3

DATE 06/29/[illegible]

TIME	PINGER CHANNEL AVE	PINGER CHANNEL SIGMA	PINGER CHANNEL B-LOSS	SPARKER CHANNEL AVE	SPARKER CHANNEL SIGMA	SPARKER CHANNEL B-LOSS	WATER DEPTH AVE	WATER DEPTH SIGMA
18.44.53	.8[illegible]	.074	1.1	.429	.104	7.9	93.0	.3
18.45.53	.6[illegible]	.232	3.4	.483	.050	6.4	91.6	5.4
18.46.53	.6[illegible]	.141	4.0	.485	.055	6.3	93.2	.3
18.47.53	.8[illegible]	.098	1.6	.437	.048	7.2	93.2	.5
18.48.53	.8[illegible]	.104	1.6	.448	.118	7.6	93.3	.5
18.49.53	.8[illegible]	.120	1.7	.508	.041	5.9	93.5	.3
18.50.53	.784	.167	2.4	.494	.053	6.2	93.7	.4
18.51.53	.758	.228	2.1	.445	.072	7.2	92.5	5.5
18.52.53	.748	.276	2.5	.448	.079	7.1	92.5	5.8
18.53.53	.776	.193	2.6	.458	.067	6.9	94.0	.5
18.54.53	.695	.301	3.4	.510	.147	6.5	93.8	7.5
18.55.53	.758	.227	2.4	.477	.052	6.5	92.6	5.4
18.56.53	.736	.260	2.6	.422	.109	8.0	92.8	5.8
18.57.53	.859	.132	1.4	.468	.051	6.6	94.4	.7
18.58.53	.581	.384	3.1	.499	.068	6.1	89.0	9.6
18.59.53	.616	.334	4.0	.454	.125	7.5	91.3	9.4
19.00.53	.636	.357	3.4	.408	.118	8.4	90.2	9.5
19.01.53	.971	.087	1.2	.445	.160	8.2	94.8	.5
19.02.53	.746	.211	3.0	.524	.059	5.7	94.9	.4
19.03.53	.693	.076	3.2	.518	.102	5.9	95.3	.5

DATE 6/29/72 ROLL NO 7

TIME	PINGER CHANNEL			SPARKER CHANNEL			WATER DEPTH	
	AVE	SIGMA	B-LOSS	AVE	SIGMA	B-LOSS	AVE	SIGMA
17.39.53	.636	.043	3.9	.639	.327	5.1	91.1	.4
17.40.53	.630	.033	4.0	.786	.382	3.3	90.9	.4
17.41.53	.619	.037	4.2	.565	.271	6.0	90.7	.5
17.42.53	.638	.039	3.9	.542	.356	7.3	90.6	.3
17.43.53	.610	.026	4.3	.617	.305	5.5	90.4	.4

DATE 06/29/72 ROLL NO 3

TIME	PINGER CHANNEL			SPARKER CHANNEL			WATER DEPTH	
	AVE	SIGMA	B-LOSS	AVE	SIGMA	B-LOSS	AVE	SIGMA
18.32.53	.573	.023	4.8	.485	.153	5.4	91.3	.3
18.33.53	.581	.045	4.7	.464	.198	4.8	91.9	.4
18.34.57	.565	.007	5.0	.543	.067	5.4	92.2	.6
18.35.53	.556	.161	4.6	.518	.148	4.8	90.6	5.4
18.39.57	.560	.064	5.1	.607	.423	2.7	93.1	.3
18.40.57	.577	.064	4.8	.582	.482	2.3	92.9	.4
18.41.57	.542	.087	5.4	.522	.550	2.5	93.1	.6

DATE 06/[illegible]

TIME	PINGER CHANNEL			SPARKER CHANNEL			WATER DEPTH	
	AVE	SIGMA	B-LOSS	AVE	SIGMA	B-LOSS	AVE	SIGMA
16.23.5[illegible]	.[illegible]21	.139	1.9	.479	.107	6.6	115.4	1.0
16.24.5[illegible]	.[illegible]49	.[illegible]77	3.8	.508	.090	6.0	114.7	5.6
16.25.5[illegible]	.65[illegible]	.[illegible]02	3.1	.640	.098	4.0	113.7	8.1
16.26.5[illegible]	.5[illegible]0	.401	3.7	.579	.091	4.9	109.3	12.1
16.27.5[illegible]	.71[illegible]	.[illegible]99	3.0	.516	.114	6.0	116.3	7.7
16.28.5[illegible]	.6[illegible]1	.[illegible]96	2.5	.524	.096	5.7	116.0	8.4
16.29.5[illegible]	.772	.[illegible]49	2.0	.499	.074	6.1	118.0	6.4

DATE 06/30/72

TIME	PINGER CHANNEL AVE	SIGMA	B-LOSS	SPARKER CHANNEL AVE	SIGMA	B-LOSS	WATER DEPTH AVE	SIGMA
15.34.5?	.65?	.187	3.2	.557	.077	5.2	91.8	6.1
15.35.5?	.724	.069	2.8	.540	.062	3.9	93.6	.4
15.36.5?	.641	.197	3.4	.564	.064	5.0	92.4	5.5
15.37.5?	.527	.369	3.8	.520	.115	5.9	88.3	10.5
15.38.5?	.72?	.066	2.9	.591	.091	4.7	94.4	.4
15.39.5?	.661	.150	3.2	.655	.086	3.7	93.3	5.4
15.40.5?	.74?	.067	2.6	.636	.039	3.9	94.7	.5
15.41.5?	.745	.061	2.6	.550	.110	5.4	95.0	.8
15.42.5?	.6??	.196	2.9	.596	.105	4.6	93.7	5.4
15.43.5?	.7?7	.156	2.3	.673	.098	3.5	95.3	.7
15.44.5?	.7?7	.?09	2.3	.625	.070	4.1	95.6	.5
15.45.5?	.7??	.204	2.6	.566	.094	5.1	94.5	5.4
15.46.5?	.6??	.266	3.0	.573	.096	4.9	93.2	8.0
15.47.5?	.7??	.?01	2.6	.549	.059	5.3	94.9	6.3
15.48.5?	.7??	.225	2.8	.527	.104	5.7	95.3	5.9
15.49.5?	.7??	.215	2.1	.549	.078	5.3	95.7	5.9
15.50.5?	.6??	.255	3.1	.548	.083	5.3	96.1	6.0
15.51.5?	.?11	.056	1.9	.588	.076	4.7	98.0	.5
15.52.5?	.7??	.067	2.0	.564	.093	5.1	99.3	.8
15.53.5?	.6?7	.?91	2.5	.568	.083	5.0	95.7	7.5
15.54.5?	.?1?	.077	1.9	.523	.090	5.7	99.1	.5
15.55.5?	.654	.?12	2.7	.563	.082	5.1	96.7	7.5
15.56.5?	.6??	.?65	2.2	.571	.096	5.0	95.0	10.0
15.57.5?	.?2?	.?90	1.8	.562	.092	5.1	95.0	10.8
15.58.5?	.7??	.244	1.7	.523	.094	5.8	97.9	7.6
15.59.5?	.9??	.?57	.5	.518	.096	5.9	101.0	.4
16.00.5?	.?41	.?51	.5	.512	.077	5.9	101.6	.7
16.01.5?	.?07	.?14	1.1	.540	.116	5.6	100.6	5.5
16.02.5?	.?3?	.?05	.8	.511	.075	5.9	102.9	1.0
16.03.5?	.?47	.?48	1.1	.561	.074	5.1	100.3	7.5
16.04.5?	.7??	.411	1.2	.516	.125	6.0	98.7	10.1
16.05.5?	.7?1	.?47	2.1	.543	.102	5.5	100.5	9.3
16.06.5?	.9??	.?40	1.3	.554	.073	5.2	102.8	6.5
16.07.5?	.?1?	.?60	1.2	.557	.075	5.2	103.9	6.1
16.08.5?	.64?	.?71	2.8	.536	.095	5.5	101.5	9.6
16.09.5?	.7?7	.?27	2.5	.529	.085	5.6	103.3	9.2
16.10.5?	.7?4	.?2?	2.8	.535	.103	5.6	105.5	6.5
16.11.5?	.?2?	.197	1.9	.579	.072	4.8	107.6	.9
16.12.5?	.617	.?5?	3.1	.529	.090	5.7	103.8	8.9
16.13.5?	.?4?	.?71	1.5	.581	.077	4.8	108.7	.7
16.14.5?	.7??	.?44	2.3	.595	.070	4.6	107.8	5.6
16.15.5?	.?1?	.?96	1.4	.592	.075	4.6	110.3	1.0
16.16.5?	.6??	.?2?	2.8	.584	.116	4.8	109.1	9.3
16.17.5?	.7??	.?67	2.0	.568	.063	5.0	106.9	9.7
16.18.5?	.?17	.124	1.9	.644	.091	3.9	111.9	.8
16.19.5?	.7??	.?5?	3.1	.596	.107	4.6	113.9	4.7
16.20.5?	.7??	.17?	3.1	.600	.?57	4.5	113.4	.8
16.21.5?	.7??	.?2?	1.8	.496	.?97	6.3	112.6	5.6
16.22.5?	.?1?	.157	2.0	.517	.079	5.8	114.7	1.1

DATE 07/06/72 [illegible] 6

TIME	PI[illegible] CHANNEL AVE	SIGMA	B-LOSS	SPARKER CHANNEL AVE	SIGMA	B-LOSS	WATER DEPTH AVE	SIGMA
17.52.5[illegible]	.6[illegible]	.10[illegible]	3.3	.635	.077	4.0	100.7	.5
17.53.5[illegible]	.75[illegible]	.[illegible]91	2.5	.548	.08[illegible]	5.3	101.4	.3
17.54.5[illegible]	.7[illegible]	.[illegible]	2.9	.56[illegible]	.076	5.1	101.6	.7
17.55.5[illegible]	.71[illegible]	.057	3.0	.530	.080	5.6	102.1	.4
17.56.5[illegible]	.6[illegible]	.19[illegible]	2.7	.457	.114	7.1	101.2	5.5
17.57.5[illegible]	.6[illegible]	.[illegible]62	3.1	.570	.077	5.0	100.2	8.2
17.58.5[illegible]	.6[illegible]	.19[illegible]	3.0	.471	.091	6.7	101.9	6.3
17.59.5[illegible]	.7[illegible]	.047	2.3	.536	.075	5.5	104.0	.6
18.00.5[illegible]	.6[illegible]	.21[illegible]	3.2	.525	.089	5.7	102.8	5.5
18.01.5[illegible]	.7[illegible]	.030	2.5	.542	.092	5.4	104.6	.4
18.02.5[illegible]	.6[illegible]	.20[illegible]	3.1	.528	.105	5.6	102.0	7.5
18.03.5[illegible]	.5[illegible]	.24[illegible]	3.6	.557	.058	5.1	101.7	8.5
18.04.5[illegible]	.77[illegible]	.03[illegible]	2.3	.555	.066	5.2	105.5	.5
18.05.5[illegible]	.76[illegible]	.046	2.4	.600	.082	4.5	105.5	.4
18.06.5[illegible]	.72[illegible]	.055	2.8	.489	.106	6.4	105.6	.6
18.07.5[illegible]	.81[illegible]	.03[illegible]	1.9	.574	.039	4.8	105.3	.4
18.08.5[illegible]	.71[illegible]	.09[illegible]	2.5	.498	.117	6.3	103.9	5.5
18.09.5[illegible]	.6[illegible]	.27[illegible]	3.3	.557	.117	5.3	102.2	7.9
18.10.5[illegible]	.7[illegible]	.110	3.2	.574	.067	4.9	104.5	.6
18.11.5[illegible]	.76[illegible]	.024	2.8	.547	.106	5.4	103.9	.5
18.12.5[illegible]	.7[illegible]	.05[illegible]	2.5	.641	.088	3.9	104.3	.5
18.13.5[illegible]	.5[illegible]	.20[illegible]	3.6	.531	.108	5.7	102.2	7.7
18.14.5[illegible]	.74[illegible]	.035	2.6	.656	.058	3.7	105.4	.5
18.15.5[illegible]	.9[illegible]	.051	1.2	.554	.122	5.3	106.3	.6
18.16.5[illegible]	.73[illegible]	.07[illegible]	2.7	.628	.063	4.1	106.9	.5
18.17.5[illegible]	.74[illegible]	.05[illegible]	2.5	.553	.071	5.2	107.5	.5
18.18.5[illegible]	.76[illegible]	.086	2.4	.546	.104	5.4	108.0	.4
18.19.5[illegible]	.74[illegible]	.06[illegible]	2.6	.581	.088	4.8	109.7	.4
18.20.5[illegible]	.7[illegible]	.13[illegible]	2.7	.651	.067	3.8	109.2	.6
18.21.5[illegible]	.6[illegible]	.21[illegible]	2.9	.512	.130	6.0	108.8	5.7
18.22.5[illegible]	.74[illegible]	.071	2.6	.651	.078	3.8	110.9	.5
18.23.5[illegible]	.4[illegible]	.33[illegible]	6.1	.555	.428	6.1	107.3	9.9

DATE 07/14/7? ROLL'C 17

TIME	PI?3-? CHANNEL			SPARKER CHANNEL			WATER DEPTH	
	AV?	SIGMA	B-LOSS	AVE	SIGMA	B-LOSS	AVE	SIGMA
14.37.5?	.4?6	.055	8.0	.509	.246	7.4	68.8	.8
14.38.5?	.415	.105	8.0	.476	.236	8.2	69.5	2.2
14.39.5?	.47?	.047	6.6	.590	.150	5.1	68.3	.4
14.40.5?	.424	.067	7.6	.579	.104	4.9	68.0	.8
14.41.5?	.449	.046	7.0	.459	.238	8.5	67.8	1.0
14.42.5?	.42?	.053	7.5	.490	.217	7.7	67.9	.4
14.43.5?	.441	.035	7.1	.560	.133	5.4	67.8	.6
14.44.5?	.3??	.163	8.4	.553	.094	5.3	64.8	7.4
14.45.5?	.419	.043	7.6	.358	.215	10.9	67.1	.5
14.46.5?	.43?	.045	7.3	.507	.220	6.9	67.4	.8
14.47.5?	.?94	.174	8.6	.371	.190	9.8	63.3	8.6
14.48.5?	.423	.047	7.5	.434	.198	8.6	67.8	.5
14.49.5?	.434	.072	7.4	.485	.193	7.1	67.9	.6
14.50.5?	.42?	.050	7.6	.541	.084	5.4	67.9	.7
14.51.5?	.410	.072	7.9	.313	.180	11.8	67.5	.8
14.52.5?	.411	.056	7.8	.560	.191	5.9	67.7	.5
14.53.5?	.46?	.098	6.9	.359	.197	10.5	67.9	.7
14.54.5?	.429	.044	7.4	.377	.206	10.0	68.7	.6
14.55.5?	.451	.018	6.9	.488	.166	7.0	69.3	1.0
14.56.5?	.425	.059	7.5	.468	.117	7.0	69.8	1.4
14.57.5?	.449	.047	7.0	.467	.107	6.8	69.6	1.1
14.58.5?	.439	.055	7.2	.519	.128	6.1	69.6	1.2
14.59.5?	.431	.075	7.5	.547	.149	5.8	70.0	.7
15.00.5?	.455	.040	6.9	.456	.157	7.5	70.5	.7
15.01.5?	.446	.044	7.0	.513	.143	6.3	70.8	.8
15.02.5?	.456	.039	6.8	.517	.200	6.6	70.9	1.2
15.03.5?	.417	.053	7.7	.454	.102	7.1	71.0	.7
15.04.5?	.432	.001	7.4	.520	.178	6.6	71.0	.7
15.05.5?	.453	.048	6.9	.616	.081	4.3	71.5	.6
15.06.5?	.425	.060	7.5	.444	.133	7.5	71.7	.6
15.07.5?	.449	.079	7.1	.524	.146	6.1	72.1	.7
15.08.5?	.437	.049	7.2	.527	.097	5.7	72.2	.5
15.09.5?	.443	.064	7.2	.482	.124	6.7	72.7	.9
15.10.5?	.430	.034	7.5	.508	.137	6.3	72.7	.5
15.11.5?	.411	.064	7.8	.581	.083	4.8	72.6	.5
15.12.5?	.454	.039	6.9	.546	.084	5.4	73.0	.5
15.13.5?	.3?4	.135	9.1	.562	.123	5.3	71.9	5.5
15.14.5?	.293	.176	9.7	.483	.211	7.5	70.8	8.0
15.15.5?	.355	.141	9.9	.520	.102	5.8	74.1	1.3
15.16.5?	.459	.024	6.8	.511	.108	6.1	73.9	.7
15.17.5?	.466	.020	6.6	.507	.109	6.1	73.9	.7
15.18.5?	.442	.050	7.1	.602	.174	4.9	74.1	.7
15.19.5?	.457	.029	6.8	.510	.151	6.3	74.2	1.0
15.20.5?	.48?	.056	7.2	.548	.154	5.5	75.1	.8
15.21.5?	.47?	.022	6.4	.500	.083	6.1	74.2	.8
15.22.5?	.339	.163	8.7	.508	.092	6.0	71.6	7.4
15.23.5?	.46?	.033	6.6	.572	.084	4.9	74.4	.5
15.24.5?	.449	.065	7.1	.493	.172	6.9	74.2	.9
15.25.5?	.471	.030	6.5	.540	.162	6.0	74.0	.4
15.26.5?	.456	.044	7.3	.537	.058	5.5	74.0	.6

DATE 07/06/72 ROLL NO 6

TIME	PINGER CHANNEL			SPARKER CHANNEL			WATER DEPTH	
	AVE	SIGMA	B-LOSS	AVE	SIGMA	B-LOSS	AVE	SIGMA
16.57.53	.785	.056	2.1	.590	.081	4.7	113.5	.4
16.58.53	.755	.048	2.5	.525	.175	4.8	112.6	.6
16.59.53	.783	.043	2.1	.540	.117	5.6	111.9	.6
17.00.53	.760	.061	2.4	.592	.065	4.6	111.3	.5
17.01.53	.761	.054	2.2	.545	.086	5.4	110.5	.3
17.02.53	.743	.047	2.6	.502	.238	4.3	109.6	.4
17.03.53	.751	.077	2.5	.523	.101	5.8	108.7	.4
17.04.53	.738	.021	2.6	.561	.081	5.1	108.5	.4
17.05.53	.762	.060	2.4	.593	.108	4.7	108.1	.5
17.06.53	.727	.040	2.8	.527	.088	5.7	107.3	.3
17.07.53	.738	.043	2.7	.577	.102	4.9	106.7	.3
17.08.53	.726	.038	2.8	.495	.110	6.3	106.4	.7
17.09.53	.732	.037	2.7	.604	.176	4.7	105.7	.5
17.10.53	.412	.400	3.8	.548	.112	5.4	95.5	10.4
17.13.53	.751	.037	2.5	.535	.078	5.5	103.2	.4
17.14.53	.740	.037	2.6	.541	.119	5.6	102.6	.5
17.15.53	.766	.052	2.3	.564	.103	5.2	102.0	.3
17.16.53	.735	.053	2.7	.537	.114	5.6	101.5	.3
17.17.53	.794	.093	2.1	.556	.114	5.3	100.8	.5
17.18.53	.753	.041	2.5	.570	.128	5.1	100.4	.5
17.19.53	.747	.023	2.5	.586	.087	4.7	100.1	.4
17.20.53	.731	.047	2.7	.557	.126	5.3	99.5	.4
17.21.53	.746	.040	2.6	.552	.118	5.4	98.9	.2
17.22.53	.734	.038	2.7	.559	.128	5.3	98.4	.2
17.23.53	.727	.027	2.8	.564	.080	5.1	98.3	.5
17.24.53	.728	.063	2.8	.571	.116	5.1	98.0	.3
17.25.53	.743	.030	2.6	.617	.073	4.3	98.1	.7
17.26.53	.744	.040	2.6	.562	.106	5.2	99.6	.3
17.27.53	.737	.056	2.7	.551	.099	5.3	100.0	.4
17.28.53	.720	.027	2.9	.499	.111	6.3	99.7	.6
17.29.53	.722	.024	2.8	.537	.091	5.5	99.6	.4
17.30.53	.678	.066	3.4	.506	.092	6.1	99.4	.4
17.31.53	.723	.048	2.8	.484	.067	6.4	99.6	.3
17.32.53	.696	.071	3.2	.540	.082	5.5	99.4	.5
17.33.53	.698	.048	3.1	.504	.105	6.1	99.0	.4
17.34.53	.696	.050	3.2	.538	.069	5.5	98.7	.2
17.35.53	.693	.037	3.2	.517	.084	5.8	98.4	.2
17.36.53	.667	.072	3.6	.542	.079	5.4	97.9	.2
17.37.53	.711	.039	3.0	.548	.066	5.3	97.8	.3
17.38.53	.704	.051	3.1	.603	.078	4.5	97.7	.5
17.39.53	.673	.047	3.5	.531	.057	5.5	97.4	.6

DATE 07/14/72 ROLL 10 17

TIME	PINGER CHANNEL			SPARKER CHANNEL			WATER DEPTH	
	AVE	SIGMA	B-LOSS	AVE	SIGMA	B-LOSS	AVE	SIGMA
15.27.5?	.442	.035	6.7	.556	.070	5.2	73.7	.7
15.28.5?	.450	.028	7.0	.481	.121	6.7	73.4	.6
15.29.5?	.449	.029	6.7	.454	.086	7.0	73.5	.4
15.30.5?	.457	.026	6.8	.544	.099	5.4	73.2	.6
15.31.5?	.441	.075	7.2	.472	.119	6.8	73.1	.8
15.32.5?	.472	.029	6.5	.560	.075	5.1	72.4	.4
15.33.5?	.434	.058	6.9	.481	.164	7.3	72.3	.8
15.34.5?	.450	.048	6.9	.634	.084	4.0	72.3	.7
15.35.5?	.476	.119	6.9	.495	.139	6.5	70.4	4.1
15.36.5?	.443	.159	7.6	.462	.160	7.0	71.4	.9

DATE 07/14/72 ROLL NO 18

TIME	PINGER CHANNEL			SPARKER CHANNEL			WATER DEPTH	
	AVE	SIGMA	B-LOSS	AVE	SIGMA	B-LOSS	AVE	SIGMA
17.41.5?	.46?	.101	6.8	.651	.182	4.1	83.7	.9
17.42.5?	.451	.074	6.5	.459	.083	6.9	84.0	1.3
17.43.5?	.464	.055	6.4	.398	.083	8.2	81.9	.7
17.44.5?	.467	.108	6.9	.499	.105	6.3	81.9	.7
17.45.5?	.461	.071	6.5	.494	.085	6.3	80.8	.9
17.46.5?	.472	.059	6.6	.445	.103	7.3	79.7	.7
17.47.5?	.427	.093	7.7	.408	.142	6.9	78.5	2.7
17.48.5?	.431	.079	7.5	.403	.072	8.0	79.3	.6
17.49.5?	.494	.031	6.1	.474	.086	6.6	78.9	1.4
17.50.5?	.417	.089	8.0	.476	.088	6.6	79.0	.8
17.51.5?	.434	.111	7.7	.543	.062	5.4	78.3	3.0
17.52.5?	.462	.144	7.5	.496	.112	6.3	76.6	4.3
17.53.5?	.479	.020	6.4	.415	.056	7.7	78.3	.8
17.54.5?	.462	.058	7.4	.462	.067	6.8	79.6	.5
17.55.5?	.429	.105	7.8	.486	.102	6.5	78.3	1.5
17.56.5?	.446	.027	6.3	.471	.080	6.7	79.8	1.0
17.57.5?	.479	.059	6.5	.445	.064	7.1	79.1	.9

DATE 07/14/7[illegible]

TIME	PI[illegible] CHANNEL AVE	SIGMA	B-LOSS	SPARKER CHANNEL AVE	SIGMA	B-LOSS	WATER DEPTH AVE	SIGMA
16.29.5[illegible]	.3[illegible]	.11[illegible]	7.9	.327	.201	11.0	68.7	2.0
16.30.5[illegible]	.3[illegible]	.10[illegible]	8.7	.489	.258	7.6	67.0	7.9
16.31.5[illegible]	.3[illegible]	.1[illegible]1	9.9	.578	.186	5.3	69.6	6.6
16.32.5[illegible]	.4[illegible]	.[illegible]	7.5	.396	.209	9.7	73.9	.8
16.33.5[illegible]	.3[illegible]	.[illegible]	7.0	.425	.124	8.0	67.0	10.2
16.34.5[illegible]	.4[illegible]	.[illegible]	7.3	.422	.170	8.4	73.3	7.7
16.35.5[illegible]	.4[illegible]	.1[illegible]	6.8	.450	.096	7.1	73.5	5.9
16.36.5[illegible]	.3[illegible]	.1[illegible]	7.7	.458	.068	6.9	71.3	7.6
16.37.5[illegible]	.4[illegible]	.1[illegible]	7.8	.479	.120	6.8	74.2	1.6
16.38.5[illegible]	.4[illegible]	.0[illegible]	6.8	.439	.074	7.4	74.5	1.3
16.39.5[illegible]	.3[illegible]	.1[illegible]	8.4	.410	.164	8.6	71.8	7.4
16.40.5[illegible]	.3[illegible]	.1[illegible]	6.7	.404	.119	8.2	70.4	10.0
16.41.5[illegible]	.4[illegible]	.1[illegible]	7.0	.414	.102	8.6	74.0	6.8
16.42.5[illegible]	.3[illegible]	.1[illegible]	7.7	.445	.109	7.4	74.6	6.1
16.43.5[illegible]	.3[illegible]	.1[illegible]	6.6	.437	.070	7.3	72.8	7.8

DATE 07/14/7? ?ILOT 12

TIME	PINGER CHANNEL			SPARKER CHANNEL			WATER DEPTH	
	AVE	SIGMA	B-LOSS	AVE	SIGMA	B-LOSS	AVE	SIGMA
18.09.5?	.4??	.1??	7.1	.519	.080	5.8	76.3	1.1
18.10.5?	.4??	.??6	6.3	.53?	.107	5.6	75.7	.6
18.11.5?	.47?	.??5	6.6	.520	.109	5.9	76.1	.7
18.12.5?	.4??	.???	6.4	.528	.106	5.7	75.7	.7
18.13.5?	.47?	.074	6.6	.551	.118	5.4	75.8	.7
18.14.5?	.474	.??1	6.6	.583	.050	4.7	75.4	.7
18.15.5?	.4??	.???	7.0	.488	.075	6.3	74.8	.8
18.16.5?	.4??	.??7	6.9	.468	.097	6.8	74.3	.5
18.17.5?	.4??	.???	6.3	.463	.094	6.9	73.9	.5
18.18.5?	.47?	.07?	7.4	.494	.083	6.2	74.2	.8
18.19.5?	.4??	.???	6.7	.467	.062	6.7	73.6	.8

DATE 07/ [illegible]

TIME	PI [illegible] CHANNEL AVE	SIGMA	N-LOSS	SPARKER CHANNEL AVE	SIGMA	N-LOSS	WATER DEPTH AVE	SIGMA
15.18.5?	.4[illegible]	.1[illegible]	8.3	.473	.072	6.6	75.0	.4
15.19.5?	.47[illegible]	.0[illegible]	6.6	.460	.054	6.8	75.3	.7
15.20.5?	.447	.077	7.1	.472	.031	6.5	75.1	1.1
15.21.5?	.4[illegible]	.045	6.9	.501	.087	6.1	75.6	.5
15.22.5?	.4[illegible]	.05[illegible]	7.1	.467	.077	6.7	76.0	.6
15.23.5?	.4[illegible]	.05[illegible]	7.5	.485	.053	6.3	76.3	.8
15.24.5?	.41[illegible]	.073	7.8	.519	.079	5.8	76.0	.4
15.25.5?	.4[illegible]	.[illegible]	7.2	.481	.045	6.4	76.8	.8
15.26.5?	.4[illegible]	.121	6.4	.471	.057	6.6	76.2	1.4
15.27.5?	.4[illegible]	.071	7.3	.479	.055	6.4	76.4	1.2
15.28.5?	.4[illegible]	.0[illegible]	7.2	.485	.038	6.3	76.9	.7
15.29.5?	.4[illegible]	.07[illegible]	7.0	.449	.069	7.1	77.1	.5
15.30.5?	.4[illegible]	.1[illegible]	6.9	.503	.060	6.0	77.2	.8
15.31.5?	.4[illegible]	.087	6.9	.459	.048	6.8	77.6	.7
15.32.5?	.4[illegible]	.0[illegible]	7.0	.496	.070	6.2	77.2	.8
15.33.5?	.4[illegible]	.0[illegible]	7.2	.498	.067	6.1	77.5	.5
15.34.5?	.41[illegible]	.07[illegible]	7.8	.496	.076	6.2	77.7	.5
15.35.5?	.4[illegible]	.143	8.5	.478	.079	6.5	74.9	7.2
15.36.5?	.44[illegible]	.0[illegible]	7.2	.547	.047	5.3	78.0	.4
15.37.5?	.4[illegible]	.087	7.6	.478	.064	6.5	78.1	1.0
15.38.5?	.43[illegible]	.1[illegible]	7.7	.499	.051	6.1	77.9	2.1
15.39.5?	.3[illegible]	.15[illegible]	9.1	.515	.054	5.8	77.5	2.8
15.40.5?	.4[illegible]	.14[illegible]	8.5	.483	.041	6.3	78.2	.6
15.41.5?	.4[illegible]	.0[illegible]	6.2	.509	.050	5.9	78.4	.6
15.42.5?	.4[illegible]	.114	7.8	.559	.074	5.1	78.2	.9
15.43.5?	.4[illegible]	.1[illegible]	7.2	.473	.052	6.6	78.5	.6
15.44.5?	.4[illegible]	.0[illegible]	6.7	.556	.067	5.2	78.5	.4
15.45.5?	.41[illegible]	.141	8.2	.494	.090	6.2	78.1	1.4
15.46.5?	.47[illegible]	.07[illegible]	6.6	.584	.121	4.8	79.0	.5
15.47.5?	.4[illegible]	.077	7.0	.492	.072	6.2	78.5	.8
15.48.5?	.5[illegible]	.0[illegible]	6.0	.559	.124	5.3	78.9	.4
15.49.5?	.4[illegible]	.147	8.3	.532	.085	5.6	77.9	1.7
15.50.5?	.47[illegible]	.0[illegible]	6.5	.493	.084	6.3	78.6	.4
15.51.5?	.5[illegible]	.0[illegible]	6.0	.519	.120	6.0	77.9	.7
15.52.5?	.4[illegible]	.0[illegible]	6.3	.507	.056	5.9	78.0	.3
15.55.5?	.44[illegible]	.0[illegible]	7.3	.597	.823	-.2	76.3	3.2
15.55.5?	.4[illegible]	.0[illegible]	7.2	.497	.057	6.1	76.3	3.2
15.56.5?	.47[illegible]	.0[illegible]	6.5	.502	.066	6.1	76.9	.3
15.58.5?	.4[illegible]	.0[illegible]	7.7	.635	.967	-.1	76.5	.7
15.59.5?	.4[illegible]	.1[illegible]	7.9	.773	.820	-.2	75.9	1.5
16.00.5?	.4[illegible]	.0[illegible]	6.9	.207	.586	-.4	75.8	.7
16.01.5?	.4[illegible]	.0[illegible]	7.0	.140	.214	2.6	75.8	.7

DATE 07/26/72 [illegible] 27

TIME	PINGER CHANNEL AVE	SIGMA	B-LOSS	SPARKER CHANNEL AVE	SIGMA	B-LOSS	WATER DEPTH AVE	SIGMA
16.07.53	.374	.127	8.3	.545	.109	5.4	75.9	6.1
16.08.53	.447	.096	7.4	.610	.090	4.4	76.9	.9
16.09.53	.274	.114	10.6	.444	.077	7.2	76.2	5.8
16.10.53	.414	.083	8.1	.533	.076	5.5	77.2	1.2
16.11.53	.345	.107	8.0	.465	.056	6.7	74.6	7.5
16.12.53	.418	.125	7.1	.539	.100	5.5	76.1	6.2
16.13.53	.345	.197	7.1	.567	.141	5.2	72.5	9.9
16.15.53	.365	.174	7.5	.685	.636	.4	74.8	9.5
16.17.53	.469	.181	6.7	.167	.209	4.5	75.5	8.8
16.19.53	.462	.069	6.8	.053	.111	2.3	79.4	.6
16.21.53	.442	.024	6.2	.470	.423	3.9	79.9	.9
16.22.53	.395	.135	7.5	.310	.575	.8	78.7	5.5
16.24.53	.513	.085	5.8	.097	.302	.6	80.0	.6
16.27.53	.424	.177	6.1	.470	.742	-.0	77.1	7.4
16.26.53	.490	.042	6.2	.058	.020	25.1	79.9	.6
16.27.53	.424	.175	6.1	.086	.029	21.7	76.9	7.5
16.28.53	.427	.124	6.5	.101	.158	23.1	77.9	6.1
16.30.53	.426	.139	7.8	.426	.103	7.9	77.6	5.7
16.31.53	.434	.092	7.5	.448	.154	7.9	79.3	.6
16.32.53	.387	.141	6.8	.456	.134	7.5	75.3	8.9
16.33.53	.417	.105	8.2	.457	.111	7.2	79.4	.6
16.34.53	.363	.163	8.6	.208	.166	16.0	74.9	7.5
16.35.53	.395	.134	7.5	.125	.028	18.3	78.0	6.1
16.36.53	.421	.072	7.6	.490	.057	6.3	79.5	1.6
16.37.53	.411	.091	8.0	.452	.057	7.0	79.9	.7
16.38.53	.408	.127	7.2	.134	.094	18.8	78.2	5.4
16.39.53	.350	.170	7.8	.372	.157	9.8	74.6	8.0
16.40.53	.416	.117	6.1	.478	.061	6.5	79.4	.5
16.41.53	.425	.102	7.8	.448	.124	7.5	79.0	2.2
16.42.53	.381	.200	6.3	.480	.071	6.5	75.1	8.9
16.43.53	.443	.070	7.2	.466	.122	7.2	79.3	.8
16.44.53	.385	.141	7.7	.466	.179	7.7	78.1	5.5
16.45.53	.391	.139	7.7	.408	.129	8.5	77.7	5.8

DATE 07/31/72 FILE 6 21

TIME	PINGER CHANNEL			SPARKER CHANNEL			WATER DEPTH	
	AVE	SIGMA	B-LOSS	AVE	SIGMA	B-LOSS	AVE	SIGMA
16.14.53	.439	.081	7.3	.617	1.075	-1.4	79.8	.5
16.16.53	.495	.053	6.1	.838	1.419	-.9	79.7	.5
16.14.53	.448	.081	7.1	.514	.048	5.8	79.8	.4
16.15.53	.507	.106	6.1	.533	.085	5.6	79.8	1.0
16.16.53	.511	.050	6.0	.567	.075	5.0	79.7	.5
16.17.53	.467	.073	6.4	.558	.060	5.1	79.9	.8
16.18.53	.431	.112	7.9	.540	.070	5.4	79.7	1.5
16.19.53	.481	.055	6.2	.552	.087	5.3	80.0	.6
16.20.53	.526	.106	5.0	.591	.088	4.7	79.8	1.0
16.21.53	.462	.069	6.9	.559	.066	5.1	80.0	.8
16.22.53	.462	.050	6.6	.545	.068	5.3	80.0	.7
16.23.53	.468	.074	6.4	.545	.031	5.3	80.0	.4
16.24.53	.469	.066	6.4	.544	.045	5.3	79.7	.4
16.25.53	.479	.061	6.5	.515	.034	5.8	79.7	.9

DATE 07/21/73 [illegible]

TIME	PINGER CHANNEL AVE	SIGMA	B-LOSS	SPARKER CHANNEL AVE	SIGMA	B-LOSS	WATER DEPTH AVE	SIGMA
15.23.53	[illegible]	.040	4.7	.531	.061	5.6	88.0	.7
15.24.53	.571	.066	4.9	.575	.029	4.8	87.6	.8
15.25.53	.566	.062	4.6	.499	.068	0.1	87.3	.8
15.26.53	.592	.100	5.8	.661	.060	3.6	87.6	.8
15.27.53	.[illegible]	.070	6.4	.644	.076	3.9	86.1	.5
15.28.53	.[illegible]	.055	5.9	.670	.055	3.5	85.1	.5
15.29.53	.[illegible]	.079	6.1	.647	.083	3.8	84.0	.6
15.30.53	.[illegible]	.075	5.7	.519	.054	5.7	82.3	.5
15.31.53	.[illegible]	.064	6.2	.545	.066	5.3	82.7	.9
15.32.53	.[illegible]	.086	6.4	.661	.074	3.6	82.5	.6
15.33.53	.[illegible]	.075	6.1	.711	.073	3.0	82.1	.8
15.34.53	.[illegible]	.065	5.7	.715	.061	2.9	82.0	.8
15.35.53	.[illegible]	.031	5.1	.620	.079	4.1	82.3	.4
15.36.53	.[illegible]	.041	5.1	.629	.076	4.1	83.0	.4
15.37.53	.[illegible]	.036	6.6	.545	.240	6.2	83.0	.8
15.38.53	.[illegible]	.079	6.5	.641	.182	4.2	82.6	.9
15.39.53	.[illegible]	.091	6.4	.659	.230	4.2	82.3	1.0
15.40.53	.[illegible]	.091	6.7	.534	.231	6.3	82.8	.9
15.41.53	.[illegible]	.064	5.8	.597	.108	4.6	83.1	.4
15.42.53	.[illegible]	.061	5.7	.573	.084	4.9	83.0	.6
15.43.53	.[illegible]	.063	6.9	.663	.099	3.7	82.7	.9
15.44.53	.[illegible]	.081	7.1	.645	.069	3.9	81.8	.7
15.45.53	.[illegible]	.032	5.4	.606	.081	4.4	80.9	.7
15.46.53	.[illegible]	.064	6.7	.564	.072	5.0	80.7	.6
15.47.53	.[illegible]	.067	6.5	.595	.076	4.6	80.5	.8
15.48.53	.[illegible]	.053	6.1	.571	.066	4.9	80.9	.3
15.49.53	.[illegible]	.080	6.5	.548	.080	5.3	81.0	.4
15.50.53	.[illegible]	.139	8.0	.558	.143	5.3	80.6	.9
15.51.53	.[illegible]	.067	6.9	.533	.064	5.5	79.9	.9
15.52.53	.467	.069	6.7	.562	.091	5.1	80.1	.8
15.53.53	.497	.062	6.1	.523	.061	5.7	79.7	.7
15.54.53	.491	.087	6.5	.566	.082	5.0	79.6	.8
15.55.53	.447	.096	7.2	.541	.046	5.4	78.8	2.8
15.56.53	.[illegible]	.143	8.6	.578	.048	4.8	77.9	3.3
15.57.53	.453	.067	7.0	.611	.049	4.3	79.2	.6
15.58.53	.478	.050	6.5	.560	.065	5.1	79.2	.7
15.59.53	.[illegible]	.061	6.7	.569	.055	4.9	78.8	.3
16.00.53	.477	.054	6.5	.551	.041	5.2	78.7	.4
16.01.53	.461	.071	6.8	.505	.068	6.0	78.5	.5
16.02.53	.429	.085	7.6	.517	.063	5.8	78.5	.5
16.03.53	.469	.067	6.7	.534	.044	5.5	79.1	.4
16.04.53	.461	.054	6.8	.528	.082	5.6	79.1	.6
16.05.53	.463	.059	6.8	.526	.054	5.6	79.2	.7
16.06.53	.466	.071	6.7	.536	.062	5.5	79.3	.4
16.07.53	.479	.055	6.5	.570	.073	5.0	79.7	.5
16.08.53	.443	.108	6.9	.531	.055	5.5	79.7	.5
16.09.53	.474	.074	6.6	.551	.043	5.2	79.6	.3
16.10.53	.454	.054	6.9	.542	.069	5.4	79.5	.8
16.11.53	.460	.084	6.9	.490	.039	6.2	79.8	.5
16.13.53	.393	.166	9.5	.056	.147	1.0	74.5	9.0

DATE 07/21/72 ROLL NO 22

TIME	PINGER CHANNEL			SPARKER CHANNEL			WATER DEPTH	
	AVE	SIGMA	B-LOSS	AVE	SIGMA	B-LOSS	AVE	SIGMA
16.56.53	.361	.057	9.0	.613	.251	4.8	77.8	.5
16.57.53	.350	.093	9.5	.472	.127	6.8	77.0	5.0
16.58.53	.346	.095	9.6	.494	.121	6.4	78.3	1.4
16.59.53	.323	.122	9.3	.514	.099	5.9	77.2	5.7
17.00.53	.350	.101	9.4	.525	.099	5.7	78.4	2.3
17.01.53	.397	.053	8.1	.558	.162	5.4	79.2	.6
17.02.53	.370	.060	8.5	.468	.132	6.9	79.4	.4
17.03.53	.334	.072	9.7	.572	.201	5.3	79.9	.6
17.04.53	.347	.064	9.5	.574	.140	5.1	80.3	.8
17.05.53	.367	.069	9.0	.542	.143	5.6	80.8	.6
17.06.53	.334	.069	9.7	.509	.160	6.2	80.6	.5
17.07.53	.318	.131	11.2	.515	.170	6.2	77.1	7.9
17.08.53	.371	.071	8.8	.500	.103	6.2	81.1	.5
17.09.53	.379	.055	8.5	.574	.200	5.2	81.0	.7
17.10.53	.380	.057	8.5	.656	.232	4.1	81.4	.5
17.11.53	.340	.055	8.3	.529	.140	5.8	81.5	.6
17.12.53	.355	.076	9.3	.700	.249	3.7	81.2	1.3
17.13.53	.350	.047	8.5	.642	.186	4.2	81.4	.6
17.14.53	.351	.062	9.2	.560	.135	5.3	81.3	.4
17.15.53	.363	.060	9.0	.557	.151	5.4	81.2	.8
17.16.53	.334	.055	9.9	.493	.100	6.3	81.2	.7
17.17.53	.350	.075	9.3	.556	.123	5.3	81.3	.6
17.18.53	.332	.084	9.9	.541	.142	5.7	80.7	2.7
17.19.53	.349	.073	9.3	.531	.129	5.7	81.3	.5
17.20.53	.340	.086	9.7	.662	.134	3.8	81.3	.5
17.21.53	.318	.085	10.3	.518	.087	5.8	81.3	.9
17.22.53	.344	.076	9.5	.613	.175	4.6	81.4	.5
17.23.53	.322	.067	10.0	.557	.092	5.2	81.4	.6
17.24.53	.323	.075	10.0	.566	.159	5.3	81.6	.5
17.25.53	.294	.081	11.0	.551	.117	5.4	80.6	3.3
17.26.53	.322	.082	10.1	.612	.119	4.4	81.7	.6
17.27.53	.367	.091	9.1	.604	.110	4.5	82.3	2.6
17.28.53	.343	.080	9.5	.533	.125	5.7	81.2	.3
17.29.53	.335	.078	9.8	.593	.103	4.7	81.8	.8
17.30.53	.340	.059	9.3	.566	.106	5.1	81.7	.6
17.31.53	.338	.100	9.8	.580	.122	4.9	80.7	5.4
17.32.53	.361	.092	9.1	.597	.082	4.6	82.2	.7
17.33.53	.339	.076	9.6	.595	.124	4.7	82.0	.5
17.34.53	.353	.082	9.3	.472	.083	6.7	82.0	.7
17.35.53	.348	.102	9.6	.559	.093	5.2	81.5	1.4
17.36.53	.366	.060	8.9	.473	.115	6.7	81.7	.7
17.37.53	.361	.080	9.1	.523	.070	5.7	81.2	2.7
17.38.53	.353	.072	9.2	.556	.127	5.3	82.2	.7
17.39.53	.369	.087	8.9	.551	.144	5.5	82.1	.7
17.40.53	.379	.054	8.5	.527	.128	5.8	82.3	.5
17.41.53	.356	.060	9.2	.561	.170	5.4	82.3	.5
17.42.53	.367	.065	8.9	.472	.101	6.7	82.1	.8
17.43.53	.367	.082	9.0	.503	.085	6.1	82.5	.4
17.44.53	.359	.075	9.1	.543	.095	5.4	83.0	.4
17.45.53	.365	.078	9.0	.582	.107	4.8	83.2	.9

DATE 07/21/72 ROLL 0 22

TIME	PINGER CHANNEL			SPARKER CHANNEL			WATER DEPTH	
	AVE	SIGMA	B-LOSS	AVE	SIGMA	B-LOSS	AVE	SIGMA
17.46.53	.387	.060	8.4	.581	.153	5.1	83.5	.6
17.47.53	.354	.094	9.4	.563	.140	5.2	83.4	1.9
17.48.53	.353	.097	9.4	.508	.121	6.2	83.4	1.9
17.49.53	.382	.071	8.5	.649	.062	3.8	84.0	.6
17.50.53	.422	.086	7.8	.591	.125	4.8	83.4	3.2
17.51.53	.448	.052	7.0	.590	.136	4.8	84.4	.4
17.52.53	.415	.083	7.8	.628	.075	4.1	84.6	.5
17.53.53	.363	.094	9.1	.541	.116	5.5	84.2	3.9
17.54.53	.446	.054	7.2	.606	.066	4.4	85.9	.8
17.55.53	.409	.109	8.2	.608	.157	4.6	84.2	4.9
17.56.53	.410	.082	7.9	.578	.140	5.0	85.2	.7
17.57.53	.424	.114	7.8	.603	.117	4.5	83.9	3.1
17.58.53	.412	.135	7.2	.540	.122	5.5	83.5	5.6
17.59.53	.424	.101	7.7	.608	.139	4.5	86.8	.7
18.00.53	.440	.110	7.4	.491	.078	6.3	87.7	.9
18.01.53	.409	.104	8.1	.607	.219	4.9	88.6	.8
18.02.53	.381	.089	8.6	.776	.261	2.8	89.8	1.1
18.03.53	.359	.089	11.2	.563	.205	5.5	87.5	4.5
18.04.53	.392	.096	8.4	.633	.403	5.6	85.0	1.0
18.05.53	.351	.085	9.1	.576	.196	5.3	82.3	.8
18.06.53	.368	.093	9.0	.580	.115	4.9	86.1	2.6
18.07.53	.312	.104	10.7	.433	.134	7.6	81.1	1.2
18.08.53	.373	.121	7.8	.538	.100	5.5	84.0	6.6
18.09.53	.418	.070	7.7	.494	.114	6.3	84.9	.7
18.10.53	.344	.119	9.9	.597	.173	4.9	84.3	4.3
18.11.53	.356	.097	9.3	.660	.169	3.9	87.3	.7
18.12.53	.367	.081	8.9	.786	.217	2.6	87.9	.8
18.13.53	.397	.061	8.1	.478	.175	6.9	88.3	.7
18.14.53	.396	.070	8.2	.573	.107	5.0	89.9	1.1
18.15.53	.378	.097	8.7	.635	.162	4.2	90.7	.7
18.16.53	.423	.049	7.9	.494	.110	6.4	90.9	3.9
18.17.53	.391	.092	8.4	.636	.186	4.4	92.3	1.0
18.18.53	.444	.065	7.2	.639	.141	4.1	92.1	.6
18.19.53	.442	.057	7.2	.518	.164	6.2	92.7	.4

DATE 07/21/72 ROLL NO 23

TIME	PINGER CHANNEL			SPARKER CHANNEL			WATER DEPTH	
	AVE	SIGMA	B-LOSS	AVE	SIGMA	B-LOSS	AVE	SIGMA
19.03.53	.532	.095	5.6	.652	.153	3.9	108.1	.8
19.04.53	.535	.074	4.7	.620	.098	4.3	107.4	.8
19.05.53	.560	.098	5.2	.597	.167	4.8	107.1	.7
19.06.53	.537	.122	5.6	.683	.178	3.6	106.6	.4
19.07.53	.569	.036	4.7	.682	.229	3.7	106.7	.8
19.08.53	.567	.094	5.1	.676	.108	3.5	106.0	1.1
19.09.53	.623	.061	4.1	.639	.158	4.2	105.1	.8
19.10.53	.570	.073	4.8	.626	.145	4.3	104.0	.4
19.11.53	.519	.094	5.8	.711	.203	3.3	103.8	.7
19.12.53	.529	.146	6.0	.614	.160	4.5	102.4	1.5
19.13.53	.514	.079	5.4	.582	.140	5.0	102.4	.7
19.16.53	.556	.105	5.3	.602	.236	5.8	101.6	.5
19.17.53	.506	.087	5.1	.671	.197	4.3	99.7	.9
19.18.53	.520	.128	6.0	.569	.331	6.9	98.5	.8
19.19.53	.531	.114	5.7	.598	.074	4.5	95.3	.8
19.20.53	.556	.069	5.0	.424	.202	8.7	94.4	.5
19.21.53	.349	.119	9.7	.295	.252	13.6	85.4	2.7
19.22.53	.356	.122	9.2	.528	.280	7.1	90.7	1.0
19.23.53	.446	.059	7.1	.297	.168	11.9	78.5	.8
19.24.53	.360	.170	10.2	.281	.242	13.8	81.3	2.3
19.25.53	.389	.139	8.8	.177	.101	16.4	86.7	.9
19.26.53	.548	.079	5.3	.518	.453	7.5	93.7	.7
19.27.53	.570	.080	5.0	1.038	.540	2.3	96.8	.8
19.28.53	.539	.155	6.0	.634	.236	5.3	97.6	4.2
19.29.53	.531	.112	5.7	.564	.199	6.1	98.4	.4
19.30.53	.612	.047	4.3	.442	.182	8.5	97.8	.6
19.31.53	.609	.040	4.3	.569	.047	4.9	96.5	.7
19.32.53	.617	.078	4.3	.518	.060	5.8	95.9	.6
19.33.53	.584	.074	5.0	.510	.121	6.4	96.1	.4
19.34.53	.609	.025	4.3	.555	.138	5.8	95.8	.4
19.35.53	.589	.129	6.2	.512	.177	7.0	95.3	2.1
19.36.53	.581	.070	4.8	.572	.148	5.5	94.8	.8
19.37.53	.529	.139	6.1	.544	.111	5.6	93.6	5.5
19.38.53	.495	.110	6.3	.617	.155	4.8	94.3	.4
19.39.53	.547	.140	5.7	.483	.256	8.8	92.5	2.9
19.40.53	.564	.058	4.7	.644	.074	3.9	93.6	.5
19.41.53	.577	.126	5.2	.545	.069	5.3	92.1	3.2
19.42.53	.569	.131	4.9	.506	.129	6.5	91.3	5.2
19.43.53	.585	.047	4.7	.575	.076	4.9	91.7	.7
19.44.53	.593	.044	4.6	.582	.064	4.7	91.4	.5
19.45.53	.582	.061	4.8	.532	.182	6.6	91.0	.7
19.46.53	.580	.035	4.7	.586	.160	5.4	90.8	.4
19.47.53	.573	.057	4.9	.464	.206	8.3	90.1	.8
19.48.53	.572	.071	4.9	.572	.143	5.5	89.8	.5
19.49.53	.536	.077	5.5	.601	.056	4.5	89.4	.3
19.50.53	.483	.154	7.1	.586	.051	4.7	86.8	6.4
19.51.53	.505	.146	6.5	.548	.143	6.0	88.3	3.1
19.52.53	.522	.079	5.7	.619	.072	4.2	88.7	.6
19.53.53	.530	.089	5.7	.616	.089	4.3	88.5	.8
19.54.53	.542	.088	5.4	.533	.142	6.1	88.1	.4

DATE 07/21/72 BUOY 23

TIME	PINGER CHANNEL AVE	SIGMA	B-LOSS	SPARKER CHANNEL AVE	SIGMA	B-LOSS	WATER DEPTH AVE	SIGMA
19.55.53	.510	.075	6.1	.606	.069	4.4	87.8	.5
19.56.53	.549	.048	5.2	.539	.202	6.7	88.1	.5
19.57.53	.347	.236	11.5	.503	.199	7.4	79.5	9.1

DATE 07/25/72 ROLL NO 24

TIME	PINGER CHANNEL			SPARKER CHANNEL			WATER DEPTH	
	AVE	SIGMA	B-LOSS	AVE	SIGMA	B-LOSS	AVE	SIGMA
17.09.53	.476	.073	6.5	.576	.069	4.8	81.2	.5
17.10.53	.470	.053	6.6	.588	.174	5.2	81.8	.5
17.11.53	.450	.094	7.2	.574	.082	4.9	82.1	.4
17.12.53	.502	.037	6.0	.569	.129	5.2	82.2	.4
17.13.53	.453	.083	7.1	.602	.182	5.0	82.7	.6
17.14.53	.497	.067	6.1	.640	.152	4.3	83.3	.5
17.15.53	.477	.045	6.5	.700	.106	3.2	83.5	.4
17.16.53	.449	.143	6.4	.629	.095	4.1	82.2	5.5
17.17.53	.486	.028	6.3	.566	.087	5.0	83.5	.4
17.18.53	.431	.114	7.7	.605	.074	4.4	84.7	4.1
17.19.53	.445	.144	6.5	.571	.125	5.1	83.1	5.4
17.20.53	.415	.161	7.3	.541	.152	5.7	83.5	5.9
17.21.53	.455	.093	7.1	.539	.170	5.9	84.8	.5
17.22.53	.485	.093	6.5	.583	.131	4.9	84.7	.5
17.23.53	.465	.096	6.9	.576	.137	5.1	85.2	.5
17.24.53	.511	.052	5.9	.584	.058	4.7	85.3	.5
17.25.53	.478	.103	6.7	.619	.161	4.6	85.1	2.0
17.26.53	.469	.092	6.8	.492	.134	6.5	84.7	3.5
17.27.53	.470	.093	6.8	.594	.098	4.6	85.1	.7
17.28.53	.474	.097	6.7	.555	.089	5.2	85.0	3.3
17.29.53	.440	.161	6.7	.562	.085	5.1	84.3	5.7
17.30.53	.498	.064	6.1	.606	.076	4.4	85.8	.6
17.31.53	.409	.184	6.5	.563	.105	5.1	83.2	7.5
17.32.53	.470	.083	6.7	.611	.110	4.4	86.0	.6
17.33.53	.487	.108	6.4	.564	.125	5.3	85.5	.3
17.34.53	.448	.081	7.1	.582	.114	4.9	86.0	.5
17.35.53	.486	.070	6.4	.559	.095	5.2	86.0	.7
17.36.53	.494	.069	6.2	.590	.070	4.6	86.0	.5
17.37.53	.474	.084	6.6	.541	.060	5.4	86.4	.3
17.38.53	.455	.113	7.2	.511	.139	6.1	85.5	2.5
17.39.53	.467	.076	6.7	.633	.104	4.1	86.2	.6
17.40.53	.426	.144	6.9	.590	.170	5.0	84.5	5.5
17.41.53	.454	.093	7.0	.644	.283	3.4	86.8	.7
17.42.53	.455	.080	7.0	.596	.135	4.8	86.7	.5
17.43.53	.472	.081	6.7	.638	.128	4.1	87.2	.5
17.44.53	.453	.109	7.2	.703	.122	3.2	88.6	3.3
17.45.53	.468	.087	6.8	.639	.113	4.0	87.2	.5
17.46.53	.403	.208	6.9	.593	.139	4.8	83.6	7.3
17.47.53	.480	.068	6.5	.611	.064	4.3	86.6	.5

DATE 07/25/72 [illegible] 2

TIME	PINGER CHANNEL AVE	SIGMA	B-LOSS	SPARKER CHANNEL AVE	SIGMA	B-LOSS	WATER DEPTH AVE	SIGMA
16.09.53	.533	.057	5.5	.707	.128	3.1	88.9	.5
16.10.53	.498	.146	5.5	.585	.092	4.8	87.9	5.5
16.11.53	.516	.047	5.8	.585	.116	4.9	89.6	.6
16.12.53	.525	.100	5.9	.635	.105	4.1	88.6	5.0
16.13.53	.524	.104	5.9	.587	.133	4.9	90.2	.7
16.14.53	.558	.032	5.1	.583	.126	4.9	90.9	.4
16.15.53	.565	.035	5.0	.546	.117	5.5	91.8	.5
16.16.53	.519	.154	5.2	.575	.107	4.9	91.0	5.6
16.17.53	.578	.022	4.8	.581	.103	4.8	93.2	.6
16.18.53	.567	.074	5.0	.495	.162	6.6	94.2	.3
16.19.53	.575	.040	4.8	.636	.178	4.3	94.8	.5
16.20.53	.534	.110	5.7	.581	.124	4.9	95.2	.6
16.21.53	.544	.056	5.3	.689	.186	3.7	96.5	.6
16.22.53	.586	.027	4.7	.542	.081	5.4	97.0	.6
16.23.53	.527	.071	5.6	.606	.198	4.9	98.1	.6
16.24.53	.559	.110	5.3	.601	.159	4.8	97.7	.5
16.25.53	.580	.038	4.6	.548	.108	5.4	97.9	.4
16.26.53	.571	.071	4.9	.592	.123	4.8	98.1	.2
16.27.53	.575	.163	4.3	.620	.235	4.7	97.4	5.6
16.28.53	.564	.097	4.8	.560	.112	5.2	99.5	.6
16.29.53	.574	.107	5.0	.597	.141	4.7	100.6	.6
16.30.53	.535	.164	5.0	.529	.213	6.3	100.8	5.9
16.31.53	.641	.046	3.9	.678	.112	3.5	103.3	.6
16.32.53	.622	.091	4.2	.544	.161	5.8	102.5	.6
16.33.53	.526	.143	6.0	.710	.207	3.4	102.9	.3
16.34.53	.598	.051	4.5	.678	.166	3.7	101.6	.5
16.35.53	.566	.080	5.0	.706	.179	3.4	100.8	.5
16.36.53	.544	.171	4.8	.720	.270	3.6	99.3	5.4
16.37.53	.465	.232	5.8	.755	.380	3.8	98.8	9.2
16.38.53	.409	.206	9.1	.434	.301	8.6	91.6	11.1
16.39.53	.467	.107	6.8	.421	.140	7.9	98.7	1.7
16.40.53	.552	.093	5.3	.541	.332	6.7	102.0	1.0
16.41.53	.487	.140	6.6	.849	.307	2.1	100.6	1.1
16.42.53	.645	.067	3.9	.698	.309	4.1	106.0	.4
16.43.53	.662	.070	3.6	.610	.152	4.6	104.2	.5
16.44.53	.411	.276	6.5	.582	.137	5.0	99.0	8.5
16.45.53	.640	.110	4.6	.755	.165	2.6	105.3	.8
16.46.53	.661	.051	3.6	.673	.185	3.7	105.8	.7
16.47.53	.644	.060	3.9	.702	.078	3.1	106.4	.5
16.48.53	.636	.063	4.0	.677	.122	3.5	106.0	.7
16.49.53	.659	.100	3.7	.787	.317	1.8	109.1	.6
16.50.53	.610	.094	4.4	.659	.143	3.8	108.4	.5
16.51.53	.586	.174	4.2	.643	.179	4.2	106.8	5.4

DATE 07/[illegible]

TIME	[illegible] CHANNEL AVE	SIGMA	B-LOSS	SPARKER CHANNEL AVE	SIGMA	B-LOSS	WATER DEPTH AVE	SIGMA
18.00.5[illegible]	.[illegible]	.[illegible]	6.0	.052	.006	25.8	[illegible]	.4
18.01.5[illegible]	.[illegible]	.11[illegible]	6.5	.050	.012	24.8	[illegible]	.3
18.02.5[illegible]	.[illegible]	.14[illegible]	6.5	.043	.012	27.6	[illegible]	5.4
18.03.5[illegible]	.[illegible]	.13[illegible]	7.6	.054	.010	25.5	[illegible]	5.3
18.04.5[illegible]	.[illegible]	.23[illegible]	7.5	.050	.007	26.2	[illegible]	10.9
18.05.5[illegible]	.[illegible]	.17[illegible]	6.2	.052	.016	26.1	[illegible]	10.0
18.06.5[illegible]	.[illegible]	.15[illegible]	6.2	.056	.011	25.2	[illegible]	6.5
18.07.5[illegible]	.[illegible]	.13[illegible]	6.7	.058	.011	24.9	[illegible]	4.9
18.08.5[illegible]	.[illegible]	.06[illegible]	5.6	.064	.016	24.3	[illegible]	.2
18.09.5[illegible]	.[illegible]	.07[illegible]	5.9	.050	.017	23.9	[illegible]	.7
18.10.5[illegible]	.[illegible]	.19[illegible]	6.5	.062	.013	24.3	[illegible]	7.8
18.11.5[illegible]	.[illegible]	.29[illegible]	7.0	.056	.012	25.2	[illegible]	8.8
18.13.5[illegible]	.[illegible]	.09[illegible]	4.7	.041	.044	12.2	[illegible]	.4

DATE 07/26/72 ROLL NO 25

TIME	PINGER CHANNEL			SPARKER CHANNEL			WATER DEPTH	
	AVE	SIGMA	B-LOSS	AVE	SIGMA	B-LOSS	AVE	SIGMA
17.23.53	.814	.057	1.9	.639	.198	4.4	114.7	.4
17.24.53	.774	.089	2.3	.688	.237	3.9	114.5	.7
17.25.53	.779	.077	2.3	.629	.111	4.2	113.9	.6
17.26.53	.765	.070	2.4	.663	.195	4.1	113.0	.5
17.27.53	.762	.069	2.4	.640	.227	4.5	112.4	.5
17.28.53	.738	.093	2.7	.689	.145	3.4	112.0	.6
17.29.53	.681	.119	3.5	.600	.252	4.1	111.1	.2
17.30.53	.720	.080	2.9	.677	.187	3.8	111.0	.4
17.31.53	.700	.069	3.1	.711	.204	3.5	110.4	.5
17.32.53	.724	.040	2.8	.720	.128	3.0	109.9	.6
17.33.53	.690	.080	3.3	.702	.154	3.3	109.5	.5
17.34.53	.674	.109	3.6	.682	.152	3.6	108.5	.9
17.35.53	.685	.071	3.3	.673	.138	3.7	108.3	.2
17.36.53	.660	.113	3.7	.689	.122	3.4	109.5	.9
17.37.53	.622	.140	4.3	.764	.218	2.8	110.8	.7
17.38.53	.701	.069	3.1	.802	.176	2.2	111.1	.8
17.39.53	.709	.084	3.1	.916	.215	1.2	110.6	.4
17.40.53	.684	.087	3.4	.642	.161	4.2	108.5	3.9
17.41.53	.668	.084	3.3	.557	.194	5.7	109.7	.7
17.42.53	.706	.087	3.1	.827	.165	1.8	108.4	.5
17.43.53	.681	.093	3.4	.637	.212	4.6	108.1	.4
17.44.53	.660	.080	3.7	.650	.113	3.9	108.1	.5
17.45.53	.612	.104	4.4	.643	.213	4.5	107.5	.4
17.46.53	.650	.052	3.4	.620	.178	4.6	106.8	.6
17.47.53	.656	.069	3.7	.519	.104	5.9	106.7	.4
17.48.53	.642	.069	3.9	.560	.135	5.3	106.0	.3
17.49.53	.614	.166	4.9	.546	.165	5.7	104.2	2.9
17.50.53	.641	.063	3.9	.649	.130	4.0	104.7	.5
17.51.53	.622	.090	4.2	.614	.178	4.8	103.7	.6
17.52.53	.633	.097	4.1	.554	.183	5.8	103.8	.4
17.53.53	.614	.054	4.3	.623	.140	4.4	102.9	.5
17.54.53	.631	.033	4.0	.596	.138	4.8	101.9	.4
17.55.53	.610	.075	4.4	.581	.143	5.1	101.6	.4
17.56.53	.633	.045	3.9	.564	.249	4.7	101.0	.4
17.57.53	.572	.076	4.9	.477	.218	6.0	100.8	.5
17.58.53	.573	.114	5.1	.588	.186	5.2	100.1	1.6
17.59.53	.596	.035	4.6	.609	.150	4.7	100.4	.6
18.00.53	.590	.028	4.5	.570	.176	5.5	100.2	.6
18.01.53	.510	.134	6.1	.679	.189	3.7	97.6	6.5
18.02.53	.554	.090	5.2	.872	.128	1.3	98.7	.5
18.03.53	.524	.134	6.0	.733	.207	3.2	98.2	.7
18.04.53	.566	.077	5.0	.552	.230	6.2	97.6	.4
18.05.53	.552	.041	5.2	.605	.141	4.7	96.3	.4
18.06.53	.547	.059	5.3	.653	.116	3.8	95.9	.5
18.07.53	.541	.034	5.0	.560	.158	5.5	95.4	.4
18.08.53	.486	.176	7.2	.498	.184	6.7	90.8	8.2
18.09.53	.490	.195	8.2	.562	.180	5.6	88.6	10.2
18.10.53	.547	.075	5.3	.569	.162	5.4	94.0	.4
18.11.53	.496	.149	6.7	.562	.098	5.1	91.2	6.1
18.12.53	.510	.220	6.6	.614	.216	4.8	90.9	7.0

DATE 07/[illegible]

TIME	[illegible] CHANNEL AVE	SIGMA	B-LOSS	SPARKER CHANNEL AVE	SIGMA	B-LOSS	WATER DEPTH AVE	SIGMA
18.13.5[illegible]	.5[illegible]	.0[illegible]	5.6	.668	.174	3.6	92.8	.5
18.14.5[illegible]	.5[illegible]	.[illegible]	5.8	.614	.121	4.4	92.6	.4
18.15.5[illegible]	.5[illegible]	.[illegible]	5.9	.580	.168	5.2	92.5	.4
18.16.5[illegible]	.4[illegible]	.[illegible]	9.0	.589	.122	4.3	87.4	7.5
18.17.5[illegible]	.4[illegible]	.[illegible]	6.7	.692	.098	3.3	90.9	3.7
18.18.5[illegible]	.3[illegible]	.[illegible]	9.4	.507	.185	6.7	86.1	8.3
18.19.5[illegible]	.4[illegible]	.[illegible]	6.5	.617	.123	4.4	90.2	4.2
18.20.5[illegible]	.5[illegible]	.[illegible]	14.1	.576	.139	5.2	80.5	6.2
18.21.5[illegible]	.3[illegible]	.[illegible]	9.7	.490	.282	3.0	84.9	8.4
18.22.5[illegible]	.4[illegible]	.[illegible]	6.5	.546	.214	6.3	89.0	5.5
18.23.5[illegible]	.4[illegible]	.[illegible]	8.1	.656	.163	4.1	87.5	8.0
18.24.5[illegible]	.4[illegible]	.[illegible]	6.5	.409	.213	9.1	90.0	2.2
18.25.5[illegible]	.4[illegible]	.[illegible]	6.7	.549	.138	5.6	89.9	.2
18.26.5[illegible]	.4[illegible]	.[illegible]	8.3	.511	.176	6.5	86.7	6.7
18.27.5[illegible]	.3[illegible]	.[illegible]	11.0	.557	.118	5.3	81.0	10.1
18.28.5[illegible]	.3[illegible]	.[illegible]	9.6	.494	.148	6.7	84.4	7.8
18.29.5[illegible]	.4[illegible]	.[illegible]	6.4	.480	.187	7.2	89.4	.3
18.30.5[illegible]	.3[illegible]	.[illegible]	9.5	.537	.153	6.2	85.5	5.9
18.31.5[illegible]	.4[illegible]	.[illegible]	7.2	.510	.168	6.4	87.8	4.1
18.32.5[illegible]	.4[illegible]	.[illegible]	7.6	.611	.120	4.4	87.5	5.0
18.33.5[illegible]	.4[illegible]	.[illegible]	6.9	.597	.146	4.9	88.2	2.1
18.34.5[illegible]	.4[illegible]	.[illegible]	7.8	.520	.163	6.2	87.2	4.7
18.35.5[illegible]	.3[illegible]	.[illegible]	9.4	.533	.164	5.9	82.5	9.6
18.36.5[illegible]	.4[illegible]	.[illegible]	8.1	.579	.133	5.1	88.1	1.5
18.37.5[illegible]	.4[illegible]	.[illegible]	8.4	.534	.167	6.1	86.0	6.0
18.38.5[illegible]	.3[illegible]	.[illegible]	9.8	.533	.109	5.7	83.5	8.0
18.39.5[illegible]	.4[illegible]	.[illegible]	6.8	.564	.174	5.5	87.9	.5
18.40.5[illegible]	.4[illegible]	.[illegible]	7.6	.494	.218	7.3	86.6	3.8
18.41.5[illegible]	.4[illegible]	.[illegible]	7.2	.538	.172	6.0	86.5	5.6
18.42.5[illegible]	.4[illegible]	.[illegible]	7.5	.568	.228	6.1	87.8	.5
18.43.5[illegible]	.3[illegible]	.[illegible]	8.9	.547	.168	5.9	86.4	3.5
18.44.5[illegible]	.3[illegible]	.[illegible]	10.7	.911	.579	2.1	90.6	4.7

DATE 07/27/72 ROLL NO 27

TIME	PINGER CHANNEL AVE	SIGMA	B-LOSS	SPARKER CHANNEL AVE	SIGMA	B-LOSS	WATER DEPTH AVE	SIGMA
15.58.53	.495	.147	6.7	.541	.218	6.5	81.9	2.1
15.59.53	.530	.093	5.6	.484	.247	8.1	81.6	2.8
16.00.53	.537	.122	5.9	.579	.141	5.2	82.9	.5
16.01.53	.581	.095	4.7	.645	.071	3.9	83.4	.3
16.02.53	.535	.125	5.9	.602	.059	4.4	82.8	3.4
16.04.53	.566	.043	5.0	.250	.186	10.4	84.4	.3
16.05.53	.473	.175	6.1	.261	.105	10.6	83.3	5.5
16.06.53	.478	.175	7.4	.148	.086	11.9	82.8	5.3
16.07.53	.581	.084	4.8	.207	.178	8.6	85.0	.6
16.08.53	.530	.110	5.7	.340	.213	9.5	85.3	.4
16.09.53	.496	.143	6.7	.230	.113	11.9	85.5	.3
16.11.53	.517	.121	6.1	.217	.160	11.4	85.7	.3
16.12.53	.519	.130	6.1	.299	.200	8.8	86.0	.3
16.13.53	.559	.126	5.5	.283	.194	10.8	86.3	.4
16.14.53	.525	.100	5.7	.218	.208	7.1	86.5	.6
16.15.53	.497	.164	5.8	.958	.742	4.0	85.2	5.5
16.16.53	.566	.050	5.0	.609	.868	4.6	86.7	.5
16.17.53	.529	.079	5.3	.680	1.304	2.7	87.1	.6
16.18.53	.425	.180	7.2	1.273	1.923	3.2	85.8	5.5
16.19.53	.446	.193	7.0	.295	.319	4.4	85.0	6.2
16.21.53	.505	.116	6.2	.583	.606	2.9	87.4	.5
16.22.53	.562	.066	5.0	.728	.804	.8	87.6	.3
16.23.53	.541	.087	5.5	.325	.268	5.8	87.9	.5
16.24.53	.514	.175	6.4	.484	.565	2.3	86.5	5.5
16.26.53	.572	.076	4.9	.594	.551	5.7	87.9	.5
16.27.53	.550	.060	4.6	.491	.248	7.2	88.0	.6
16.28.53	.540	.107	5.6	.349	.240	7.7	88.5	.5
16.29.53	.471	.202	6.5	.698	.557	3.1	88.2	6.9
16.30.53	.552	.084	5.3	.250	.201	8.9	88.3	.5
16.31.53	.539	.123	5.6	.194	.181	6.1	89.6	4.1
16.32.53	.530	.103	5.5	.565	.633	7.3	88.9	.6
16.33.53	.577	.070	4.9	.394	.500	3.5	88.9	.4
16.34.53	.519	.126	6.1	.414	.280	6.5	89.2	.5
16.35.53	.520	.150	5.3	.294	.173	8.7	87.6	5.4
16.36.53	.544	.128	5.7	.394	.255	8.1	89.2	2.4
16.37.53	.560	.079	5.1	.313	.250	7.4	89.9	.4
16.38.53	.525	.123	5.9	.402	.336	5.9	90.2	.4
16.39.53	.509	.152	5.8	.793	.803	3.6	90.0	7.0
16.41.53	.543	.161	5.9	.302	.239	7.7	90.6	1.1

DATE 07/27/7[illegible] [illegible] 27

TIME	PINGER CHANNEL AVE	SIGMA	B-LOSS	SPARKER CHANNEL AVE	SIGMA	B-LOSS	WATER DEPTH AVE	SIGMA
18.56.53	.[illegible]84	.173	7.1	.590	.125	4.9	84.8	3.1
18.57.53	.4[illegible]5	.193	9.2	.565	.145	5.4	82.0	6.1
18.58.53	.517	.102	5.9	.487	.151	6.8	85.9	.4
18.59.53	.4[illegible]7	.153	8.0	.465	.178	7.4	85.1	1.5
19.00.53	.514	.135	6.2	.562	.134	5.3	84.9	.9
19.01.53	.511	.123	6.1	.572	.207	5.6	83.2	4.6
19.02.53	.497	.152	7.7	.579	.166	5.3	82.1	5.4
19.03.53	.514	.125	6.2	.607	.056	4.4	83.6	2.7
19.04.53	.503	.124	6.4	.539	.178	6.1	83.1	3.9
19.05.53	.541	.064	5.4	.497	.135	6.5	83.8	.4
19.06.53	.547	.053	5.3	.546	.141	5.6	83.6	.4
19.07.53	.459	.136	7.3	.587	.155	5.1	80.7	4.9

DATE 07/27/7[illegible]

TIME	PINGER CHANNEL AVE	SIGMA	B-LOSS	SPARKER CHANNEL AVE	SIGMA	B-LOSS	WATER DEPTH AVE	SIGMA
18.33.5[illegible]	[illegible]	[illegible]	4.1	.590	.155	4.9	107.5	.7
18.34.5[illegible]	[illegible]	[illegible]	3.7	.577	.097	4.9	106.8	.6
18.35.5[illegible]	[illegible]	[illegible]	4.1	.550	.164	4.3	105.8	1.9
18.36.5[illegible]	[illegible]	[illegible]	3.9	.579	.143	5.2	105.6	.5
18.37.5[illegible]	[illegible]	[illegible]	4.0	.561	.167	5.6	104.7	.6
18.38.5[illegible]	[illegible]	[illegible]	5.3	.582	.074	4.8	103.4	1.6
18.39.5[illegible]	[illegible]	[illegible]	4.1	.626	.155	4.7	103.1	.8
18.40.5[illegible]	[illegible]	[illegible]	3.9	.518	.169	6.4	102.4	.8
18.41.5[illegible]	[illegible]	[illegible]	4.2	.605	.155	4.9	101.8	.5
18.42.5[illegible]	[illegible]	[illegible]	4.8	.557	.138	5.6	100.3	3.9
18.43.5[illegible]	[illegible]	[illegible]	4.4	.583	.058	4.7	100.5	.8
18.44.5[illegible]	[illegible]	[illegible]	4.4	.630	.098	4.1	100.2	.7
18.45.5[illegible]	[illegible]	[illegible]	4.5	.501	.213	7.4	99.9	.7
18.46.5[illegible]	[illegible]	[illegible]	4.5	.555	.090	5.2	99.3	.3
18.47.5[illegible]	[illegible]	[illegible]	4.7	.663	.103	3.7	98.8	.6
18.48.5[illegible]	[illegible]	[illegible]	4.5	.554	.197	6.2	98.0	.5
18.49.5[illegible]	[illegible]	[illegible]	4.7	.651	.381	5.2	97.4	.5
18.50.5[illegible]	[illegible]	[illegible]	4.5	.596	.123	4.7	97.3	.5
18.51.5[illegible]	[illegible]	[illegible]	5.5	.567	.144	5.4	95.5	5.2
18.52.5[illegible]	[illegible]	[illegible]	4.7	.690	.130	3.4	94.3	.5
18.53.5[illegible]	[illegible]	[illegible]	5.7	.644	.145	4.0	95.6	1.6
18.54.5[illegible]	[illegible]	[illegible]	4.8	.705	.126	3.2	95.6	.8
18.55.5[illegible]	[illegible]	[illegible]	5.9	.603	.243	4.3	94.2	4.3
18.56.5[illegible]	[illegible]	[illegible]	5.2	.615	.129	4.4	95.0	.7
18.57.5[illegible]	[illegible]	[illegible]	6.1	.625	.201	3.4	93.6	2.9
18.58.5[illegible]	[illegible]	[illegible]	5.7	.629	.161	4.6	94.5	.6
18.59.5[illegible]	[illegible]	[illegible]	5.7	.559	.280	6.6	93.5	2.7
19.00.5[illegible]	[illegible]	[illegible]	5.3	.471	.156	7.2	93.9	.5
19.01.5[illegible]	[illegible]	[illegible]	5.6	.630	.107	4.0	93.6	.6
19.02.5[illegible]	[illegible]	[illegible]	5.6	.634	.213	4.7	93.5	.6
19.03.5[illegible]	[illegible]	[illegible]	5.7	.653	.125	3.8	93.0	.6
19.05.5[illegible]	[illegible]	[illegible]	5.8	.226	.142	10.7	92.5	1.0
19.06.5[illegible]	[illegible]	[illegible]	6.1	.143	.047	17.3	92.5	.9
19.07.5[illegible]	[illegible]	[illegible]	6.2	.133	.036	17.8	92.1	1.9
19.08.5[illegible]	[illegible]	[illegible]	6.0	.131	.065	14.4	92.5	1.1
19.09.5[illegible]	[illegible]	[illegible]	5.6	.148	.061	15.2	92.7	1.4
19.10.5[illegible]	[illegible]	[illegible]	5.4	.157	.083	16.5	92.4	1.1
19.11.5[illegible]	[illegible]	[illegible]	6.6	.151	.084	15.6	92.0	1.7
19.12.5[illegible]	[illegible]	[illegible]	6.5	.159	.058	16.4	92.0	.5
19.13.5[illegible]	[illegible]	[illegible]	6.4	.145	.085	15.7	90.8	4.0
19.14.5[illegible]	[illegible]	[illegible]	6.1	.121	.050	16.9	91.7	.5
19.15.5[illegible]	[illegible]	[illegible]	5.7	.123	.028	18.4	91.3	.5
19.16.5[illegible]	[illegible]	[illegible]	6.6	.135	.032	17.6	91.2	.6
19.17.5[illegible]	[illegible]	[illegible]	5.9	.152	.108	15.7	90.9	.4
19.05.5[illegible]	[illegible]	[illegible]	5.9	.197	.161	11.2	92.6	1.0
19.06.5[illegible]	[illegible]	[illegible]	6.3	.153	.106	15.9	92.5	1.0
19.07.5[illegible]	[illegible]	[illegible]	6.4	.144	.035	17.0	92.1	1.8
19.08.5[illegible]	[illegible]	[illegible]	6.1	.121	.071	13.3	92.6	1.0
19.09.5[illegible]	[illegible]	[illegible]	5.8	.192	.150	12.4	92.8	1.4
19.10.5[illegible]	[illegible]	[illegible]	5.6	.160	.064	16.5	92.1	1.1

DATE 07/27/72 ROLL NO 20

TIME	PINGER CHANNEL			SPARKER CHANNEL			WATER DEPTH	
	AVE	SIGMA	B-LOSS	AVE	SIGMA	B-LOSS	AVE	SIGMA
19.05.53	.517	.069	5.8	.586	.244	4.1	92.2	1.0
19.06.53	.490	.102	6.2	.715	.092	3.0	92.2	1.0
19.07.53	.502	.114	6.3	.574	.260	6.4	91.8	1.9
19.08.53	.512	.075	5.9	.555	.305	6.8	92.2	1.0
19.09.53	.523	.070	5.7	.720	.221	3.5	92.4	1.4
19.10.53	.537	.061	5.5	.600	.237	5.5	92.1	1.1
19.11.53	.464	.107	6.6	.777	.224	2.9	91.7	1.7
19.12.53	.481	.108	6.5	.654	.099	3.8	91.9	.5
19.13.53	.491	.117	6.6	.588	.175	5.3	90.5	4.0
19.14.53	.482	.116	6.7	.666	.219	4.4	91.1	1.3
19.15.53	.523	.010	5.6	.623	.251	5.5	91.0	.5
19.16.53	.483	.104	6.6	.572	.252	6.4	91.0	.6
19.17.53	.516	.060	5.8	.583	.339	6.8	90.5	.4
19.18.53	.492	.072	6.3	.668	.232	4.3	90.7	.5
19.19.53	.521	.062	5.7	.717	.143	3.1	90.4	.7
19.20.53	.479	.132	7.1	.627	.216	4.8	89.7	1.7
19.21.53	.491	.117	6.6	.442	.278	8.2	88.8	4.8
19.22.53	.457	.070	6.3	.626	.161	4.7	89.8	.7
19.23.53	.491	.060	6.2	.531	.190	6.1	89.2	.4
19.24.53	.519	.053	5.7	.720	.210	3.2	89.0	.5
19.25.53	.495	.094	6.3	.540	.201	6.2	88.8	.4
19.26.53	.509	.060	6.1	.696	.206	3.5	88.7	.6
19.27.53	.531	.027	5.5	.658	.205	4.4	88.5	.4
19.28.53	.469	.057	6.3	.615	.273	5.7	88.4	.5
19.29.53	.507	.044	5.9	.627	.324	5.6	88.1	.5
19.30.53	.500	.048	5.9	.720	.202	3.5	87.9	.4
19.31.53	.506	.042	5.9	.761	.280	1.9	87.4	.4
19.32.53	.495	.061	6.2	.687	.241	4.1	87.3	.4
19.33.53	.513	.024	5.8	.117	.044	17.0	87.0	.4

DATE 07/28/72 ROLL NO 37

TIME	PINGER CHANNEL AVE	SIGMA	B-LOSS	SPARKER CHANNEL AVE	SIGMA	B-LOSS	WATER DEPTH AVE	SIGMA
16.31.53	.707	.212	2.7	.572	.164	5.4	123.4	3.4
16.32.53	.748	.091	2.7	.610	.162	4.9	124.1	.6
16.33.53	.764	.066	2.4	.703	.100	3.2	123.5	1.0
16.34.53	.727	.103	2.9	.642	.134	4.1	122.7	.5
16.35.53	.736	.073	3.1	.618	.104	4.3	122.2	.5
16.36.53	.727	.060	2.8	.650	.075	3.8	121.3	.4
16.37.53	.650	.093	3.7	.506	.236	7.5	120.8	.9
16.38.53	.693	.087	3.3	.568	.186	5.7	120.4	.8
16.39.53	.703	.059	3.1	.574	.173	5.5	119.2	.8
16.40.53	.676	.068	3.4	.468	.188	7.7	118.6	.8
16.41.53	.679	.090	3.5	.662	.085	3.7	118.3	.8
16.42.53	.662	.111	3.7	.721	.061	2.9	118.1	.8
16.43.53	.695	.052	3.2	.680	.101	3.5	117.5	.4
16.44.53	.661	.083	3.6	.589	.110	4.8	117.2	.6
16.45.53	.678	.054	3.4	.663	.162	4.2	116.6	.6
16.46.53	.665	.111	3.4	.501	.182	7.1	116.0	.9
16.47.53	.706	.067	3.1	.511	.204	7.0	115.1	.6
16.48.53	.688	.059	3.3	.472	.222	8.0	115.0	.4
16.49.53	.694	.084	3.2	.627	.161	4.7	114.2	.6
16.50.53	.649	.096	3.9	.570	.215	6.1	113.5	.8
16.51.53	.673	.086	3.5	.671	.123	3.6	113.0	.5
16.52.53	.595	.110	4.7	.612	.166	5.0	112.2	1.0
16.53.53	.632	.100	4.1	.663	.174	4.3	111.5	.8
16.54.53	.590	.108	4.7	.538	.195	6.6	111.0	.5
16.55.53	.632	.123	4.3	.612	.128	4.5	110.4	.4
16.56.53	.642	.057	3.9	.499	.229	7.9	109.4	.4
16.57.53	.625	.096	4.2	.580	.143	5.3	109.0	.5
16.58.53	.646	.043	3.8	.588	.122	4.8	108.5	.7
16.59.53	.610	.079	4.4	.552	.209	6.4	107.9	.5
17.00.53	.639	.053	3.9	.652	.090	3.8	107.4	.8
17.01.53	.610	.099	4.4	.545	.178	6.1	106.9	.7
17.02.53	.633	.051	4.0	.575	.214	6.2	106.7	.8
17.03.53	.653	.032	3.7	.417	.262	9.6	106.0	.4
17.04.53	.612	.043	4.3	.667	.085	3.6	105.4	.6
17.05.53	.602	.033	4.4	.635	.064	4.0	104.8	1.0
17.06.53	.615	.019	4.2	.465	.222	8.1	104.4	.9
17.07.53	.590	.046	4.5	.558	.136	5.7	103.9	.6
17.08.53	.593	.023	4.5	.592	.115	4.7	103.3	.7
17.09.53	.590	.014	4.6	.633	.117	4.2	103.1	.4
17.10.53	.608	.025	4.3	.675	.093	3.5	102.5	1.0
17.11.53	.586	.043	4.7	.597	.165	5.3	102.1	.9
17.12.53	.590	.018	4.6	.519	.175	6.3	101.6	.5
17.13.53	.583	.014	4.6	.587	.226	6.0	101.2	.7
17.14.53	.579	.024	4.8	.606	.146	4.8	100.5	.6
17.15.53	.583	.033	4.7	.593	.216	6.0	100.1	.5
17.16.53	.577	.024	4.8	.580	.221	6.2	100.0	.5
17.17.53	.571	.021	4.9	.592	.095	4.7	99.7	.5
17.18.53	.583	.021	4.7	.630	.186	4.9	99.4	.8
17.19.53	.592	.022	4.6	.556	.075	5.2	99.0	.6
17.20.53	.579	.016	4.8	.567	.181	5.8	98.5	.6

DATE 07/25/72 ROLL NO 33

TIME	PINGER CHANNEL AVE	SIGMA	B-LOSS	SPARKER CHANNEL AVE	SIGMA	B-LOSS	WATER DEPTH AVE	SIGMA
17.21.53	.545	.052	5.3	.675	.093	3.5	98.1	.8
17.22.53	.555	.027	5.0	.485	.220	8.2	99.0	.4
17.23.53	.527	.107	6.0	.605	.226	5.9	96.5	3.5
17.24.53	.543	.056	5.2	.558	.210	6.1	97.3	.8
17.25.53	.571	.044	4.9	.625	.198	5.0	96.7	.7
17.26.53	.557	.025	5.1	.532	.207	5.8	96.4	.8
17.27.53	.546	.027	5.3	.561	.221	6.5	96.2	.5
17.28.53	.547	.045	5.3	.536	.253	7.5	96.0	.8
17.29.53	.564	.056	5.4	.550	.263	7.2	95.4	.8
17.30.53	.547	.026	5.3	.528	.202	7.0	95.5	.5
17.31.53	.516	.100	6.1	.616	.068	4.3	94.8	1.2
17.32.53	.534	.057	5.5	.560	.209	6.1	94.7	1.0
17.33.53	.543	.051	5.7	.615	.158	5.0	94.5	.7
17.34.53	.503	.098	6.1	.428	.267	10.5	94.6	.7
17.35.53	.524	.044	5.6	.556	.204	6.2	93.8	.8
17.36.53	.514	.040	5.8	.234	.275	17.3	93.7	.6
17.37.53	.495	.130	7.4	.534	.190	6.5	94.5	3.5
17.38.53	.493	.078	6.2	.524	.205	6.9	93.6	.7
17.39.53	.496	.117	6.5	.686	.051	3.3	92.3	2.6
17.40.53	.503	.075	6.1	.468	.208	8.1	93.3	.7
17.41.53	.491	.097	6.4	.563	.218	6.6	91.7	5.0

DATE 07/2[illegible]/73 [illegible] 31

TIME	PINGER CHANNEL AVE	SIGMA	B-LOSS	SPARKER CHANNEL AVE	SIGMA	B-LOSS	WATER DEPTH AVE	SIGMA
19.21.5[illegible]	.697	.162	3.5	.426	.211	8.9	111.3	.6
19.22.5[illegible]	.6[illegible]	.21[illegible]	2.9	.46[illegible]	.142	7.0	109.7	5.4
19.23.5[illegible]	.735	.12[illegible]	2.8	.539	.141	5.9	110.5	.7
19.24.5[illegible]	.697	.156	3.5	.554	.074	5.2	110.9	3.9
19.25.5[illegible]	.583	.311	4.4	.504	.171	6.7	105.8	7.1
19.26.5[illegible]	.762	.051	2.4	.596	.118	4.7	108.5	.5
19.27.5[illegible]	.717	.16[illegible]	3.3	.510	.086	6.0	106.9	3.3
19.28.5[illegible]	.729	.11[illegible]	2.9	.616	.113	4.4	107.5	1.2
19.29.5[illegible]	.630	.169	3.6	.607	.072	4.4	106.4	1.7
19.30.5[illegible]	.748	.067	2.6	.528	.191	6.3	106.2	.7
19.31.5[illegible]	.[illegible]66	.20[illegible]	2.9	.667	.091	3.6	104.3	5.2
19.32.5[illegible]	.627	.227	5.0	.581	.186	5.5	100.7	8.7
19.33.5[illegible]	.650	.233	3.6	.566	.131	5.2	101.5	7.6
19.34.5[illegible]	.71[illegible]	.07[illegible]	2.9	.605	.143	4.7	103.8	.9
19.35.5[illegible]	.717	.066	2.9	.502	.175	7.1	103.0	.3
19.36.5[illegible]	.694	.077	3.2	.497	.174	6.9	102.7	.7
19.37.5[illegible]	.708	.045	3.1	.618	.165	4.9	102.2	.7
19.38.5[illegible]	.734	.047	2.7	.622	.083	4.2	101.7	.7
19.39.5[illegible]	.7[illegible]	.044	2.5	.667	.080	3.6	101.6	.5
19.40.5[illegible]	.675	.207	3.1	.643	.184	4.6	99.7	5.2
19.41.5[illegible]	.6[illegible]4	.21[illegible]	3.7	.666	.094	3.6	101.4	5.2
19.42.5[illegible]	.6[illegible]	.06[illegible]	3.2	.574	.142	5.1	100.0	.5
19.43.5[illegible]	.6[illegible]	.19[illegible]	4.7	.538	.186	6.1	97.9	4.6
19.44.5[illegible]	.674	.131	3.7	.665	.097	3.6	98.9	.7
19.45.5[illegible]	.6[illegible]1	.06[illegible]	3.4	.600	.219	5.8	98.6	.6
19.46.5[illegible]	.67[illegible]	.056	3.4	.662	.091	3.7	98.4	.5
19.47.5[illegible]	.6[illegible]9	.16[illegible]	4.5	.543	.149	5.7	97.0	4.6
19.48.5[illegible]	.6[illegible]0	.19[illegible]	3.8	.541	.211	6.7	96.2	5.7
19.49.5[illegible]	.67[illegible]	.06[illegible]	3.4	.591	.177	5.4	97.3	.9
19.50.5[illegible]	.6[illegible]	.18[illegible]	3.7	.427	.264	10.4	95.7	5.4
19.51.5[illegible]	.66[illegible]	.04[illegible]	3.6	.662	.109	3.7	96.8	.4
19.52.5[illegible]	.6[illegible]	.13[illegible]	4.3	.566	.227	6.4	96.7	.7
19.53.5[illegible]	.516	.24[illegible]	4.9	.430	.279	9.4	93.2	7.1
19.54.5[illegible]	.5[illegible]0	.19[illegible]	5.9	.385	.257	11.2	93.9	5.0
19.55.5[illegible]	.5[illegible]3	.14[illegible]	5.0	.650	.182	4.5	95.9	.5
19.56.5[illegible]	.57[illegible]	.17[illegible]	4.4	.657	.104	3.8	94.3	5.3
19.57.5[illegible]	.61[illegible]	.14[illegible]	4.8	.382	.231	10.4	93.9	5.5
19.58.5[illegible]	.5[illegible]9	.10[illegible]	4.7	.512	.225	7.3	95.3	.9
19.59.5[illegible]	.5[illegible]	.09[illegible]	4.8	.491	.161	6.8	95.2	.8
20.00.5[illegible]	.55[illegible]	.10[illegible]	5.2	.546	.211	6.6	95.0	1.0
20.01.5[illegible]	.53[illegible]	.171	6.2	.551	.151	5.7	93.2	4.2
20.02.5[illegible]	.544	.07[illegible]	4.7	.648	.181	4.5	94.6	.6
20.03.5[illegible]	.54[illegible]	.14[illegible]	5.7	.523	.155	6.1	94.2	.7
20.04.5[illegible]	.54[illegible]	.12[illegible]	5.0	.565	.223	5.9	93.0	5.4
20.05.5[illegible]	.56[illegible]	.11[illegible]	4.6	.629	.177	4.8	94.2	.6
20.06.5[illegible]	.59[illegible]	.14[illegible]	5.0	.624	.137	4.3	92.6	5.1
20.07.5[illegible]	.55[illegible]	.111	5.2	.503	.199	7.1	93.6	.8
20.08.5[illegible]	.641	.06[illegible]	3.9	.614	.08[illegible]	4.3	93.6	.7
20.09.5[illegible]	.64[illegible]	.045	3.8	.523	.167	6.4	93.2	1.2
20.10.5[illegible]	.5[illegible]	.11[illegible]	5.2	.617	.081	4.3	92.9	.7

DATE 07/[illegible]

TIME	PINGER CHANNEL AVE	PINGER CHANNEL SIGMA	PINGER CHANNEL B-LOSS	SPARKER CHANNEL AVE	SPARKER CHANNEL SIGMA	SPARKER CHANNEL B-LOSS	WATER DEPTH AVE	WATER DEPTH SIGMA
17.51.53	.544	.136	5.8	.570	.153	5.3	90.6	4.4
17.52.53	.517	.107	4.4	.589	.058	4.6	90.5	5.2
17.53.53	.574	.151	5.4	.527	.201	7.0	91.4	1.3
17.54.53	.[illegible]	.[illegible]	4.5	.591	.164	5.3	91.5	.6
17.55.53	.[illegible]	.[illegible]	5.2	.579	.088	5.0	91.5	.9
17.56.53	.[illegible]	.[illegible]	6.6	.532	.146	6.2	89.0	5.9
17.57.53	.[illegible]	.[illegible]	5.0	.575	.149	5.6	91.1	.6
17.58.53	.[illegible]	.[illegible]	4.9	.560	.151	5.7	90.6	.6
17.59.53	.[illegible]	.[illegible]	7.7	.174	.177	18.0	89.1	3.5
18.00.53	.[illegible]	.[illegible]	5.8	.543	.110	5.5	90.6	.4
18.01.53	.[illegible]	.[illegible]	4.9	.539	.105	5.6	90.6	.4
18.02.53	.[illegible]	.[illegible]	6.1	.567	.062	5.0	89.8	1.4
18.03.53	.[illegible]	.[illegible]	8.8	.523	.098	5.8	85.5	7.2
18.04.53	.[illegible]	.[illegible]	5.6	.493	.300	9.4	89.9	.5
18.05.53	.[illegible]	.[illegible]	5.8	.546	.152	6.0	88.5	5.4
18.06.53	.[illegible]	.[illegible]	5.7	.627	.054	4.1	89.4	1.2
18.07.53	.[illegible]	.[illegible]	5.4	.528	.115	5.8	89.2	1.5
18.08.53	.[illegible]	.[illegible]	6.7	.595	.058	4.5	87.7	5.0
18.09.53	.[illegible]	.[illegible]	5.4	.602	.048	4.4	89.5	.7
18.10.53	.[illegible]	.[illegible]	6.7	.605	.096	4.5	88.8	1.5
18.11.53	.[illegible]	.[illegible]	5.6	.547	.154	6.0	88.2	3.6
18.12.53	.[illegible]	.[illegible]	4.9	.567	.047	5.0	88.7	.6
18.13.53	.[illegible]	.[illegible]	5.6	.500	.192	7.3	87.4	3.4
18.14.53	.[illegible]	.[illegible]	5.5	.551	.143	6.0	88.4	.3
18.15.53	.[illegible]	.[illegible]	7.1	.552	.153	5.9	86.4	4.3
18.16.53	.[illegible]	.[illegible]	4.5	.590	.043	4.6	89.1	.5
18.17.53	.[illegible]	.[illegible]	7.7	.507	.198	7.4	85.7	5.3

DATE 07/28/72 POLL NO 31

TIME	PINGER CHANNEL			SPARKER CHANNEL			WATER DEPTH	
	AVE	SIGMA	B-LOSS	AVE	SIGMA	B-LOSS	AVE	SIGMA
20.11.53	.609	.131	4.6	.545	.183	5.9	92.6	1.0
20.12.53	.534	.127	5.7	.515	.214	6.9	91.3	5.3
20.13.53	.566	.100	5.1	.547	.179	6.0	92.4	.7
20.14.53	.546	.127	5.5	.583	.107	4.8	92.4	.3
20.15.53	.500	.130	6.4	.509	.246	7.9	93.2	5.0
20.16.53	.549	.126	5.5	.471	.231	8.6	90.5	4.7
20.17.53	.564	.168	4.5	.489	.165	7.1	90.0	5.7

DATE 08/01/72 ROLL NO 32

TIME	PINGER CHANNEL AVE	SIGMA	B-LOSS	SPARKER CHANNEL AVE	SIGMA	B-LOSS	WATER DEPTH AVE	SIGMA
17.17.53	.701	.068	3.1	.606	.094	4.4	124.7	.4
17.18.53	.620	.230	3.9	.470	.181	7.5	122.6	5.2
17.19.53	.684	.070	3.3	.584	.157	5.3	123.2	.6
17.20.53	.677	.105	3.5	.648	.112	3.9	122.5	1.6
17.21.53	.660	.105	3.7	.466	.184	7.6	122.0	.9
17.22.53	.707	.121	3.2	.623	.173	4.9	121.4	1.1
17.23.53	.668	.143	3.8	.662	.071	3.6	120.0	2.7
17.24.53	.654	.109	3.8	.581	.132	4.9	119.8	.6
17.25.53	.680	.100	3.4	.657	.089	3.7	119.1	.9
17.26.53	.673	.059	3.5	.608	.171	5.2	118.4	.8
17.27.53	.676	.053	3.4	.615	.077	4.3	117.7	.6
17.28.53	.643	.115	4.0	.585	.168	5.4	116.8	.4
17.29.53	.676	.049	3.4	.579	.138	5.0	116.1	.7
17.30.53	.676	.036	3.4	.630	.164	4.8	115.5	1.4
17.31.53	.630	.101	4.0	.593	.106	4.7	114.7	.8
17.32.53	.635	.074	4.0	.486	.218	8.2	113.9	1.0
17.33.53	.644	.063	3.9	.528	.211	6.9	113.2	.5
17.34.53	.657	.053	3.7	.522	.248	7.5	112.5	.8
17.35.53	.614	.137	4.7	.482	.169	7.1	111.4	1.7
17.36.53	.628	.073	4.1	.626	.165	4.9	111.1	.7
17.37.53	.645	.075	3.9	.591	.073	4.6	110.4	.8
17.38.53	.635	.071	4.0	.555	.139	5.5	109.9	.8
17.39.53	.616	.121	4.5	.549	.153	6.0	109.0	2.2
17.40.53	.624	.080	4.2	.600	.153	5.2	108.6	1.1
17.41.53	.607	.148	4.8	.541	.201	6.8	106.8	4.5
17.42.53	.633	.071	4.1	.577	.170	5.6	107.7	1.4
17.43.53	.670	.043	3.5	.601	.061	4.5	107.0	.7
17.44.53	.622	.089	4.1	.588	.046	4.6	105.9	.6
17.45.53	.655	.057	3.7	.519	.156	6.5	105.8	.9
17.46.53	.613	.134	4.6	.502	.135	6.7	104.1	4.7
17.47.53	.644	.106	4.0	.509	.142	6.6	103.2	4.7
17.48.53	.674	.024	3.4	.525	.197	7.1	104.2	1.2
17.49.53	.631	.075	4.1	.617	.073	4.2	103.6	.5
17.50.53	.651	.040	3.8	.491	.187	7.4	103.0	.6
17.51.53	.648	.077	4.2	.504	.167	6.9	102.4	.7
17.52.53	.650	.044	3.8	.481	.228	8.5	102.2	1.1
17.55.53	.638	.062	3.9	.506	.555	9.9	100.6	.7
17.56.53	.644	.037	3.8	.285	.214	13.0	100.1	.6
17.58.53	.617	.129	4.7	.195	.162	16.1	98.5	2.2
17.53.53	.646	.137	4.1	.148	.098	17.8	100.0	5.9
17.53.53	.673	.021	3.4	.543	.054	5.3	101.6	.3
17.54.53	.670	.042	3.5	.526	.117	5.8	101.2	.5
17.55.53	.675	.021	3.4	.531	.140	6.3	100.6	.7
17.56.53	.648	.032	3.6	.484	.189	7.6	100.1	.5
17.57.53	.650	.027	3.6	.521	.202	7.2	99.8	1.0
17.58.53	.634	.133	4.3	.509	.204	7.4	98.5	2.2
17.59.53	.650	.027	3.6	.479	.131	7.1	98.7	.4
18.00.53	.643	.035	3.9	.561	.121	5.3	98.4	.4
18.01.53	.634	.125	4.6	.534	.154	6.1	97.5	2.6
18.02.53	.630	.023	4.0	.408	.192	9.5	97.6	.7

DATE 08/01/72 ROLL NO 32

TIME	PINGER CHANNEL			SPARKER CHANNEL			WATER DEPTH	
	AVE	SIGMA	B-LOSS	AVE	SIGMA	B-LOSS	AVE	SIGMA
18.03.53	.619	.042	4.2	.542	.174	6.3	97.3	.5
18.04.53	.603	.043	4.4	.549	.116	5.4	97.0	.7
18.05.53	.662	.314	4.0	.444	.181	8.2	97.9	5.4
18.06.53	.559	.116	5.4	.503	.177	7.0	95.5	2.7
18.07.53	.557	.062	5.1	.520	.189	7.0	95.8	.9
18.08.53	.556	.029	5.1	.603	.080	4.5	95.7	1.1
18.09.53	.519	.036	5.2	.468	.221	8.5	95.2	.7
18.10.53	.526	.070	5.7	.511	.249	8.2	95.1	1.2
18.11.53	.554	.081	5.2	.537	.134	5.9	94.7	.5
18.12.53	.519	.082	6.0	.573	.057	4.9	94.9	1.5
18.13.53	.520	.113	5.9	.502	.188	7.5	93.5	5.0
18.14.53	.519	.123	6.1	.370	.204	10.8	93.2	4.6
18.15.53	.514	.107	6.1	.516	.175	6.7	93.4	2.3
18.16.53	.541	.030	5.4	.522	.178	6.8	94.0	.9
18.17.53	.526	.080	5.7	.288	.221	14.1	93.9	1.3
18.18.53	.516	.110	6.3	.442	.165	8.3	93.8	.8
18.19.53	.445	.141	7.6	.500	.225	8.1	93.0	1.5
18.20.53	.536	.027	5.4	.493	.182	7.5	93.3	.9
18.21.53	.469	.110	6.9	.509	.148	6.7	93.0	1.8

DATE 08/01/72 PELAO 33

TIME	PINGER CHANNEL			SPARKER CHANNEL			WATER DEPTH	
	AVE	SIGMA	B-LOSS	AVE	SIGMA	B-LOSS	AVE	SIGMA
18.51.53	.537	.180	6.2	.458	.122	7.3	89.9	5.7
18.52.53	.437	.215	8.5	.476	.229	8.8	87.8	8.4
18.53.53	.565	.174	4.5	.303	.239	13.7	91.8	7.0
18.55.53	.569	.218	4.8	.135	.088	18.6	91.2	7.0
18.56.53	.600	.130	4.8	.105	.027	19.8	94.2	.8
18.57.53	.550	.181	5.9	.108	.035	19.7	91.4	6.4
18.55.53	.569	.216	4.8	.367	.188	11.0	91.4	6.2
18.56.53	.609	.128	4.7	.544	.146	6.2	94.2	.8
18.57.53	.569	.180	5.6	.520	.136	6.3	91.4	6.4
18.58.53	.561	.192	6.9	.342	.252	13.1	93.2	4.0
18.59.53	.539	.150	5.9	.386	.186	10.3	92.7	5.7
19.00.53	.463	.255	5.0	.414	.195	9.7	90.3	9.5
19.01.53	.501	.210	4.9	.368	.221	11.5	91.0	8.7
19.02.53	.506	.091	4.8	.421	.245	10.5	93.3	5.1
19.03.53	.515	.193	5.5	.357	.229	11.9	92.8	5.7
19.04.53	.559	.171	4.7	.324	.242	13.2	93.0	5.8
19.05.53	.469	.186	7.5	.257	.197	14.7	92.8	3.9
19.06.53	.492	.211	6.1	.259	.214	14.9	92.0	6.0
19.07.53	.446	.226	6.1	.241	.155	14.4	91.4	8.3
19.08.53	.463	.263	7.1	.212	.191	17.1	91.1	7.7
19.09.53	.401	.231	7.4	.353	.225	12.0	87.4	10.9
19.10.53	.484	.226	5.4	.322	.248	13.8	90.6	9.9
19.11.53	.401	.292	5.8	.436	.129	8.1	88.0	12.0
19.12.53	.568	.092	5.0	.302	.238	14.1	95.5	.5
19.13.53	.382	.282	6.2	.361	.235	12.0	88.7	10.0
19.14.53	.525	.176	6.2	.306	.201	13.2	94.6	4.6
19.15.53	.586	.086	4.8	.246	.197	15.1	96.3	.8
19.16.53	.452	.254	5.2	.301	.207	13.4	92.3	8.7
19.17.53	.513	.204	5.7	.415	.193	9.3	94.6	6.7
19.18.53	.410	.244	7.2	.388	.206	10.5	93.2	8.3
19.19.53	.529	.177	5.1	.362	.255	11.9	95.4	6.4
19.20.53	.535	.217	5.4	.362	.212	11.4	95.8	5.9
19.21.53	.572	.142	5.3	.288	.214	13.9	96.1	5.7
19.22.53	.478	.265	4.8	.180	.155	17.5	93.2	9.2
19.23.53	.748	.304	5.1	.198	.184	17.5	87.5	12.8
19.24.53	.505	.215	5.9	.166	.151	18.3	95.1	8.8
19.25.53	.531	.190	5.3	.260	.219	15.0	96.6	6.2
19.26.53	.341	.310	5.5	.379	.180	10.5	88.8	11.4
19.29.53	.470	.267	5.1	.221	.184	13.7	93.3	13.1
19.30.53	.533	.234	4.5	.192	.208	18.1	96.2	9.7
19.31.53	.378	.292	6.5	.103	.059	20.8	90.2	12.4
19.27.53	.616	.192	4.0	.226	.175	15.3	97.4	6.2
19.28.53	.634	.141	4.2	.352	.231	12.3	99.4	.9
19.29.53	.526	.303	4.3	.339	.241	12.1	95.4	8.7
19.30.53	.583	.253	3.8	.464	.178	8.1	96.5	8.9
19.31.53	.462	.302	4.6	.425	.189	9.2	93.5	11.1
19.32.53	.560	.175	4.6	.158	.128	18.5	98.7	7.2
19.33.53	.574	.168	4.4	.318	.192	12.7	99.3	6.0
19.34.53	.543	.176	4.9	.285	.231	14.4	99.5	5.9
19.35.53	.431	.244	7.8	.504	.202	7.7	96.5	8.7

DATE 08/01/7[illegible] FILE 0 33

TIME	FI[illegible] CHANNEL			SPARKED CHANNEL			WATER DEPTH	
	AV[illegible]	SIGMA	B-LOSS	AVE	SIGMA	B-LOSS	AVE	SIGMA
19.36.57	.5[illegible]	.172	5.9	.476	.148	7.1	100.6	5.0
19.37.57	.4[illegible]	.[illegible]85	6.0	.378	.224	11.2	96.0	9.7
19.38.57	.4[illegible]	.[illegible]35	8.6	.247	.209	15.6	93.3	12.1
19.39.57	.5[illegible]	.211	5.1	.331	.235	13.6	99.2	10.9
19.40.57	.5[illegible]7	.[illegible]63	5.0	.396	.238	10.8	101.4	10.1
19.41.57	.5[illegible]1	.180	4.8	.402	.221	10.8	102.7	6.2
19.42.57	.5[illegible]2	.217	4.8	.411	.238	10.4	101.6	8.1
19.43.57	.5[illegible]7	.180	4.7	.460	.170	8.2	104.9	.7
19.44.57	.5[illegible]1	.167	5.6	.352	.206	11.5	104.3	4.8
19.45.57	.3[illegible]2	.[illegible]27	5.3	.378	.248	12.0	95.8	12.0
19.46.57	.4[illegible]7	.264	6.0	.492	.140	7.0	100.1	12.9
19.47.57	.4[illegible]5	.[illegible]46	5.7	.468	.175	8.2	102.9	9.8
19.48.57	.5[illegible]0	.[illegible]33	4.8	.459	.175	8.3	104.7	7.6
19.49.57	.4[illegible]3	.[illegible]04	5.2	.268	.193	14.3	100.3	11.7
19.50.57	.4[illegible]0	.054	4.0	.325	.227	12.5	108.8	1.2
19.51.57	.5[illegible]3	.151	5.1	.420	.241	10.2	108.9	1.6
19.52.57	.5[illegible]6	.[illegible]10	4.5	.465	.175	7.8	105.5	9.1
19.53.57	.5[illegible]0	.[illegible]92	4.3	.416	.267	11.0	107.1	9.0
19.54.57	.5[illegible]4	.[illegible]07	5.0	.470	.171	7.7	107.8	8.7
19.55.57	.4[illegible]0	.[illegible]06	7.1	.448	.236	9.4	111.5	.7
19.56.57	.4[illegible]4	.251	5.5	.438	.201	8.8	109.4	7.7
19.58.57	.4[illegible]2	.[illegible]75	6.0	.169	.138	17.3	105.7	10.6
19.59.57	.5[illegible]0	.[illegible]67	6.1	.101	.097	15.4	106.6	11.9
20.00.57	.7[illegible]7	.358	10.9	2.118	5.407	4.5	94.5	18.7

DATE 08/[illegible]

TIME	PINGER CHANNEL			SPARKER CHANNEL			WATER DEPTH	
	AVE	SIGMA	B-LOSS	AVE	SIGMA	B-LOSS	AVE	SIGMA
18.31.5[illegible]	.[illegible]	.[illegible]	4.1	.490	.171	7.0	91.9	1.0
18.32.5[illegible]	.[illegible]	.[illegible]	5.2	.344	.245	12.7	91.3	.8
18.33.5[illegible]	.[illegible]	.[illegible]	4.4	.410	.257	11.0	91.7	.7
18.34.5[illegible]	.[illegible]	.[illegible]	4.8	.441	.227	9.6	91.4	.4
18.35.5[illegible]	.[illegible]	.[illegible]	4.8	.514	.181	7.0	91.3	.7
18.36.5[illegible]	.[illegible]	.[illegible]	5.7	.384	.220	10.7	91.2	.6
18.37.5[illegible]	.[illegible]	.[illegible]	5.5	.390	.224	10.7	89.8	5.1
18.38.5[illegible]	.[illegible]	.[illegible]	5.6	.488	.192	7.8	89.9	5.5
18.39.5[illegible]	.[illegible]	.[illegible]	4.5	.440	.180	8.3	91.3	1.0
18.40.5[illegible]	.[illegible]	.[illegible]	5.0	.464	.212	8.9	90.2	3.3
18.41.5[illegible]	.[illegible]	.[illegible]	8.0	.434	.239	10.1	86.4	8.2
18.42.5[illegible]	.[illegible]	.[illegible]	4.5	.389	.243	11.5	91.2	.5
18.43.5[illegible]	.[illegible]	.[illegible]	6.7	.204	.170	16.7	88.3	6.3
18.44.5[illegible]	.[illegible]	.[illegible]	4.9	.466	.224	8.7	90.7	.9
18.45.5[illegible]	.[illegible]	.[illegible]	5.0	.541	.184	6.4	90.3	.9

DATE 08/02/7? ROLL'D 34

TIME	PINGER CHANNEL			SPARKER CHANNEL			WATER DEPTH	
	AVE	SIGMA	B-LOSS	AVE	SIGMA	B-LOSS	AVE	SIGMA
16.55.5?	.?7?	.156	1.3	.649	.073	3.8	122.0	.9
16.56.5?	.?9?	.120	1.2	.650	.095	3.8	121.3	.9
16.57.5?	.6??	.079	3.4	.626	.105	4.2	120.3	.8
16.58.5?	.6??	.079	3.3	.592	.182	3.8	119.3	.7
16.59.5?	.?8?	.137	1.6	.568	.241	3.2	118.4	.6
17.00.5?	.?3?	.119	2.7	.662	.094	3.7	117.5	1.0
17.01.5?	.?6?	.101	1.4	.619	.205	3.4	116.4	.5
17.02.5?	.737	.077	2.7	.629	.076	4.1	115.7	.9
17.03.5?	.745	.147	2.8	.555	.178	4.3	114.5	.9
17.04.5?	.?9?	.144	2.2	.611	.115	4.5	114.0	1.1
17.05.5?	.751	.082	2.5	.592	.111	4.7	113.2	.7
17.06.5?	.?2?	.098	2.9	.626	.073	4.1	112.6	.5
17.07.5?	.?64	.097	2.4	.623	.090	4.2	111.9	.8
17.08.5?	.764	.092	2.2	.641	.066	3.9	110.9	.7
17.09.5?	.77?	.060	2.3	.624	.088	4.2	110.1	.9

DATE 08/02/72 ROLL 0 35

TIME	PINGER CHANNEL			SPARKER CHANNEL			WATER DEPTH	
	AVE	SIGMA	B-LOSS	AVE	SIGMA	B-LOSS	AVE	SIGMA
17.21.53	.960	.199	1.1	.713	.093	3.0	103.2	.2
17.22.53	.913	.164	.9	.704	.130	3.2	102.5	.4
17.23.53	.749	.188	2.8	.702	.103	3.2	102.1	.9
17.24.53	.746	.081	2.6	.695	.085	3.2	101.5	.6
17.25.53	.903	.185	2.3	.624	.131	4.3	100.1	5.4
17.26.53	.816	.049	1.8	.757	.129	2.5	101.1	.7
17.27.53	.792	.062	2.2	.711	.103	3.1	100.3	.4
17.28.53	.953	.260	1.7	.740	.243	2.9	100.3	.5
17.29.53	.852	.116	1.5	.654	.214	3.0	100.0	.5
17.30.53	.748	.071	2.6	.660	.095	3.7	99.6	.4
17.31.53	.770	.062	2.2	.719	.076	2.9	99.6	.8
17.32.53	.832	.052	1.6	.668	.178	3.9	99.2	.9
17.33.53	.760	.156	2.7	.640	.058	3.9	98.4	2.7
17.34.53	.870	.036	1.2	.673	.137	3.7	98.7	.5
17.35.53	.847	.050	1.5	.629	.093	4.1	98.4	.6
17.36.53	.788	.165	2.4	.740	.093	2.7	97.8	1.7
17.37.53	.817	.055	1.8	.687	.090	3.3	97.9	.5
17.38.53	.718	.226	2.6	.532	.182	6.3	96.0	5.2
17.39.53	.750	.157	2.8	.688	.143	3.5	96.6	1.2
17.40.53	.764	.044	2.1	.686	.103	3.4	96.9	.8
17.41.53	.762	.082	2.8	.701	.102	3.2	96.9	.8
17.42.53	.669	.137	4.0	.713	.140	3.1	94.0	5.4
17.43.53	.698	.100	3.2	.682	.094	3.4	95.9	.5
17.44.53	.750	.079	2.5	.744	.090	2.6	95.8	.7
17.45.53	.685	.147	3.5	.690	.093	3.3	95.4	.6
17.46.53	.744	.122	2.7	.672	.090	3.5	95.3	.6
17.47.53	.660	.141	3.7	.627	.074	4.1	93.7	4.7
17.48.53	.709	.091	3.1	.663	.135	3.6	95.1	.3
17.49.53	.703	.080	3.1	.675	.115	3.5	94.8	.9
17.50.53	.748	.070	2.6	.592	.146	4.8	94.7	.5
17.51.53	.724	.066	2.8	.708	.091	3.1	94.7	.5
17.52.53	.742	.067	2.6	.645	.128	4.0	94.9	1.0
17.53.53	.739	.100	2.7	.642	.102	4.0	95.4	1.0
17.54.53	.691	.160	3.6	.647	.118	3.9	94.2	4.6
17.55.53	.694	.156	3.6	.652	.078	3.8	94.3	4.9
17.56.53	.719	.084	2.9	.678	.092	3.4	95.5	.8
17.57.53	.660	.215	4.1	.601	.094	4.5	93.3	4.9
17.58.53	.747	.090	2.6	.695	.065	3.2	95.0	.6
17.59.53	.715	.141	3.2	.718	.173	3.1	94.7	1.1
18.00.53	.729	.090	2.8	.657	.090	3.7	94.7	1.0
18.01.53	.614	.219	5.3	.684	.068	3.3	91.4	6.2
18.02.53	.650	.144	4.3	.722	.073	2.9	93.6	.8
18.03.53	.715	.077	3.1	.734	.087	2.7	93.5	1.1

DATE 08/02/72 FOLIO 35

TIME	PINGER CHANNEL			SPARKER CHANNEL			WATER DEPTH	
	AVE	SIGMA	B-LOSS	AVE	SIGMA	B-LOSS	AVE	SIGMA
18.51.53	.774	.109	2.3	.741	.104	2.7	95.7	1.2
18.52.53	.719	.241	2.9	.665	.130	3.7	93.1	7.2
18.53.53	.771	.091	2.3	.650	.089	3.8	95.9	.6
18.54.53	.652	.167	4.2	.688	.122	3.4	96.5	1.2
18.55.53	.715	.161	3.3	.677	.083	3.4	95.1	5.2
18.56.53	.633	.145	3.5	.655	.111	3.8	97.0	.5
18.57.53	.685	.184	3.7	.578	.093	4.9	97.3	.8
18.58.53	.568	.309	4.6	.566	.096	5.1	94.4	7.4
18.59.53	.765	.099	2.4	.650	.122	3.9	97.2	1.1
19.00.53	.626	.237	4.0	.633	.088	4.1	96.0	5.5
19.01.53	.630	.222	4.6	.654	.141	3.9	96.5	5.0
19.02.53	.611	.256	5.4	.619	.102	4.3	93.8	7.9
19.03.53	.672	.228	3.2	.705	.086	3.1	95.7	6.3
19.04.53	.655	.184	4.2	.734	.113	2.8	97.4	.7
19.05.53	.657	.224	4.5	.689	.093	3.3	97.2	1.1
19.06.53	.641	.150	4.2	.739	.092	2.7	96.4	1.7
19.07.53	.557	.278	4.5	.681	.151	3.6	93.7	7.4
19.08.53	.620	.277	3.3	.636	.093	4.0	92.8	8.1
19.09.53	.607	.246	4.3	.690	.106	3.3	95.1	6.6
19.10.53	.561	.303	4.6	.549	.125	5.4	92.0	8.6
19.11.53	.632	.208	4.7	.658	.098	3.7	96.2	1.4
19.12.53	.620	.277	3.4	.645	.104	3.9	93.9	7.6
19.13.53	.516	.318	4.6	.557	.085	5.2	91.2	10.3
19.14.53	.696	.201	2.8	.661	.157	3.9	95.5	7.0
19.15.53	.511	.352	4.1	.632	.114	4.1	91.1	10.3
19.16.53	.690	.153	3.5	.624	.104	4.2	97.7	.7
19.17.53	.376	.358	5.1	.599	.216	3.8	88.3	11.1
19.18.53	.525	.328	4.6	.588	.162	4.9	90.1	14.1
19.19.53	.726	.103	2.9	.783	.120	2.2	98.5	.9
19.20.53	.523	.227	5.5	.746	.057	2.6	99.0	7.8
19.21.53	.580	.032	4.8	.646	.066	3.8	99.2	.6
19.22.53	.403	.215	5.3	.644	.086	3.9	96.8	7.5
19.23.53	.445	.224	6.3	.639	.122	4.0	95.1	9.4
19.24.53	.584	.028	4.7	.776	.059	2.2	100.2	1.2
19.25.53	.447	.243	6.4	.633	.128	4.1	95.7	8.4
19.26.53	.561	.037	4.7	.627	.091	4.1	100.6	.7
19.27.53	.480	.231	5.6	.694	.066	3.2	98.2	7.6
19.28.53	.602	.023	4.4	.671	.159	3.7	101.3	1.0
19.29.53	.594	.133	5.1	.677	.108	3.5	100.8	3.0
19.30.53	.595	.187	4.1	.562	.163	5.4	100.6	5.8
19.31.53	.506	.306	4.2	.652	.140	3.9	98.2	8.4

DATE 08/03/73 BOILER 36

TIME	PINGER CHANNEL			SPARKER CHANNEL			WATER DEPTH	
	AVE	SIGMA	B-LOSS	AVE	SIGMA	B-LOSS	AVE	SIGMA
17.42.53	.738	.119	2.8	.719	.117	3.0	109.0	.8
17.43.53	.733	.132	2.9	.645	.079	3.9	109.7	.7
17.44.53	.743	.171	2.9	.619	.113	4.3	111.6	4.6
17.45.53	.621	.205	3.8	.633	.084	4.1	110.0	5.4
17.46.53	.712	.160	3.4	.631	.120	4.1	112.4	1.1
17.47.53	.760	.062	2.4	.641	.071	3.9	112.6	.7
17.48.53	.614	.268	4.5	.545	.123	5.5	110.9	6.9
17.49.53	.707	.127	3.2	.636	.096	4.0	114.1	.7
17.50.53	.645	.185	3.4	.616	.108	4.4	113.3	5.7
17.51.53	.721	.092	2.9	.645	.076	3.9	115.5	.7
17.52.53	.751	.068	2.5	.620	.101	4.3	116.2	.7
17.53.53	.631	.290	3.3	.599	.091	4.5	114.1	7.7
17.54.53	.676	.090	3.5	.622	.081	4.2	117.6	.6
17.55.53	.694	.201	2.9	.650	.141	4.0	116.8	5.6
17.56.53	.694	.320	3.3	.585	.119	4.8	119.1	7.9
17.57.53	.751	.114	2.6	.651	.092	3.8	120.2	.7
17.58.53	.665	.247	3.2	.634	.101	4.1	119.6	5.7
17.59.53	.776	.112	2.3	.534	.175	4.6	122.0	.8

DATE 08/03/72 ROLLNO 35

TIME	PINGER CHANNEL AVE	SIGMA	B-LOSS	SPARKER CHANNEL AVE	SIGMA	B-LOSS	WATER DEPTH AVE	SIGMA
19.40.53	.337	.247	9.0	.589	.144	4.8	92.3	10.0
19.41.53	.553	.273	4.5	1.644	.537	-4.0	101.7	12.3
19.42.53	.509	.338	4.1	.682	.245	4.0	100.2	12.1
19.43.53	.499	.291	5.4	.602	.286	2.9	102.0	11.7
19.44.53	.577	.237	4.8	.610	.122	4.4	106.5	7.1
19.45.53	.721	.145	3.0	.660	.130	3.8	109.7	4.9
19.46.53	.608	.181	3.9	.714	.078	3.0	109.2	5.4
19.47.53	.481	.304	5.1	.646	.120	4.0	106.0	9.8
19.48.53	.610	.264	3.6	.646	.110	3.9	107.2	8.9
19.49.53	.473	.303	5.3	.779	.127	2.3	106.7	10.6
19.50.53	.684	.091	3.4	.655	.096	3.8	111.7	.7
19.51.53	.363	.276	6.6	.575	.112	5.0	107.3	9.1
19.52.53	.543	.301	3.9	.656	.118	3.6	107.8	11.0
19.53.53	.659	.152	4.0	.710	.091	3.0	113.5	.9
19.54.53	.560	.306	3.9	.688	.122	3.4	109.9	8.9
19.55.53	.604	.233	5.3	.693	.097	3.3	111.7	8.2
19.56.53	.624	.230	4.0	.707	.105	3.1	113.8	6.4
19.57.53	.655	.267	3.7	.743	.106	2.7	114.5	6.1
19.58.53	.567	.325	4.7	.789	.090	2.1	113.8	8.2
19.59.53	.734	.109	2.8	.634	.076	4.0	117.5	.7

DATE 08/04/72 PULSE 37

TIME	PINGER CHANNEL AVE	SIGMA	B-LOSS	SPARKER CHANNEL AVE	SIGMA	B-LOSS	WATER DEPTH AVE	SIGMA
19.25.53	.772	.115	2.3	.503	.111	6.2	122.7	.8
19.26.53	.742	.078	2.6	.556	.115	5.3	121.8	.5
19.27.53	.854	.155	1.5	.604	.127	4.6	120.8	.6
19.28.53	.745	.124	2.7	.565	.138	5.3	120.0	.4
19.29.53	.774	.050	2.2	.613	.100	4.4	119.0	.5
19.30.53	.719	.075	2.9	.570	.104	5.0	118.2	.5
19.31.53	.713	.126	3.1	.605	.066	4.4	117.4	.4
19.32.53	.737	.097	2.8	.588	.090	4.7	116.9	.9
19.33.53	.661	.159	3.7	.608	.142	4.5	114.7	4.8
19.34.53	.655	.173	4.2	.580	.121	4.9	114.1	4.1
19.35.53	.677	.164	3.9	.558	.120	5.3	113.2	4.3
19.36.53	.763	.103	2.4	.581	.145	5.0	113.7	.7
19.37.53	.721	.174	3.2	.555	.076	5.2	112.5	2.6
19.38.53	.750	.047	2.5	.323	10.527	2.2	112.3	.8
19.39.53	.815	.070	1.8	.540	.182	4.6	111.7	.8
19.40.53	.849	.247	1.5	.567	.142	5.2	109.9	3.7
19.41.53	.842	.247	1.1	.541	.176	4.5	108.8	5.0
19.42.53	.775	.071	2.3	.560	.119	5.2	109.7	.5
19.43.53	.868	.097	.4	.536	.289	3.5	108.2	.7
19.44.53	.851	.097	.5	.619	.186	4.5	108.1	.4
19.45.53	.677	.154	3.8	.565	.113	5.2	106.4	4.0
19.46.53	.914	.086	.9	.703	.131	3.2	107.2	.6
19.47.53	.664	.124	3.7	.573	.133	5.1	105.3	4.2
19.48.53	.870	.093	.3	.635	.134	4.1	106.0	.5
19.49.53	.901	.062	.9	.589	.128	4.6	104.2	4.9
19.50.53	.867	.152	1.4	.605	.174	4.7	105.2	.5
19.51.53	.853	.207	1.8	.576	.135	5.0	104.4	.8
19.52.53	.698	.058	3.2	.596	.145	4.8	104.3	1.1
19.53.53	.874	.124	.3	.635	.275	3.5	103.8	.4
19.54.53	.838	.079	1.6	.578	.107	4.9	103.1	.4
19.55.53	.731	.208	3.2	.579	.085	4.8	102.3	1.5
19.56.53	.910	.086	.9	.668	.122	3.6	102.5	.5
19.57.53	.820	.105	1.8	.603	.195	3.7	101.8	.4
19.58.53	.906	.139	1.4	.569	.165	5.3	100.6	4.2
19.59.53	.878	.202	1.5	.693	.131	3.3	100.6	3.1
20.00.53	.863	.075	1.3	.602	.185	4.8	100.9	.9
20.01.53	.757	.213	2.9	.574	.092	4.9	98.7	4.4
20.02.53	.767	.282	3.0	.632	.193	4.4	97.9	5.9
20.03.53	.824	.086	1.7	.671	.138	3.7	99.9	.7
20.04.53	.772	.124	2.4	.570	.149	5.0	99.4	.5
20.05.53	.773	.102	2.3	.617	.164	4.5	98.7	.6
20.06.53	.621	.069	4.2	.596	.072	4.6	98.3	.5
20.07.53	.847	.110	1.9	.509	.117	6.1	98.2	.5
20.08.53	.632	.059	4.0	.543	.107	5.5	98.0	.5
20.09.53	.607	.038	4.4	.617	.094	4.3	97.3	.3
20.10.53	.502	.150	5.5	.602	.089	4.5	94.4	7.2
20.11.53	.625	.068	4.1	.648	.133	3.9	95.4	5.7
20.12.53	.642	.110	4.0	.612	.057	4.3	96.8	.5
20.13.53	.556	.198	6.0	.574	.187	4.1	94.8	4.3

DATE 08/04/72 POLL NO 38

TIME	PINGER CHANNEL AVE	SIGMA	B-LOSS	SPARKER CHANNEL AVE	SIGMA	B-LOSS	WATER DEPTH AVE	SIGMA
20.23.53	.644	.079	3.9	.596	.235	5.9	97.4	1.1
20.24.53	.495	.144	6.6	.502	.330	9.4	94.4	6.7
20.25.53	.555	.060	5.2	.336	.292	12.9	96.4	.6
20.26.53	.553	.050	5.2	.585	.273	6.8	96.2	.5
20.27.53	.510	.134	6.3	.592	.273	6.3	94.2	5.5
20.35.53	.547	.121	5.7	.633	.285	5.9	96.6	4.9
20.36.53	.495	.188	5.9	.550	.242	6.8	94.4	8.0
20.37.53	.499	.182	7.0	.530	.286	7.8	95.2	7.4
20.38.53	.497	.186	7.0	15.65158	.098	1.1	95.9	6.8
20.39.53	.474	.209	7.7	.438	.307	10.6	93.8	8.1
20.40.53	.550	.129	5.5	.385	.345	12.9	97.4	6.1
20.41.53	.544	.100	5.5	.490	.293	8.7	96.9	6.3
20.50.53	.712	.128	3.1	.525	.281	8.0	97.1	6.8
20.51.53	.541	.122	5.7	.630	.115	4.2	98.9	3.1
20.52.53	.588	.068	4.8	.558	.275	7.1	100.2	.5
20.53.53	.561	.100	5.2	.525	.286	8.0	98.7	4.6
20.54.53	.540	.134	5.7	.512	.310	8.7	98.1	6.1
20.55.53	.608	.043	4.3	.505	.278	8.4	99.8	2.3
20.56.53	.720	.094	2.9	.606	.232	5.5	100.8	.6
20.57.53	.749	.022	2.5	.499	.350	9.7	100.6	.4
20.58.53	.661	.222	3.4	.549	.301	7.5	100.2	7.1
20.59.53	.693	.155	3.5	.448	.311	10.0	98.3	4.6
21.00.53	.712	.124	3.2	.792	.105	2.1	98.7	.8
21.01.53	.650	.222	3.5	.643	.303	8.0	98.2	7.2
21.02.53	.709	.157	3.4	.612	.291	6.4	96.4	7.0
20.56.53	.669	.113	3.8	.515	.275	7.9	100.7	.6
20.57.53	.629	.024	4.0	.635	.293	6.1	100.6	.4
20.58.53	.594	.217	4.4	.525	.287	8.1	100.0	6.8
20.59.53	.629	.148	4.4	.526	.284	8.0	99.4	.5
21.00.53	.696	.127	3.4	.668	.233	4.7	97.5	4.5
21.01.53	.528	.179	5.2	.636	.251	5.4	98.1	7.5
21.02.53	.652	.159	4.2	.720	.205	3.6	97.5	5.7
21.03.53	.924	.180	.9	.840	.618	4.9	100.5	4.4
21.04.53	.597	.184	5.2	.169	.121	16.6	99.3	1.3
21.05.53	.777	.068	2.2	.156	.065	16.6	100.0	.6
21.06.53	.748	.041	2.5	.155	.040	16.4	100.4	.8
21.07.53	.746	.041	2.6	.219	.141	14.6	100.8	.8
21.08.53	.747	.058	2.6	.196	.218	14.4	101.2	.6
21.09.53	.673	.190	3.0	.223	.230	15.8	100.3	5.6
21.02.53	.660	.151	4.0	.578	.313	7.2	96.3	7.0
21.03.53	.961	.126	1.4	.845	.638	5.4	99.3	.6
21.05.53	.732	.119	2.8	.600	.267	6.4	100.0	.6
21.06.53	.744	.040	2.6	.596	.270	6.3	100.4	.8
21.07.53	.635	.162	4.5	.492	.268	8.5	99.7	4.2
21.08.53	.601	.217	5.4	.497	.269	8.5	98.7	6.2
21.09.53	.634	.182	3.9	.576	.267	6.7	100.0	6.3
21.10.53	.684	.078	3.4	.595	.282	6.4	102.3	.6
21.11.53	.623	.046	4.1	.606	.272	6.4	103.7	.6
21.12.53	.838	.046	1.5	.668	.170	4.2	103.4	.7
21.13.53	.795	.069	2.0	.493	.309	8.9	103.7	.8

DATE 08/04/7[illegible]

TIME	PINGER CHANNEL			SPARKER CHANNEL			WATER DEPTH	
	AVE	SIGMA	B-LOSS	AVE	SIGMA	B-LOSS	AVE	SIGMA
21.14.53	.8[illegible]4	.125	2.0	.549	.333	8.2	104.3	.4
21.15.53	.8[illegible]4	.030	1.9	.646	.296	5.9	104.7	.6
21.16.53	.754	.090	2.5	.351	.283	12.5	105.3	.5
21.17.53	.774	.110	2.3	.662	.241	4.8	105.6	.8
21.18.53	.6[illegible]5	.100	4.1	.621	.285	6.1	105.5	2.5
21.19.53	.641	.170	4.3	.654	.236	5.0	104.9	5.3
21.20.53	.690	.161	3.6	.660	.234	4.8	106.4	4.5
21.21.53	.8[illegible]5	.065	1.8	.599	.260	6.1	108.0	.6
21.22.53	.7[illegible]0	.104	2.1	.489	.328	9.5	108.2	.7
21.23.53	.799	.060	2.0	.568	.296	7.0	108.8	.7
21.24.53	.810	.050	1.8	.604	.265	6.2	109.5	.8
21.25.53	.841	.055	1.5	.547	.329	8.2	110.0	.9
21.26.53	.7[illegible]0	.214	2.0	.660	.251	5.0	109.2	5.6
21.27.53	.8[illegible]0	.063	1.9	.506	.296	8.5	110.9	.7
21.28.53	.741	.107	3.0	.650	.237	4.9	110.8	3.2
21.29.53	.757	.145	2.3	.584	.314	7.2	112.1	.7
21.30.53	.817	.087	1.8	.629	.273	5.8	112.9	.6
21.31.53	.794	.124	2.1	.667	.298	5.5	113.4	.4
21.32.53	.814	.112	2.0	.633	.283	5.9	114.2	.6
21.33.53	.7[illegible]8	.135	2.5	.661	.231	4.7	115.6	4.2
21.34.53	.7[illegible]6	.155	2.6	.609	.322	6.7	115.4	1.3
21.35.53	.867	.057	1.3	.607	.318	6.7	116.6	.9
21.36.53	.857	.118	1.4	.724	.119	2.9	117.6	.5
21.37.53	.853	.065	1.4	.641	.238	5.1	117.5	.8
21.38.53	.857	.107	1.4	.667	.307	5.6	117.2	.7
21.39.53	.8[illegible]0	.160	2.2	.687	.241	4.5	118.3	1.3
21.40.53	.741	.274	2.5	.693	.166	3.7	116.5	6.6
21.41.53	.8[illegible]0	.114	1.6	.607	.319	6.7	119.8	.7
21.42.53	.774	.255	2.0	.704	.260	4.5	119.1	5.6
21.43.53	.844	.160	1.7	.536	.278	7.6	121.4	.7

DATE 08/03/72 ROLL NO 39

TIME	PINGER CHANNEL			SPARKER CHANNEL			WATER DEPTH	
	AVE	SIGMA	B-LOSS	AVE	SIGMA	B-LOSS	AVE	SIGMA
17.14.57	.696	.079	3.2	.616	.158	4.9	99.7	.6
17.15.57	.760	.089	2.4	.606	.179	5.2	100.1	.4
17.16.57	.724	.096	2.9	.673	.175	4.2	100.3	.7
17.17.57	.673	.076	3.5	.549	.246	7.2	100.7	.4
17.18.57	.692	.157	3.5	.667	.103	3.6	100.0	4.6
17.19.57	.753	.124	2.6	.688	.058	3.3	101.4	.4
17.20.57	.691	.079	3.3	.717	.071	2.9	101.3	.4
17.21.57	.729	.097	2.8	.677	.196	4.3	101.8	.5
17.22.57	.656	.047	3.7	.646	.054	3.8	102.1	.4
17.23.57	.693	.038	3.3	.663	.073	3.6	102.4	.3
17.24.57	.692	.086	3.2	.655	.071	3.7	102.6	.4
17.25.57	.677	.043	3.4	.675	.083	3.5	102.5	.3
17.26.57	.695	.027	3.2	.627	.082	4.1	102.5	.6
17.27.57	.672	.038	3.4	.660	.044	3.6	102.3	.5
17.28.57	.660	.038	3.5	.648	.276	10.2	102.7	.4
17.29.57	.675	.025	3.4	.650	.102	3.9	102.0	.4
17.30.57	.663	.014	3.6	.664	.084	3.6	100.8	.4
17.31.57	.687	.033	3.5	.622	.162	4.8	100.5	.5
17.32.57	.697	.025	3.6	.670	.079	3.5	100.9	.4
17.33.57	.693	.046	3.9	.625	.161	4.9	101.4	.5
17.34.57	.653	.026	3.7	.615	.159	5.0	101.7	.3
17.35.57	.681	.029	3.6	.645	.070	3.9	102.3	.4
17.36.57	.693	.043	3.6	.475	.256	9.0	102.8	.4
17.37.57	.681	.045	3.3	.491	.263	8.7	103.3	.5
17.38.57	.736	.061	3.0	.513	.229	7.8	104.0	.3
17.39.57	.646	.033	3.6	.312	.254	13.8	104.5	.5
17.40.57	.676	.039	3.4	.525	.242	7.7	105.2	.5
17.41.57	.666	.026	3.3	.509	.226	7.7	105.6	.6
17.42.57	.687	.134	3.6	.451	.277	9.9	106.0	.3
17.43.57	.735	.139	3.1	.402	.262	10.7	106.7	.5
17.44.57	.715	.070	2.9	.638	.056	3.9	107.3	.6
17.45.57	.748	.048	2.7	.632	.166	4.7	107.9	.5
17.46.57	.757	.068	2.3	.677	.160	4.2	108.3	.5
17.47.57	.737	.075	2.7	.624	.232	5.6	108.8	.5
17.49.57	.907	.070	.9	.530	.235	7.1	110.3	.3
17.50.57	.954	.052	.4	.585	.151	5.3	111.0	.4
17.51.57	.949	.021	.5	.561	.207	6.3	111.4	.6
17.52.57	.974	.057	.2	.705	.061	3.1	112.0	.6
17.53.57	.961	.042	.4	.598	.151	5.1	112.6	.6
17.54.57	.935	.103	.9	.675	.053	3.4	113.4	.6
17.55.57	.941	.180	.8	.684	.185	3.9	114.1	.5
17.56.57	.900	.257	.7	.628	.169	4.7	113.3	5.6
17.57.57	.980	.052	.2	.694	.103	3.3	115.3	.6
17.58.57	.941	.080	.6	.655	.078	3.7	116.1	.5
17.59.57	.977	.065	.2	.712	.148	3.1	117.0	.6
18.00.57	.913	.122	.9	.684	.067	3.3	117.9	.6
18.01.57	.954	.111	.5	.661	.104	3.7	118.6	.6
18.02.57	.928	.120	.7	.681	.092	3.4	119.3	.7
18.03.57	.977	.070	.2	.645	.103	3.9	120.4	.7

DATE 8/29/72 PILOT 69

TIME	PINGER CHANNEL AVE	SIGMA	B-LOSS	SPARKER CHANNEL AVE	SIGMA	S-LOSS	WATER DEPTH AVE	SIGMA
20.00.00	.7[illegible]	.314	2.8	.477	.098	6.6	44.7	.7
20.01.00	.7[illegible]	.[illegible]	3.1	.473	.092	6.7	44.7	.6
20.02.00	.772	.231	2.6	.500	.075	6.1	44.6	.6
20.03.00	.6[illegible]7	.123	3.7	.421	.027	7.5	43.8	.3
20.04.00	.6[illegible]	.[illegible]91	3.9	.378	.073	8.6	43.7	.6
20.05.00	.674	.[illegible]40	4.0	.332	.056	9.7	43.7	.9
20.06.00	.9[illegible]	.346	1.7	.402	.063	8.0	43.3	.7
20.07.00	.6[illegible]1	.[illegible]55	4.5	.355	.164	6.9	43.8	.5
20.08.00	.72[illegible]	.145	2.9	.329	.078	9.9	42.9	.4
20.10.00	.6[illegible]1	.[illegible]06	4.4	.435	.091	7.4	42.7	.9
20.11.00	.6[illegible]0	.225	3.8	.431	.068	7.4	42.1	.6
20.12.00	.7[illegible]2	.[illegible]40	3.3	.428	.083	7.5	42.4	1.0
20.13.00	.7[illegible]1	.[illegible]42	3.6	.477	.057	6.5	41.5	.5
20.14.00	.6[illegible]1	.[illegible]26	4.1	.415	.177	8.4	42.2	.8
20.15.00	.4[illegible]7	.[illegible]89	8.1	.385	.066	8.4	41.1	.5
20.16.00	.3[illegible]4	.11[illegible]	8.7	.501	.059	6.1	40.9	.3
20.17.00	.217	.[illegible]37	8.6	.484	.072	6.4	42.3	5.6
20.18.00	.2[illegible]5	.[illegible]29	8.8	.479	.099	6.6	42.5	6.3
20.19.00	.13[illegible]	.13[illegible]	-.2	.551	.268	5.9	43.8	8.1
20.17.00	.6[illegible]9	.313	4.8	.429	.100	7.6	39.1	.5
20.18.00	.614	.212	4.8	.275	.091	11.6	39.4	.[illegible]
20.19.00	.5[illegible]2	.274	6.2	.363	.151	9.5	38.3	.7
20.20.00	.5[illegible]5	.[illegible]62	5.2	.285	.110	11.[illegible]	38.0	.8
20.21.00	.643	.210	4.3	.297	.078	10.9	37.3	.8
20.22.00	.6[illegible]4	.190	4.8	.229	.069	13.1	36.9	.7
19.49.00	.5[illegible]1	.[illegible]52	6.0	.602	.158	4.6	49.4	.6
19.50.00	.5[illegible]7	.178	5.6	.620	.107	4.3	48.7	.6
19.51.00	.6[illegible]	.291	3.9	.659	.103	3.7	48.1	.6
19.52.00	.6[illegible]1	.257	5.0	.606	.104	4.5	48.0	.6
19.53.00	.6[illegible]0	.[illegible]50	4.6	.451	.049	7.0	47.3	.4
19.54.00	.6[illegible]4	.190	3.6	.460	.058	6.8	46.7	.4
19.55.00	.6[illegible]3	.195	4.1	.422	.064	7.6	46.3	.5
19.56.00	.6[illegible]6	.[illegible]36	4.0	.457	.076	6.9	45.8	.5
19.57.00	.7[illegible]3	.173	3.1	.474	.090	6.6	45.3	.5
19.58.00	.5[illegible]7	.171	5.0	.431	.050	7.4	45.3	.8
19.59.00	.6[illegible]3	.198	3.7	.383	.062	8.4	44.8	.3

DATE 8/29/72 ROLL NO 58

TIME	PINGER CHANNEL AVE	SIGMA	B-LOSS	SPARKER CHANNEL AVE	SIGMA	B-LOSS	WATER DEPTH AVE	SIGMA
19.01.00	.677	.194	3.7	.537	.071	5.5	42.9	.3
19.02.00	.636	.247	4.7	.443	.121	7.4	44.1	.9
19.03.00	.610	.248	5.1	.513	.116	4.4	44.8	.9
19.04.00	.595	.218	5.0	.538	.104	5.5	45.4	.8
19.05.00	.592	.190	4.9	.592	.169	4.9	46.5	.5
19.06.00	.782	.309	2.9	.538	.123	5.6	46.3	.5
19.07.00	.660	.313	4.6	.557	.077	5.2	47.3	.9
19.08.00	.626	.236	4.6	.543	.266	6.2	48.0	.8
19.09.00	.538	.190	6.0	.556	.184	5.6	47.1	1.1
19.10.00	.810	.163	2.1	.485	.078	6.4	47.9	.7
19.11.00	.676	.147	3.6	.509	.095	6.0	47.8	.7
19.12.00	.624	.134	4.3	.454	.073	7.0	48.3	.8
19.13.00	.726	.272	3.4	.463	.073	6.8	48.7	.4
19.14.00	.661	.165	3.9	.552	.061	5.2	49.2	.6
19.15.00	.643	.269	4.4	.441	.146	7.5	49.3	.4
19.16.00	.595	.132	6.3	.428	.066	7.5	49.4	.5
19.17.00	.537	.200	6.0	.487	.077	6.4	50.1	.5
19.18.00	.706	.215	3.4	.452	.096	7.1	50.3	.5
19.19.00	.680	.195	3.7	.467	.080	6.7	50.3	.3
19.20.00	.726	.164	3.0	.480	.123	6.7	50.5	.6
19.21.00	.747	.173	2.7	.474	.074	6.6	50.4	.7
19.22.00	.743	.164	2.8	.494	.077	6.2	51.1	.8
19.23.00	.697	.131	3.3	.487	.077	6.4	51.2	.9
19.24.00	.738	.121	2.8	.465	.047	6.7	51.6	.8
19.25.00	.796	.151	2.1	.518	.079	5.8	51.7	.3
19.26.00	.734	.155	2.9	.497	.097	6.2	51.5	.8
19.27.00	.725	.144	3.1	.515	.080	5.9	51.6	.5
19.28.00	.825	.177	1.9	.530	.099	5.6	51.8	.4
19.29.00	.760	.194	3.0	.513	.068	5.9	51.9	.4
19.30.00	.741	.198	2.4	.575	.073	4.9	52.4	.5
19.31.00	.636	.220	4.5	.537	.093	5.5	52.1	.8
19.32.00	.689	.211	4.8	.481	.063	6.4	52.7	.5
19.33.00	.634	.196	3.5	.563	.087	5.1	53.1	.4
19.34.00	.675	.250	4.1	.549	.112	5.4	53.7	.8
19.35.00	.714	.209	3.7	.609	.084	4.4	54.0	.6

DATE 8/29/72 ROLLNO 58

TIME	PINGER CHANNEL			SPARKER CHANNEL			WATER DEPTH	
	AVE	SIGMA	B-LOSS	AVE	SIGMA	B-LOSS	AVE	SIGMA
18.21.53	.364	.018	8.8	.651	.110	3.8	56.1	.3
18.22.53	.362	.026	8.8	.678	.141	3.6	55.9	.6
18.23.53	.329	.062	9.9	.572	.112	5.0	54.7	2.2
18.24.53	.347	.040	9.2	.671	.116	3.6	54.8	.7
18.25.53	.357	.014	9.0	.615	.114	4.4	54.4	.5
18.26.53	.347	.027	9.2	.560	.096	5.2	54.0	.7
18.27.53	.325	.032	9.8	.528	.090	5.7	54.7	.4
18.28.53	.308	.087	10.7	.624	.155	4.4	53.3	3.1
18.29.53	.332	.037	9.6	.623	.104	4.2	53.9	.6
18.30.53	.341	.023	9.4	.603	.068	4.5	53.5	.4
18.31.53	.342	.019	9.3	.599	.084	4.5	52.9	.6
18.32.53	.341	.012	9.4	.538	.093	5.5	52.8	.3
18.33.53	.345	.036	9.3	.600	.073	4.5	52.6	.5
18.34.53	.351	.022	9.1	.539	.107	5.5	52.5	.6
18.35.53	.340	.013	9.4	.577	.132	5.1	52.2	.5